SMALL MOLECULE MODULATORS OF BCL-2 FAMILY PROTEINS

IDENTIFICATION AND CHARACTERIZATION OF SMALL MOLECULE MODULATORS OF BCL-2 FAMILY PROTEINS

By HETAL BRAHMBHATT, B.Sc.

A Thesis Submitted to the School of Graduate Studies in Partial Fulfilment of the Requirements for the Degree Doctor of Philosophy

McMaster University DOCTOR OF PHILOSOPHY (2016) Hamilton, Ontario

(Biochemistry and Biomedical Sciences)

TITLE: Identification and characterization of small molecule modulators of Bcl-2 family proteins

AUTHOR: Hetal Brahmbhatt, B.Sc. (McMaster University)

SUPERVISOR: Dr. David W. Andrews

NUMBER OF PAGES: xviii, 220

LAY ABSTRACT

Apoptosis is one process by which cells commit suicide. Alterations in the amounts of cell suicide are linked with many diseases; decreased cell death is characteristic of cancers while increased cell death is associated with neurodegenerative diseases. During apoptosis, the proteins Bax and Bak make a hole on the power house of the cell, the mitochondria, leaking components which trigger the demolition of cells. In this study chemicals were identified that promote or prevent the formation of holes in mitochondria were identified. The compounds were used to demonstrate the stage at which the hole formation can be blocked, identify an alternative way of triggering Bax to form holes, and to accelerate hole formation in cancers. Taken together this work increases the understanding of the events leading the formation of the hole and demonstrates how manipulation of these events is important for the treatment of apoptosis- linked diseases.

ABSTRACT

Apoptosis is a tightly regulated form of cell death fundamental to multi-cellular organisms for maintaining cellular homeostasis and removing damaged or dangerous cells. Disruptions in the apoptotic pathway that result in excessive or insufficient apoptosis are associated with many conditions including cancer, auto-immune diseases and neurodegenerative diseases. The Bcl-2 family proteins are the central regulators and executors of apoptotic signals at the mitochondrial outer membrane (MOM). Permeabilization of the MOM by the Bcl-2 family proteins, Bax and Bak, marks commitment to death and is considered to be the point of no return for most cells. Therefore, restoring normal apoptosis by targeting the Bcl-2 family proteins represents a potentially important avenue for novel therapeutics. Small molecules targeting Bcl-2 family proteins are important for mechanistic studies and serve as potential leads for novel therapeutics. The findings presented in this thesis were focused on identifying and characterizing small molecules that promote or inhibit Bax and/or Bak mediated MOM permeabilization. Four small molecules, MSN-50, MSN-125, OICR766A and SRI-O13 were identified by screening compound libraries for molecules that inhibit or promote Bax mediated permeabilization. MSN-50 and MSN-125 inhibit Bax and Bak mediated membrane permeabilization and confer protection of cells against apoptotic stimuli. The compounds inhibit Bax mediated MOMP by disrupting partial, but not all, interfaces of the Bax dimer. OICR766A activates Bax by a

mechanism distinct from activator BH3 proteins and cysteine 126 of Bax is required for activation by this compound. SRI-O13 enhances Bax and Bak mediated MOM permeabilization and displays anti-tumor activity in mice. Additionally, SRI-O13 synergizes with various apoptosis inducing agents to promote MOM permeabilization. Taken together, this work has increased the understanding of the mechanisms and interactions of Bcl-2 family proteins highlights the benefits of pharmacologically targeting Bcl-2 family proteins.

.

ACKNOWLEDGEMENTS

I would like to express my deepest appreciation and gratitude to all the following individuals for their contributions towards the success of my thesis.

I thank Dr. David Andrews and Dr. Brian Leber for the tremendous support, encouragement, patience, direction and constructive criticism provided to me during the course of my graduate studies. It has truly been an honor and privilege working under your supervision. I am also very grateful to my committee member, Dr. Radhey Gupta for giving me new ideas for my projects and always engaging in helpful discussions. The three of you always challenged me to think critically about my research work and this was very helpful in my training in research.

I would like to thank all past and present DWA lab members for being a great family to me away from home. I could have not asked to work with any other lab mates. I thank you all for the helpful ideas, discussions, friendship and doses of daily entertainment. I am particularly thankful to Lieven and Candis for training me as an undergraduate, Jarkko for help with the Opera, Santosh for always assisting me with my data analysis, Sina and Elizabeth for their contributions towards the introduction of my thesis, and Dr. Yuval Shaked for conducting the mice experiments and always providing me with very important tips. A very special heartfelt thank you to Aisha, Mina, Weijia, Justin, Xiaoke,

Frank, Fei, Santosh, Qian, Wiebke, Elizabeth and Vicki for always standing by me, supporting me and helping me during my good and bad lab days.

To all my family members, I would like to thank you for all your love, support, prayers and blessings. Mum and Dad, you have always been my greatest pillars of strength. I thank you for all your hard work, sacrifices, and efforts for making it possible for me to pursue and complete my graduate studies. I worked long and odd hours and it was only possible because you took care of everything else for me. You always had faith in me and your love for me provided me with the strength to stay determined. Riddhi, I thank you for always patiently listening to my endless stories and providing me with guidance on dealing with the ups and downs on lab life. Even though you live in a different country, you have always been there for me when I needed you the most. You are my angel. Aayushi, your innocent cute actions and laughter was the best medicine to help with cope with stress.

Lastly, to my husband Soham, I thank you for standing by my side and being so kind, caring, loving, patient, helpful, and understanding. Your positive attitude and smile lifted my spirits and provided me with the courage that I needed to complete this long journey. I am forever grateful for your countless efforts in making our dream come true.

TABLE OF CONTENTS

LIST OF FIGURES

CHAPTER I

CHAPTER II

CHAPTER III

CHAPTER IV

CHAPTER V

LIST OF TABLES

CHAPTER I

CHAPTER II

CHAPTER III

CHAPTER IV

LIST OF ABBREVIATIONS

ActD	Actinomycin D
Ala	Alanine
ANTS	8-Aminonaphthalene-1, 3, 6-Trisulfonic Acid, Disodium Salt
ATF6	Activating transcription factor 6
Bad	Bcl-2-associated death promoter
Bak	Bcl-2 antagonist/killer
Bap31	B-cell receptor associated protein 31
Bax	Bcl-2 associated X protein
Bcl-2	B-cell lymphoma 2
Bcl-XL	B-cell lymphoma – extra large
BH	Bcl-2 homology
Bid	BH3 interacting death-domain agonist
Bik	Bcl-2 interacting killer
Bim	Bcl-2 interacting mediator of cell death
Bmf	Bcl-2 modifying factor
BMK	Baby mouse kidney
C- terminal	Carboxyl terminal
CHOP	CCAAT/enhancer-binding protein homologous protein
CI	Combination index
CLL	Chronic lymphocytic leukemia

CuPhe	Copper (II)(1,10-phenanthroline)3
Cys	Cysteine
DAC	N-(7-dimethylamino-4-methylcoumarin-3-yl) maleimide
DAP1	4',6-diamidino-2-phenylindole
DKO	Double knock out
DMEM	Dulbecco's Modified Eagle Medium
DMSO	Dimethyl sulfoxide
DNA	Deoxyribonucleic acid
DPX	p-Xylene-Bis-Pyridinium Bromide
DSS	Disuccinimidyl suberate
ER	Endoplasmic reticulum
FBS	Fetal Bovine Serum
FDA	Food and drug administration
FLIM	Fluorescence lifetime imaging microscopy
FRET	Förster resonance energy transfer
HCT116	Human colon cancer cells
HDAC	Histone deacetylase
Hrk	Harakiri, Bcl-2 interacting protein
IANBD	N-N'-dimethyl-N-(iodoacetyl)-N'-(7-nitrobenzene-2-oxa-1, 3-diazol-4-yl) ethylenediamine
IgG	Immunoglobulin G

IL-3	Interleukin -3
IMM	Inner mitochondrial membrane
IP3	Inositol triphosphate
IRE-1	Inositol-requiring enzyme 1
ITC	Isothermal Calorimetry
IVT	in vitro translation
Mcl-1	Myeloid cell leukemia 1
MEF	Mouse embryonic fibroblast
MLM	Mouse liver mitochondria
MOM	Mitochondrial outer membrane
MOMP	Mitochondrial outer membrane permeabilization
mRNA	Messenger ribonucleic acid
MTD	Maximal tolerated dose
NAF1	Nuclear assembly factor 1
NEM	N-ethylmaleimide
NMR	Nuclear magnetic resonance
OICR	Ontario Institute for Cancer Research
PERK	Protein kinase RNA-like endoplasmic reticulum kinase
PMA	Phenylmercuric acetate
Puma	p53 upregulated modulator of apoptosis
SAR	Structure-activity relationship

SD	Standard deviation
SEM	Standard error of the mean
STAT5	Signal transducer and activator of transcription 5
Tb/DPA	terbium-dipicolinic acid
TM	Transmembrane
TMRE	Tetramethylrhodamine, Ethyl Ester
TNF	Tumor necrosis factor
TNT	Transcription/translation
TUNEL	Terminal deoxynucleotidyl transferase dUTP nick end labeling
UPR	Unfolded protein response
VDAC	Voltage-dependent anion channel
Wt	Wild type

DECLARATION OF ACADEMIC ACHIEVEMENT

The research work presented in this thesis has been conducted under the supervision and guidance of Dr. Andrews and Dr. Leber. The preface of each chapter summarizes my contributions and those of other colleagues.

CHAPTER I: Introduction

Preface

The work presented here has been previously published as a chapter in:

Andrews D.W., Brahmbhatt H., and Leber B., The Bcl-2 Family Proteins: Insights into Their Mechanism of Action and Therapeutic Potential. In: Ralph A Bradshaw and Philip D Stahl (Editors-in-Chief), Encyclopedia of Cell Biology, Vol 3, Waltham, MA: Academic Press, 2016, pp. 379-389.

Permission has been granted by the publisher to reproduce the material presented here.

Contribution of authors:

Brahmbhatt H wrote all sections of the chapter and prepared the tables and figures. Andrews D.W and Leber B directed the layout of the chapter and edited the manuscript.

The Bcl-2 family proteins: Insights into their mechanism of action and therapeutic potential

The Bcl-2 Family Proteins: Insights into Their Mechanism of Action and Therapeutic Potential

DW Andrews and H Brahmbhatt, Sunnybrook Research Institute, Toronto, ON, Canada
B Leber, Hamilton, ON, Canada

Apoptosis and the Bcl-2 Family: A Historical Perspective

Apoptosis was first described in 1972 as a controlled form of programmed cell death distinct from necrosis that is required during development and in the maintenance of homeostasis of multi-cellular organisms (Kerr *et al.*, 1972). In 1985, the gene encoding B-cell lymphoma-2 (Bcl-2), the founding member of the family, was identified from a follicular lymphoma patient where a chromosomal translocation t(14;18) resulted in dysregulated Bcl-2 expression (Tsujimoto *et al.*, 1985). The link between Bcl-2, apoptosis, and cancer was established when the *BCL-2* gene product was shown to block cell death rather than to enhance cell proliferation as was expected as the mode of action of oncogenes at that time (Vaux *et al.*, 1988; Hockenbery *et al.*, 1990). This seminal observation led to the concept that impaired apoptosis was critical for tumorigenesis (Hanahan and Weinberg, 2000).

The Pathway of Apoptosis

Cellular signals that initiate apoptosis originate from many different types of intracellular stresses such as DNA damage and the unfolded protein response (UPR), or from external signals like the engagement of extracellular death receptors by ligands such as binding of tumor necrosis factor alpha (TNFα) or Fas to their cognate receptors on cancer cells (Fulda and Debatin, 2006). While both these cell intrinsic and extrinsic pathways are regulated by the Bcl-2 family of proteins, the former is more tightly regulated by the Bcl-2 family proteins because these apoptotic signals ultimately converge to cause mitochondrial outer membrane permeabilization (MOMP). As a consequence of MOMP, factors such as cytochrome c are released from the mitochondrial intermembrane space into the cytoplasm, which leads to the activation of a cascade of proteases termed caspases that cleave a distinct population of subcellular substrates that yields the characteristic apoptotic phenotype (Garrido *et al.*, 2006; Chipuk *et al.*, 2006). Therefore by initiating this final effector phase of apoptosis MOMP is typically regarded as the point of no return for a cell. The crucial role of Bcl-2 family of proteins is to regulate MOMP by a coordinated series of protein–protein and protein–membrane interactions (Leber *et al.*, 2010, 2007).

The Bcl-2 Family of Proteins: Classification and Structure

More than 20 Bcl-2 family proteins have been identified and are classified into three groups based on function and sequence similarity within four conserved Bcl-2 homology (BH) regions (**Figure 1(a)**; Sato *et al.*, 1994). The first group comprises the anti-apoptotic proteins, Bcl-2, Bcl-XL, Bcl-w, Mcl-1, and AI, which contain all four BH regions. The pro-apoptotic family members are distributed in two groups: (1) Bax and Bak, the proteins that form the pore in the mitochondrial outer membrane to mediate MOMP share sequence similarity in the BH1-3 regions and a modified BH4 region, and (2) the BH3 proteins such as Bid, Bim, Puma, Bad, Noxa, Bmf, Bik, Beclin-1 and Hrk which function as stress sensors and only share homology in the BH3 region (Kvansakul *et al.*, 2008). A feature found in many Bcl-2 family proteins is a carboxyl-terminal (C-terminal) transmembrane region (TM) which anchors proteins to intracellular membranes such as the mitochondrial outer membrane (MOM), endoplasmic reticulum (ER) and nucleus (Shamas-Din *et al.*, 2013b).

Although Bcl-2 family proteins vary in function and in amino acid sequence, the multi-region Bcl-2 family proteins show a similar structural fold thus providing insights into binding interactions that explains their mechanism of action. The three-dimensional solution structures show a common fold where two central hydrophobic α-helices form a hairpin surrounded by 6–7 amphipathic α-helices. Additionally, a long unstructured flexible loop is present between helix 1 and helix 2. The loop acts as a regulatory region and is sensitive to posttranslational modifications. The BH1-3 regions form a hydrophobic groove of different sizes (Petros *et al.*, 2004), and these grooves serve as the docking sites for specific BH3 regions of other Bcl-2 family members in a fashion analogous to ligand-receptor interactions (**Figure 1(b)**; Sattler *et al.*, 1997; Petros *et al.*, 2000; Liu *et al.*, 2003; Czabotar *et al.*, 2013; Dewson *et al.*, 2008). In Bax and Bcl-w, the hydrophobic C- terminal TM region occludes the hydrophobic groove from the aqueous environment of the cytoplasm (Suzuki *et al.*, 2000; Denisov *et al.*, 2003).

In contrast to the multi-region Bcl-2 proteins, NMR studies of Bim, Bad, Bmf and sequence analysis of BH3 proteins other than Bid and Bik suggest that they are intrinsically unstructured, but that the BH3 region becomes structured after interaction with the binding groove in anti-apoptotic members (Hinds *et al.*, 2007). Bid is an exception as it has a defined structure similar to the multi-region members, rather than its BH3 protein counterparts (Shamas-Din *et al.*, 2013a; Billen *et al.*, 2008b). From an evolutionary perspective, the multi-region Bcl-2 family members and Bid share a common ancestral origin whereas the BH3 proteins evolved later and separately (Aouacheria *et al.*, 2005). There is no structural information available for Bik but sequence analysis suggests that it may also be an all helical protein similar to the multi-region Bcl-2 family proteins. Unlike other family members, several BH3 proteins appear to have functions unrelated their apoptotic activity or to the functions of other BH3 proteins.

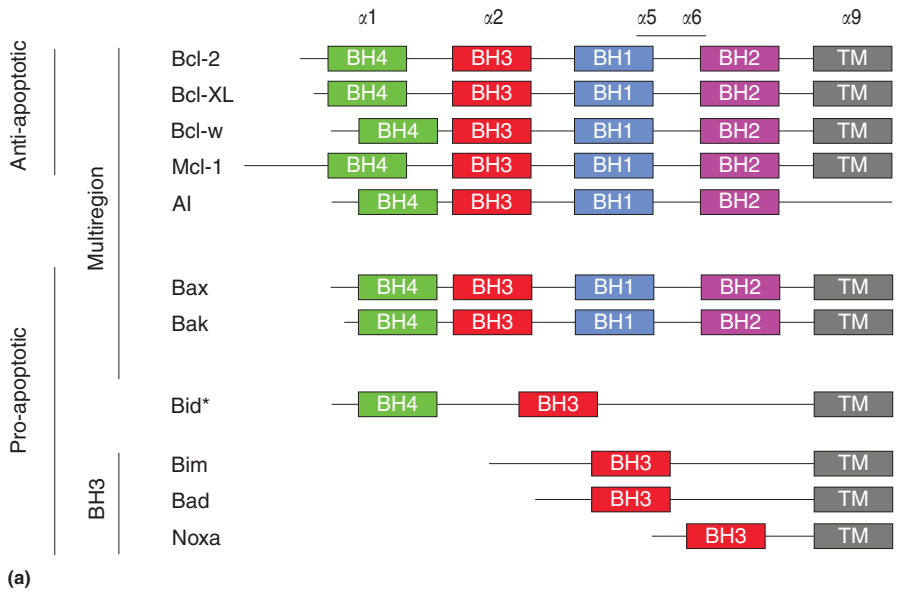

Figure 1 Schematic overview of the Bcl-2 family of proteins. (a) The Bcl-2 family of proteins is divided into three groups based on function and the presence of up to four Bcl-2 homology (BH) regions. The anti-apoptotic proteins and the multi-region pro-apoptotic proteins contain all four BH regions. The BH3 proteins contain only one conserved BH3 region. Most Bcl-2 family members contain a putative hydrophobic transmembrane (TM) region at the C-terminus that targets the proteins to intracellular membranes. *Bid is an example of an exceptional BH3 protein as it contains multiple BH regions. (b) The BH1-3 regions form a hydrophobic groove which serves as the interaction site for the BH3 region of other Bcl-2 family proteins. This figure is based on the crystal structure of Bcl-XL bound to the BH3 peptide of Bim (Liu, X., Dai, S., Zhu, Y., Marrack, P., Kappler, J.W., 2003. The structure of a Bcl-xL/Bim fragment complex: Implications for Bim function. Immunity 19, 341–352).

How Do Bcl-2 Family Proteins Regulate MOMP?

As the critical step in committing a cell to apoptosis, Bax and/or Bak oligomerize in the MOM forming a pore through which cytochrome c and other apoptogenic factors are released. Because both these proteins are present as monomers in cells, several models have been proposed to explain how their activation leads to oligomerization and how that is regulated by other Bcl-2 family members to ensure that MOMP only occurs in the appropriate cellular context (**Figure 2(a)**). According to the displacement model, Bax and Bak are constitutively active and therefore cell survival requires continuous inhibition of these proteins by binding to the anti-apoptotic proteins. During apoptosis, BH3 proteins displace activated Bax and Bak from the anti-apoptotic proteins allowing them to oligomerize, enabling MOMP (Willis *et al.*, 2005, 2007; Chen *et al.*, 2005). In contrast, the direct activation model postulates that Bax and Bak are inactive and require activation to execute MOMP. As a consequence, BH3 proteins can be pro-apoptotic in two different ways, and can be classified as activators or sensitizers based on binding affinities for different sub-types of the multi-region Bcl-2 members (**Figure 2(b)**). Activator BH3 proteins bind to Bax and/or Bak directly to cause their activation, but also bind to anti-apoptotic proteins; this latter interaction does not necessarily lead to MOMP and is one mechanism by which anti-apoptotic proteins prevent apoptosis. By contrast BH3 sensitizers only bind to anti-apoptotic proteins. If the anti-apoptotic protein is already bound to an

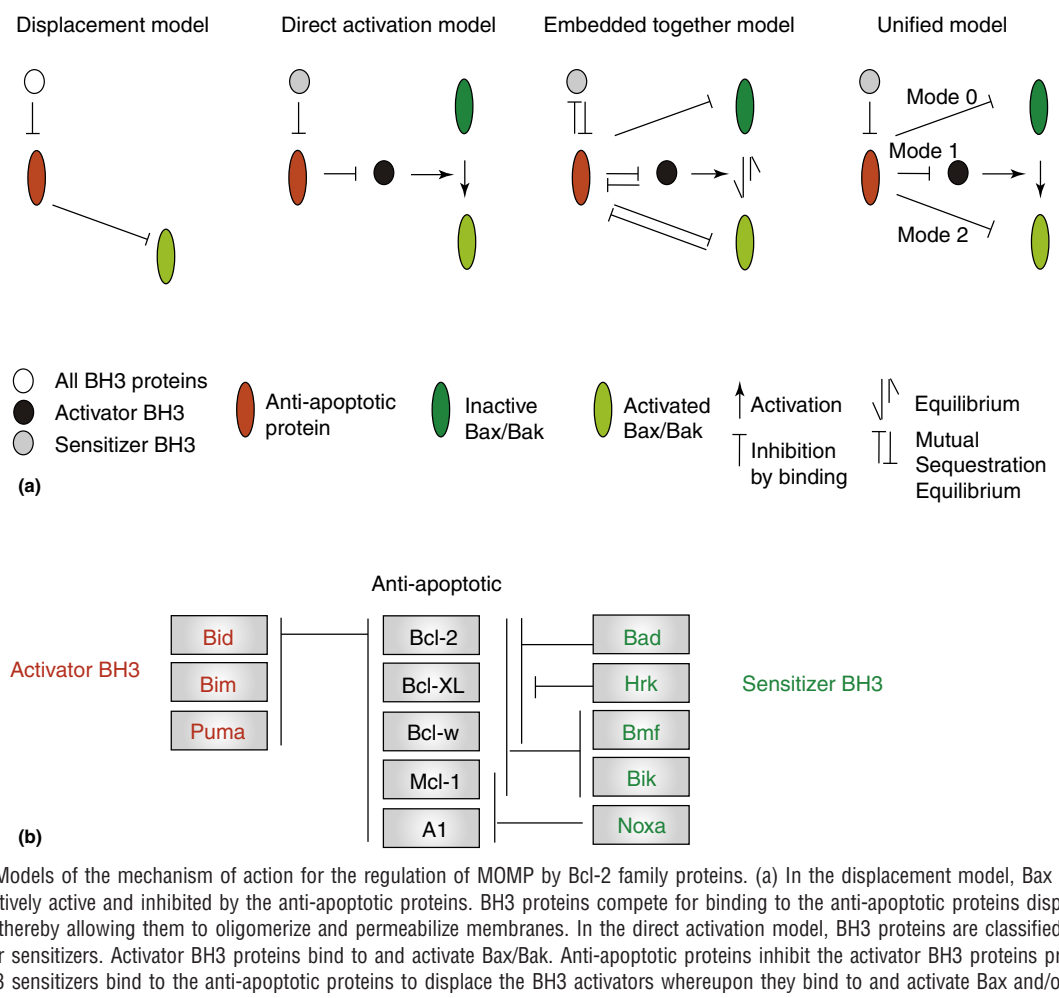

Figure 2 Models of the mechanism of action for the regulation of MOMP by Bcl-2 family proteins. (a) In the displacement model, Bax and/or Bak are constitutively active and inhibited by the anti-apoptotic proteins. BH3 proteins compete for binding to the anti-apoptotic proteins displacing Bax and/or Bak thereby allowing them to oligomerize and permeabilize membranes. In the direct activation model, BH3 proteins are classified as activators or sensitizers. Activator BH3 proteins bind to and activate Bax/Bak. Anti-apoptotic proteins inhibit the activator BH3 proteins preventing MOMP. BH3 sensitizers bind to the anti-apoptotic proteins to displace the BH3 activators whereupon they bind to and activate Bax and/or Bak. The embedded together model includes both displacement and activation mechanisms and suggests that the interactions of Bcl-2 family proteins with membranes results in conformational changes that change the affinities of the proteins for each other. Thus implicit in this model is that all interactions including those with membranes are reversible and governed equilibria. At membranes, the anti-apoptotic proteins inhibit the activator proteins as well as Bax and Bak by sequestering them or preventing their binding to the membrane. Both activator and sensitizer proteins can recruit and sequester anti-apoptotic proteins in the membrane, a term defined as mutual sequestration. The unified model defines anti-apoptotic sequestration of activator proteins and Bax or Bak as mode 1 and mode 2, respectively. Inhibition by mode 1 is less effective than mode 2. Mode 2 also prevents mitochondrial fusion and promotes mitochondrial fragmentation. (b) Classification of BH3 proteins as activators or sensitizers and selectivity of binding between BH3 proteins and anti-apoptotic members. This figure is based on binding affinities obtained from Certo, M., Del Gaizo Moore, V., Nishino, M., *et al.*, 2006. Mitochondria primed by death signals determine cellular addiction to antiapoptotic BCL-2 family members. Cancer Cell 9, 351–365.

activator, the activator is displaced whereupon it can bind to and activate Bax and/or Bak. Thus, sensitizers cause MOMP indirectly, and only if the anti-apoptotic protein bound has a 'pre-bound' activator (Letai *et al.*, 2002; Kuwana *et al.*, 2005). Thus, these models differ significantly as to the functional state of Bax and Bak monomers and the mechanism by which anti-apoptotic proteins inhibit MOMP (Leber *et al.*, 2007).

Based on experiments that measured these binding interactions *in vitro*, the embedded together model proposed that the distinction between activator and sensitizer BH3 proteins was valid, but incomplete. This model suggested that anti-apoptotic family members inhibit MOMP by binding to and sequestering both the activators and activated Bax and/or Bak (Leber *et al.*, 2007; Lovell *et al.*, 2008; Billen *et al.*, 2008a). Furthermore it assigns the membrane a critical role in the process, not only as a locus of interaction that is ultimately altered during MOMP, but also as a regulator of binding interactions as after interaction with membranes Bcl-2 family members undergo conformational changes that affect subsequent binding interactions. For example, Bid binds to and activates Bax only when both proteins are membrane bound. As a result, the entire process is governed by a series of reversible equilibria of protein–protein and protein–membrane interactions and the functional outcome depends on the relative protein concentrations and binding affinities. An additional feature of this model is that it assigns a dual role to BH3 proteins in that activators and sensitizers can also 'activate' their anti-apoptotic binding partners by promoting their insertion into the membrane. As binding of a membrane-bound anti-apoptotic protein to a BH3 protein or to Bax

and/or Bak inactivates both proteins, this mechanism is termed mutual sequestration (Leber *et al.*, 2010).

The unified model also recognizes that there are multiple mechanisms whereby anti-apoptotic proteins function by designating the sequestration of activators as MODE 1 and sequestration of activated Bax and/or Bak as MODE 2. In this model, inhibition of MODE 1 is less efficient and more easily de-repressed than MODE 2. As an important extension related to, but independent of apoptosis, inhibition by MODE 2 also prevents mitochondrial fusion and promotes mitochondrial fragmentation (Llambi *et al.*, 2011). Recently, the mechanism by which in healthy cells Bcl-XL transiently binds to peripherally membrane-bound Bax causing its relocation to the cytoplasm has been ascribed MODE 0 (Billen *et al.*, 2008a; Todt *et al.*, 2013; Edlich *et al.*, 2011; Westphal *et al.*, 2014).

Conformational Changes Associated with Bax and Bak Activation

In most cells Bax and Bak are described as functionally equivalent. However, evidence from animals (described below) suggests this may not be entirely correct. After binding to activator BH3 proteins both Bax and Bak undergo conformation changes permitting oligomerization that leads to the pore formation that is the structural basis for MOMP (Degenhardt *et al.*, 2002; Hsu and Youle, 1997; Griffiths *et al.*, 1999). Both Bax and Bak are composed of nine α helices: α5 and α6 are the two central hairpin helices, α9 contains the C-terminal TM region, and α2-4 forms the hydrophobic pocket (Suzuki *et al.*, 2000; Moldoveanu *et al.*, 2006). Despite these similarities in structure, conformational changes and function, there are still important differences between them.

In healthy cells, Bax is primarily cytosolic whereas Bak is inserted in the mitochondria and ER membrane. This difference in localization is attributed differences in the structure and configuration of the C-terminal TM region in α9 in the two proteins. After binding to BH3 activators, α9 of Bax is dislodged from the hydrophobic pocket allowing Bax to insert into membranes (Wolter *et al.*, 1997; Schinzel *et al.*, 2004; Annis *et al.*, 2005). In contrast, Bak bypasses this step since it is constitutively integrated in the membrane via its α9; this difference in spontaneous membrane insertion may be due to the increased hydrophobicity of the TM region of Bak compared to Bax (Ferrer *et al.*, 2012).

A common conformational change that occurs after activation of both Bax and Bak is the rearrangement of an amino terminal sequence that generates a neo-epitope (Hsu and Youle, 1997; Griffiths *et al.*, 1999). A transient interaction of Bax with membranes triggers this conformation change that is detected by the 6A7 antibody. This change is largely irreversible after binding to BH3 proteins and membranes (Yethon *et al.*, 2003). Structurally this neo-epitope emerges due to the unwinding of part of the Bax α1 helix after activation (Peyerl *et al.*, 2007). The specific change leading to epitope exposure after Bak activation has not been elucidated, but is proposed to be similar.

Another difference (albeit controversial) between Bax and Bak is the location and number of BH3 protein binding sites. The common interaction involves the BH3 region and the hydrophobic groove of BH1-3 that leads to conformational change favoring the formation of oligomers. While the Bid BH3 peptide binds Bak at this canonical site, an alternative binding hydrophobic pocket termed the 'rear pocket' was identified as the interaction site for the Bim BH3 peptide on Bax (Gavathiotis *et al.*, 2008; Leshchiner *et al.*, 2013). Notably this pocket is located at the 'opposite side' of the protein compared to the canonical site (termed 'front pocket'). The α1 and 6 helices form the rear pocket and is masked by the α1, 2 loop in the unbound state. Binding of the Bim BH3 peptide results in a conformation change that facilitates the displacement of C-terminal α9 that mediates membrane binding, and also exposes the BH3 region (Kim *et al.*, 2009; **Figure 3(a)**). Displacement of α9 is followed by the insertion of α5, α6 and α9 onto or into the membrane (Czabotar *et al.*, 2013; Annis *et al.*, 2005).

Regardless of whether there are one or two activation binding sites on Bax, activation results in the exposure of the hydrophobic BH3 region required for Bax homodimerization (Dewson *et al.*, 2008; George *et al.*, 2007). However, the type of dimer that is formed will depend on which binding pocket this newly exposed BH3 region finds. There are two competing models to explain the propagation of Bax dimers into large pore forming oligomers. In the asymmetric dimer model, the exposed BH3 region of one Bax molecule activates another Bax molecule through binding to the rear pocket (**Figure 3(b)**; Gavathiotis *et al.*, 2008). In contrast, the symmetric dimer model predicts that a Bax dimer forms when the BH3 region of one Bax molecule binds to the BH3 groove of another Bax molecule. Oligomer propagation occurs as a consequence of the interaction of two dimers via the rear pocket (**Figure 3(c)**; Czabotar *et al.*, 2013; Brouwer *et al.*, 2014).

Physiology and Regulation of Bcl-2 Family Members

Although the role of Bcl-2 family members in regulating apoptosis was initially recognized in the context of overexpression secondary to a chromosomal translocation found in a human cancer, our understanding of the physiological functions of specific Bcl-2 family members has been greatly aided by genetic knockout mice studies. Mice with a genetic deletion of *BCL-2*, *BCL-XL* or *MCL-1* are not viable. *MCL-1* -/- mice display a failure in embryonic implantation (Rinkenberger *et al.*, 2000). *BCL-XL* -/- mice die during embryonic development and exhibit extensive neuronal and hematopoietic progenitor cell death (Motoyama *et al.*, 1995). *BCL-2* -/- mice complete embryonic development but die postnatally displaying growth retardation, renal failure, extensive lymphocyte cell death and defects in hair pigmentation (Veis *et al.*, 1993). In contrast, Bcl-w knockout males are sterile and A1 knockout mice have accelerated neutrophil apoptosis (Hamasaki *et al.*, 1998; Print *et al.*, 1998).

Pro-apoptotic proteins are also important during development. While *BAK*-/- mice are developmentally normal and *BAX*-/- mice have limited abnormalities restricted to hyperplasia of lymphoid tissues and male sterility, mice lacking both *BAX* and *BAK* die perinatally from the accumulation of excessive cells in the hematopoietic and central nervous system. As expected, cells from these mice are resistant to various apoptotic stimuli (Knudson *et al.*, 1995; Lindsten *et al.*, 2000).

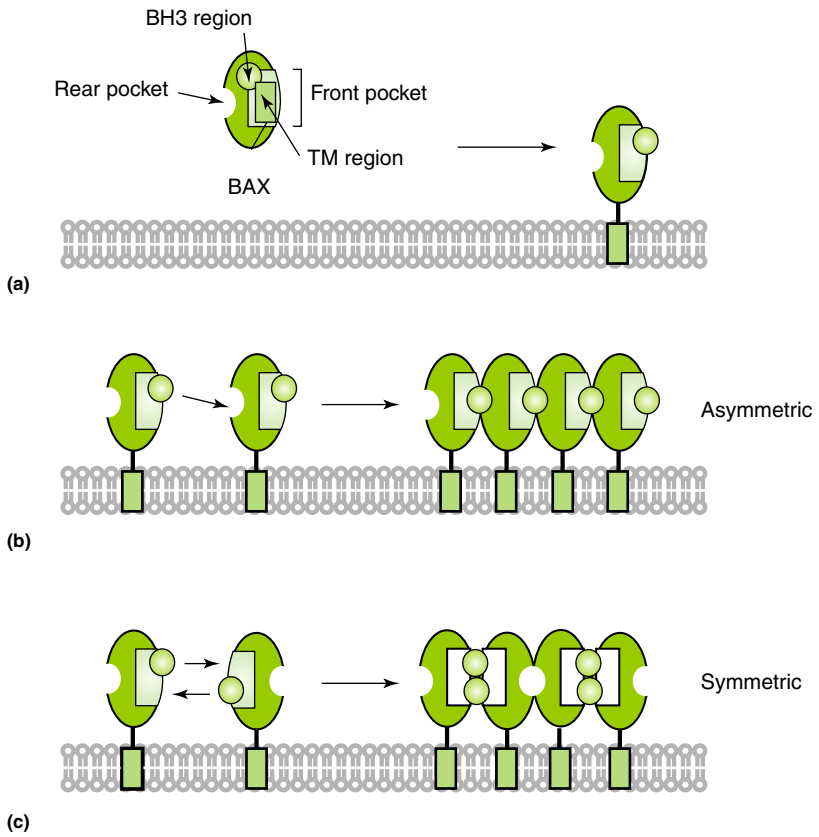

Figure 3 Models of Bax dimer formation. (a) Bax activation is triggered by interaction of a BH3 protein on the rear or front pocket. This interaction triggers the exposure of the BH3 region of Bax and insertion of the Bax into the membrane via the TM region. (b) Formation of asymmetric dimers: The exposed BH3 region of Bax and Bak interacts with the rear pocket of an adjacent Bax or Bak. Oligomer formation occurs by the subsequent interaction of the rear pocket and the BH3 regions. (c) Formation of symmetric dimers. The exposed BH3 regions of Bax and Bak interact with the hydrophobic groove of an adjacent Bax or Bak forming a homo-dimer. Pore formation occurs by subsequent oligomerization of homodimers presumably via interactions with the rear pocket.

In contrast, most mice lacking BH3 proteins are not affected developmentally, but display various tissue specific and signaling abnormalities (**Table 1**). As the BH3 domain is generally not required for the diverse non-apoptotic functions of BH3 proteins, it is likely that many of the defects observed in knockout animals are not due to alterations in apoptosis. Moreover, it is an open question for each family member as to which function evolved first. These proteins therefore serve as examples of intersecting nodes between cell death and metabolism, two processes that are tightly linked at many levels (Green *et al.*, 2014).

Since Bcl-2 family proteins are critical for maintaining the balance between life and death, their expression and activity is tightly controlled at multiple levels. At a transcriptional level, the expression of Bcl-2 family proteins is often increased in response to death or survival signals. For example, DNA damage results in the transcriptional activation by the tumor-suppressor P53 of pro-apoptotic *NOXA*, *PUMA* and *BAX* (Oda *et al.*, 2000; Nakano and Vousden, 2001; Miyashita *et al.*, 1994). By contrast, growth or survival signals cause the phosphorylation of STAT5 which acts as a transcriptional enhancer of *BCL-XL* (Silva *et al.*, 1999).

Function can also be regulated by alternative splicing: Bcl-XL and Bcl-XS are splice variants; the former anti-apoptotic and the latter pro-apoptotic due to the absence of a critical domain (Grillot *et al.*, 1997; Boise *et al.*, 1993). Bim has three isoforms, of which BimS is constitutively active in cells because it lacks a dynein light chain binding domain that normally sequesters BimL and BimEL to the micro-tubule associated dynein motor complex (O'Connor *et al.*, 1998). The latter proteins are therefore held inactive but able to respond more rapidly than BimS that is regulated transcriptionally.

At the posttranslational level, many Bcl-2 proteins are regulated by posttranslational modifications including phosphorylation, myristoylation, ubiquitin-mediated degradation and proteolytic cleavage, most commonly in the unstructured loop region, BH3 region and in the TM (Kutuk and Letai, 2008). These posttranslational modifications directly affect protein localization, half-life (and therefore concentration), and binding affinity to other Bcl-2 family members. The modifications also affect binding to other regulatory proteins outside the Bcl-2 family. For example, in the presence of the IL-3 survival factor the pro-apoptotic Bad is phosphorylated, binds to 14-3-3 complexes and is thereby sequestered in the cytoplasm. Therefore the phosphorylation status of Bad can serve as a switch in function as de-phosphorylation of Bad results in dissociation from the 14-3-3 complex and binding to Bcl-XL at the membrane as a pro-apoptotic sensitizer

Table 1 Phenotypes of mice deficient in BH3 proteins

BH3 protein deletion	*Phenotypes in mice*	*References*
Bid	Mice are resistant to Fas mediated fatal hepatocyte apoptosis and hemorrhagic necrosis	Yin *et al.* (1999)
Bim	Mice have hyperplasia of lymphoid and myeloid cells and T cell development is perturbed. Lymphocytes are resistant to apoptosis induced by elevated Ca^{2+} by ionomycin, micro-tubule stabilization by taxol, and cytokine deprivation. With age, mice develop lymphadenopathy and a fatal systemic autoimmune disease	Bouillet *et al.* (1999)
Puma	Various cell types are resistant to apoptosis induced by DNA damage, cytokine deprivation and glucocorticoid exposure	Jeffers *et al.* (2003); Villunger *et al.* (2003)
Bad	Certain cell types display an increased resistance to epidermal or insulin-like growth factor mediated apoptosis. Lymphocytes have decreased IgG production. With age, mice develop B-cell lymphoma	Ranger *et al.* (2003)
Noxa	Mice exhibit increased resistance toward X-ray irradiation induced gastrointestinal death. Fibroblasts display mild resistance toward etoposide or γ irradiation	Villunger *et al.* (2003); Shibue *et al.* (2003)
Bmf	Mice have hyperplasia of B cells and mild hypergammaglobulinemia Thymocytes and pre-B cells are mildly resistant to apoptosis induced by glucocorticoids, and histone- deacetylase inhibition	Labi *et al.* (2008)
Bik	No obvious detectable defects	Coultas *et al.* (2005)
Beclin	Early embryonic lethality. Embryonic stem cells display abnormalities in autophagy induction	Yue *et al.* (2003)
Hrk	Some neuronal cell types displayed delayed apoptosis induced by nerve growth factor withdrawal	Coultas *et al.* (2007); Imaizumi *et al.* (2004)

(Zha *et al.*, 1996). Additionally in healthy cells, Bak is bound to mitochondrial outer membrane protein VDAC2, thereby preventing activation until it is displaced during death signal initiation by tBid, Bim or Bad (Cheng *et al.*, 2003).

Bcl-2 Proteins at the Endoplasmic Reticulum

While much research has focused on the regulation of MOMP by Bcl-2 family proteins, they have also been implicated in important processes at the ER such as modulation of calcium signaling (Oakes *et al.*, 2006; Rong and Distelhorst, 2008). During endoplasmic reticulum stress, Bax and Bak oligomerize at the endoplasmic reticulum causing the release of calcium into the cytosol (Scorrano *et al.*, 2003; Zong *et al.*, 2003; Nutt *et al.*, 2002). This can lead to both mitochondrial dependent and independent pathways of cells death although the latter is less well characterized (Heath-Engel *et al.*, 2008). As a potential mediator of this process, the BH3 protein Bik induces ER resident Bax and Bak to oligomerize and release calcium ultimately leading to MOMP and the release of cytochrome *c* (Mathai *et al.*, 2005). ER resident Bcl-2 affects calcium flux by directly or indirectly binding to the IP3 receptor calcium channel (Rong *et al.*, 2009). Additionally, Bcl-2 localized at the endoplasmic reticulum can inhibit apoptosis triggered by various stress signals (Zhu *et al.*, 1996; Bhatt *et al.*, 2008). Furthermore, Bcl-2 has been found to be present in a complex which includes the ER protein Bap31, another transmitter of apoptotic signals from the endoplasmic reticulum to mitochondria (Chami *et al.*, 2004; Rong *et al.*, 2009; Breckenridge *et al.*, 2003; Ng *et al.*, 1997).

The unfolded protein response (UPR) and autophagy are two additional complex cellular responses mediated at the ER that are also regulated by Bcl-2 family proteins. UPR occurs as a consequence of the accumulation of unfolded or misfolded proteins in the lumen of the ER and triggers three signaling pathways mediated by ER localized ATF6, PERK and IRE-1, to restore normal function. Prolonged or excessive UPR results in apoptosis through PERK activation leading to CHOP-dependent transcriptional upregulation of *PUMA* and *BIM* (Puthalakath *et al.*, 2007; Ghosh *et al.*, 2012). A second arm of UPR mediation also requires the Bcl-2 family as Bax and Bak promote IRE-1 signaling (Hetz *et al.*, 2006).

Autophagy is a cell survival mechanism in which double membrane organelles called autophagosomes are induced to form around damaged cellular components such as misfolded proteins, protein aggregates and dysfunctional organelles. By regulated fusion with lysosomes the contents are catabolized and can be re-used to maintain cellular energy levels (Levine and Kroemer, 2008). Autophagy is therefore a survival mechanism, but autophagy can be driven to cell death through extensive degradation of critical organelles (Mukhopadhyay *et al.*, 2014). The initiation of autophagosome formation at the ER requires the BH3 protein Beclin-1 to co-ordinate a multiprotein complex (Axe *et al.*, 2008). Bcl-2 inhibits autophagy by directly binding to Beclin-1 in the presence of NAF-1 (Chang *et al.*, 2010; Rong *et al.*, 2008; Pattingre *et al.*, 2005). The BH3 protein Bad stimulates autophagy by displacing Beclin-1 from binding to Bcl-2 and Bcl-XL and allowing formation of the pre-autophagosome complex; thus there is direct cross talk between autophagy and apoptosis (Maiuri *et al.*, 2007).

Bcl-2 Family Proteins and Cancer

Cancers arise when cells acquire genetic or epigenetic abnormalities that cause uncontrolled proliferation. Apoptosis acts as a physiologic brake to this context-independent cell division (Meier *et al.*, 2000). Therefore the evasion of apoptosis is one of the required features for tumorigenesis and

many direct and indirect mediators of cell death are known to be abnormal in human and experimental cancer models, including Bcl-2 family proteins. In addition to the chromosomal translocations which led to the original discovery of *BCL-2*, many more common mechanisms have been observed including the amplification of the *BCL-2* gene as observed in small cell lung cancer and the loss of endogenous microRNAs that repress *BCL-2* gene expression as seen in chronic lymphocytic leukemia (Ikegaki *et al.*, 1994; Cimmino *et al.*, 2005). Amplification of *MCL-1* is one of the most common genetic abnormalities across cancers (Beroukhim *et al.*, 2010). Additionally, the inactivation of *BAX* by microsatellite insertions is common amongst many malignancies (Rampino *et al.*, 1997; Yamamoto *et al.*, 1997). Point mutations or posttranslational modifications altering the activity of BH3 proteins have also been reported, such as the somatic missense mutations reported in *BAD* in cases of colon adenocarcinoma. These mutations are predicted to reduce the binding affinity of Bad for Bcl-2 and Bcl-XL (Lee *et al.*, 2004).

Cancer and Addiction to Bcl-2 Family Proteins

Because of the requirement for preventing apoptosis to maintain continued proliferation of cancer cells, tumors are essentially 'addicted' to this inhibition. As critical regulators of MOMP, Bcl-2 family proteins are good (but not the only) candidates to achieve this (Certo *et al.*, 2006; Del Gaizo Moore *et al.*, 2007). Thus selective antagonism of anti-apoptotic Bcl-2 family proteins should be sufficient to kill those cancers where this represents the locus of addiction. The BH3 profiling assay is a powerful predictive tool to determine if regulation of MOMP by Bcl-2 family proteins is the locus, and to identify the nature of the addiction. To determine this, mitochondria are isolated from tumor cells and exposed to a panel of BH3 peptides representing the BH3 proteins. MOMP is measured by quantifying the release of cytochrome c from the mitochondria (Del Gaizo Moore and Letai, 2013). When MOMP is elicited, the pattern of release by effective and ineffective peptides can be divided into three classes with functional significance (**Figure 4**). The 'Class A' block occurs due to insufficient BH3 protein activation, and is overcome by adding activator BH3 peptides. 'Class B' block occurs due to a loss of the executors, Bax and Bak. Mitochondria with this block are insensitive to all BH3 peptides. In the 'Class C' block, MOMP is prevented by the overexpression of anti-apoptotic proteins which sequester the pro-activator molecules, and can be overcome by adding sensitizer BH3 peptides. Because of the specificity of BH3 sensitizers to different anti-apoptotic Bcl-2 family members, BH3 profiling can reveal which inhibitor(s) are present (**Figure 2(b)**). For example, Bad binds Bcl-2 and Bcl-XL (but not Mcl-1), whereas Noxa binds Mcl-1 and A1 (but not Bcl-2 or Bcl-XL). Thus mitochondria with a 'Class C' block are described as being 'primed' for death as an increase in the concentration of the relevant BH3 protein (or its mimetic as described in the next section) should elicit cell death in that tumor.

Bcl-2 Family Proteins as Therapeutic Targets

Targeting cell death with agents that affect Bcl-2 family proteins represents a new way to selectively target cancer cells that contrasts with the broad toxicity of most standard anti-cancer drugs that are often selective only at concentrations that kill only dividing cells. As a result there is an emerging strategy to restore apoptosis in cancers is by antagonizing the activity of anti-apoptotic proteins using small molecules. Although several putative anti-apoptotic protein inhibitors have been identified, not all these agents have shown specificity for Bcl-2 family proteins as their mechanism of action (Vogler *et al.*, 2009).

The best characterized and furthest developed series of truly selective molecules have been designed by Abbot Laboratories and provide an instructive lesson in Bcl-2 family protein physiology. ABT 737 is a mimetic of the BH3 region of Bad and as such is a potent inhibitor of Bcl-2, Bcl-XL and Bcl-w; the closely related but better absorbed ABT-263 has been taken forward into clinical trials (Tse *et al.*, 2008). As a single agent, the results in hematological malignancies were encouraging. However, a dose limiting decrease in platelet counts (thrombocytopenia) was observed that represents an 'on-target' effect, as inhibition of Bcl-XL is known to predictably decrease platelet life-span (Vogler *et al.*, 2011). As this effect is limited to Bcl-XL among the anti-apoptotic proteins, a new compound, ABT-199 was designed which binds to Bcl-2 but not to Bcl-XL or Bcl-w (Souers *et al.*, 2013). While ABT-199 works extremely efficiently for some hematological malignancies, presumably there will be some tumors that are resistant because they are addicted to Bcl-XL rather than Bcl-2. Furthermore, solid tumors are also more resistant, and this phenomenon may be attributed to resistance conferred by Mcl-1 which is not affected by ABT-199 (or ABT-263), and thus represents another important target (van Delft *et al.*, 2006; Varin *et al.*, 2010). An important unanswered question for all approaches that inhibit anti-apoptotic Bcl-2 family proteins is whether specificity for cytotoxicity against cancer cells will be retained when these agents are combined with other cancer therapies.

While restoring apoptosis in addicted cancers by antagonizing the activity of the anti-apoptotic proteins using small molecules is promising and in clinical development, the pharmacologic modulation of pro-apoptotic Bax and Bak activity is another promising approach that is being explored. The small molecules BAM7, SMBA1 and compound 106, have been identified as potential candidates with differing putative mechanisms of action. While BAM7 activates Bax by binding the rear pocket similar to the Bim peptide, compound 106 is predicted to bind to the front pocket (Gavathiotis *et al.*, 2012; Zhao *et al.*, 2014). In contrast, SMBA1 is proposed to block the phosphorylation of Bax at serine 184. This phosphorylation is a negative regulator of Bax function, and preventing it should de-repress Bax (Xin *et al.*, 2014).

Summary

The Bcl-2 family proteins are critical regulators of cell death at the mitochondria and the ER. Bcl-2 family proteins regulate this process by a series of protein–protein and protein–membrane interactions that are associated with complex conformational changes in the proteins that ultimately control

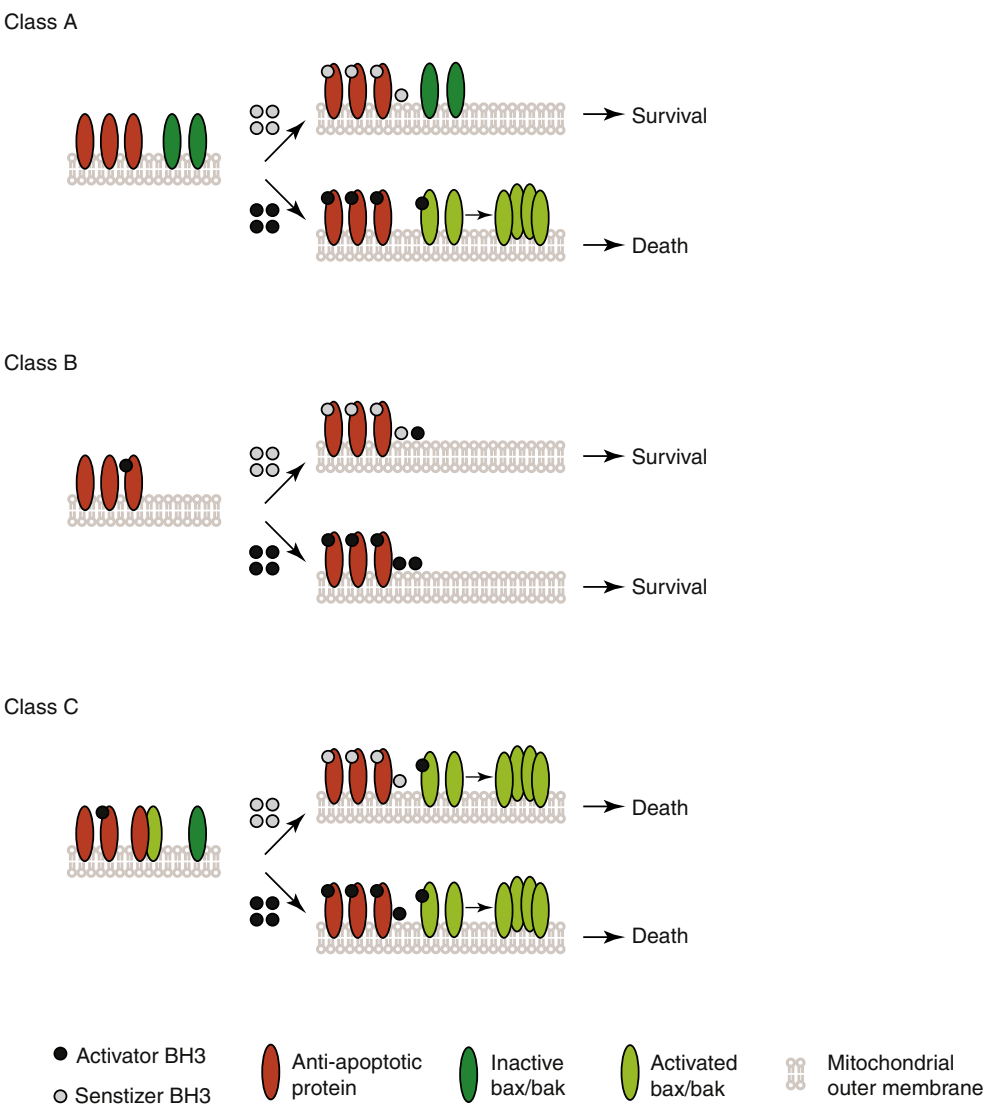

Figure 4 BH3 profiling to identify blocks in apoptosis. In BH3 profiling, mitochondria are incubated with BH3 peptides as representatives of their cognate proteins to examine the pattern of apoptosis response as measured by MOMP *in vitro*. In the 'Class A' block, Bax and Bak are inactive and functional BH3 proteins are low or missing and hence MOMP occurs only in response to added activators but not sensitizers. In the 'Class B' block, Bax and/or Bak are absent or nonfunctional. Thus, the mitochondria do not respond to the addition of any BH3 peptide. In the 'Class C' block, mitochondria are sequestering activator BH3 proteins or activated Bax or Bak. In this scenario, sensitizer peptides induce MOMP based on their specific binding affinities to different anti-apoptotic members. These cancers are said to be 'primed' and are candidates for therapies based on inhibitors the anti-apoptotic proteins.

the formation of pores in organelle membranes. Although most, if not all, of the players have been identified, rigorous quantitative modeling of these interactions is still in its infancy and promises great insights in the future (Gaudet *et al.*, 2012). From a therapeutic point of view the concept that 'addiction' to anti-apoptotic Bcl-2 members is relevant for cancer maintenance has led to the development of small molecule Bcl-2 inhibitors designed based on structural and functional insights derived from two decades of research. From this perspective, it will be exciting to investigate small molecules that target other interactions among Bcl-2 family members, and to see how such agents fit into treatment as monotherapy or combined with other drugs.

See also: Cell Division/Death: Apoptosis: Apoptosis; Caspases

References

Annis, M.G., Soucie, E.L., Dlugosz, P.J., *et al.*, 2005. Bax forms multispanning monomers that oligomerize to permeabilize membranes during apoptosis. EMBO Journal 24, 2096–2103.

Aouacheria, A., Brunet, F., Gouy, M., 2005. Phylogenomics of life-or-death switches in multicellular animals: Bcl-2, BH3-Only, and BNip families of apoptotic regulators. Molecular Biology and Evolution 22, 2395–2416.

Axe, E.L., Walker, S.A., Manifava, M., *et al.*, 2008. Autophagosome formation from membrane compartments enriched in phosphatidylinositol 3-phosphate and dynamically connected to the endoplasmic reticulum. Journal of Cell Biology 182, 685–701.

Beroukhim, R., Mermel, C.H., Porter, D., *et al.*, 2010. The landscape of somatic copy-number alteration across human cancers. Nature 463, 899–905.

Bhatt, K., Feng, L., Pabla, N., *et al.*, 2008. Effects of targeted Bcl-2 expression in mitochondria or endoplasmic reticulum on renal tubular cell apoptosis. American Journal of Physiology. Renal Physiology 294, F499–F507.

Billen, L.P., Kokoski, C.L., Lovell, J.F., Leber, B., Andrews, D.W., 2008a. Bcl-XL inhibits membrane permeabilization by competing with Bax. PLoS Biology 6, e147.

Billen, L.P., Shamas-Din, A., Andrews, D.W., 2008b. Bid: A Bax-like BH3 protein. Oncogene 27 (Suppl. 1), S93–104.

Boise, L.H., Gonzalez-Garcia, M., Postema, C.E., *et al.*, 1993. bcl-x, a bcl-2-related gene that functions as a dominant regulator of apoptotic cell death. Cell 74, 597–608.

Bouillet, P., Metcalf, D., Huang, D.C., *et al.*, 1999. Proapoptotic Bcl-2 relative Bim required for certain apoptotic responses, leukocyte homeostasis, and to preclude autoimmunity. Science 286, 1735–1738.

Breckenridge, D.G., Stojanovic, M., Marcellus, R.C., Shore, G.C., 2003. Caspase cleavage product of BAP31 induces mitochondrial fission through endoplasmic reticulum calcium signals, enhancing cytochrome c release to the cytosol. Journal of Cell Biology 160, 1115–1127.

Brouwer, J.M., Westphal, D., Dewson, G., *et al.*, 2014. Bak core and latch domains separate during activation, and freed core domains form symmetric homodimers. Molecular Cell 55, 938–946.

Certo, M., Del Gaizo Moore, V., Nishino, M., *et al.*, 2006. Mitochondria primed by death signals determine cellular addiction to antiapoptotic BCL-2 family members. Cancer Cell 9, 351–365.

Chami, M., Prandini, A., Campanella, M., *et al.*, 2004. Bcl-2 and Bax exert opposing effects on Ca2 + signaling, which do not depend on their putative pore-forming region. Journal of Biological Chemistry 279, 54581–54589.

Chang, N.C., Nguyen, M., Germain, M., Shore, G.C., 2010. Antagonism of Beclin 1-dependent autophagy by BCL-2 at the endoplasmic reticulum requires NAF-1. EMBO Journal 29, 606–618.

Chen, L., Willis, S.N., Wei, A., *et al.*, 2005. Differential targeting of prosurvival Bcl-2 proteins by their BH3-only ligands allows complementary apoptotic function. Molecular Cell 17, 393–403.

Cheng, E.H., Sheiko, T.V., Fisher, J.K., Craigen, W.J., Korsmeyer, S.J., 2003. VDAC2 inhibits BAK activation and mitochondrial apoptosis. Science 301, 513–517.

Chipuk, J.E., Bouchier-Hayes, L., Green, D.R., 2006. Mitochondrial outer membrane permeabilization during apoptosis: The innocent bystander scenario. Cell Death & Differentiation 13, 1396–1402.

Cimmino, A., Calin, G.A., Fabbri, M., *et al.*, 2005. miR-15 and miR-16 induce apoptosis by targeting BCL2. Proceedings of the National Academy of Sciences of the United States of America 102, 13944–13949.

Coultas, L., Bouillet, P., Loveland, K.L., *et al.*, 2005. Concomitant loss of proapoptotic BH3-only Bcl-2 antagonists Bik and Bim arrests spermatogenesis. EMBO Journal 24, 3963–3973.

Coultas, L., Terzano, S., Thomas, T., *et al.*, 2007. Hrk/DP5 contributes to the apoptosis of select neuronal populations but is dispensable for haematopoietic cell apoptosis. Journal of Cell Science 120, 2044–2052.

Czabotar, P.E., Westphal, D., Dewson, G., *et al.*, 2013. Bax crystal structures reveal how BH3 domains activate Bax and nucleate its oligomerization to induce apoptosis. Cell 152, 519–531.

van Delft, M.F., Wei, A.H., Mason, K.D., *et al.*, 2006. The BH3 mimetic ABT-737 targets selective Bcl-2 proteins and efficiently induces apoptosis via Bak/Bax if Mcl-1 is neutralized. Cancer Cell 10, 389–399.

Degenhardt, K., Sundararajan, R., Lindsten, T., Thompson, C., White, E., 2002. Bax and Bak independently promote cytochrome C release from mitochondria. Journal of Biological Chemistry 277, 14127–14134.

Del Gaizo Moore, V., Brown, J.R., Certo, M., *et al.*, 2007. Chronic lymphocytic leukemia requires BCL2 to sequester prodeath BIM, explaining sensitivity to BCL2 antagonist ABT-737. Journal of Clinical Investigation 117, 112–121.

Del Gaizo Moore, V., Letai, A., 2013. BH3 profiling – Measuring integrated function of the mitochondrial apoptotic pathway to predict cell fate decisions. Cancer Letters 332, 202–205.

Denisov, A.Y., Madiraju, M.S., Chen, G., *et al.*, 2003. Solution structure of human BCL-w: Modulation of ligand binding by the C-terminal helix. Journal of Biological Chemistry 278, 21124–21128.

Dewson, G., Kratina, T., Sim, H.W., *et al.*, 2008. To trigger apoptosis, Bak exposes its BH3 domain and homodimerizes via BH3:groove interactions. Molecular Cell 30, 369–380.

Edlich, F., Banerjee, S., Suzuki, M., *et al.*, 2011. Bcl-x(L) retrotranslocates Bax from the mitochondria into the cytosol. Cell 145, 104–116.

Ferrer, P.E., Frederick, P., Gulbis, J.M., Dewson, G., Kluck, R.M., 2012. Translocation of a Bak C-terminus mutant from cytosol to mitochondria to mediate cytochrome C release: Implications for Bak and Bax apoptotic function. PLoS One 7, e31510.

Fulda, S., Debatin, K.M., 2006. Extrinsic versus intrinsic apoptosis pathways in anticancer chemotherapy. Oncogene 25, 4798–4811.

Garrido, C., Galluzzi, L., Brunet, M., *et al.*, 2006. Mechanisms of cytochrome c release from mitochondria. Cell Death & Differentiation 13, 1423–1433.

Gaudet, S., Spencer, S.L., Chen, W.W., Sorger, P.K., 2012. Exploring the contextual sensitivity of factors that determine cell-to-cell variability in receptor-mediated apoptosis. PLoS Computational Biology 8, e1002482.

Gavathiotis, E., Reyna, D.E., Bellairs, J.A., Leshchiner, E.S., Walensky, L.D., 2012. Direct and selective small-molecule activation of proapoptotic BAX. Nature Chemical Biology 8, 639–645.

Gavathiotis, E., Suzuki, M., Davis, M.L., *et al.*, 2008. BAX activation is initiated at a novel interaction site. Nature 455, 1076–1081.

George, N.M., Evans, J.J., Luo, X., 2007. A three-helix homo-oligomerization domain containing BH3 and BH1 is responsible for the apoptotic activity of Bax. Genes & Development 21, 1937–1948.

Ghosh, A.P., Klocke, B.J., Ballestas, M.E., Roth, K.A., 2012. CHOP potentially co-operates with FOXO3a in neuronal cells to regulate PUMA and BIM expression in response to ER stress. PLoS One 7, e39586.

Green, D.R., Galluzzi, L., Kroemer, G., 2014. Cell biology. Metabolic control of cell death. Science 345, 1250256.

Griffiths, G.J., Dubrez, L., Morgan, C.P., *et al.*, 1999. Cell damage-induced conformational changes of the pro-apoptotic protein Bak *in vivo* precede the onset of apoptosis. Journal of Cell Biology 144, 903–914.

Grillot, D.A., Gonzalez-Garcia, M., Ekhterae, D., *et al.*, 1997. Genomic organization, promoter region analysis, and chromosome localization of the mouse bcl-x gene. Journal of Immunology 158, 4750–4757.

Hamasaki, A., Sendo, F., Nakayama, K., *et al.*, 1998. Accelerated neutrophil apoptosis in mice lacking A1-a, a subtype of the bcl-2-related A1 gene. Journal of Experimental Medicine 188, 1985–1992.

Hanahan, D., Weinberg, R.A., 2000. The hallmarks of cancer. Cell 100, 57–70.

Heath-Engel, H.M., Chang, N.C., Shore, G.C., 2008. The endoplasmic reticulum in apoptosis and autophagy: Role of the BCL-2 protein family. Oncogene 27, 6419–6433.

Hetz, C., Bernasconi, P., Fisher, J., *et al.*, 2006. Proapoptotic BAX and BAK modulate the unfolded protein response by a direct interaction with IRE1alpha. Science 312, 572–576.

Hinds, M.G., Smits, C., Fredericks-Short, R., *et al.*, 2007. Bim, Bad and Bmf: intrinsically unstructured BH3-only proteins that undergo a localized conformational change upon binding to prosurvival Bcl-2 targets. Cell Death & Differentiation 14, 128–136.

Hockenbery, D., Nunez, G., Milliman, C., Schreiber, R.D., Korsmeyer, S.J., 1990. Bcl-2 is an inner mitochondrial membrane protein that blocks programmed cell death. Nature 348, 334–336.

Hsu, Y.T., Youle, R.J., 1997. Nonionic detergents induce dimerization among members of the Bcl-2 family. Journal of Biological Chemistry 272, 13829–13834.

Ikegaki, N., Katsumata, M., Minna, J., Tsujimoto, Y., 1994. Expression of bcl-2 in small cell lung carcinoma cells. Cancer Research 54, 6–8.

Imaizumi, K., Benito, A., Kiryu-Seo, S., *et al.*, 2004. Critical role for DP5/Harakiri, a Bcl-2 homology domain 3-only Bcl-2 family member, in axotomy-induced neuronal cell death. Journal of Neuroscience 24, 3721–3725.

Jeffers, J.R., Parganas, E., Lee, Y., *et al.*, 2003. Puma is an essential mediator of p53-dependent and -independent apoptotic pathways. Cancer Cell 4, 321–328.

Kerr, J.F., Wyllie, A.H., Currie, A.R., 1972. Apoptosis: A basic biological phenomenon with wide-ranging implications in tissue kinetics. British Journal of Cancer 26, 239–257.

Kim, H., Tu, H.C., Ren, D., *et al.*, 2009. Stepwise activation of BAX and BAK by tBID, BIM, and PUMA initiates mitochondrial apoptosis. Molecular Cell 36, 487–499.

Knudson, C.M., Tung, K.S., Tourtellotte, W.G., Brown, G.A., Korsmeyer, S.J., 1995. Bax-deficient mice with lymphoid hyperplasia and male germ cell death. Science 270, 96–99.

Kutuk, O., Letai, A., 2008. Regulation of Bcl-2 family proteins by posttranslational modifications. Current Molecular Medicine 8, 102–118.

Kuwana, T., Bouchier-Hayes, L., Chipuk, J.E., *et al.*, 2005. BH3 domains of BH3-only proteins differentially regulate Bax-mediated mitochondrial membrane permeabilization both directly and indirectly. Molecular Cell 17, 525–535.
Kvansakul, M., Yang, H., Fairlie, W.D., *et al.*, 2008. Vaccinia virus anti-apoptotic F1L is a novel Bcl-2-like domain-swapped dimer that binds a highly selective subset of BH3-containing death ligands. Cell Death & Differentiation 15, 1564–1571.
Labi, V., Erlacher, M., Kiessling, S., *et al.*, 2008. Loss of the BH3-only protein Bmf impairs B cell homeostasis and accelerates gamma irradiation-induced thymic lymphoma development. Journal of Experimental Medicine 205, 641–655.
Leber, B., Lin, J., Andrews, D.W., 2007. Embedded together: The life and death consequences of interaction of the Bcl-2 family with membranes. Apoptosis 12, 897–911.
Leber, B., Lin, J., Andrews, D.W., 2010. Still embedded together binding to membranes regulates Bcl-2 protein interactions. Oncogene 29, 5221–5230.
Lee, J.W., Soung, Y.H., Kim, S.Y., *et al.*, 2004. Inactivating mutations of proapoptotic Bad gene in human colon cancers. Carcinogenesis 25, 1371–1376.
Leshchiner, E.S., Braun, C.R., Bird, G.H., Walensky, L.D., 2013. Direct activation of full-length proapoptotic BAK. Proceedings of the National Academy of Sciences of the United States of America 110, E986–E995.
Letai, A., Bassik, M.C., Walensky, L.D., *et al.*, 2002. Distinct BH3 domains either sensitize or activate mitochondrial apoptosis, serving as prototype cancer therapeutics. Cancer Cell 2, 183–192.
Levine, B., Kroemer, G., 2008. Autophagy in the pathogenesis of disease. Cell 132, 27–42.
Lindsten, T., Ross, A.J., King, A., *et al.*, 2000. The combined functions of proapoptotic Bcl-2 family members bak and bax are essential for normal development of multiple tissues. Molecular Cell 6, 1389–1399.
Liu, X., Dai, S., Zhu, Y., Marrack, P., Kappler, J.W., 2003. The structure of a Bcl-xL/Bim fragment complex: Implications for Bim function. Immunity 19, 341–352.
Llambi, F., Moldoveanu, T., Tait, S.W., *et al.*, 2011. A unified model of mammalian BCL-2 protein family interactions at the mitochondria. Molecular Cell 44, 517–531.
Lovell, J.F., Billen, L.P., Bindner, S., *et al.*, 2008. Membrane binding by tBid initiates an ordered series of events culminating in membrane permeabilization by Bax. Cell 135, 1074–1084.
Maiuri, M.C., Le Toumelin, G., Criollo, A., *et al.*, 2007. Functional and physical interaction between Bcl-X(L) and a BH3-like domain in Beclin-1. EMBO Journal 26, 2527–2539.
Mathai, J.P., Germain, M., Shore, G.C., 2005. BH3-only BIK regulates BAX,BAK-dependent release of Ca2+ from endoplasmic reticulum stores and mitochondrial apoptosis during stress-induced cell death. Journal of Biological Chemistry 280, 23829–23836.
Meier, P., Finch, A., Evan, G., 2000. Apoptosis in development. Nature 407, 796–801.
Miyashita, T., Krajewski, S., Krajewska, M., *et al.*, 1994. Tumor suppressor p53 is a regulator of bcl-2 and bax gene expression *in vitro* and *in vivo*. Oncogene 9, 1799–1805.
Moldoveanu, T., Liu, Q., Tocilj, A., *et al.*, 2006. The X-ray structure of a BAK homodimer reveals an inhibitory zinc binding site. Molecular Cell 24, 677–688.
Motoyama, N., Wang, F., Roth, K.A., *et al.*, 1995. Massive cell death of immature hematopoietic cells and neurons in Bcl-x-deficient mice. Science 267, 1506–1510.
Mukhopadhyay, S., Panda, P.K., Sinha, N., Das, D.N., Bhutia, S.K., 2014. Autophagy and apoptosis: where do they meet? Apoptosis 19, 555–566.
Nakano, K., Vousden, K.H., 2001. PUMA, a novel proapoptotic gene, is induced by p53. Molecular Cell 7, 683–694.
Ng, F.W., Nguyen, M., Kwan, T., *et al.*, 1997. p28 Bap31, a Bcl-2/Bcl-XL- and procaspase-8-associated protein in the endoplasmic reticulum. Journal of Cell Biology 139, 327–338.
Nutt, L.K., Pataer, A., Pahler, J., *et al.*, 2002. Bax and Bak promote apoptosis by modulating endoplasmic reticular and mitochondrial Ca2+ stores. Journal of Biological Chemistry 277, 9219–9225.
O'Connor, L., Strasser, A., O'Reilly, L.A., *et al.*, 1998. Bim: a novel member of the Bcl-2 family that promotes apoptosis. EMBO Journal 17, 384–395.
Oakes, S.A., Lin, S.S., Bassik, M.C., 2006. The control of endoplasmic reticulum-initiated apoptosis by the BCL-2 family of proteins. Current Molecular Medicine 6, 99–109.
Oda, E., Ohki, R., Murasawa, H., *et al.*, 2000. Noxa, a BH3-only member of the Bcl-2 family and candidate mediator of p53-induced apoptosis. Science 288, 1053–1058.
Pattingre, S., Tassa, A., Qu, X., *et al.*, 2005. Bcl-2 antiapoptotic proteins inhibit Beclin 1-dependent autophagy. Cell 122, 927–939.
Petros, A.M., Nettesheim, D.G., Wang, Y., *et al.*, 2000. Rationale for Bcl-xL/Bad peptide complex formation from structure, mutagenesis, and biophysical studies. Protein Science 9, 2528–2534.
Petros, A.M., Olejniczak, E.T., Fesik, S.W., 2004. Structural biology of the Bcl-2 family of proteins. Biochimica et Biophysica Acta 1644, 83–94.
Peyerl, F.W., Dai, S., Murphy, G.A., *et al.*, 2007. Elucidation of some Bax conformational changes through crystallization of an antibody-peptide complex. Cell Death & Differentiation 14, 447–452.
Print, C.G., Loveland, K.L., Gibson, L., *et al.*, 1998. Apoptosis regulator bcl-w is essential for spermatogenesis but appears otherwise redundant. Proceedings of the National Academy of Sciences of the United States of America 95, 12424–12431.
Puthalakath, H., O'Reilly, L.A., Gunn, P., *et al.*, 2007. ER stress triggers apoptosis by activating BH3-only protein Bim. Cell 129, 1337–1349.
Rampino, N., Yamamoto, H., Ionov, Y., *et al.*, 1997. Somatic frameshift mutations in the BAX gene in colon cancers of the microsatellite mutator phenotype. Science 275, 967–969.
Ranger, A.M., Zha, J., Harada, H., *et al.*, 2003. Bad-deficient mice develop diffuse large B cell lymphoma. Proceedings of the National Academy of Sciences of the United States of America 100, 9324–9329.
Rinkenberger, J.L., Horning, S., Klocke, B., Roth, K., Korsmeyer, S.J., 2000. Mcl-1 deficiency results in peri-implantation embryonic lethality. Genes & Development 14, 23–27.
Rong, Y., Distelhorst, C.W., 2008. Bcl-2 protein family members: versatile regulators of calcium signaling in cell survival and apoptosis. Annual Review of Physiology 70, 73–91.
Rong, Y.P., Aromolaran, A.S., Bultynck, G., *et al.*, 2008. Targeting Bcl-2-IP3 receptor interaction to reverse Bcl-2's inhibition of apoptotic calcium signals. Molecular Cell 31, 255–265.
Rong, Y.P., Bultynck, G., Aromolaran, A.S., *et al.*, 2009. The BH4 domain of Bcl-2 inhibits ER calcium release and apoptosis by binding the regulatory and coupling domain of the IP3 receptor. Proceedings of the National Academy of Sciences of the United States of America 106, 14397–14402.
Sato, T., Irie, S., Krajewski, S., Reed, J.C., 1994. Cloning and sequencing of a cDNA encoding the rat Bcl-2 protein. Gene 140, 291–292.
Sattler, M., Liang, H., Nettesheim, D., *et al.*, 1997. Structure of Bcl-xL-Bak peptide complex: recognition between regulators of apoptosis. Science 275, 983–986.
Schinzel, A., Kaufmann, T., Schuler, M., *et al.*, 2004. Conformational control of Bax localization and apoptotic activity by Pro168. Journal of Cell Biology 164, 1021–1032.
Scorrano, L., Oakes, S.A., Opferman, J.T., *et al.*, 2003. BAX and BAK regulation of endoplasmic reticulum Ca2+: A control point for apoptosis. Science 300, 135–139.
Shamas-Din, A., Bindner, S., Zhu, W., *et al.*, 2013a. tBid undergoes multiple conformational changes at the membrane required for Bax activation. Journal of Biological Chemistry 288, 22111–22127.
Shamas-Din, A., Kale, J., Leber, B., Andrews, D.W., 2013b. Mechanisms of action of Bcl-2 family proteins. Cold Spring Harbor Perspectives in Biology 5, a008714.
Shibue, T., Takeda, K., Oda, E., *et al.*, 2003. Integral role of Noxa in p53-mediated apoptotic response. Genes & Development 17, 2233–2238.
Silva, M., Benito, A., Sanz, C., *et al.*, 1999. Erythropoietin can induce the expression of bcl-x(L) through Stat5 in erythropoietin-dependent progenitor cell lines. Journal of Biological Chemistry 274, 22165–22169.
Souers, A.J., Leverson, J.D., Boghaert, E.R., *et al.*, 2013. ABT-199, a potent and selective BCL-2 inhibitor, achieves antitumor activity while sparing platelets. Nature Medicine 19, 202–208.
Suzuki, M., Youle, R.J., Tjandra, N., 2000. Structure of Bax: Coregulation of dimer formation and intracellular localization. Cell 103, 645–654.
Todt, F., Cakir, Z., Reichenbach, F., Youle, R.J., Edlich, F., 2013. The C-terminal helix of Bcl-x(L) mediates Bax retrotranslocation from the mitochondria. Cell Death & Differentiation 20, 333–342.
Tse, C., Shoemaker, A.R., Adickes, J., *et al.*, 2008. ABT-263: a potent and orally bioavailable Bcl-2 family inhibitor. Cancer Research 68, 3421–3428.
Tsujimoto, Y., Cossman, J., Jaffe, E., Croce, C.M., 1985. Involvement of the bcl-2 gene in human follicular lymphoma. Science 228, 1440–1443.
Varin, E., Denoyelle, C., Brotin, E., *et al.*, 2010. Downregulation of Bcl-xL and Mcl-1 is sufficient to induce cell death in mesothelioma cells highly refractory to conventional chemotherapy. Carcinogenesis 31, 984–993.
Vaux, D.L., Cory, S., Adams, J.M., 1988. Bcl-2 gene promotes haemopoietic cell survival and cooperates with c-myc to immortalize pre-B cells. Nature 335, 440–442.

Veis, D.J., Sorenson, C.M., Shutter, J.R., Korsmeyer, S.J., 1993. Bcl-2-deficient mice demonstrate fulminant lymphoid apoptosis, polycystic kidneys, and hypopigmented hair. Cell 75, 229–240.
Villunger, A., Michalak, E.M., Coultas, L., *et al.*, 2003. p53- and drug-induced apoptotic responses mediated by BH3-only proteins puma and noxa. Science 302, 1036–1038.
Vogler, M., Dinsdale, D., Dyer, M.J., Cohen, G.M., 2009. Bcl-2 inhibitors: small molecules with a big impact on cancer therapy. Cell Death & Differentiation 16, 360–367.
Vogler, M., Hamali, H.A., Sun, X.M., *et al.*, 2011. BCL2/BCL-X(L) inhibition induces apoptosis, disrupts cellular calcium homeostasis, and prevents platelet activation. Blood 117, 7145–7154.
Westphal, D., Kluck, R.M., Dewson, G., 2014. Building blocks of the apoptotic pore: How Bax and Bak are activated and oligomerize during apoptosis. Cell Death & Differentiation 21, 196–205.
Willis, S.N., Chen, L., Dewson, G., *et al.*, 2005. Proapoptotic Bak is sequestered by Mcl-1 and Bcl-xL, but not Bcl-2, until displaced by BH3-only proteins. Genes & Development 19, 1294–1305.
Willis, S.N., Fletcher, J.I., Kaufmann, T., *et al.*, 2007. Apoptosis initiated when BH3 ligands engage multiple Bcl-2 homologs, not Bax or Bak. Science 315, 856–859.
Wolter, K.G., Hsu, Y.T., Smith, C.L., *et al.*, 1997. Movement of Bax from the cytosol to mitochondria during apoptosis. Journal of Cell Biology 139, 1281–1292.
Xin, M., Li, R., Xie, M., *et al.*, 2014. Small-molecule Bax agonists for cancer therapy. Nature Communications 5, 4935.
Yamamoto, H., Sawai, H., Perucho, M., 1997. Frameshift somatic mutations in gastrointestinal cancer of the microsatellite mutator phenotype. Cancer Research 57, 4420–4426.
Yethon, J.A., Epand, R.F., Leber, B., Epand, R.M., Andrews, D.W., 2003. Interaction with a membrane surface triggers a reversible conformational change in Bax normally associated with induction of apoptosis. Journal of Biological Chemistry 278, 48935–48941.
Yin, X.M., Wang, K., Gross, A., *et al.*, 1999. Bid-deficient mice are resistant to Fas-induced hepatocellular apoptosis. Nature 400, 886–891.
Yue, Z., Jin, S., Yang, C., Levine, A.J., Heintz, N., 2003. Beclin 1, an autophagy gene essential for early embryonic development, is a haploinsufficient tumor suppressor. Proceedings of the National Academy of Sciences of the United States of America 100, 15077–15082.
Zha, J., Harada, H., Yang, E., Jockel, J., Korsmeyer, S.J., 1996. Serine phosphorylation of death agonist BAD in response to survival factor results in binding to 14-3-3 not BCL-X(L). Cell 87, 619–628.
Zhao, G., Zhu, Y., Eno, C.O., *et al.*, 2014. Activation of the proapoptotic Bcl-2 protein Bax by a small molecule induces tumor cell apoptosis. Molecular and Cellular Biology 34, 1198–1207.
Zhu, W., Cowie, A., Wasfy, G.W., *et al.*, 1996. Bcl-2 mutants with restricted subcellular location reveal spatially distinct pathways for apoptosis in different cell types. EMBO Journal 15, 4130–4141.
Zong, W.X., Li, C., Hatzivassiliou, G., *et al.*, 2003. Bax and Bak can localize to the endoplasmic reticulum to initiate apoptosis. Journal of Cell Biology 162, 59–69.

Further Reading

Chi, X., Kale, J., Leber, B., Andrews, D.W., 2014. Regulating cell death at, on, and in membranes. Biochimica et Biophysica Acta 1843, 2100–2113.
Czabotar, P.E., Lessene, G., Strasser, A., Adams, J.M., 2014. Control of apoptosis by the BCL-2 protein family: Implications for physiology and therapy. Nature Reviews Molecular Cell Biology 15, 49–63.
Galluzzi, L., Aaronson, S.A., Abrams, J., *et al.*, 2009. Guidelines for the use and interpretation of assays for monitoring cell death in higher eukaryotes. Cell Death & Differentiation 16, 1093–1107.
Kale, J., Liu, Q., Leber, B., Andrews, D.W., 2012. Shedding light on apoptosis at subcellular membranes. Cell 151, 1179–1184.
Kroemer, G., Marino, G., Levine, B., 2010. Autophagy and the integrated stress response. Molecular Cell 40, 280–293.
Tait, S.W., green, D.R., 2012. Mitochondria and cell signalling. Journal of Cell Science 125, 807–815.

Relevant Websites

http://www.cellsignal.com/common/content/content.jspid=science-pathways-apoptosis
Cell Signalling. 'Apoptosis resources'.
http://www.biooncology.com/research-education/apoptosis/apoptosis
Genetech Biooncology. 'Apoptosis: A Critical Process in Homeostasis'.
http://www.rndsystems.com/molecule_group.aspxg=464
R&D systems. 'Bcl-2 Proteins and Regulators'.
http://www.nature.com/scitable/topicpage/the-discovery-of-lysosomes-and-autophagy-14199828
Susana Castro-Obregon. 'The Discovery of Lysosomes and Autophagy'.
http://www.asbmb.org/asbmbtoday/201408/JournalNews/JBC/UPR/
Teodora Donisan. 'Unfolded Protein response signaling and metabolic diseases'.

Preface

The work presented here has been previously published as a review in:

Brahmbhatt, H., Oppermann, S., Osterlund, E.J., Leber, B. & Andrews, D.W. Molecular Pathways: Leveraging the BCL-2 Interactome to Kill Cancer Cells--Mitochondrial Outer Membrane Permeabilization and Beyond. Clin Cancer Res 21, 2671-6 (2015).

Contribution of authors:

Brahmbhatt, H wrote the abstract, background, the section on 'The BCL-2 family interactome and cancer, the second paragraph in the section on 'The BCL-2–BAD interaction at mitochondria: a promising clinical target', the first four paragraphs in the section on 'Targeting other BCL-2 family interactions' and prepared Figure 1 and Table 1.

Oppermann, S wrote the first and third paragraph in the section on, 'The BCL-2–BAD interaction at mitochondria: a promising clinical target', the last paragraph in the section on 'Assessing apoptotic modulators in cells and tissues' and assisted in preparing Table 1.

Osterlund E wrote the last two paragraphs in the section on ‘Targeting other BCL-2 family interactions’, the first paragraph in the section on ‘Assessing apoptotic modulators in cells and tissues’ and prepared Figure 1.

Leber, B and Andrews, D.W edited and directed the book review.

Molecular Pathways: Leveraging the BCL-2 Interactome to Kill Cancer Cells—Mitochondrial Outer Membrane Permeabilization and Beyond

Published OnlineFirst April 2, 2015; DOI: 10.1158/1078-0432.CCR-14-0959

Molecular Pathways

Clinical Cancer Research

Molecular Pathways: Leveraging the BCL-2 Interactome to Kill Cancer Cells—Mitochondrial Outer Membrane Permeabilization and Beyond

Hetal Brahmbhatt[1,2], Sina Oppermann[2], Elizabeth J. Osterlund[2,3], Brian Leber[4], and David W. Andrews[1,2,3]

Abstract

The inhibition of apoptosis enables the survival and proliferation of tumors and contributes to resistance to conventional chemotherapy agents and is therefore a very promising avenue for the development of new agents that will enhance current cancer therapies. The BCL-2 family proteins orchestrate apoptosis at the mitochondria and endoplasmic reticulum and are involved in other processes such as autophagy and unfolded protein response (UPR) that lead to different types of cell death. Over the past decade, significant efforts have been made to restore apoptosis using small molecules that modulate the activity of BCL-2 family proteins. The small molecule ABT-199, which antagonizes the activity of BCL-2, is currently the furthest in clinical trials and shows promising activity in many lymphoid malignancies as a single agent and in combination with conventional chemotherapy agents. Here, we discuss strategies to improve the specificity of pharmacologically modulating various antiapoptotic BCL-2 family proteins, review additional BCL-2 family protein interactions that can be exploited for the improvement of conventional anticancer therapies, and highlight important points of consideration for assessing the activity of small-molecule BCL-2 family protein modulators. *Clin Cancer Res; 21(12); 2671–6. ©2015 AACR.*

Background

Tumorigenesis is a complex multistep process that occurs when normal cells acquire genetic or epigenetic alterations that cause dysregulated cell proliferation. Preventing apoptosis is an essential component of this process, as programmed cell death is frequently activated in response to such transformations (1). The effect of most cytotoxic chemotherapy agents that impair DNA synthesis or mitosis is to restore apoptosis. However, this strategy is often ineffective, as many tumors have acquired aberrant apoptotic signaling either during initiation or clonal progression (2). Using drugs that specifically target key components of these blocked apoptotic pathways may kill tumor cells while minimizing the severe side effects on normal cells, and therefore represents a promising strategy to improve the efficacy and specificity of anticancer therapies.

Apoptosis can be initiated via two pathways, the extrinsic and the intrinsic pathway. Whereas the extrinsic pathway is initiated through stimulation of cell surface death receptors, the intrinsic pathway is activated by many different intracellular stresses and is elicited by most chemotherapy agents. The BCL-2 family proteins are predominantly involved in the intrinsic pathway, in which they regulate mitochondrial outer membrane permeabilization (MOMP). MOMP results in the release of apoptosis-triggering factors, such as cytochrome c, from the mitochondrial intermembrane space into the cytoplasm in which they activate a cascade of caspases that execute widespread proteolytic events leading to cellular demise (3). MOMP marks commitment to death and is often considered to be the point of no return for a cell. Here, we review the rationale and preliminary results of recent efforts to elicit MOMP by exploiting BCL-2 family proteins as an anticancer therapy and discuss other related targets for drug development.

The BCL-2 family interactome and cancer

Over 25 BCL-2 family proteins have been identified and are classified into three groups based on function and the presence of conserved BCL-2 homology (BH) regions: (i) proapoptotic multiregion BAX and BAK oligomerize to form pores that permeabilize the mitochondrial outer membrane (MOM); (ii) proapoptotic BH3 proteins such as BID, BIM, BAD, NOXA, and PUMA are activated by various stress stimuli and directly (activator BH3) or indirectly (sensitizer BH3) activate BAX and BAK; and (iii) antiapoptotic multiregion proteins such as BCL-2, BCL-XL, and MCL-1 inhibit both classes of proapoptotic proteins. The BCL-2 family proteins are predominantly localized to the mitochondria, endoplasmic reticulum (ER) and perinuclear membrane.

The membrane is the locus of interaction and an active regulator governing binding interactions between among BCL-2 family proteins (4). Upon binding to membranes, BCL-2 family proteins undergo conformational changes that affect subsequent binding interactions. The process is initiated when activator BH3 proteins are stimulated by cellular stress signals and rapidly

[1]Department of Biochemistry and Biomedical Sciences, McMaster University, Hamilton, Ontario, Canada. [2]Sunnybrook Research Institute, University of Toronto, Toronto, Ontario, Canada. [3]Department of Biochemistry, University of Toronto, Toronto, Ontario, Canada. [4]Department of Medicine, McMaster University, Hamilton, Ontario, Canada.

Corresponding Author: David W. Andrews, Sunnybrook Research Institute, 2075 Bayview Avenue, Toronto, ON M4N 3M5, Canada. Phone: 416-480-5120; Fax: 416-480-4375; E-mail: david.andrews@sri.utoronto.ca

doi: 10.1158/1078-0432.CCR-14-0959

Published OnlineFirst April 2, 2015; DOI: 10.1158/1078-0432.CCR-14-0959

translocate to the membranes where they interact with cytoplasmic BAX or membrane-bound BAK. As a result of this binding, BAX inserts into the membrane, and both BAX and BAK undergo a series of conformational changes that allow these proteins to oligomerize, thereby forming pores which cause MOMP (5, 6). Antiapoptotic proteins inhibit activator BH3 proteins as well as activated BAX/BAK at the membrane (7, 8). Inhibition of BH3 proteins when they are sequestered by antiapoptotic proteins is called Mode 1 inhibition, and inhibition of activated BAX/BAK by antiapoptotic proteins is designated as Mode 2 (9). Sensitizer proteins function to displace activator BH3 proteins or activated BAX/BAK from antiapoptotic proteins (Fig. 1).

On the basis of the specific requirements to induce MOMP, the blocks in apoptosis that confer tumor survival can be subdivided into three classes (10). Mitochondria with a class A block have insufficient activated BH3 proteins, or all available activator BH3 proteins are sequestered by the antiapoptotic members (Mode 1 inhibition), resulting in insufficient MOMP. Mitochondria with a class B block have inactive or low levels of BAX and BAK and remain insensitive to MOMP induction even in the presence of activator BH3 proteins. Because of repeat sequences, *BAX* is susceptible to inactivation by microsatellite insertions (11). Mitochondria with a class C block overexpress antiapoptotic BCL-2 family members that sequester and inhibit activator BH3 proteins and activated BAX and BAK (Mode 1 or Mode 2). Overexpression of BCL-2, BCL-XL, and MCL-1 is observed in many cancers and is associated with poor survival and resistance to therapy (12, 13).

Cancer cells with a class C block can be considered "addicted" to high levels of the antiapoptotic BCL-2 proteins for survival (14). Selective antagonism of these antiapoptotic proteins using BH3 mimetics should overcome this block with reduced toxicities to normal cells. Because antiapoptotic proteins have different affinities for BH3 proteins (e.g., BCL-2 and BCL-XL bind to BAD but not NOXA whereas MCL-1 binds to NOXA but not BAD), identifying which inhibitor is involved could theoretically lead to more selective therapy (14). Using peptides from

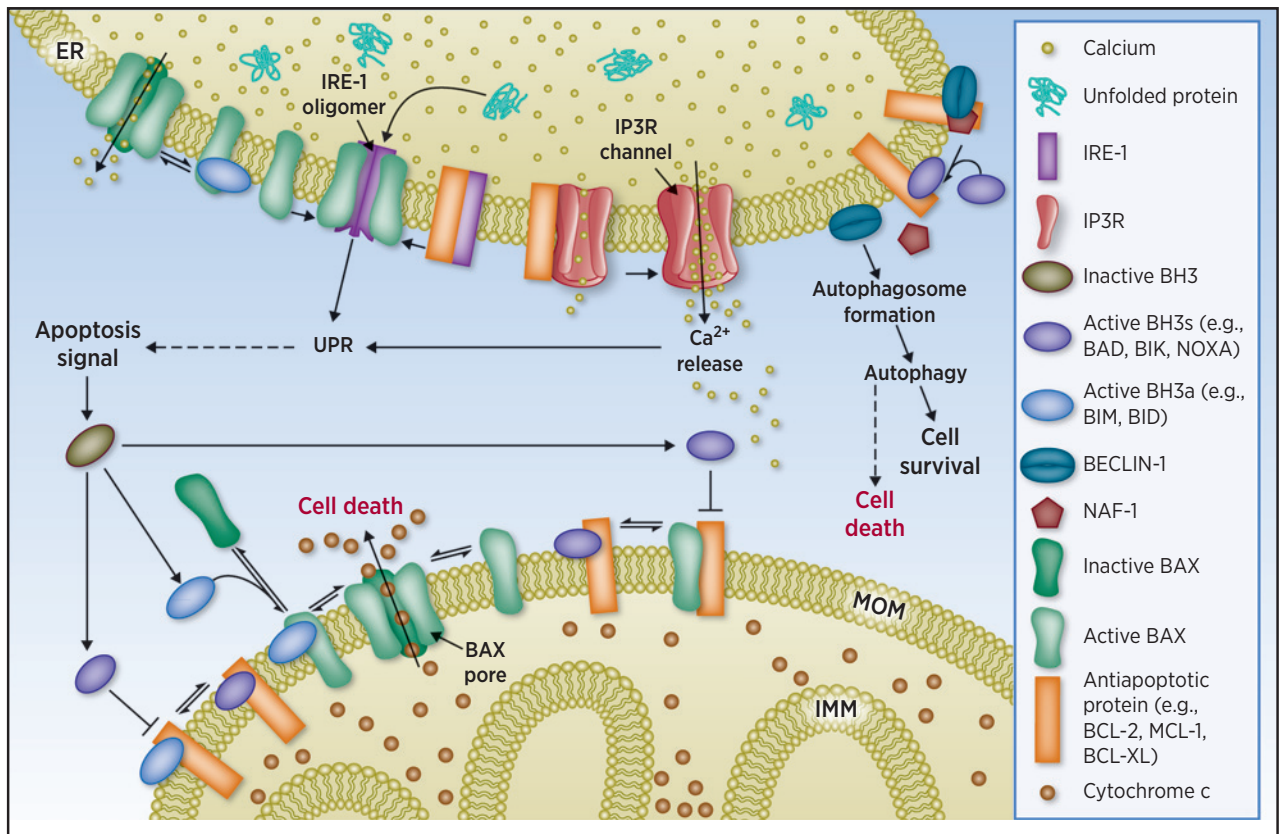

Figure 1.
Schematic of the BCL-2 family interactions at the mitochondria and ER. BCL-2 family proteins are involved in cellular processes such as apoptosis, autophagy, and the UPR, and localize at the mitochondria and ER. Various stress stimuli activate BH3 proteins. Activator BH3 proteins (BH3a) translocate to the membrane to activate BAX. BAX translocates and inserts into the MOM, where it oligomerizes to form pores releasing cytochrome c from the mitochondrial intermembrane space into the cytoplasm. Antiapoptotic proteins function by binding and sequestering activator BH3 proteins and activated BAX at the membrane. Sensitizer BH3 proteins (BH3s) displace activator BH3 proteins or activated BAX from antiapoptotic proteins. The interactions at the ER are not well studied and the model at the ER is more speculative. At the ER, the accumulation of unfolded proteins triggers the UPR, which is mediated by IRE-1. BAX interacts with IRE-1 to sustain IRE-1 activation. In addition, pore formation by BAX oligomerization at the ER results in the release of calcium. BCL-2 interacts with IP3R to inhibit the release of calcium and with BECLIN-1 preventing autophagosome assembly to inhibit autophagy; IMM, inner mitochondrial membrane.

Published OnlineFirst April 2, 2015; DOI: 10.1158/1078-0432.CCR-14-0959

specific BH3 proteins to elicit MOMP in clinical cancer samples *in vitro* is a powerful tool to tailor patient-specific treatment approaches (10).

Clinical–Translational Advances

The BCL-2–BAD interaction at mitochondria: a promising clinical target

There is a strong rationale to interfere with antiapoptotic BCL-2 family members to induce selective apoptosis in cancer cells. Downregulating the expression of the prosurvival BCL-2 family proteins is one approach. Indeed, as might be expected, conventional chemotherapy drugs often modulate the expression the BCL-2 family proteins as an indirect downstream consequence (Table 1). The first intentional approach used antisense oligonucleotide targeting of *BCL-2* mRNA. This agent, oblimersen sodium, showed moderate activity in phase III clinical trials for melanoma, chronic lymphocytic leukemia (CLL), and multiple myeloma but was not approved by the FDA when it failed to reach primary survival endpoints in a phase III melanoma trial (15). Because antisense oligonucleotide therapies are limited by poor drug delivery and pharmacokinetics, modulating the interaction of BCL-2 family proteins presents an attractive alternative approach when potentially targetable binding interfaces are known.

Thus, the cytoplasmic structures of the BCL-2 family complexed with BH3 peptides from BH3 proteins have guided the discovery of small molecules that disrupt heterodimeric interactions between antiapoptotic proteins and their binding partners. The small molecules compete with the BH3 region of BH3 proteins for binding to a hydrophobic groove formed by the BH1-3 regions of the multiregion antiapoptotic proteins (16). High-throughput screening techniques and structure-based design have resulted in identification of several small-molecule antiapoptotic protein inhibitors that have relevant clinical activity when used as single agents or in combination therapy (17). Agents such as obatoclax and gossypol (AT-101) have shown some activity in phase II clinical trials as single agents and in combination with chemotherapy (Table 1; ref. 18). Unfortunately, many of these compounds have off-target cytotoxicity causing cell death even in the absence of BAX and BAK that will likely severely impair cancer cell specificity (19).

Exceptions to this observation are the AbbVie compounds. The lead compound ABT-737 was designed using nuclear magnetic resonance structure-based screening to mimic the BH3 region of BAD that binds with high affinity to BCL-2, BCL-XL and BCL-W (but not to MCL-1) and induces significant cytotoxicity in experimental studies in cell lines derived from acute lymphoblastic leukemia and small cell lung cancer (SCLC; ref. 20). ABT-263 (navitoclax) was developed as an orally available derivative of ABT-737 that retains similar binding profiles and affinities. ABT-263 has demonstrated strong activity as a single agent and in combination with other chemotherapeutic drugs in many lymphoid malignancies such as CLL and has single-agent activity against SCLC solid tumor cell lines (21–23). However, a major barrier to further clinical development noted in phase I/II trials was dose-dependent thrombocytopenia due to on-target inhibition of BCL-XL in platelets (24). This problem was circumvented by the development of a related compound, ABT-199, that selectively targets BCL-2 not BCL-XL, and therefore does not cause thrombocytopenia (25). Although ABT-199 is active as a single agent in lymphoid malignanices such as CLL and non-Hodgkin lymphoma, tumors addicted to BCL-XL will presumably be resistant, and this remains an unmet medical need (26). Nevertheless, a strong measure of the efficacy of ABT-199 in lymphoid malignancies and the biologic importance of BCL-2 addiction was the

Table 1. Effect of anticancer therapies on BCL-2 family proteins

Type of anticancer therapy	Class of anticancer drug	Compound (e.g.)	Effect of compound on BCL-2 family proteins	References
Classical chemotherapy	Mitotic inhibitor	Docetaxel	Increase in BCL-2 phosphorylation; decrease in MCL-1, BCL-XL, and BIM protein levels	(47)
	Alkylating agent	Cisplatin	Activation of BAX and BAK; decrease in BCL-XL and increase in BAK and PUMA protein levels	(48, 49)
	Antimetabolites	Methotrexate	Decrease in *BCL-2* mRNA levels	(50)
	Topoisomerase II inhibitors	Etoposide	Increase in BAX/BCL-2 protein ratio	(51)
	Anthracycline	Doxorubicin	Decrease in BCL-2, BID and increase in BAD, BAX protein levels	(52)
	Intercalators	Mitomycin C	Decrease in BCL-2, BCL-XL, MCL-1 and increase in BIM and BAX protein levels	(53)
Targeted therapy	Monoclonal antibodies	Rituximab	Decrease in BCL-2, MCL-1 and increase in BAX levels	(54)
	Tyrosine kinase inhibitor	Sorefenib	Decrease in BCL-2, BCL-XL, and MCL-1 and increase in BAD protein levels	(55, 56)
	Proteasome inhibitor	Bortezomib	Decrease in BCL-2 and increase in BIK, NOXA, BIK, and MCL-1 protein levels	(57)
BCL-2 family modulators	Antisense deoxynucleotide	Oblimersen sodium	Decrease in cellular BCL-2 levels	(58)
	Small molecules	Obatoclax (GX15–070)	Pan–BCL-2 inhibitor; inhibition of BCL-2, BCL-XL, BCL-W	(59)
		AT101 (gossypol)	Pan–BCL-2 inhibitor; inhibition of BCL-2, BCL-XL, MCL-1	(59)
		ABT-737	Inhibition of BCL-2, BCL-XL, BCL-W	(20)
		ABT-263 (navitoclax)	Inhibition of BCL-2, BCL-XL, BCL-W	(60)
		ABT-199	Inhibition of BCL-2	(25)

Published OnlineFirst April 2, 2015; DOI: 10.1158/1078-0432.CCR-14-0959

occurrence of tumor lysis syndrome in initial phase I trials in CLL. A gradual dose-escalation schedule has been designed and tested to prevent this and forms the basis of the current registration trials.

Targeting other BCL-2 family interactions

In live breast cancer cells, ABT-263 and ABT-737 disrupt the BCL-XL/BCL-2 complexes with BID but not with BIM at the mitochondria. This suggests that the binding properties of BIM to BCL-XL/BCL-2 differ compared with other BH3 proteins. Determining whether this is an inherent property of BIM at mitochondria or mediated by another binding site may provide useful leads for drug discovery, especially as the BIM–BCL-XL interaction does not mediate platelet survival (27).

Another important target that is not affected by ABT 263 or 199 is the antiapoptotic protein MCL-1, and tumors with higher levels of MCL-1 and lower BIM–MCL-1 ratio are associated with chemoresistance to ABT-263 treatment (12, 28, 29). MCL-1 is structurally unique from its prosurvival counterparts making targeting with small molecules challenging; as a consequence current lead compounds for MCL-1 inhibitors have weak binding affinities and lack convincing *in vivo* activities (30). The BH3 region recognizes four hydrophobic residue binding sites, P1–4 in the hydrophobic-binding groove. In comparison with BCL-XL, the P2 pocket of MCL-1 is larger, deeper, and expands in the presence of hydrophobic ligands; the P4 pocket is also more solvent exposed (31). ABT-737 was discovered by linking two moieties that bind the P2 and P4 pocket (20). Thus, to target MCL-1, it may be advantageous to link hydrophobic moieties that bind to the P2 while avoiding the P4 pocket to retain specificity to MCL-1. Another unique feature of MCL-1 among the antiapoptotic proteins is its short half-life due to constitutive ubiquitin-mediated proteasomal degradation (32). This is therapeutically exploitable, as many current drugs such as seliciclib and sorafenib, indirectly downregulate MCL-1 levels and may be particularly useful in combination with BCL-2 family inhibitors (33, 34).

As an alternative to targeting the antiapoptotic BCL-2 family proteins, pharmacologic activation of BAX and BAK might also serve as a promising strategy to overcome a class C block in cancer cells. In this case, the search would be for activators of these pore-forming proteins. Aside from the hydrophobic groove that binds to the BH3 region of activator proteins, an alternative binding region termed the "rear" pocket has been identified in BAX as the interaction site for BIM–BAX (35). Furthermore, after activation both BAX and BAK must oligomerize to form pores. On the basis of these multiple steps in the mediation of MOMP, several small molecules have been identified as modulators of BAX activity, each acting by a different putative mechanism that may be suited to specific combination chemotherapy with BCL-2 family inhibitors (36, 37).

The regulation of MOMP has attracted the most interest as a point of no return in cell death. However, many BCL-2 family members are also localized to the ER, where several processes relevant for cell survival are regulated by these proteins (Fig. 1). There is growing evidence that increased autophagy and activation of the unfolded protein response (UPR) drive the survival of carcinomas, leukemias, lymphomas, and gliomas in the tumor microenvironment (38). Preventing UPR may sensitize cancer cells and overcome resistance to other chemotherapy agents. BAX and BAK are inhibited by IRE-1, one of the three effector arms of UPR. Hence, either disrupting the IRE-1–BAX interaction or directly activating BAX to form pores to release intraluminal ER residing calcium may be particularly useful in cancers with constitutive UPR activation (39).

The BH3 protein BECLIN-1 is required for the initiation of autophagy but is inhibited by ER-localized BCL-2 (40). Autophagy is a survival response; however, prolonged stimulation leads to cell death (41). Disruption of the BECLIN-1–BCL-2 complex by the BH3 sensitizer protein, BAD, stimulates autophagy. Therefore, treatment with BAD mimetics, ABT-199 or ABT-737, should presumably have a similar effect. BAD mimetics alone may not be sufficient to push cells toward autophagic cell death, and consequently may confer stress tolerance and cell survival. Thus, a combination treatment with an additional autophagy-inducing agent may be more effective. In support of this strategy, ABT-737 and rapamycin showed synergistic cytotoxicity in breast cancers overexpressing BCL-2 (42). In contrast, combination treatment with an autophagy inhibitor to reduce the cytoprotective autophagy effects of BAD mimetics may enhance apoptotic cell death induced by these agents (41). It remains to be resolved which is the better combination approach, and may be worth considering in tailoring patient treatments.

Another binding target of ER-localized BCL-2 is the 1,4,5-trisphosphate receptor (IP3R); this interaction suppresses calcium release and apoptotic signaling, and is mediated by the BH4 domain of BCL-2 binding to the regulatory coupling domain (RCD) of IP3R (43). Current BCL-2 inhibitors do not target the BH4 region. A 20–amino acid peptide of the RCD was able to disrupt the interaction between IP3R and BCL-2, and exposure to the RCD peptide significantly enhanced cell killing by ABT-737 in CLL cells (43). Because the peptide has poor cellular penetration, small peptidomimetic compounds represent a promising new approach.

Assessing apoptotic modulators in cells and tissues

Because BCL-2 family proteins adopt a different conformation in the membrane *in vivo* compared with isolated recombinant proteins and peptide fragments that have been used in the current screening approaches, some interactions may be missed, and the affinities of others underestimated or overestimated. For example, the detergents commonly used for immunoprecipitiation to assess BCL-2 family interactions in cells can artifactually create or abolish binding surfaces (4). An elegant alternative that avoids these problems is assessment of interactions by fluorescent lifetime imaging microscopy-Förster resonance energy transfer (FLIM-FRET) in live cells as we have described for BIM–BCL-XL above. This is a relatively labor-intensive process, but recent advances in fluorescent microscopy, the development of better fluorescent probes, and automated image analysis have now made high-throughput drug screening via FLIM-FRET possible (44). This technique has other desirable features, as it can be used to study interactions that have not yet been tested *in vitro* due to difficulty in purifying full-length proteins, and can be tailored to measure quantitatively interactions at different subcellular localizations. In the near future, we anticipate that this technology will be able to measure protein–protein interactions in three-dimensional cultures of various cell types.

Although the circumvention of apoptosis is likely to be a widely applicable strategy to improve cancer therapy, a major clinical challenge arises from the fact that cancer is very variable genetically even within pathologic tumor subtypes, and this

Published OnlineFirst April 2, 2015; DOI: 10.1158/1078-0432.CCR-14-0959

variability will contribute to differing responses to therapy. Recent attempts suggest that personalized prescriptions of anticancer drugs will be more effective than classic generic treatment protocols that are based on pathologic grade and stage. It is likely that drugs targeting the BCL-2 family proteins will have therapeutic benefit as they will synergize with conventional chemotherapies that indirectly modulate BCL-2 family protein expression (Table 1). Automated high-throughput screening of drug libraries can be used for quantitative analysis of drug synergy effects of cancer cell lines, and importantly can also assay primary cells obtained from patients with advanced forms of cancer (45, 46). In contrast with the liquid tumors, cultivation of patient-derived cancer cells from solid tumors has been challenging in the past. However, using culture techniques adapted from stem cell research, it is now feasible to investigate drug sensitivities and acquired drug resistance in cell culture models derived from biopsy samples of solid tumors (45). Using this approach, combining conventional or targeted chemotherapy and available or emerging BCL-2 family modulators will uncover exploitable private pathways to apoptosis with great clinical benefit.

Disclosure of Potential Conflicts of Interest

B. Leber reports receiving speakers bureau honoraria from AMGEN Canada, Bristol-Myers Squibb Canada, Celgene Canada, Novartis Canada, and Pfizer Canada. No potential conflicts of interest were disclosed by the other authors.

Authors' Contributions

Conception and design: H. Brahmbhatt, S. Oppermann, E.J. Osterlund, B. Leber

Development of methodology: D.W. Andrews

Writing, review, and/or revision of the manuscript: H. Brahmbhatt, S. Oppermann, E.J. Osterlund, B. Leber, D.W. Andrews

Acknowledgments

The authors thank Tracy Krebs for technical assistance and Dr. Cristina Magi-Galluzzi for help with pathologic assessment and critique.

Grant Support

This work was supported by grant FRN12517 to B. Leber and D.W. Andrews from the Canadian Institute of Health Research (CIHR).

Received January 19, 2015; revised March 5, 2015; accepted March 6, 2015; published OnlineFirst April 2, 2015.

References

1. Hanahan D, Weinberg RA. The hallmarks of cancer. Cell 2000;100:57–70.
2. Kontos CK, Christodoulou MI, Scorilas A. Apoptosis-related BCL2-family members: key players in chemotherapy. Anticancer Agents Med Chem 2014;14:353–74.
3. Youle RJ, Strasser A. The BCL-2 protein family: opposing activities that mediate cell death. Nat Rev Mol Cell Biol 2008;9:47–59.
4. Leber B, Lin J, Andrews DW. Embedded together: the life and death consequences of interaction of the Bcl-2 family with membranes. Apoptosis 2007;12:897–911.
5. Annis MG, Soucie EL, Dlugosz PJ, Cruz-Aguado JA, Penn LZ, Leber B, et al. BAX forms multispanning monomers that oligomerize to permeabilize membranes during apoptosis. EMBO J 2005;24:2096–103.
6. Dewson G, Kratina T, Sim HW, Puthalakath H, Adams JM, Colman PM, et al. To trigger apoptosis, Bak exposes its BH3 domain and homodimerizes via BH3:groove interactions. Mol Cell 2008;30:369–80.
7. Willis SN, Chen L, Dewson G, Wei A, Naik E, Fletcher JI, et al. Proapoptotic Bak is sequestered by Mcl-1 and Bcl-xL, but not Bcl-2, until displaced by BH3-only proteins. Genes Dev 2005;19:1294–305.
8. Billen LP, Kokoski CL, Lovell JF, Leber B, Andrews DW. Bcl-XL inhibits membrane permeabilization by competing with BAX. PLoS Biol 2008;6:e147.
9. Llambi F, Moldoveanu T, Tait SW, Bouchier-Hayes L, Temirov J, McCormick LL, et al. A unified model of mammalian BCL-2 protein family interactions at the mitochondria. Mol Cell 2011;44:517–31.
10. Deng J, Carlson N, Takeyama K, Dal Cin P, Shipp M, Letai A. BH3 profiling identifies three distinct classes of apoptotic blocks to predict response to ABT-737 and conventional chemotherapeutic agents. Cancer Cell 2007;12:171–85.
11. Yamamoto H, Sawai H, Perucho M. Frameshift somatic mutations in gastrointestinal cancer of the microsatellite mutator phenotype. Cancer Res 1997;57:4420–6.
12. Beroukhim R, Mermel CH, Porter D, Wei G, Raychaudhuri S, Donovan J, et al. The landscape of somatic copy-number alteration across human cancers. Nature 2010;463:899–905.
13. Minn AJ, Rudin CM, Boise LH, Thompson CB. Expression of bcl-xL can confer a multidrug resistance phenotype. Blood 1995;86:1903–10.
14. Certo M, Del Gaizo Moore V, Nishino M, Wei G, Korsmeyer S, Armstrong SA, et al. Mitochondria primed by death signals determine cellular addiction to antiapoptotic BCL-2 family members. Cancer Cell 2006;9:351–65.
15. Gleave ME, Monia BP. Antisense therapy for cancer. Nat Rev Cancer 2005;5:468–79.
16. Petros AM, Olejniczak ET, Fesik SW. Structural biology of the Bcl-2 family of proteins. Biochim Biophys Acta 2004;1644:83–94.
17. Davids MS, Letai A. Targeting the B-cell lymphoma/leukemia 2 family in cancer. J Clin Oncol 2012;30:3127–35.
18. Billard C. BH3 mimetics: status of the field and new developments. Mol Cancer Ther 2013;12:1691–700.
19. Vogler M, Weber K, Dinsdale D, Schmitz I, Schulze-Osthoff K, Dyer MJ, et al. Different forms of cell death induced by putative BCL2 inhibitors. Cell Death Differ 2009;16:1030–9.
20. Oltersdorf T, Elmore SW, Shoemaker AR, Armstrong RC, Augeri DJ, Belli BA, et al. An inhibitor of Bcl-2 family proteins induces regression of solid tumours. Nature 2005;435:677–81.
21. Roberts AW, Seymour JF, Brown JR, Wierda WG, Kipps TJ, Khaw SL, et al. Substantial susceptibility of chronic lymphocytic leukemia to BCL2 inhibition: results of a phase I study of navitoclax in patients with relapsed or refractory disease. J Clin Oncol 2012;30:488–96.
22. Ackler S, Mitten MJ, Chen J, Clarin J, Foster K, Jin S, et al. Navitoclax (ABT-263) and bendamustine +/− rituximab induce enhanced killing of non-Hodgkin's lymphoma tumours *in vivo*. Br J Pharmacol 2012;167:881–91.
23. Lam LT, Zhang H, Chyla B. Biomarkers of therapeutic response to BCL2 antagonists in cancer. Mol Diagn Ther 2012;16:347–56.
24. Wilson WH, O'Connor OA, Czuczman MS, LaCasce AS, Gerecitano JF, Leonard JP, et al. Navitoclax, a targeted high-affinity inhibitor of BCL-2, in lymphoid malignancies: a phase 1 dose-escalation study of safety, pharmacokinetics, pharmacodynamics, and antitumour activity. Lancet Oncol 2010;11:1149–59.
25. Souers AJ, Leverson JD, Boghaert ER, Ackler SL, Catron ND, Chen J, et al. ABT-199, a potent and selective BCL-2 inhibitor, achieves antitumor activity while sparing platelets. Nat Med 2013;19:202–8.
26. BCL-2 inhibitor yields high response in CLL and SLL. Cancer Discov 2014;4:OF5.
27. Liu Q, Leber B, Andrews DW. Interactions of pro-apoptotic BH3 proteins with anti-apoptotic Bcl-2 family proteins measured in live MCF-7 cells using FLIM FRET. Cell Cycle 2012;11:3536–42.
28. van Delft MF, Wei AH, Mason KD, Vandenberg CJ, Chen L, Czabotar PE, et al. The BH3 mimetic ABT-737 targets selective Bcl-2 proteins and efficiently induces apoptosis via Bak/BAX if Mcl-1 is neutralized. Cancer Cell 2006;10:389–99.
29. Wuilleme-Toumi S, Robillard N, Gomez P, Moreau P, Le Gouill S, Avet-Loiseau H, et al. Mcl-1 is overexpressed in multiple myeloma and associated with relapse and shorter survival. Leukemia 2005;19:1248–52.

Published OnlineFirst April 2, 2015; DOI: 10.1158/1078-0432.CCR-14-0959

30. Belmar J, Fesik SW. Small molecule Mcl-1 inhibitors for the treatment of cancer. Pharmacol Ther 2015;145C:76–84.
31. Friberg A, Vigil D, Zhao B, Daniels RN, Burke JP, Garcia-Barrantes PM, et al. Discovery of potent myeloid cell leukemia 1 (Mcl-1) inhibitors using fragment-based methods and structure-based design. J Med Chem 2013; 56:15–30.
32. Zhong Q, Gao W, Du F, Wang X. Mule/ARF-BP1, a BH3-only E3 ubiquitin ligase, catalyzes the polyubiquitination of Mcl-1 and regulates apoptosis. Cell 2005;121:1085–95.
33. Rahmani M, Davis EM, Bauer C, Dent P, Grant S. Apoptosis induced by the kinase inhibitor BAY 43-9006 in human leukemia cells involves down-regulation of Mcl-1 through inhibition of translation. J Biol Chem 2005; 280:35217–27.
34. Lacrima K, Valentini A, Lambertini C, Taborelli M, Rinaldi A, Zucca E, et al. *In vitro* activity of cyclin-dependent kinase inhibitor CYC202 (Seliciclib, R-roscovitine) in mantle cell lymphomas. Ann Oncol 2005; 16:1169–76.
35. Gavathiotis E, Suzuki M, Davis ML, Pitter K, Bird GH, Katz SG, et al. BAX activation is initiated at a novel interaction site. Nature 2008;455:1076–81.
36. Gavathiotis E, Reyna DE, Bellairs JA, Leshchiner ES, Walensky LD. Direct and selective small-molecule activation of proapoptotic BAX. Nat Chem Biol 2012;8:639–45.
37. Xin M, Li R, Xie M, Park D, Owonikoko TK, Sica GL, et al. Small-molecule BAX agonists for cancer therapy. Nat Commun 2014;5:4935.
38. Wang M, Kaufman RJ. The impact of the endoplasmic reticulum protein-folding environment on cancer development. Nat Rev Cancer 2014;14: 581–97.
39. Mathai JP, Germain M, Shore GC. BH3-only BIK regulates BAX, BAK-dependent release of Ca2+ from endoplasmic reticulum stores and mitochondrial apoptosis during stress-induced cell death. J Biol Chem 2005; 280:23829–36.
40. Chang NC, Nguyen M, Germain M, Shore GC. Antagonism of Beclin 1-dependent autophagy by BCL-2 at the endoplasmic reticulum requires NAF-1. EMBO J 2010;29:606–18.
41. Toton E, Lisiak N, Sawicka P, Rybczynska M. Beclin-1 and its role as a target for anticancer therapy. J Physiol Pharmacol 2014;65:459–67.
42. Vaillant F, Merino D, Lee L, Breslin K, Pal B, Ritchie ME, et al. Targeting BCL-2 with the BH3 mimetic ABT-199 in estrogen receptor-positive breast cancer. Cancer Cell 2013;24:120–9.
43. Rong YP, Bultynck G, Aromolaran AS, Zhong F, Parys JB, DeSmedt H, et al. The BH4 domain of Bcl-2 inhibits ER calcium release and apoptosis by binding the regulatory and coupling domain of the IP3 receptor. Proc Natl Acad Sci U S A 2009;106:14397–402.
44. Kumar S, Alibhai D, Margineanu A, Laine R, Kennedy G, McGinty J, et al. FLIM FRET technology for drug discovery: automated multiwell-plate high-content analysis, multiplexed readouts and application in situ. Chemphyschem 2011;12:609–26.
45. Crystal AS, Shaw AT, Sequist LV, Friboulet L, Niederst MJ, Lockerman EL, et al. Patient-derived models of acquired resistance can identify effective drug combinations for cancer. Science 2014;346:1480–6.
46. Shen M, Zhang Y, Saba N, Austin CP, Wiestner A, Auld DS. Identification of therapeutic candidates for chronic lymphocytic leukemia from a library of approved drugs. PLoS ONE 2013;8:e75252.
47. Mhaidat NM, Zhang XD, Jiang CC, Hersey P. Docetaxel-induced apoptosis of human melanoma is mediated by activation of c-Jun NH2-terminal kinase and inhibited by the mitogen-activated protein kinase extracellular signal-regulated kinase 1/2 pathway. Clin Cancer Res 2007; 13:1308–14.
48. Kutuk O, Arisan ED, Tezil T, Shoshan MC, Basaga H. Cisplatin overcomes Bcl-2-mediated resistance to apoptosis via preferential engagement of Bak: critical role of Noxa-mediated lipid peroxidation. Carcinogenesis 2009; 30:1517–27.
49. Jiang M, Wei Q, Wang J, Du Q, Yu J, Zhang L, et al. Regulation of PUMA-alpha by p53 in cisplatin-induced renal cell apoptosis. Oncogene 2006; 25:4056–66.
50. Floros KV, Talieri M, Scorilas A. Topotecan and methotrexate alter expression of the apoptosis-related genes BCL2, FAS and BCL2L12 in leukemic HL-60 cells. Biol Chem 2006;387:1629–33.
51. Sawada M, Nakashima S, Banno Y, Yamakawa H, Hayashi K, Takenaka K, et al. Ordering of ceramide formation, caspase activation, and BAX/Bcl-2 expression during etoposide-induced apoptosis in C6 glioma cells. Cell Death Differ 2000;7:761–72.
52. Malugin A, Kopeckova P, Kopecek J. HPMA copolymer-bound doxorubicin induces apoptosis in ovarian carcinoma cells by the disruption of mitochondrial function. Mol Pharm 2006;3:351–61.
53. Cheng H, Hong B, Zhou L, Allen JE, Tai G, Humphreys R, et al. Mitomycin C potentiates TRAIL-induced apoptosis through p53-independent upregulation of death receptors: evidence for the role of c-Jun N-terminal kinase activation. Cell Cycle 2012;11:3312–23.
54. Hou Y, Wang HQ, Ba Y. Effects of CDC7 gene silencing and Rituximab on apoptosis in diffuse large B cell lymphoma cells. J Cancer Res Clin Oncol 2012;138:2027–34.
55. Lopez-Fauqued M, Gil R, Grueso J, Hernandez-Losa J, Pujol A, Moline T, et al. The dual PI3K/mTOR inhibitor PI-103 promotes immunosuppression, *in vivo* tumor growth and increases survival of sorafenib-treated melanoma cells. Int J Cancer 2010;126:1549–61.
56. Galmiche A, Ezzoukhry Z, Francois C, Louandre C, Sabbagh C, Nguyen-Khac E, et al. BAD, a proapoptotic member of the BCL2 family, is a potential therapeutic target in hepatocellular carcinoma. Mol Cancer Res 2010;8: 1116–25.
57. Fennell DA, Chacko A, Mutti L. BCL-2 family regulation by the 20S proteasome inhibitor bortezomib. Oncogene 2008;27:1189–97.
58. Oblimersen: Augmerosen, BCL-2 antisense oligonucleotide - Genta, G 3139, GC 3139, oblimersen sodium. Drugs R D 2007;8:321–34.
59. Zhai D, Jin C, Satterthwait AC, Reed JC. Comparison of chemical inhibitors of antiapoptotic Bcl-2-family proteins. Cell Death Differ 2006;13:1419–21.
60. Tse C, Shoemaker AR, Adickes J, Anderson MG, Chen J, Jin S, et al. ABT-263: a potent and orally bioavailable Bcl-2 family inhibitor. Cancer Res 2008;68:3421–8.

Study rationale and goals

Apoptosis is an intricately regulated form of programmed cell death pivotal for development and the maintenance of tissue homeostasis. When perturbed, apoptosis contributes to a number of human diseases. Insufficient apoptosis has been implicated in cancers, viral infections, autoimmune disorders whereas excessive apoptosis has been implicated in neurodegenerative diseases, AIDS and stroke. The Bcl-2 family proteins are the central players regulating and executing this process. Therefore, understanding the fundamental mechanisms by which Bcl-2 family proteins regulate and execute this process and functionally modulating their activity is pivotal for the treatment of apoptosis- linked diseases.

Multiple signaling pathways converge to result in MOMP. Therefore strategies aimed to promote or inhibit MOMP have been attractive from a therapeutic perspective. Using small molecules to therapeutically exploit Bcl-2 family proteins has been an alternative strategy to gene manipulation strategies and extensive research has already been conducted to identify several small molecules, of which ABT-263 and ABT-199 have been most promising for cancer therapy. As discussed earlier, new sets of problems have arisen due to the on-target toxicities and selectivity against only a subset of the Bcl-2 family proteins. To overcome this, the aim of this thesis was to identify new small molecules that target additional Bcl-2 family proteins to serve as mechanistic tools and as potential leads for therapies for apoptosis-linked diseases.

In this thesis, we employed *in vitro* liposome based screens to identify small molecules that a) inhibit Bax and Bak, b) activate Bax, and c) enable Bax to escape inhibition by Bcl-XL. In Chapters II-IV, we describe the rationale of these screens and analyze the activity of the compounds. Furthermore we discuss how these compounds were used as tools for obtaining further mechanistic insights into the steps that occur during apoptosis, and how they may serve as leads for the development of therapeutics.

CHAPTER II:

Small molecule inhibition of pro-apoptotic Bax and Bak promotes long term cell survival and protects primary neurons from excitotoxicity

Preface

The work presented here has been submitted to *Nature Chemical Biology* (NCHEMB-A160103325) as a research article.

Contribution of authors:

J.Y. and D.W.A designed and X.N. conducted the secondary screen with the 38 compounds, measured the IC_{50} values for MSN-50, MSN-125, BJ-1 and BJ-1-BP, performed the immunofluorescence 6A7 experiments and conducted the Bax-Bax FRET experiments. H.B. tested the activity of DAN004 in the liposome based assay and in the HCT116 cells, examined the efficacy of the compounds in the mitochondria based assay, conducted the DSS crosslinking studies, compared inhibition of cBid/Bim- Bax by the compounds, conducted the isothermal calorimetry studies with Bax. P.M. designed the assay and tested the activity of MSN-125 in primary neurons. J.L. designed and Z.Z. conducted the Copper (II)(1,10-phenanthroline)3 crosslinking studies. J.S. conducted the SAR studies in the liposome based assay shown in the supplementary table. W.E.D. CC, D.W.A. designed, DAN004. W.E.D. designed the synthetic strategy and M.D. and F.G.R.E. synthesized DAN004. CC designed and performed preliminary tests on the compound. E.W. conducted the primary screen with 86 compounds.

W.Z. conducted the clonal survival assays in the HCT116 cells. J.P. conducted the experiments with Nutlin-3a. P.A designed and Jyoti Nandy, Maragani

Satyanaraya, and Ravi Jimmidi synthesized MSN-50, MSN-125 and the SAR compounds. X.N., H.B., P.M., B.L., and D.W.A analyzed the data and wrote the paper. D.W.A, B.L and J.Y. conceived and directed the project.

Research Objective:

To identify and characterize novel small molecule inhibitors of Bax and Bak and evaluate their ability to protect cells against apoptotic stimuli.

Research Highlights:

- MSN-125 and MSN-50 inhibit Bax and Bak mediated membrane permeabilization in a dose dependent manner.
- MSN-125 and MSN-50 conferred protection of immortalized and primary neuronal cultures against apoptotic stimuli.
- DAN004 is more potent than MSN-50 and MSN-125 at inhibiting Bax and Bak mediated membrane permeabilization but displays off- target activities in cells.
- MSN-125, MSN-50 and DAN004 have a pronounced effect on the formation of Bax oligomers than dimers.
- MSN-125 disrupts partial, not all, interfaces of the Bax dimer.

Small molecule inhibition of pro-apoptotic Bax and Bak promotes long term cell survival and protects primary neurons from excitotoxicity

Xin Niu[1,2,*], Hetal Brahmbhatt[1,3,*], Philipp Mergenthaler[3,*], Zhi Zhang[4], Jing Sang[2,3], Michael Daude[5], Fabian G. R. Ehlert[5], Wibke E. Diederich[5], Eve Wong[1], Weijia Zhu[1], Justin Pogmore[3],Jyoti P. Nandy[7,8], Maragani Satyanarayana[7,9], Ravi K. Jimmidi[10], Prabhat Arya[7,11], Brian Leber[1,12] Jialing Lin[4], Carsten Culmsee[6], Jing Yi[2] and David W. Andrews[1,3**]

[1]Department of Biochemistry and Biomedical Sciences, McMaster University, Hamilton, Ontario, Canada, L8S 4L8
[2]Department of Biochemistry and Molecular Cell Biology, Institutes of Medical Sciences, Shanghai Jiao Tong University School of Medicine, Shanghai 200025, China
[3]Present address: Department of Biological Sciences, Sunnybrook Research Institute, Toronto, Ontario, Canada, M4N 3M5
[4]Department of Biochemistry and Molecular Biology, Peggy and Charles Stephenson Cancer Center, University of Oklahoma Health Sciences Center, Oklahoma City, Oklahoma 73126
[5]Department of Medicinal Chemistry and Center for Tumor Biology and Immunology, Philipps-Universität Marburg, Hans-Meerwein-Straße 3, Marburg 35043, Germany
[6]Institut für Pharmakologie und Klinische Pharmazie, Philipps Universität Marburg
[7]Ontario Institute for Cancer Research, MaRS Centre, South Tower, 101 College Street, Toronto, Ontario, M5G 0A3, Canada
[8]Present address: Therapeutic Product Directorate, Health Canada, 101 Tunney's Pasture Driveway, Ottawa, Ontario, K1A 0K9, Canada.
[9]Present address: TCG Life Sciences, Bio Resource Centre, Gensis Campus,Hinjewadi, Pune-411057, Maharashtra, India
[10]Present address: SAI Life Sciences Limited, unit-II, IKP knowledge Park, Shameerpet, Hyderabad, 500078, India
[11]Present address: Dr. Reddy's Institute of Life Sciences, University of Hyderabad Campus, Gachibowli, Hyderabad 500046, India
[12]Department of Medicine, McMaster University, Hamilton, Ontario, L8S 4L8, Canada

*These authors contributed equally to this work

**Correspondence should be addressed to: david.andrews@sri.utoronto.ca
Correspondence for MSN-50 and MSN125 should be addressed prabhata@drils.org

Running title: Small Molecule Inhibitors of Bax and Bak

Graphical Abstract

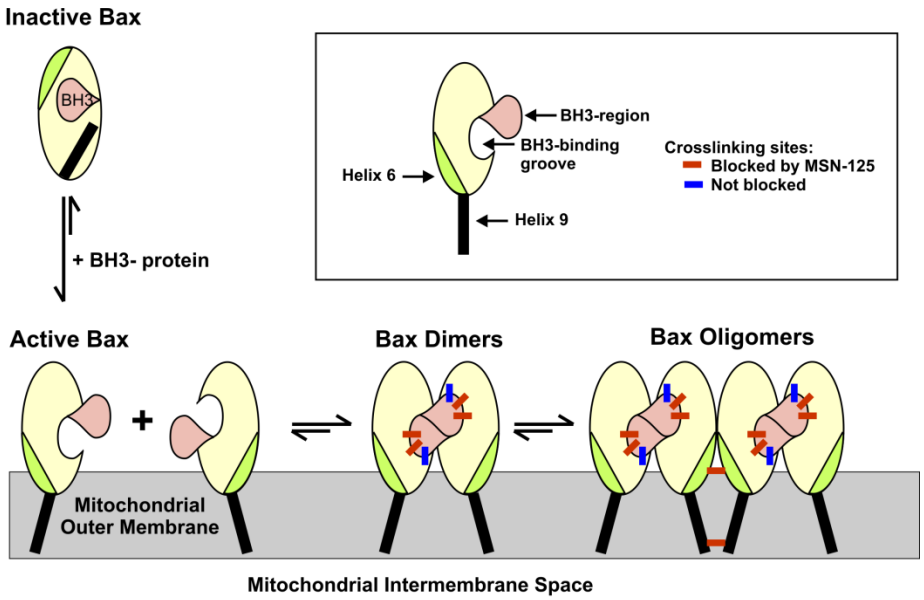

Abstract

Excess cell death via apoptosis is associated with acute and degenerative diseases. Small molecules that interfere with the ordered series of protein-protein interactions leading to lethal Bax and Bak pores are desirable as leads for novel therapeutics and as tools for mechanistic studies. As candidates for disrupting protein-protein interactions we screened a library of small molecules to identify compounds that inhibit Bax and Bak mediated membrane permeabilization. Two compounds displayed cytoprotective activity against lethal stimuli in primary neuron cultures and immortalized colon cancer cells. We demonstrate that the

compounds inhibit Bax oligomerization primarily at the dimer stage by disruption of multiple, but not all, interactions at the BH3-groove, helix 6 and helix 9 dimer interfaces. Our results suggest that oligomerization of Bax beyond dimer formation is essential for membrane permeabilization activity and that pharmacologic inhibition of Bax and Bak has therapeutic potential to promote cellular survival and treat excitotoxic neurodegeneration.

Introduction

The transient prevention of programmed cell death is predicted to be of potential therapeutic benefit when cells are subjected to acute stress such as during ischemia, ischemia-reperfusion, inflammation as well as when exposed to other forms of stress, for example macular degeneration and in normal tissues during cancer chemotherapy (Mergenthaler, Dirnagl et al. 2004; Szeto 2008; Leber, Geng et al. 2010; Hardwick and Soane 2013). While cells have evolved many strategies for avoiding apoptosis (Delbridge, Valente et al. 2012), development of pharmacological strategies to inhibit apoptosis has not been widely investigated. The multi-domain pro-apoptotic Bcl-2 family members Bax and Bak are attractive targets for the development of small molecule inhibitors due to their central importance in Mitochondrial Outer Membrane Permeabilization (MOMP), an event widely accepted as committing most cells to apoptosis (Moldoveanu, Follis et al. 2014; Uchime, Dai et al. 2016).

MOMP results from an ordered series of steps beginning with activation of one or more Bcl-2 homology 3 proteins (BH3-proteins). Once activated, BH3-proteins bind to mitochondria, directly recruit and activate cytoplasmic Bax and the constitutively membrane bound Bak (Lovell, Billen et al. 2008; Sarosiek, Chi et al. 2013). In some cases 'activation' involves releasing a previously activated Bax or Bak from inhibition by an anti-apoptotic protein of the Bcl-2 family (Wilson-Annan, O'Reilly et al. 2003; Willis, Fletcher et al. 2007). Activated membrane-bound Bax recruits and activates more Bax and Bak by catalyzing insertion of the central helices 5-6 into the lipid bilayer of the mitochondrial outer membrane (MOM) as part of a yet to be fully defined structure (Ruffolo and Shore 2003; Annis, Soucie et al. 2005; Tan, Dlugosz et al. 2006; Czabotar, Westphal et al. 2013). Oligomerization of membrane-bound Bax or Bak culminates in MOMP (Dewson, Ma et al. 2012; Ma, Hockings et al. 2013; Zhang, Subramaniam et al. 2015). Thus, pharmacological protection of cells from apoptosis would require inhibition of both proteins.

MOMP could also be prevented by inhibiting any one of the individual steps that lead to the oligomerization of Bax and Bak in the outer mitochondrial membrane. However, the multiple different BH3-proteins that activate Bax and Bak are structurally disparate therefore inhibiting Bax and Bak serves as the optimal target.

Three classes of Bax inhibitors have been reported (Bombrun, Gerber et al. 2003; Polster, Basanez et al. 2003; Hetz, Vitte et al. 2005; Jiang, Pabla et al. 2007; Peixoto, Ryu et al. 2009; Peixoto, Teijido et al. 2015); one of which is sufficiently hydrophobic that it is expected to partition into membrane (Polster, Basanez et al. 2003). While access to these molecules has been limited, it has been shown that most of them inhibit Bax and the effect on Bak activity remains to be determined (Hetz, Vitte et al. 2005). Furthermore, electrophysiology studies suggested that they act as channel blockers rather than inhibiting Bax oligomerization (Bombrun, Gerber et al. 2003; Hetz, Vitte et al. 2005; Peixoto, Ryu et al. 2009). In addition to inhibiting the MDM2/p53 interaction, Nutlins have been reported to block Bax and Bak oligomerization thereby attenuating cytochrome c release (Jiang, Pabla et al. 2007). Assessment of the molecular mechanism of inhibition of Bax and Bak by Nutlins has not elucidated how they confer protective effects in kidney tubular cells but also potentiate cancer cell death (Tovar, Rosinski et al. 2006). Thus, additional tool compounds that inhibit defined steps during Bax and Bak activation would be a key advancement.

The identification of efficient small molecule inhibitors of Bax and Bak is complicated by the viscous lipidic environment of the membrane in which the proteins are active. Furthermore, the lack of structural information about and the overall dynamic nature of Bax and Bak protein complexes inside cellular membranes have prohibited rationally designing small molecule inhibitors.

Here, we screened a natural product-inspired compound library (Reayi and Arya 2005) to identify small molecules that would inhibit the activity of Bax and Bak in the MOM, their primary functional location (Leber, Lin et al. 2007). Two small molecules that share a common active core structure were identified and inhibited Bax and Bak mediated apoptosis in live cells. The molecular mechanism of their function was determined using a combination of *in vitro* and live cell assays. The identified small molecules partially disrupt the normal Bax dimerization interfaces thereby preventing dimers from oligomerizing further. Using these inhibitors, we further demonstrate that pharmacological inhibition of Bax and Bak allows cells to survive an otherwise lethal challenge and rescues neurons from prior excitotoxic damage.

Results

Screening for small molecule inhibitors of Bax

To identify novel Bax inhibitors, we screened a collection of benzofuran-based flavonoid-inspired, and several tetrahydroquinoline alkaloid-inspired compounds for inhibition of tBid/Bax mediated membrane permeabilization in a MOMP-mimicking liposome dye release assay (Billen, Kokoski et al. 2008) (Fig. 1a). In total, 86 compounds were individually added to liposomes encapsulating both 8-aminonaphthalene1,3,6-trisulfonic acid (ANTS) and its quencher p-xylene-bis-pyridinium (DPX). Bax and tBid were added to induce permeabilization of the

liposomes (Fig. 1b). Small molecules that inhibited liposome permeabilization with a Z-score greater than 2 were re-assayed manually.

We synthesized a secondary library of 37 compounds based on the molecular structures of the compounds with the highest activity in the manual analyses (BJ-1 and BJ-1-BP). In this set, two compounds (MSN-125 and MSN-50) efficiently inhibited liposome permeabilization (Fig. 1c and 2a).

Small molecule inhibition of liposome permeabilization by tBid and Bax is concentration-dependent

In validation experiments we found that BJ-1, BJ-1-BP, MSN-125, and MSN-50 all inhibited dye-release from liposomes in a concentration-dependent fashion (Fig. 2b,c). Consistent with previous reports (Jiang, Pabla et al. 2007) Nutlin-3a also inhibited liposome permeabilization in this assay in a concentration-dependent fashion but was poorly active with isolated mitochondria (Supplementary Fig. 1a-b). However, as shown below, MSN-50 and MSN-125 were active in mitochondria and in cells. Structure-activity relationship (SAR) experiments suggested that most modifications of these compounds reduced activity significantly (Supplementary Table 1). Therefore, in an attempt to identify the pharmacophore common to MSN-125 and MSN-50, we synthesized DAN004 (Fig. 2a). Like the parent compounds, DAN004 showed concentration-dependent inhibition of liposome permeabilization but with improved activity *in vitro* (Fig. 2d).

This assay does not permit determination of conventional kinetic parameters since new oligomers form in liposomes that have already been permeabilized and existing Bax oligomers can continue to expand until they contain hundreds of Bax molecules(Satsoura, Kucerka et al. 2012). Neither of these events is recorded in our assay as liposome permeabilization is an all-or-nothing event. Nevertheless, the assay does permit concentration response curves to be generated that are useful for quantitatively comparing different compounds, provided they are analyzed using the same protein and liposome concentrations. The concentration of compound required to inhibit 50% of the maximal dye release (IC_{50} values) obtained for MSN-125, MSN-50, BJ-1 and BJ-1-BP in this assay were approximately 4, 6, 9 and 6 μM, respectively (Fig. 2b,c). Consistent with DAN004 being the pharmacophore, it exhibited the most potent inhibitory activity (IC_{50} ~0.7 μM, Fig. 2d).

MSN-125, MSN-50, and DAN004 inhibit Bax and Bak on mitochondria

In order to investigate whether the compounds identified above inhibited tBid-activated Bax and/or Bak in mitochondria, they were assayed using mitochondria isolated from *Bax*$^{-/-}$ or *Bax*$^{-/-}$ *Bak*$^{-/-}$ baby mouse kidney (BMK) cell lines stably expressing Smac-mCherry(Shamas-Din, Satsoura et al. 2014), an intermembrane space localized fluorescent protein which is released upon MOMP (Fig. 2e,f). At concentrations of 40 μM none of the compounds alone

resulted in significant mitochondrial permeabilization (Supplementary Fig. 2a). Therefore, this concentration was chosen as the maximum for the assays used to assess inhibition of Bax/Bak. Both MSN-125 and MSN-50 inhibited tBid/Bax mediated MOMP in a concentration dependent manner (Fig. 2e). However, BJ-1 and BJ-1-BP failed to inhibit Bax-induced MOMP (Supplementary Fig. 2b) and Nutlin-3a inhibited tBid/Bax mediated permeabilization of mitochondria poorly (Supplementary Fig. 1b). As expected, mitochondria from *Bax*$^{-/-}$ cells were efficiently permeabilized by tBid alone due to activation of endogenous Bak in the MOM and/or release of activated Bak from endogenous anti-apoptotic proteins (Fig. 2f). It was not possible to measure the amount of endogenous Bak on the MOM with sufficient accuracy to compare quantitatively compound mediated inhibition of Bak with inhibition of the known quantities of Bax added to mitochondria from *Bax*$^{-/-}$ *Bak*$^{-/-}$ cells. Nevertheless, both MSN-125 and MSN-50 showed a concentration-dependent inhibition of Bak mediated Smac-mCherry release (Fig. 2f) and there was no inhibition by BJ-1 or BJ-1-BP (Supplementary Fig. 2c). As expected from our results in the liposome assays (Fig. 2c, d), compared to the other compounds, DAN004 inhibited Bax and Bak mediated MOMP more potently (Fig. 2g and Supplementary Fig. 2d). Taken together, unlike Bax inhibitors described previously (Bombrun, Gerber et al. 2003; Polster, Basanez et al. 2003; Hetz, Vitte et al. 2005; Peixoto, Ryu et al. 2009) these compounds inhibit both Bax and Bak.

As MSN-125, MSN-50 and DAN004 inhibited both Bax and Bak it suggests that the step inhibited is common to both proteins. Therefore it is unlikely that inhibition of Bax recruitment to membranes plays a significant role as Bak is a constitutive MOM transmembrane protein. As tBid was used to activate both Bax and Bak it was common to both assays for MOMP. Therefore, we assessed whether inhibition was selective to tBid by using Bim to activate Bax. Consistent with the target of the compounds being Bax and Bak, all three compounds inhibited Bim-activated Bax mediated liposome permeabilization in a dose dependent fashion (Supplementary Fig. 3). Furthermore, inhibition of Bim- or cBid-activated Bax was comparable (Supplementary Fig. 3).

MSN-125 and MSN-50 inhibit apoptosis in cells

We investigated inhibition of Bax/Bak-mediated apoptosis by MSN-125, MSN-50, and DAN004 in live HCT-116 cells and primary cortical neurons. To assess inhibition of Bax and Bak separately and together, wild-type (Wt), *Bax*$^{-/-}$, *Bak*$^{-/-}$, and *Bax*$^{-/-}$ *Bak*$^{-/-}$ (DKO) human colon cancer (HCT116) cells were assessed for survival and growth after inducing Bax-/Bak-dependent apoptosis by treating these cells with actinomycin D. As expected, in the absence of the inhibitor compounds, only *Bax*$^{-/-}$*Bak*$^{-/-}$ cells survived and proliferated after replating (Fig. 3a). Pre-treatment of the cells with MSN-50 or MSN-125 conferred survival to the Wt, *Bax*$^{-/-}$, and *Bak*$^{-/-}$ cells. This is consistent with our previous

observation that these compounds inhibit both Bax and Bak (Fig. 3a). ILS-JRK-C95-182, a compound structurally similar to MSN-125 and MSN-50 that displayed minimal inhibitory effect in the liposome permeabilization assay (Supplementary Table 1) also lacked protective activity in live cells (Fig. 3a, "ILS-JRK-C95-182"). Control wells with no apoptosis inducing drug demonstrated that alone 5 or 10μM MSN-125 and MSN-50 had negligible effects on cell growth and proliferation (Fig. 3a).

Although DAN004 exhibited potent inhibitory activity *in vitro,* this molecule exhibited marked toxicity at 10 μM in cell replating assays (Supplementary Fig. 4a). Furthermore, at sub-toxic doses it did not confer protection against actinomycin D treatment (Supplementary Fig. 4b). Due to the large number of potential reasons for the marked increase in off-target toxicity for DAN004 the compound was not pursued further here.

To correlate functional inhibition of apoptosis by MSN-125 to inhibition of Bax in cells, we performed immunofluorescence with the conformation-specific anti-Bax-6A7 antibody that binds to an N-terminal epitope of Bax that is exposed upon activation(Hsu and Youle 1998). In the controls actinomycin D treatment triggered the endogenous Bax to adopt the 6A7-positive conformation and at least partial cytochrome c release from mitochondria in HCT116 Wt cells as expected (Fig. 3b). Consistent with MSN-125 potently inhibiting Bax and Bak,

addition of the compound protected cells from both Bax activation and cytochrome c release (Fig. 3b).

MSN-125 protects cultured primary neurons against glutamate excitotoxicity

Glutamate excitotoxicity can be mediated by Bax-dependent pathways (D'Orsi, Bonner et al. 2012) and excessive release of glutamate after ischemic stroke contributes to neuronal cell death (Mergenthaler, Dirnagl et al. 2004). We therefore assessed whether MSN-125 would protect cultured primary embryonic mouse brain cortical neurons from glutamate excitotoxicity. We treated neurons with 25 or 100 μM glutamate for 30 minutes, which leads to substantial neuronal cell death after 24 hours (Fig. 4c). However, treatment with 5 μM MSN-125 directly after the excitotoxic insult elicited neuroprotection as indicated by increased neuronal viability. At this concentration and time point, treatment with MSN-125 alone did not result in neuronal damage. This result demonstrates not only that unlike other neuroprotective agents MSN-125 mediated inhibition of Bax and/or Bak protects neurons when administered after the initial insult but it also validates Bax and/or Bak as potential therapeutic targets.

Molecular mechanism of small molecule inhibition of Bax

Bax mediated membrane permeabilization proceeds as an ordered series of steps including tBid binding to the MOM, recruitment of Bax to tBid, insertion of Bax into the MOM, Bax oligomerization and finally permeabilization of the MOM (Lovell, Billen et al. 2008). The most likely explanation for inhibition of Bax by the small molecules is direct binding to Bax. However, it was not possible to measure direct binding of MSN-125 or MSN-50 to Bax due to limited solubility of the compounds and protein when mixed in solutions containing the more than 100 nM Bax required for isothermal calorimetry (ITC) or nuclear magnetic resonance (NMR) experiments. Although DAN004 is much more soluble in aqueous solutions in ITC studies, we did not detect direct binding to Bax in solution. However, this compound inhibits Bax activation by both tBid and Bim. Although a formal possibility, it is unlikely that inhibition of Bax was due to partitioning of the compounds into the liposome bilayer, thereby changing its physical properties because adding the compounds to the liposomes and then re-isolating the liposomes by gel filtration chromatography had no effect on Bax mediated membrane permeabilization (Supplementary Fig. 5). Furthermore, many structurally similar compounds of the same or higher hydrophobicity had no detectable effect on inhibition of membrane permeabilization (Supplementary Table 1). Finally, it is unlikely that inhibiting Bax and Bak by changing the lipid properties of subcellular membranes would both function and be tolerated in the wide variety of systems reported here.

The molecular mechanism(s) by which the compounds inhibit Bax oligomerization in membranes was examined using Förster resonance energy transfer (FRET) and chemical crosslinking. To measure Bax oligomerization by FRET, single-cysteine mutants of Bax were labelled with diaminomethyl-coumarin (DAC-Bax-134C) or with 7-nitrobenzene-2-oxa-1,3-diazol-4-yl-ethylenediamine (NBD-Bax-126C) as donor and acceptor respectively(Lovell, Billen et al. 2008). In reactions containing liposomes and tBid, addition of MSN-125 or MSN-50, inhibited FRET between DAC-Bax-134C and NBD-Bax-126C (Fig. 4a and Supplementary Fig. 6a). These data indicate that MSN-125 and MSN-50 inhibit Bax oligomerization.

The FRET measurements do not distinguish effects on dimer and oligomer formation. Therefore, we directly assessed the oligomerization state by chemical crosslinking of purified Bax. Crosslinking data obtained using the amine-specific crosslinker DSS clearly demonstrate that MSN-125, MSN-50, and DAN004 inhibit tBid-induced Bax oligomerization in liposomes with a more pronounced effect on the formation of higher order oligomers than dimers (Fig. 4b,c and Supplementary Fig. 6b-e). At the highest concentration tested MSN-125 also inhibited Bax dimerization to a limited extent, an effect not seen for MSN-50. DAN004 also inhibited Bax oligomerization to a much greater extent than it inhibited Bax dimerization. At high concentrations MSN-125, MSN-50, DAN004

and the positive control Bcl-XL inhibited large oligomers of Bax to a similar extent (Fig. 4b,c and Supplementary Fig. 6b-e).

MSN-125 inhibits Bax oligomerization at defined dimer:dimer interfaces

Previous disulfide crosslinking studies identified three dimer interfaces in Bax oligomers bound to the mitochondria (Zhang, Zhu et al. 2010; Dewson, Ma et al. 2012; Zhang, Subramaniam et al. 2015). Binding of the BH3-region of one Bax to the canonical BH1-3-groove of other Bax forms a BH3-groove interface, and binding of the two helices 6 and 9 in the neighboring Bax molecules forms the other two interfaces. To determine whether MSN-125 inhibits the formation of a specific dimer interfaces in the Bax oligomer, we used site-specific disulfide crosslinking. To this end, single-cysteine Bax mutants previously shown to form a disulfide-linked Bax homodimer when activated by a Bax BH3-peptide and targeted mitochondria lacking Bax and Bak (Zhang, Subramaniam et al. 2015) were oxidized on mitochondria to induce disulfide crosslinking in the absence or presence of MSN-125. In the absence of MSN-125, a Bax mutant with the single cysteine at position 146 (Bax E146C) in helix 6 or 183 (Bax A183C) in helix 9 formed a disulfide-linked homodimer (Fig. 4d, lane 16 or 18, arrow). Addition of MSN-125 inhibited formation of both dimers (Fig. 4d, lanes 14 and 20). Similarly, two pairs of Bax mutants with the single cysteine in the BH3/helix 2 region (Bax L59C, and T56C) and in the canonical groove (Bax M79C in helix 3, and R94C in

helix 4) also generated disulfide-linked dimers (Fig. 4d, lanes 2 and 6) that were inhibited by MSN-125 (Fig. 4d, lanes 4 and 8).

In contrast, another pair of Bax mutants with the single cysteine L63C in BH3/helix 2 and A112C in groove/helix 5 resulted in relatively weak disulfide-crosslinking that was not inhibited by MSN-125 (Fig 4d, compare lane 10 to 12). A similar result was obtained when we used a fully coupled in vitro transcription translation system to produce more Bax L63C and A112C proteins to increase the disulfide-crosslinking (Supplementary Fig. 6f). A schematic of the MSN-125 affected and unaffected interactions in the BH3-groove interface is shown in Fig. 4e. Taken together these results suggest that the three dimer interfaces are at least partially disrupted by MSN-125.

As expected from previous data suggesting that oligomerization occurs after binding to membranes (Annis, Soucie et al. 2005), the targeting of the wild-type and mutant Bax proteins to mitochondria was largely unaffected by MSN-125 (Fig. 4d, open circle). Therefore, MSN-125 does not significantly interfere with targeting of Bax monomers to the mitochondria, but blocks assembly of Bax oligomers at the MOM by interfering with multiple, yet not all, Bax:Bax interactions at the three dimer interfaces. MSN-125, MSN-50 and DAN004 prevent Bax oligomerization predominantly beyond the formation of dimers suggesting that correct formation of all the interfaces is required for oligomerization beyond a dimer. Thus, our data also suggest that when activated

by a BH3-protein, Bax oligomerization beyond the formation of dimers is essential for Bax mediated MOMP.

Discussion

Here, we report the discovery of small molecule inhibitors of the pro-apoptotic Bcl-2 family proteins, Bax and Bak. We highlight the use of these molecules as important tools for dissecting molecular mechanisms of cell death pathways and as molecular probes for assessing the therapeutic potential of targeting Bax and Bak.

Commitment of a cell to apoptosis involves the convergence of pro-apoptotic signaling by BH3-proteins and the anti-apoptotic activities of multi-BH region Bcl-2 family proteins at Bax and Bak. These pro- and anti-apoptotic signals are integrated by competitive binding between the membrane bound forms of the proteins acting in concert to mediate membrane permeabilization by Bax and Bak (Hsu, Wolter et al. 1997; Wei, Lindsten et al. 2000). In most cell types, Bax and Bak functionally substitute for each other (Degenhardt, Sundararajan et al. 2002; Mikhailov, Mikhailova et al. 2003) and it is therefore essential to inhibit both proteins to study the effects of acute inhibition of apoptosis in living cells. Unlike previously identified molecules that inhibited only Bax (Bombrun, Gerber et al. 2003; Polster, Basanez et al. 2003; Hetz, Vitte et al. 2005; Peixoto, Ryu et al. 2009), MSN-125, MSN-50, and DAN004 also inhibit Bak.

MSN-50 and MSN-125 were the most promising candidates inhibiting Bax and Bak in live cell and mitochondria-based assays (Fig. 2 e-g and Fig. 3). Unlike these molecules there was no response to BJ-1 or BJ-1-BP at concentrations up to 40 μM. Complete lack of response could be attributed to inefficient entry of the compounds into cells, metabolic breakdown within cells or non-specific binding of the compounds to proteins, membranes or other cellular constituents. In contrast, DAN004 was somewhat toxic suggesting off-target effects in cells. Therefore, this structurally simpler and more soluble compound is most promising as a tool for structural and mechanistic studies using purified proteins.

Our studies using MSN-50 and MSN-125 indicate that there may be therapeutic benefit to inhibition of Bax and Bak. We measured survival after re-plating to eliminate cells which were unable to proliferate or in which cell death was delayed. By using cells with genetic deletion of Bax and/or Bak it was possible to demonstrate that increased survival of HCT-116 cells was due to inhibition of both proteins (Fig. 3 a-b). However, primary neurons lack such replicative potential and therefore, we measured retention of neuronal viability after an apoptotic stimulus. Our data demonstrate that primary neurons can be protected from prior glutamate excitotoxicity in the presence of MSN-125 (Fig. 3c) suggesting that targeting Bax and/or Bak in neurons may be of therapeutic benefit. As neurons express an alternate isoform of Bak suggested not to be pro-apoptotic, the major therapeutic target in these cells is likely Bax (Sun, Yu et al.

2001). Excitotoxicity is one of the damaging mechanisms contributing to acute neuronal degeneration after stroke (Mergenthaler, Dirnagl et al. 2004), traumatic brain injury and epileptic seizures (Engel, Plesnila et al. 2011). Damage after an excitotoxic insult has been demonstrated to be at least in part mediated through Bax-dependent signaling mechanisms (D'Orsi, Bonner et al. 2012). Our data demonstrating that MSN-125 protects neurons from cell death after glutamate excitotoxicity are corroborated by genetic models where deletion of Bax protected neurons from cell death after stroke in mice (D'Orsi, Kilbride et al. 2015).

However the requirement of Bak as a crucial player in neuronal apoptosis is not clear. Bak may promote neuronal survival under certain conditions and during neuronal development, while promoting neuronal cell death after insults such as stroke (Fannjiang, Kim et al. 2003; Hardwick and Soane 2013). Additionally, although full length Bak is ubiquitously expressed in most cells, central and peripheral neurons express a splice variant, N-Bak and has been reported to have both anti- and pro-death functions (Sun, Yu et al. 2001; Uo, Kinoshita et al. 2005). Thus, further studies are warranted to dissect the function of the pore forming proteins in different settings. The molecules described in this paper are ideal tools for these studies as they appear to function via a well-defined molecular mechanism.

To permeabilize membranes, Bax and Bak homodimerize via the BH3-groove interfaces to nucleate oligomerization of heterogeneously-sized higher-order

oligomers via additional dimer interfaces (Dewson, Ma et al. 2012; Czabotar, Westphal et al. 2013; Ma, Hockings et al. 2013; Iyer, Bell et al. 2015; Subburaj, Cosentino et al. 2015). To assess the contribution of these interfaces to Bax oligomeric pore formation, we have shown that the BH3-groove dimer nucleates the assembly of Bax oligomeric pore which is enlarged by dimerization at the helix 9 interface (Zhang, Subramaniam et al. 2015). Using MSN-125 as a tool to dissect the molecular mechanism of Bax activation, we show that blocking Bax at the dimer stage is sufficient to inhibit MOMP. Furthermore, crosslinking analysis revealed that MSN-125 disrupts the helix 6 and helix 9, and some, but not all, interactions in the BH3-groove interface. Therefore MSN-125 and MSN-50 can serve as important tools for identifying molecular interactions critical for forming functional Bax oligomers. We expect that by limiting Bax oligomerization to dimers that the compounds will also be useful for future structure-function studies of Bax and Bak.

Some molecules identified from previous screens of inhibitors of tBid-Bax mediated liposome permeabilization inhibited Bax channel activity without disrupting Bax oligomerization in the MOM or inhibiting Bak (Polster, Basanez et al. 2003; Hetz, Vitte et al. 2005). Using fluorescence spectroscopy and biochemical crosslinking, we show that MSN-50 and MSN-125 disrupt Bax oligomer formation suggesting that these compounds do not act as channel blockers. Nutlin-3a, which we used as a control, has also been reported to inhibit

Bax and Bak oligomerization thereby attenuating cytochrome c release in addition to its intended inhibitory effect on MDM2:p53 interaction(Jiang, Pabla et al. 2007). Unlike MSN-50 and MSN-125, Nutlin-3a inhibited Bax dimerization (Jiang, Pabla et al. 2007), and in mitochondria and cells it was much less potent than MSN-50 and MSN-125 (Supplementary Fig. 1b) therefore the molecular mechanism is likely different.

Bax and Bak have to insert into and permeabilize membranes therefore it is not surprising that small molecules that alter the physical properties of membranes such as dibucaine, propranolol and cholesterol have all been shown to partially inhibit the insertion of Bax into membranes thereby reducing apoptosis (Polster, Basanez et al. 2003; Christenson, Merlin et al. 2008). However, gross perturbation of cellular membranes is likely to have wide ranging effects on cellular physiology (e.g. dibucaine is an anesthetic and propranolol is beta-adrenergic antagonist used to treat high blood pressure), meaning such molecules are unlikely to be useful probes for studying the molecular mechanism of Bax and Bak activation or as leads for the development of apoptosis inhibiting pharmaceuticals.

In addition to molecular mechanism studies, small molecules that disrupt both Bax and Bak protein-protein interactions are desirable for cellular analyses. For example, prior to our studies the potential biological benefit of inhibiting Bax and Bak was not clear. Pharmacological inhibition of MOMP by blocking Bax and

Bak oligomerization may have generated 'undead' cells unable to replicate and that may have very limited biological activity. However, our data with HCT116 cells demonstrates that if apoptosis is inhibited prior to MOMP it allows cells that would otherwise die to survive and grow suggesting that inhibition of Bax and Bak could be of therapeutic benefit. Finally, we speculate that the relatively long and variable lag time between the intoxication and the onset of MOMP enables inhibition of Bax and Bak subsequent to exposure to glutamate to inhibit death of primary neurons. Our result with in vitro cultured neurons has confirmed this speculation and strongly suggests that transient inhibition of Bax and/or Bak may be of therapeutic benefit in treating acute cell stress in circumstances like ischemia reperfusion, epileptic seizures, for burn patients or for mitigating dose limiting side effects of some cancer treatments.

Methods

Compounds

Diversity-oriented synthesis of the compounds screened including MSN125, MSN50 and the synthesis of DAN004 is described in the Supplementary Information section. Nutlin-3a was obtained from Selleck.

Protein purification

Recombinant murine tBid or cBid were purified as described previously (Shamas-Din, Bindner et al. 2013). Recombinant murine Bim was purified as described previously (Sarosiek, Chi et al. 2013). Recombinant human Bcl-XL, Bax and the mutants of Bax with a single cysteine at position 126 or 134 were expressed and purified as described previously (Billen, Kokoski et al. 2008; Lovell, Billen et al. 2008).

Liposome preparation and permeabilization assay

Liposomes of mitochondria-like composition encapsulating ANTS/DPX (Life Technologies) were prepared and assayed as described previously (Billen, Kokoski et al. 2008). To assay compounds as Bax inhibitors, fluorescence (excition at 355 nm and emission 520 nm) was measured in the Tecan microplate reader for 15-30 min at 37^0C in the presence of compounds and liposomes but without Bax and tBid to obtain background values and correct for compound fluorescence (F_0). Bax and tBid (added in that order) were added at t_0, and then fluorescence (F) was measured for at least 2 h at 37^0C. Triton X-100 was added to a final concentration of 0.2% (w/v), and fluorescence was measured for 10 min at 37^0C and taken as F_{100}. The percentage release of ANTS/DPX was calculated as $[(F - F_0)/(F_{100} - F_0)]\times100$. For compound screening, the % inhibition was calculated by $[(\%\ Release_{Bax\ +\ tBid} - \%Release_{Bax\ +\ tBid+\ compound})/\ \%\ Release_{Bax\ +\ tBid}]*100$. Z-scores were calculated by $[(\%\ inhibition - \%\ inhibition_{population\ mean})/$

Standard deviation]. Unless indicated, all assays used 20 nM tBid and 100 nM Bax.

Mitochondria isolation and permeabilization assay

BMK mitochondria: Bax$^{-/-}$ Bak$^{-/-}$ or *Bax$^{-/-}$* baby mouse kidney (BMK) cells stably expressing the mitochondrial import peptide of Smac (1-58) fused to the red fluorescence protein, mCherry were maintained in 3 µg/ml Blasticidin (Bioshop) in DMEM containing 10% FBS (Life Technologies). Heavy membranes containing mitochondria were isolated and assayed as described previously (Shamas-Din, Satsoura et al. 2014). Briefly, membrane fractions (0.2 mg/ml) were incubated with the compound, followed by the addition of 2 nM tBid and 20 nM Bax for the *Bax$^{-/-}$ Bak$^{-/-}$* mitochondria, or 0.5 nM tBid for the *Bax$^{-/-}$* mitochondria for 30 min at 37°C. Mitochondria were then pelleted by centrifugation at 13000 *g* for 10 min. The release of Smac-mCherry was assessed by fluorometric analysis of the supernatant and pellet fractions at excitation of 580 nm and emission of 610 nm in the Tecan microplate reader. The percentage release of Smac-mCherry was calculated as $[F_{supernatant} / (F_{supernatant} + F_{pellet})] \times 100$.

Mouse liver mitochondria: Mitochondria were isolated from livers of *Bax$^{-/-}$* mice and frozen as described previously (Yamaguchi, Andreyev et al. 2007). After thawing, membrane fractions (1 mg/ml) were incubated with compound and 5 nM cBid and pelleted as described above. The supernatant and pellet fractions were

analyzed by immunoblotting using a cytochrome c antibody raised in rabbits and affinity purified in our laboratory. Immunoblots were developed using chemiluminescence and intensities were recorded using a CCD camera (DNR). Image analysis was conducted using ImageJ to quantify the release of cytochrome c.

Long term survival after replating.

HCT116 cells were seeded at a cell density of 3000 cells/well in a 96 well plate (Sarstedt) in DMEM (Life Technologies) containing 10% FBS (Sigma). After adhering, cells were treated with the indicated concentration of the inhibitors for three hours followed by actinomycin D (Sigma) for the next 4 hours. The actinomycin D containing media was replaced with drug-free media and cells were re-plated after 4 days into 24 well plates. Surviving cells were allowed to grow until the controls treated with DMSO instead of actinomycin D, reached confluence and then all the plates were stained with crystal violet (Sigma). Images of the plates were obtained using a flat-bed scanner. The fractional area of each well stained by crystal violet was determined by background detection and thresholding using Image J.

Immunofluorescence

HCT116 cells were pre-treated with 10 μM MSN-125 for three hours, followed by the addition of actinomycin D (50 ng/ml final) for 24 hours. Cells were fixed using paraformaldehyde and analyzed by immunofluorescence by double staining with primary sheep anti-cytochrome c antibody (Caprilogics) and mouse anti-Bax 6A7 monoclonal antibodies. Secondary donkey anti-sheep-Alexa Fluor 488 and goat anti-mouse-Alexa Fluor 555 (Invitrogen) antibodies were used for microscopy. The nuclei of HCT116 cells were stained with DAPI according to the manufacturer's instructions (Sigma). Cells were imaged using a Zeiss LSM710 confocal microscope and associated software.

Primary neuronal cultures

Primary neuron cultures of cerebral cortex from mouse embryos (embryonic day 14.5-15) were dissected and cultured for up to 10 days to ensure maturation of neurons as described(Mergenthaler, Kahl et al. 2012). Neurons from one embryo were considered as one independent experiment. A maximum of 3 embryos per litter were used. All animal procedures were performed in accordance with the local standards for animal care. Briefly, neurons were cultured in Neurobasal-A medium (Life Technologies) supplemented with B-27 (Life Technolgies), 0.5 mM L-glutamine and 25 μM glutamate. The medium was partially replaced on day 6 in culture with Neurobasal-A supplemented with B-27 and L-glutamine. On day 9, neurons were treated with either 25 μM or 100 μM glutamate in BSS_0 (116 mM

NaCl, 5.4 mM KCl, 0.8 mM $MgSO_4$, 1 mM NaH_2PO_4, 26.2 mM $NaHCO_3$, 10 µM glycine, 1.8 mM $CaCl_2$, 10 mM HEPES pH 7.4) for 30 minutes (37°C, 5% CO_2) after washing the cultures with PBS. Medium was pooled and added to cultures after the incubation period with or without addition of 5 µM MSN-125. Cell death was analyzed 20-24 hours after glutamate treatment by measuring lactate dehydrogenase release as previously described(Mergenthaler, Kahl et al. 2012) and normalized to total lactate dehydrogenase after volume correction. Briefly, lactate dehydrogenase concentration in medium was analyzed by measuring NADH to NAD^+ turnover (absorbance at 340 nm) in a coupled spectrophotometric assay on the Tecan microplate reader. Total lactate dehydrogenase release was measured after incubating neuronal cultures with 0.5% TritonX-100 for 30 minutes (37° C). Statistical analysis was performed in Prism 5.0 (GraphPad) or SPSS 23 (IBM). ANOVA was performed after normality testing.

Bax-Bax FRET assay

Dye- labelling of proteins: Bax mutants with a single cysteine at position 126 or 134 were labelled as described previously(Lovell, Billen et al. 2008). For labeling with fluorescent dyes, the Bax proteins were prepared without reducing agent. The concentration of Bax, was determined spectrophotometrically at 280 nm using the molar extinction coefficient 37,000 $M^{-1}cm^{-1}$. For labeling, N-N'-dimethyl-N-(iodoacetyl)-N'-(7-nitrobenzene-2-oxa-1, 3-diazol-4-yl) ethylenediamine

(IANBD; Life Technologies) or N-(7-dimethylamino-4-methylcoumarin-3-yl) maleimide (DACM; Anaspec) were prepared in DMSO and the concentrations were determined after dilution in methanol by absorbance using the dye molar extinction coefficients 25,000 $M^{-1}cm^{-1}$ at 479 nm or 27,000 $M^{-1}cm^{-1}$ at 380 nm, respectively. Bax was labeled by incubation of the protein with a 10 fold molar excess of dye in labeling buffer (10 mM HEPES pH 7, 0.2 M NaCl, 0.2 mM EDTA, 0.5% CHAPS w/v and 10% glycerol v/v) with rotation at room temperature for 2 hours in the dark. The reaction was quenched with 1mM dithiothreitol. Free dye was removed from the sample by gel filtration chromatography (Sephadex G-25 Fine, GE Healthcare Life Sciences) in the labeling buffer without CHAPS.

Bax:Bax FRET measurements: Bax:Bax binding was assessed using the FRET assay described previously in a PTI Quantamaster fluorimeter (Lovell, Billen et al. 2008). Compounds dissolved in DMSO or for controls an equivalent volume of DMSO were added after liposomes but prior to the proteins, thereby allowing correction for fluorescence that originated from the compounds. Liposomes were then equilibrated with DAC-134C- Bax and fluorescence measurements were made at an excitation of 380 nm and emission at 460 nm (F_0). A decrease in DAC fluorescence was measured upon the addition of NBD-126C-Bax and tBid (F) and results are represented as F/F_0 for reactions with and without compound.

Disuccinimidyl suberate (DSS) crosslinking

Mitochondria-like liposomes were prepared as described previously (Billen, Kokoski et al. 2008). Samples containing liposomes (125 μM total lipids) were incubated with the compounds and 5 nM tBid and 100 nM Bax at 30°C for 2 hr in a low protein binding microtiter plate (Corning). DSS (Pierce) crosslinking was performed at a final concentration of 2mM for 30min at room temperature followed by quenching with 20 mM Tris-Cl (pH 8) as described previously (Billen, Kokoski et al. 2008). Bax was detected on immunoblots using the monoclonal antibody 2D2 at a dilution of 1:10,000. Quantitative analysis of the immunoblots was performed using Image J to measure the total intensity of the dimers and larger oligomers. To combine the data from multiple independent experiments the blots were normalized using the intensity in the “no compound” lane. One sample t-test was performed in GraphPad Prism.

Disulfide crosslinking

The single-cysteine Bax mutants were constructed and designated as described before (Zhang, Subramaniam et al. 2015). The [^{35}S]Met-labeled Bax mutant proteins were synthesized in either a wheat germ-based in vitro translation (IVT) system or a transcription/translation (TNT) coupled SP6 RNA polymerase/reticulocyte lysate system (Promega) as described (Lin, Liang et al. 2001; Zhang, Subramaniam et al. 2015). After adding 20 μg/ml of cycloheximide to terminate translation, 15 or 7 μl of the resultant Bax proteins from the IVT or

TNT system, respectively, were mixed with mitochondria containing 0.5 mg/ml total protein. The mitochondria were purified from liver of *Bak*$^{-/-}$ mice, thereby also lacking Bax as it is a cytosolic protein in the liver. Mitochondria were treated with 18 mM N-ethylmaleimide (NEM) to block the sulfhydryl groups of mitochondrial proteins, thereby preventing them from crosslinking with the single-cysteine Bax mutants via disulfides in the following oxidation reactions. In addition, 16 μM of a peptide containing residues 53-86 of Bax including the BH3-region (BH3-peptide) that activates Bax (Tan, Dlugosz et al. 2006), MSN-125 of indicated concentration, and 1 mM of DTT were added and the samples were incubated at 37^{o}C for 1 h. The resulting mitochondria and bound Bax were pelleted by centrifugation at 4^{o}C and 13,000 g for 5 min, and then suspended in 100 μl buffer A (110 mM KOAc, 1 mM $Mg(OAc)_2$ and 25 mM Hepes, pH 7.5). The resulting samples were treated with 1 mM $NaAsO_4$ to eliminate the residual DTT, and then divided into two aliquots. One aliquot was treated with redox catalyst copper (II)(1,10-phenanthroline)$_3$ (CuPhe; consisting of 0.3 mM $CuSO_4$ and 1 mM 1,10-phenanthroline) to induce disulfide crosslinking. After incubation on ice for 30 min, the oxidation reactions were quenched with 18 mM NEM, 100mM ethylenediaminetetraacetic acid (EDTA) and 1 mM $NaAsO_4$. As the “0 min” control, the other aliquot was treated with NEM, EDTA and $NaAsO_4$ to block the disulfide crosslinking prior to the addition of CuPhe. The resulting samples were precipitated with Cl_3CCOOH, and then analyzed with non-reducing and as

controls (not shown) reducing SDS-PAGE (15%), followed by phosphor-imaging to detect the radioactive Bax proteins and their adducts.

References

Annis, M. G., E. L. Soucie, et al. (2005). "Bax forms multispanning monomers that oligomerize to permeabilize membranes during apoptosis." EMBO J 24(12): 2096-2103.

Billen, L. P., C. L. Kokoski, et al. (2008). "Bcl-XL inhibits membrane permeabilization by competing with Bax." PLoS Biol 6(6): e147.

Bombrun, A., P. Gerber, et al. (2003). "3,6-dibromocarbazole piperazine derivatives of 2-propanol as first inhibitors of cytochrome c release via Bax channel modulation." J Med Chem 46(21): 4365-4368.

Christenson, E., S. Merlin, et al. (2008). "Cholesterol effects on BAX pore activation." J Mol Biol 381(5): 1168-1183.

Czabotar, P. E., D. Westphal, et al. (2013). "Bax crystal structures reveal how BH3 domains activate Bax and nucleate its oligomerization to induce apoptosis." Cell 152(3): 519-531.

D'Orsi, B., H. Bonner, et al. (2012). "Calpains are downstream effectors of bax-dependent excitotoxic apoptosis." J Neurosci 32(5): 1847-1858.

D'Orsi, B., S. M. Kilbride, et al. (2015). "Bax regulates neuronal Ca2+ homeostasis." J Neurosci 35(4): 1706-1722.

Degenhardt, K., R. Sundararajan, et al. (2002). "Bax and Bak independently promote cytochrome C release from mitochondria." J Biol Chem 277(16): 14127-14134.

Delbridge, A. R., L. J. Valente, et al. (2012). "The role of the apoptotic machinery in tumor suppression." Cold Spring Harb Perspect Biol 4(11).

Dewson, G., S. Ma, et al. (2012). "Bax dimerizes via a symmetric BH3:groove interface during apoptosis." Cell Death Differ 19(4): 661-670.

Engel, T., N. Plesnila, et al. (2011). "In vivo contributions of BH3-only proteins to neuronal death following seizures, ischemia, and traumatic brain injury." J Cereb Blood Flow Metab 31(5): 1196-1210.

Fannjiang, Y., C. H. Kim, et al. (2003). "BAK alters neuronal excitability and can switch from anti- to pro-death function during postnatal development." Dev Cell 4(4): 575-585.

Hardwick, J. M. and L. Soane (2013). "Multiple functions of BCL-2 family proteins." Cold Spring Harb Perspect Biol 5(2).

Hetz, C., P. A. Vitte, et al. (2005). "Bax channel inhibitors prevent mitochondrion-mediated apoptosis and protect neurons in a model of global brain ischemia." J Biol Chem 280(52): 42960-42970.

Hsu, Y. T., K. G. Wolter, et al. (1997). "Cytosol-to-membrane redistribution of Bax and Bcl-X(L) during apoptosis." Proc Natl Acad Sci U S A 94(8): 3668-3672.

Hsu, Y. T. and R. J. Youle (1998). "Bax in murine thymus is a soluble monomeric protein that displays differential detergent-induced conformations." J Biol Chem 273(17): 10777-10783.

Iyer, S., F. Bell, et al. (2015). "Bak apoptotic pores involve a flexible C-terminal region and juxtaposition of the C-terminal transmembrane domains." Cell Death Differ 22(10): 1665-1675.

Jiang, M., N. Pabla, et al. (2007). "Nutlin-3 protects kidney cells during cisplatin therapy by suppressing Bax/Bak activation." J Biol Chem 282(4): 2636-2645.

Leber, B., F. Geng, et al. (2010). "Drugs targeting Bcl-2 family members as an emerging strategy in cancer." Expert Rev Mol Med 12: e28.

Leber, B., J. Lin, et al. (2007). "Embedded together: the life and death consequences of interaction of the Bcl-2 family with membranes." Apoptosis 12(5): 897-911.

Lin, J., Z. Liang, et al. (2001). "Membrane topography and topogenesis of prenylated Rab acceptor (PRA1)." J Biol Chem 276(45): 41733-41741.

Lovell, J. F., L. P. Billen, et al. (2008). "Membrane binding by tBid initiates an ordered series of events culminating in membrane permeabilization by Bax." Cell 135(6): 1074-1084.

Ma, S., C. Hockings, et al. (2013). "Assembly of the Bak apoptotic pore: a critical role for the Bak protein alpha6 helix in the multimerization of homodimers during apoptosis." J Biol Chem 288(36): 26027-26038.

Mergenthaler, P., U. Dirnagl, et al. (2004). "Pathophysiology of stroke: lessons from animal models." Metab Brain Dis 19(3-4): 151-167.

Mergenthaler, P., A. Kahl, et al. (2012). "Mitochondrial hexokinase II (HKII) and phosphoprotein enriched in astrocytes (PEA15) form a molecular switch governing cellular fate depending on the metabolic state." Proc Natl Acad Sci U S A 109(5): 1518-1523.

Mikhailov, V., M. Mikhailova, et al. (2003). "Association of Bax and Bak homo-oligomers in mitochondria. Bax requirement for Bak reorganization and cytochrome c release." J Biol Chem 278(7): 5367-5376.

Moldoveanu, T., A. V. Follis, et al. (2014). "Many players in BCL-2 family affairs." Trends Biochem Sci 39(3): 101-111.

Peixoto, P. M., S. Y. Ryu, et al. (2009). "MAC inhibitors suppress mitochondrial apoptosis." Biochem J 423(3): 381-387.

Peixoto, P. M., O. Teijido, et al. (2015). "MAC inhibitors antagonize the pro-apoptotic effects of tBid and disassemble Bax / Bak oligomers." J Bioenerg Biomembr.

Polster, B. M., G. Basanez, et al. (2003). "Inhibition of Bax-induced cytochrome c release from neural cell and brain mitochondria by dibucaine and propranolol." J Neurosci 23(7): 2735-2743.

Reayi, A. and P. Arya (2005). "Natural product-like chemical space: search for chemical dissectors of macromolecular interactions." Curr Opin Chem Biol 9(3): 240-247.

Ruffolo, S. C. and G. C. Shore (2003). "BCL-2 selectively interacts with the BID-induced open conformer of BAK, inhibiting BAK auto-oligomerization." J Biol Chem 278(27): 25039-25045.

Sarosiek, K. A., X. Chi, et al. (2013). "BID preferentially activates BAK while BIM preferentially activates BAX, affecting chemotherapy response." Mol Cell 51(6): 751-765.

Satsoura, D., N. Kucerka, et al. (2012). "Interaction of the full-length Bax protein with biomimetic mitochondrial liposomes: a small-angle neutron scattering and fluorescence study." Biochim Biophys Acta 1818(3): 384-401.

Shamas-Din, A., S. Bindner, et al. (2013). "tBid undergoes multiple conformational changes at the membrane required for Bax activation." J Biol Chem.

Shamas-Din, A., D. Satsoura, et al. (2014). "Multiple partners can kiss-and-run: Bax transfers between multiple membranes and permeabilizes those primed by tBid." Cell Death Dis 5: e1277.

Subburaj, Y., K. Cosentino, et al. (2015). "Bax monomers form dimer units in the membrane that further self-assemble into multiple oligomeric species." Nat Commun 6: 8042.

Sun, Y. F., L. Y. Yu, et al. (2001). "Neuron-specific Bcl-2 homology 3 domain-only splice variant of Bak is anti-apoptotic in neurons, but pro-apoptotic in non-neuronal cells." J Biol Chem 276(19): 16240-16247.

Szeto, H. H. (2008). "Mitochondria-targeted cytoprotective peptides for ischemia-reperfusion injury." Antioxid Redox Signal 10(3): 601-619.

Tan, C., P. J. Dlugosz, et al. (2006). "Auto-activation of the apoptosis protein Bax increases mitochondrial membrane permeability and is inhibited by Bcl-2." J Biol Chem 281(21): 14764-14775.

Tan, C., P. J. Dlugosz, et al. (2006). "Auto-activation of the apoptosis protein Bax increases mitochondrial membrane permeability and is inhibited by Bcl-2." J. Biol. Chem. 281(21): 14764-14775, PMCID: PMC2826894.

Tovar, C., J. Rosinski, et al. (2006). "Small-molecule MDM2 antagonists reveal aberrant p53 signaling in cancer: implications for therapy." Proc Natl Acad Sci U S A 103(6): 1888-1893.

Uchime, O., Z. Dai, et al. (2016). "Synthetic Antibodies Inhibit Bcl-2-associated X Protein (BAX) through Blockade of the N-terminal Activation Site." J Biol Chem 291(1): 89-102.

Uo, T., Y. Kinoshita, et al. (2005). "Neurons exclusively express N-Bak, a BH3 domain-only Bak isoform that promotes neuronal apoptosis." J Biol Chem 280(10): 9065-9073.

Wei, M. C., T. Lindsten, et al. (2000). "tBID, a membrane-targeted death ligand, oligomerizes BAK to release cytochrome c." Genes Dev 14(16): 2060-2071.

Willis, S. N., J. I. Fletcher, et al. (2007). "Apoptosis initiated when BH3 ligands engage multiple Bcl-2 homologs, not Bax or Bak." Science 315(5813): 856-859.

Wilson-Annan, J., L. A. O'Reilly, et al. (2003). "Proapoptotic BH3-only proteins trigger membrane integration of prosurvival Bcl-w and neutralize its activity." J Cell Biol 162(5): 877-887.

Yamaguchi, R., A. Andreyev, et al. (2007). "Mitochondria frozen with trehalose retain a number of biological functions and preserve outer membrane integrity." Cell Death Differ 14(3): 616-624.

Zhang, Z., S. Subramaniam, et al. (2015). "BH3-in-groove dimerization initiates and helix 9 dimerization expands Bax pore assembly in membranes." EMBO J.

Zhang, Z., W. Zhu, et al. (2010). "Bax forms an oligomer via separate, yet interdependent, surfaces." J Biol Chem 285(23): 17614-17627.

Acknowledgements

The 6A7 and 2D2 antibodies for Bax were a generous gift from Richard Youle. The BMK cells were a generous gift from Dr. Eileen White. We thank Mina Falcone for conducting the compound partitioning experiments and Corrie Griffiths for her assistance in conducting the screen.

Funding

This work was supported by the Ontario Institute for Cancer Research through funding provided by the Government of Ontario, the Terry Fox Research Institute and the Canada Research Chairs program (DWA), the National Cancer Institute of Canada (PA), Department of Science and Technology (PA), Council of Scientific and Industrial Research (PhD fellowship to RJ), the Shanghai Municipal Science and Technology Commission 10410704000 (JY and DWA), the Shanghai Municipal Education Commission J50201 (JY), the Seventh Framework Programme for Research and Technological Development of the European Union (FP7/2008–2013) under Grant Agreement 627951 (Marie Curie IOF to PM), and the United States National Institute of Health grant GM062964 (JL).

The authors declare no competing interests.

Figures

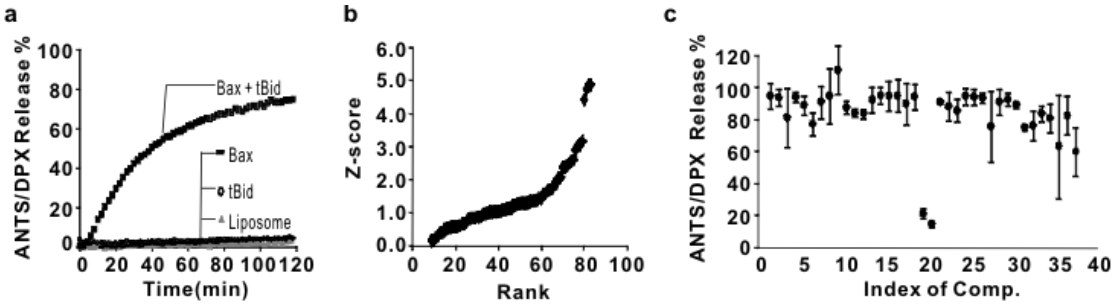

Figure 1. Identification of inhibitors of tBid and Bax mediated liposome permeabilization.

(a) Bax and tBid permeabilize liposomes releasing encapsulated ANTS and DPX resulting in an increase in fluorescence. Fluorescence measurements were recorded every 2 min for 120 min.

(b) Z-score versus rank for 86 benzofuran- and tetrahydroaninoquinoline-based compounds screened in triplicate at 10 μM final concentration. All compounds with a Z-score >0 for inhibiting tBid/Bax mediated liposome permeabilization are shown. Hits were defined as compounds that reduced normalized ANTS/DPX release by at least 2 standard deviations below the plate mean ($Z \geq 2$).

(c) Primary ANTS/DPX release screening data for 37 tetrahydroquinoline-based compounds designed based on the structures of BJ-1 and BJ-1-BP. MSN-125 and MSN-50 (Index 19 and 20) inhibited liposomes permeabilization normalized to dye release by tBid and Bax alone. End-point release was measured after incubation for duplicate samples for 120 min. Mean ± range.

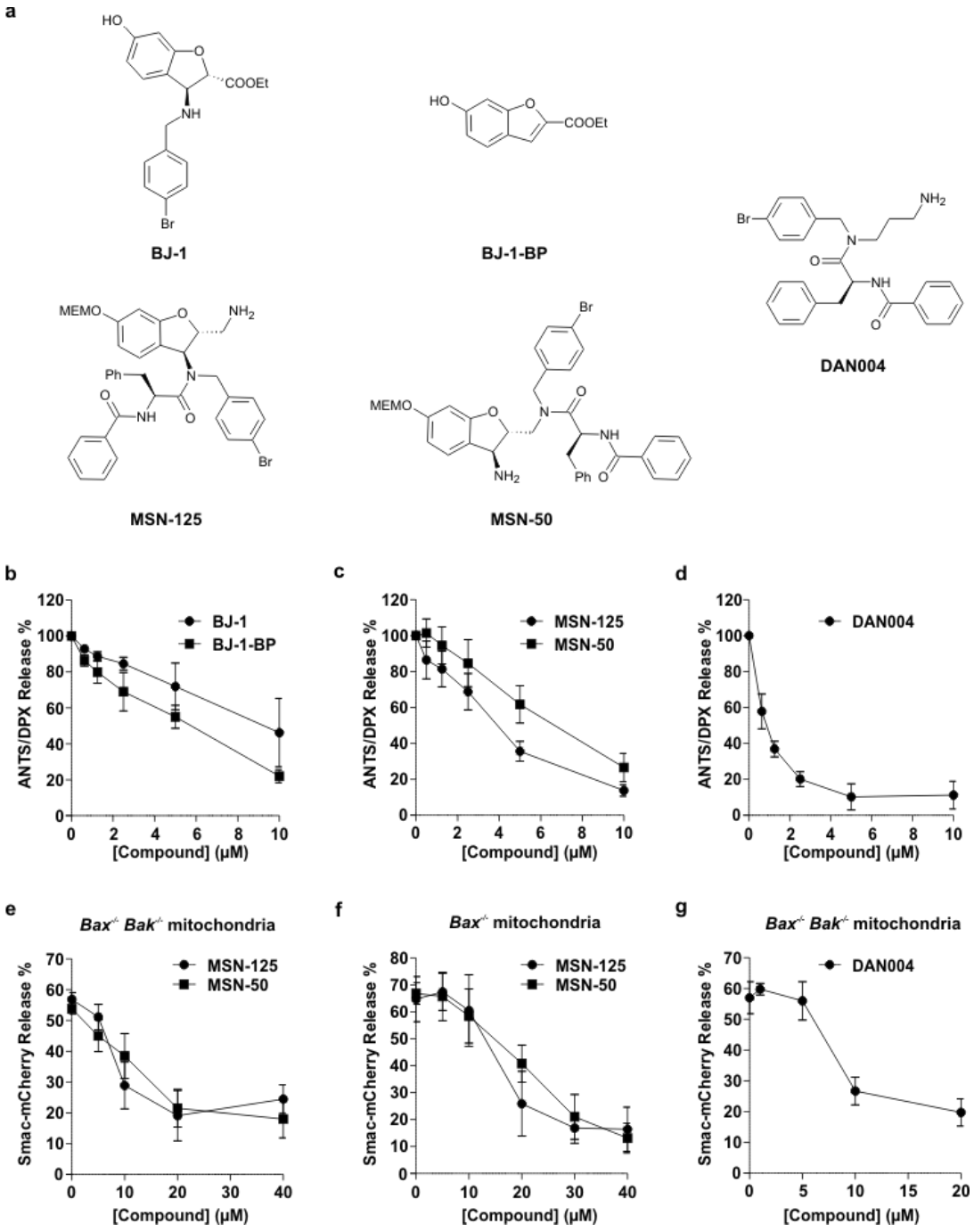

Figure 2. Small molecule inhibitors that prevent Bax mediated permeabilization of liposomes and mitochondria.

(a) Molecular structures of BJ-1, BJ-1-BP, MSN-125, MSN-50 and DAN004. MEMO is β-MethoxyEthoxyMethylether.

(b-d) Concentration-dependent inhibition of liposome permeabilization by tBid and Bax by the indicated concentrations of (b) BJ-1 and BJ-1-BP, (c) MSN-125 and MSN-50, and (d) DAN004. Results are normalized to reactions without compound. Mean ± SD, n≥3.

(e-g) Permeabilization of mitochondria isolated from (e.g.) *Bax*$^{-/-}$ *Bak*$^{-/-}$ or (f) *Bax*$^{-/-}$ BMK cells expressing Smac-mCherry incubated with (e.g.) tBid and Bax or (f) tBid and the compounds as indicated. Release of Smac-mCherry was determined by pelleting the mitochondria by centrifugation and measuring the mCherry fluorescence in the supernatant and pellet fractions. Mean ± SD, n≥3.

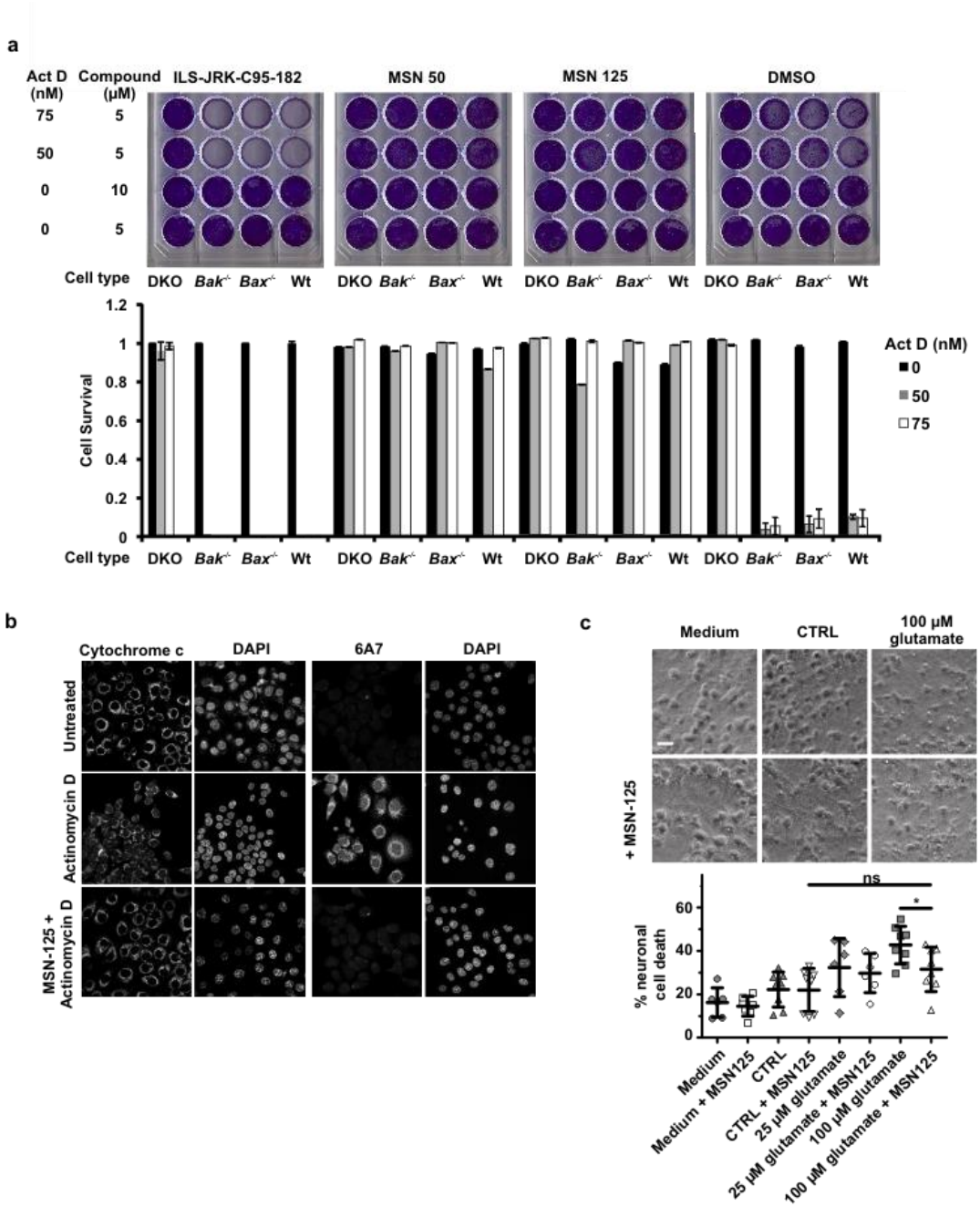

Figure 3. MSN-50 and MSN-125 protect HCT116 cells and primary cortical neurons from apoptosis.

(a) MSN-50 and MSN-125 but not the negative controls ILS-JRK-C95-182 and DMSO conferred long term survival to HCT-116 cells exposed to actinomycin D. After replating viable cells were stained with crystal violet (top panel). Bottom panel: quantification of cell growth after treatment as in the top panel, mean +/- SD, n=3.

(b) In cells treated with actinomycin D MSN-125 prevents exposure of the N-terminal Bax epitope that indicates activation. HCT116 cells were treated with 10 μM MSN-125 for 3 hours before actinomycin D treatment for 24 hours. Cells were fixed and immunofluorescence was performed with primary antibodies against active Bax (6A7) or cytochrome c. Nuclei were stained with DAPI.

(c) MSN-125 (5 μM) protects neurons from prior treatment with 100 μM glutamate (in BSS_0) to induce glutamate excitotoxicity. Medium – neurons incubated in the culture medium without wash; CTRL – neurons incubated in BSS_0. Phase contrast images (upper panels) and lactate dehydrogenase release (Lower panel). Individual data points and mean ± SD are displayed, n=6-8 individual experiments. * $p<0.05$, one-way ANOVA, Bonferroni post-hoc; ns = non-significant.

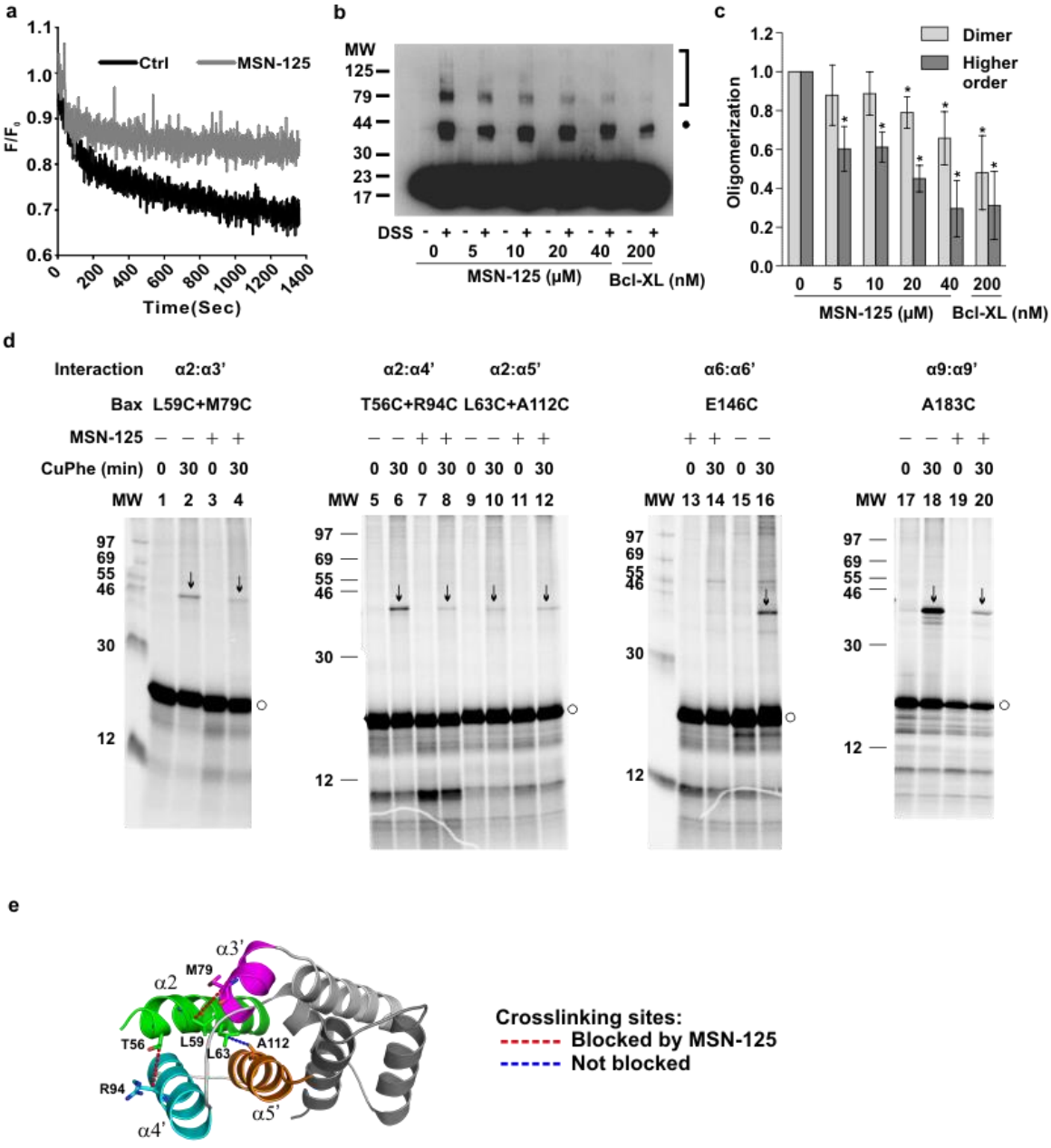

Figure 4. MSN-125 restricts Bax oligomerization beyond dimer formation.

(a) MSN-125 (10 μM) interferes with DAC-Bax-134C binding to NBD-Bax-126C on liposomes measured by FRET. F_0 is DAC-Bax-134C fluorescence before addition of NBD-Bax-126C. Binding of the proteins resulted in a time dependent

decrease in DAC-Bax-134C fluorescence (F) due to FRET between DAC and NBD. Addition of MSN-125 decreased FRET compared to no compound control (Ctrl). One representative measurement from n=3 is shown.

(b) MSN-125 blocks tBid-induced Bax oligomerization in liposomes. Bax oligomers were detected after chemical crosslinking with DSS by immunoblotting for Bax. Bax monomers migrate at ~ 20 kDa; dimers, solid dot; larger oligomers, bracket. MW, migration of molecular weight markers (kDa). One representative immunoblot of n=3 is shown.

(c) Quantification of crosslinking data from b. Mean ± SD for n=3. * $p<0.05$; one-sample t- test compared to the mean of the no compound control.

(d) MSN-125 inhibits some, but not all, interactions in Bax oligomers. Disulfide crosslinking of radioactive Bax with a single cysteine at the indicated positions incubated with mitochondria lacking Bax and Bak in the absence or presence of MSN-125. MW, migration positions of molecular weight markers (kDa); Bax monomers, circles; Disulfide-linked Bax dimers, arrows. Representative data from n ≥ 2 experiments is shown.

(e) Cartoon representation of the Bax BH3-groove dimer structure (PDB#4BDU) shown with the green BH3/α2 helix of one monomer binding to the groove of the other monomer comprised of magenta α3', cyan α4', and orange α5' helices. Disulfide crosslinking: dotted line-linked residues.

Supplementary Figures

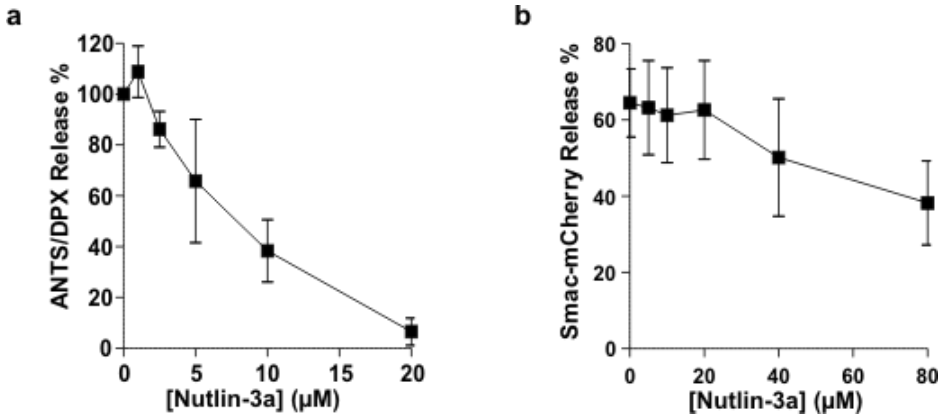

Supplementary Figure 1. Nutlin-3a inhibits Bax mediated permeabilization of liposomes and mitochondria

(a) Inhibition of cBid and Bax mediated liposome permeabilization by the indicated concentrations of Nutlin-3a. Mean ± SD, n=3.

(b) Inhibition of cBid and Bax mediated permeabilization of *Bax*$^{-/-}$ *Bak*$^{-/-}$ mitochondria by the indicated concentrations of Nutlin-3a. Mean ± SD, n=3.

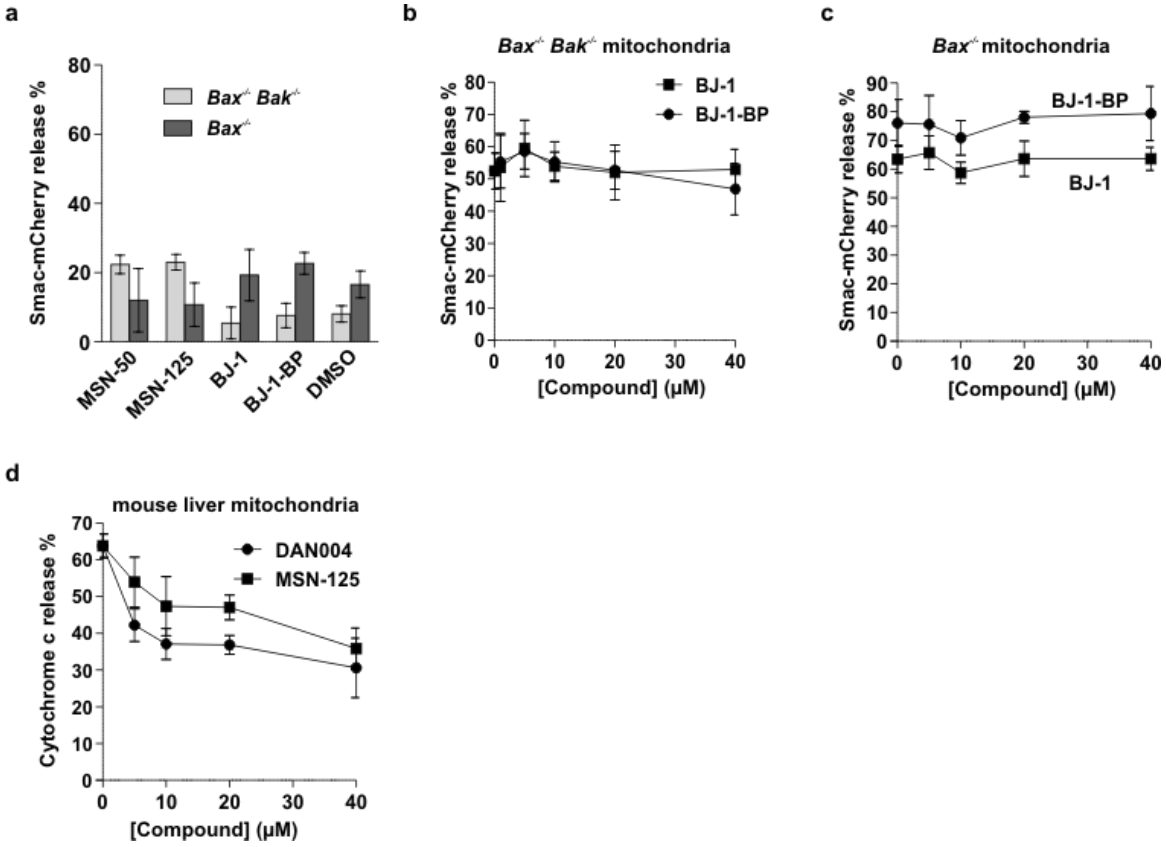

Supplementary Figure 2: DAN004 inhibits but BJ-1 and BJ-BP do not inhibit MOMP.

(a-c) Permeabilization of mitochondria isolated from BMK cells stably expressing Smac-mCherry assayed as described in Figure 2e-f.

(a) Controls illustrate that 40 μM of the indicated compounds do not permeabilize *Bax*$^{-/-}$ *Bak*$^{-/-}$ or *Bax*$^{-/-}$ mitochondria. Mean ± SD, n=3.

(b) BJ-1 and BJ-1-BP do not prevent permeabilization of *Bax*$^{-/-}$ *Bak*$^{-/-}$ mitochondria by tBid and Bax. Mean ± SD, n=3.

(c) BJ-1 and BJ-1-BP do not prevent permeabilization of *Bax*$^{-/-}$ mitochondria by tBid. Mean ± SD, n=3.

(d) DAN004 and MSN-125 inhibit Bak mediated permeabilization of *Bax*$^{-/-}$ mitochondria incubated with tBid. Permeabilization was measured by % of cytochrome c released from the mitochondria determined by immunoblotting. Mean ± SD, n = 3.

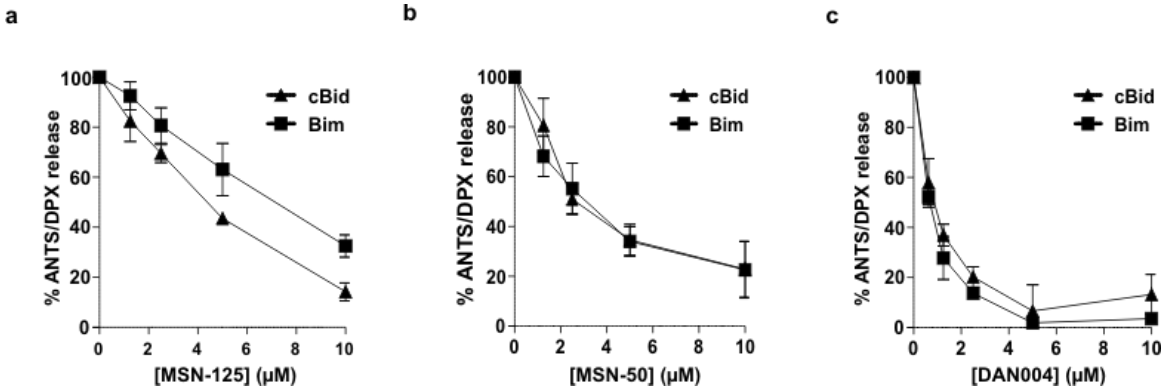

Supplementary Figure 3: MSN-125, MSN-50 and DAN004 inhibit BH3-protein activated Bax mediated liposome permeabilization

(a-c) Inhibition of liposome permeabilization by Bax and 5nM cBid or 5nM Bim by the indicated concentrations of (a) MSN-125, (b) MSN-50 or (c) DAN004.

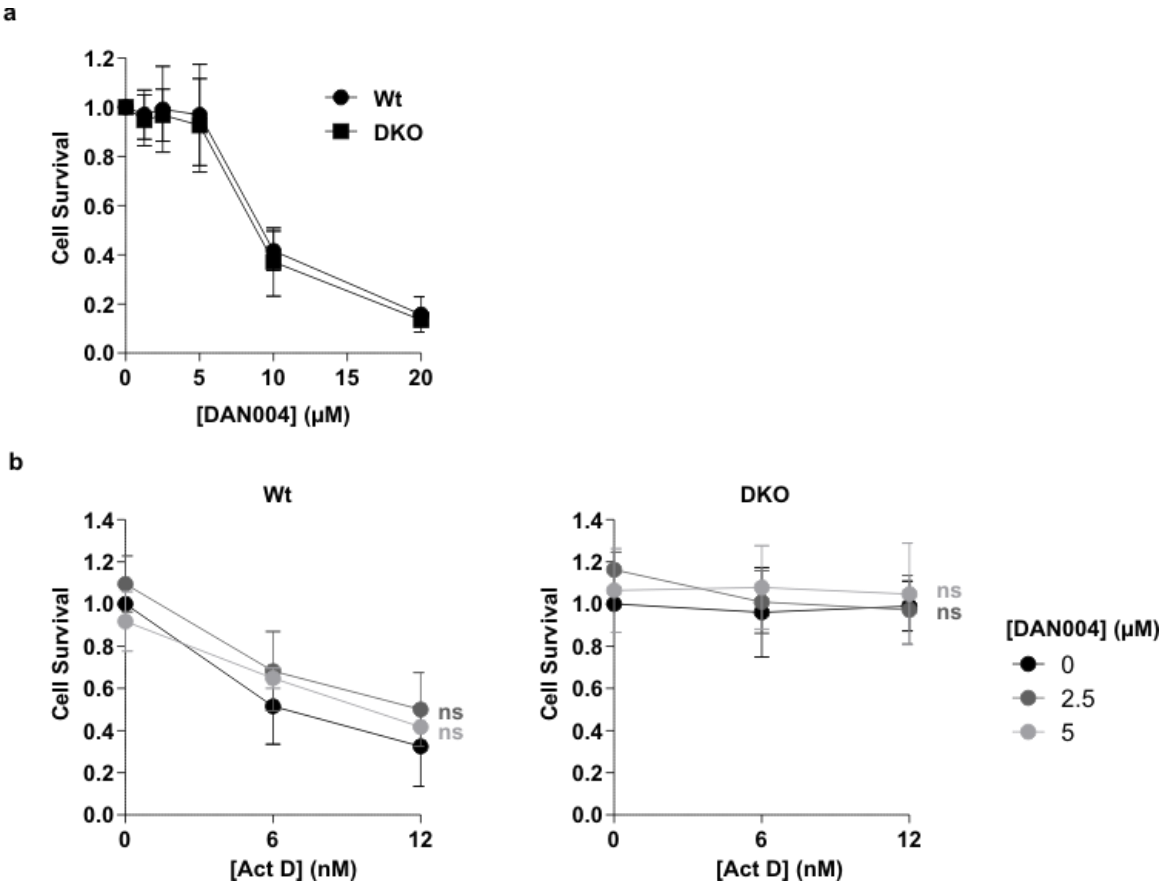

Supplementary Figure 4: DAN004 kills Wt and DKO cells and does not confer protection against actinomycin D.

(a) Cell viability of HCT116 Wt and *Bax*$^{-/-}$ *Bak*$^{-/-}$ DKO cells exposed to DAN004 for 8 hours. Cells were replated after 4 days and surviving cells were stained with crystal violet. Results are normalized to DMSO treated controls. Mean ± SD, n=4 independent experiments.

(b) HCT116 Wt and DKO cells treated with DAN004 for 4 hours followed by treatment with both DAN004 and the indicated doses of actinomycin D for 4 hours. Cells were replated after 4 days and cell survival was assessed as described above. Statistical analysis was conducted using two-way ANOVA with the Bonferroni post- test comparing respective DAN004 treated cells versus untreated cells. ns= non-significant for P values >0.05; Mean ± SD, n=3 independent experiments.

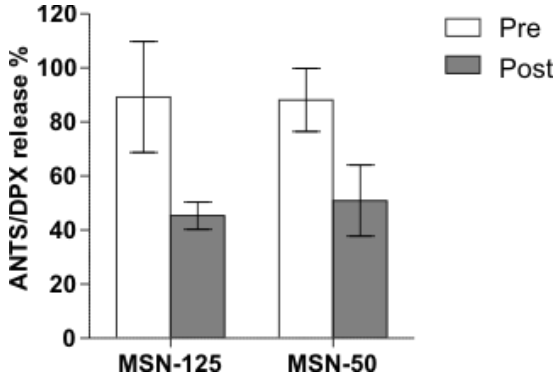

Supplementary Figure 5: MSN-50 and MSN-125 do not inhibit liposome permeabilization by partitioning into the membrane.

Liposomes pre-incubated with 10 μM MSN-125 or MSN-50 and passed over a gel filtration column to remove unpartitioned compound (Pre) released ANTS/DPX in response to tBid and Bax. In control reactions, MSN-125 or MSN-50 was added after liposomes were passed over the column (Post).

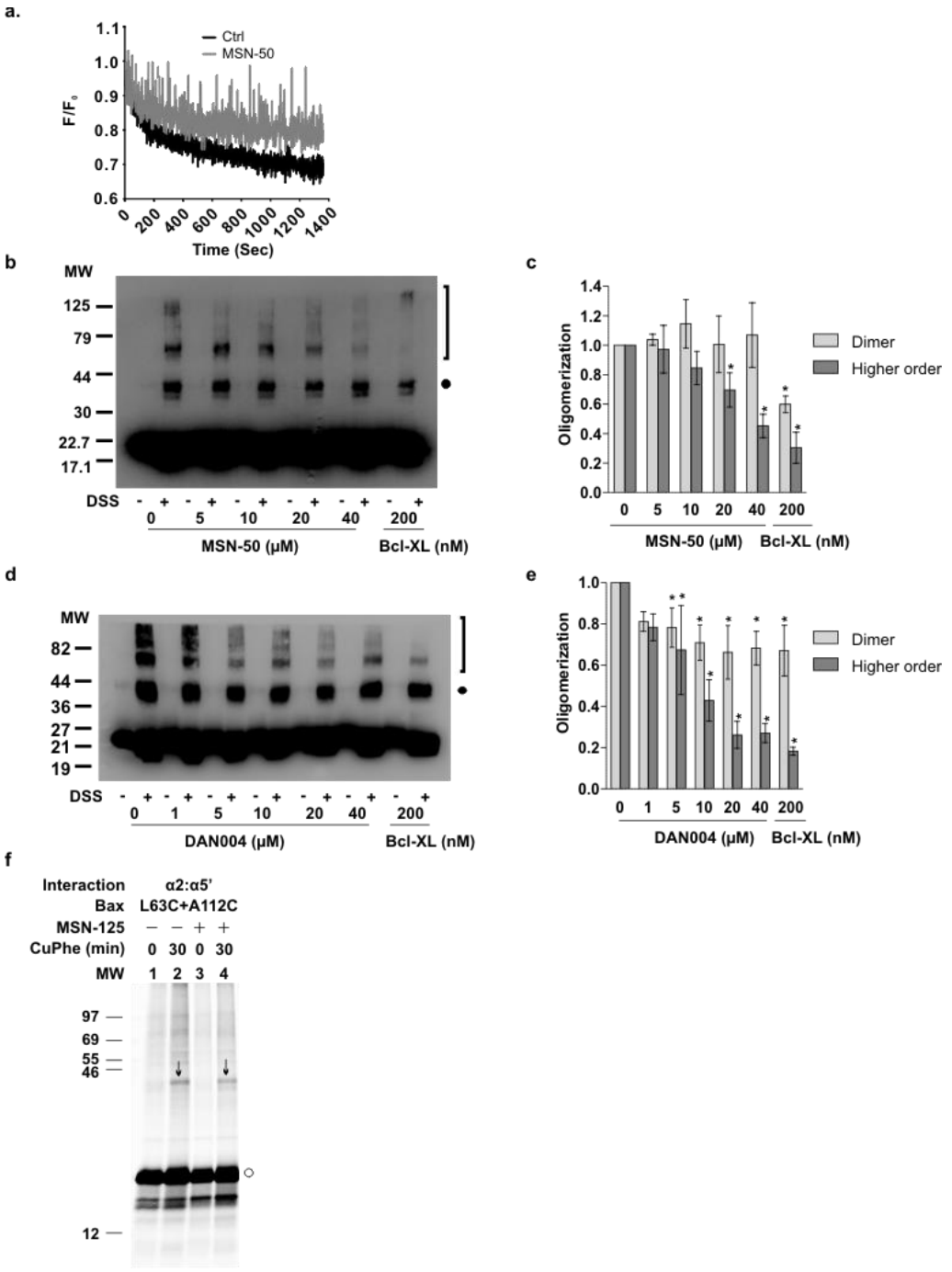

Supplementary Figure 6: MSN-50 and DAN004 disrupt Bax oligomerization. (a) Disruption of FRET between DAC-Bax-134C and NBD-Bax-126C by 10 μM MSN-50 in the presence of liposomes assayed as described in Fig. 4a.

(b-e) Chemical crosslinking of Bax oligomers assayed as described in Fig. 4b. One representative immunoblot of n=3 is are shown in (b,d) and immunoblot band intensities quantified for three independent replicates (c,e).

(f) Disulfide crosslinking of the indicated single-cysteine Bax mutants assayed as described in Fig. 4d, except that the Bax proteins were synthesized in the TNT system. One representative data from n=2 experiments is shown.

Supplementary Table

Supplementary Table 1: Inhibition of cBid and Bax mediated liposome permeabilization by analogs of MSN-50 and MSN-50

Compound ID:	Structure	ANTS/ DPX Release %
ILS-JRK-3-37	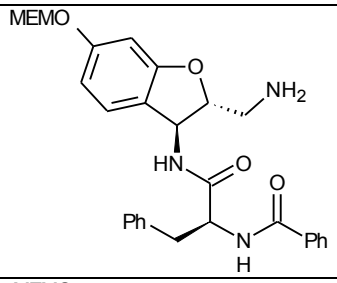	68
ILS-JRK-3-41	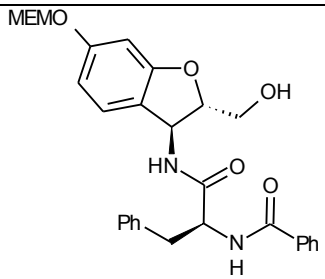	91
ILS-JRK-3-45	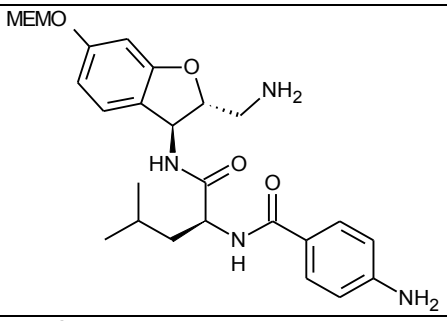	94
ILS-JRK-3-31	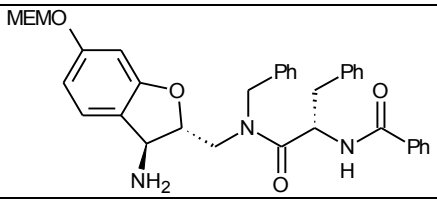	45

ILS-JRK-3-39	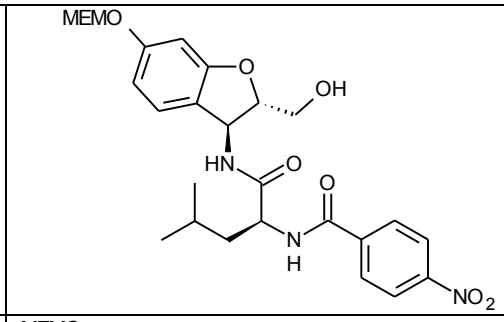	104
ILS-JRK-3-29	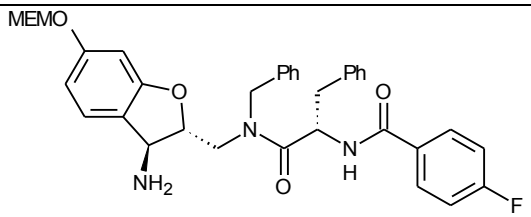	94
ILS-JRK-3-34	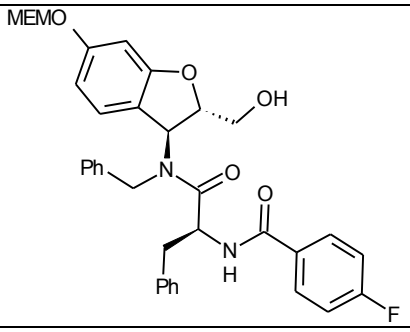	95
ILS-JRK-3-32	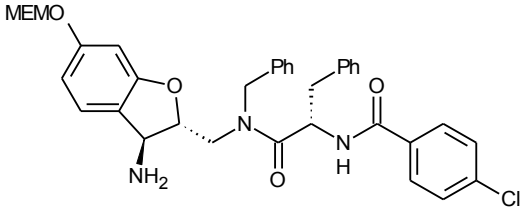	145
ILS-JRK-C95-124 (1)	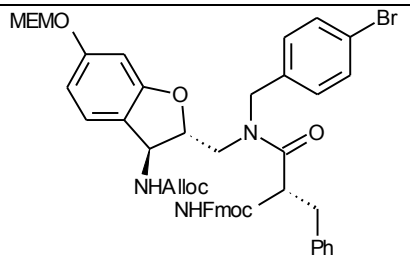	93

ILS-JRK-C95-140	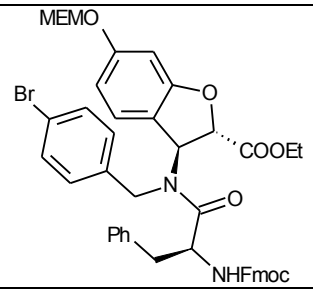	93
ILS-JRK-C95-182	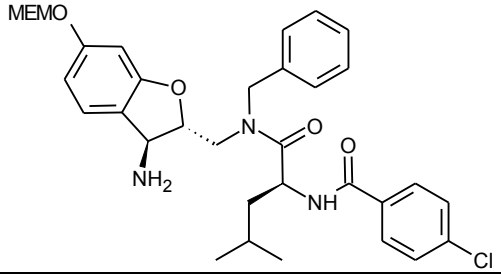	76

Supplementary Methods

Supplementary Information: Synthesis of MSN-50, MSN-125 and DAN004

Experimental Section for the Synthesis of Small Molecules MSN-50 and MSN-125

Scheme 1: Synthesis of enantioenriched benzofuran-based diamine scaffold

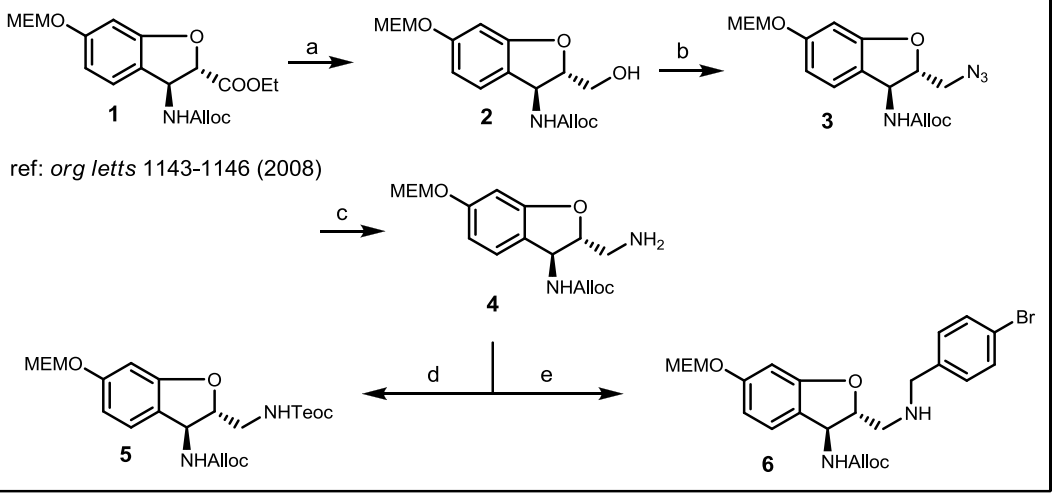

Reagents and conditions: a) $LiBH_4$, THF, 0° C to rt, 2 h; b) DPPA, TPP, DEAD, THF, 0 °C, 2h; c) TPP, H_2O, THF, rt, 12 h; d) triphosgene, trimethylsilyl ethanol, py, CH_2Cl_2, 0 °C, 4h; e) *p*-bromobenzaldehyde, $NaCNBH_3$, TMOF, AcOH, MeOH, rt, 4 h.

Scheme 2

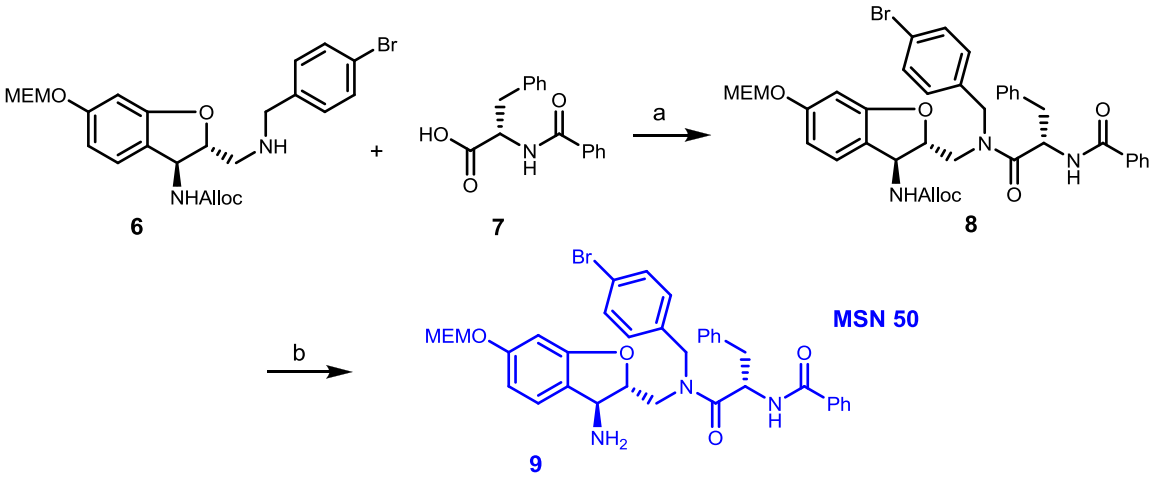

Reagents and conditions: a) PyBop, DIPEA, CH_2Cl_2, rt, 12 h; b) $Pd(PPh_3)_4$, morpholine, CH_2Cl_2, 0 °C to rt, 2 h.

Scheme 3

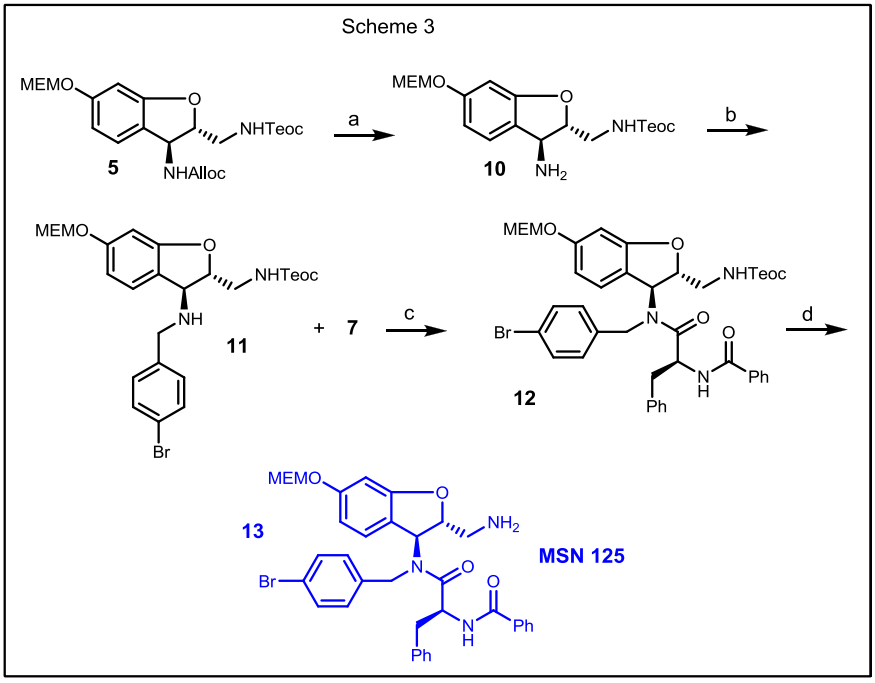

Reagents and conditions: a) $Pd(PPh_3)_4$, morpholine, CH_2Cl_2, 0 °C to rt, 2h; b) *p*-bromobenzaldehyde, $NaCNBH_3$, TMOF, AcOH, MeOH, rt, 4 h; c) PyBop, DIPEA, CH_2Cl_2, rt, 12 h; d) TBAF, THF, 0 °C to rt, 2 h.

Experimental Section

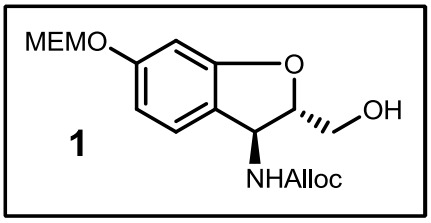

To a stirred solution of compound **1** 0.5 g, 1.26 mmol) in dry THF (10 mL) was added a solution of 2M $LiBH_4$ in THF of (0.62 mL, 1.26 mmol) at 0 °C under inert atmosphere. The reaction was allowed to warm to room temperature and stirred for 3 hours. The reaction

mixture was quenched by addition of a saturated *aq*. NH_4Cl, extracted with ethyl acetate, washed with brine, dried over anhydrous $MgSO_4$ and concentrated *in vacuo*. Purification by flash chromatography (40% ethyl acetate in hexane) afforded compound **2** (0.38 g, 80 %) as a white solid. ^1H NMR ($CDCl_3$, 400 MHz): 3.21 (s, 3H), 3.39 (m, 2H), 3.81-3.88 (m, 4H), 4.59-4.61 (m, 3H), 5.14-5.35 (m, 6H), 5.90-5.94 (m, 1H), 6.58 (s, 1H), 6.63 (d, *J* = 2.0 Hz, 1H), 7.16 (d, *J* = 2.0 Hz, 1H); ^{13}C NMR ($CDCl_3$, 100 MHz): 56.0, 59.4, 63.9, 66.5, 68.1, 71.9, 91.8, 93.9, 98.4, 99.4, 109.9, 118.6, 118.7, 125.8, 132.7, 156.5, 160.0, 161.2; MS: (ES_+) m/z = 354 (m+1), HPLC purity (>97%).

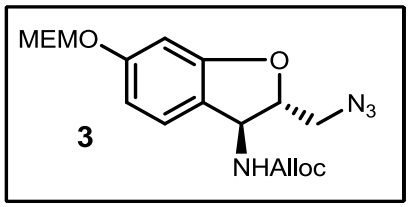

3

To a solution of alcohol **2** (0.047 g, 0.097 mmol) in 3.88 mL of THF was added triphenylphosphine (0.026 g, 0.099 mmol), DEAD (0.019 mL, 0.099 mmol), and diphenylphosphoryl azide (0.021 mL, 0.099 mmol) at 0 °C and stirred for 3 hours. The reaction was quenched with saturated $NaHCO_3$ and extracted with ethyl acetate (3 x 10 mL). The combined organics were dried over anhydrous Mg_2SO_4, concentrated in vacuo and purified by silica gel column chromatography to afford azide **3** (0.042 g, 85%) as brownish liquid. ^1H NMR ($CDCl_3$, 400 MHz):3.39 (s, 3H), 3.50-3.60 (m, 3H), 3.70-3.74 (m, 1H), 3.81-3.84 (m, 2H), 4.61 (d, *J* = 5.52 Hz, 2H), 4.65-4.69 (m, 1H), 5.04-5.07 (m, 1H), 5.12-5.14 (m, 1H), 5.25-5.27 (m, 3H), 5.28-5.35 (d, *J* = 17.5 Hz, 1H), 5.87-5.98 (m, 1H) 6.62 (d, *J* = 2.0 Hz, 1H), 6.65-6.68 (m, 1H), 7.17-7.19 (m, 1H); ^{13}C NMR ($CDCl_3$, 100 MHz): 53.8, 56.1, 59.4, 66.3, 68.2, 71.9, 90.2, 94.0, 99.5, 110.1, 118.4, 125.7, 132.8, 156.0, 160.2, 161.1; MS: (ES_+) m/z = 379 (m+1), HPLC purity (>97%).

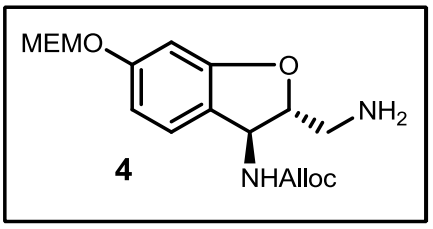

4

To a stirred solution of azide compound **3** (0.225 g, 0.595 mmol) in THF (3 mL) was added TPP (0.166 g, 0.636 mmol) and water (100 µL). The reaction mixture was left for stirring for 12 h at room temperature. After the completion of the reaction THF was removed under vacuuo and purified by flash column using DCM, MeOH solvent system to afford pure amine **4** as colorless liquid in 80 % yield. ^{1}H NMR ($CDCl_3$, 400 MHz): 2.96-3.03 (m, 1H), 3.09-3.14 (m, 1H), 3.40 (s, 3H), 3.56-3.59 (m, 2H), 3.81-3.84 (m, 2H), 4.48-4.53(m, 1H), 4.62 (d, *J* = 5.0 Hz, 2H), 5.05-5.12 (m, 1H), 5.25-5.28 (m, 3H), 5.31-5.38 (d, *J* = 16.5 Hz, 1H), 5.87-5.99 (m, 1H), 6.57 (d, *J* = 2.0 Hz, 1H), 6.64 (dd, *J* = 2.5 Hz, 1H), 7.18 (d, *J* = 8.0 Hz, 1H); ^{13}C NMR ($CDCl_3$, 100 MHz): 45.4, 56.1, 59.4, 66.2, 68.1, 71.9, 93.2, 94.0, 99.3, 109.6, 118.4, 119.3, 125.9, 132.9, 156.0, 160.0, 161.3. MS: (ES_+) m/z = 353 (m+1), HPLC purity (>97%).

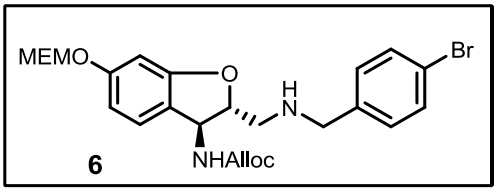

6

The pure amine **4** (0.318 g, 0.9 mmol) and *p*-bromobenzaldehyde (0.183 g, 0.993 mmol) dissolved in triethyl orthoformate (4.0 mL), and a solution of $NaCNBH_4$ (85 mg, 1.355 mmol) in TMOF/MeOH/AcOH (3 mL/720 µL/80 µL) was added to the above mixture at room temperature. The reaction mixture was stirred for 4 h. The reaction was quenched with saturated NH_4Cl solution and washed with water and brine. The organic layer was dried over sodium sulfate, filtered, and concentrated under reduced pressure. The crude product was purified by column chromatography on silica gel (1:1 ethyl acetate/hexanes) to give the product **6** (0.36 g, 77%). ^{1}H NMR ($CDCl_3$, 400 MHz): 2.90-2.95 (m, 1H), 3.0-3.04 (m, 1H), 3.39 (s, 3H), 3.56-3.58 (m, 2H), 3.81-3.83 (m, 4H), 4.60-4.65 (m, 3H) 5.03 (d, *J* =

7.5 Hz, 1H), 5.14-5.17 (m, 1H), 5.23-5.26 (m, 3H), 5.31-5.35 (m, 1H) 5.89-5.99 (m, 1H), 6.56 (d, *J* = 2.0 Hz, 1H), 6.61 (dd, *J* = 2.0 Hz, 1H), 7.16 (d, *J* = 8.5 Hz, 1H), 7.21 (d, *J* = 8.5 Hz, 1H) 7.44 (d, J = 8.5 Hz, 2H); ^{13}C NMR ($CDCl_3$, 100 MHz):52.1, 53.5, 56.6, 59.4, 66.2, 68.1, 71.9, 91.0, 94.0, 99.3, 109.7, 118.4, 119.3, 121.1, 125.9, 130.2, 131.8, 132.9, 139.5, 156.0, 160.0, 161.2; MS: (ES_+) m/z = 521 (M+1), 523 (M+3) HPLC purity (>97%).

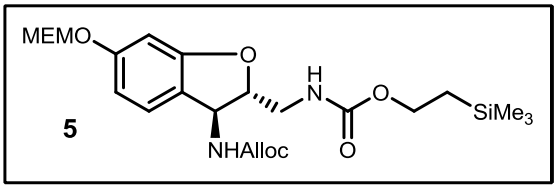

5

Triphosgene (33 mg, 0.112 mmol) was added to the round bottom flask and cooled to 0 °C. This was then followed by a slow addition of 3 mL of anhydrous CH_2Cl_2, and 2-(trimethylsilyl) ethanol (49 µL, 0.34 mmol) was added in one portion to the reaction mixture. Then pyridine (27.6 µL, 0.34 mmol) was added drop wise to the reaction mixture and stirred for 2 h at 0 °C. Then a solution of free amine **4** (60 mg, 0.17 mmol) and pyridine (42 µL, 0.51 mmol) in 3 mL of anhydrous CH_2Cl_2 was added via cannula over a period of 5 min. The mixture was stirred continuously for 2 h at 0 °C. When the TLC showed no starting material, the reaction mixture was quenched via the addition of a saturated solution of $NaHCO_3$, and the aqueous layer was extracted with CH_2Cl_2 (3 x 10 mL). The organic layer was dried over $MgSO_4$, filtered, and concentrated under vacuum,

and the crude product was chromatographed on silica gel with (hexane/ ethyl acetate 7/3) to give **5** (77 mg, 91%) as a white solid. ^1H NMR ($CDCl_3$, 400 MHz):1.0 (t, *J* = 8.5Hz, 2H), 3.4 (s, 3H), 3.5-3.59 (m, 4H) 3.81-3.84 (m, 2H), 4.18 (t, *J* = 8.5Hz, 2H), 4.57-4.63 (m, 1H) 5.03-5.09 (m, 1H), 5.25-5.27 (m, 3H), 5.31-5.35 (d, *J* = 17.0Hz, 1H), 6.57 (d, *J* = 2.0 Hz, 1H), 6.65 (dd, *J* = 2.0 Hz, 1H), 7.18 (d, *J* = 8.0 Hz, 1H); MS: (ES_+) m/z = 497 (M+1), 498 (M+2) HPLC purity (>95%).

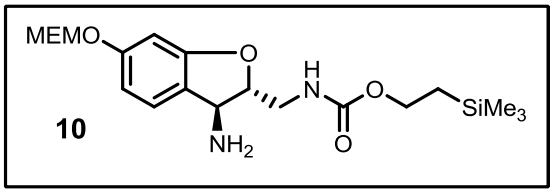

10

To a solution of **5** (77 mg, 0.155 mmol) in dry CH_2Cl_2 (5 mL) under organ atmosphere at 0 °C, was added morpholine (27.6 µL, 0.317 mmol) and tetrakis(triphenylphosphine) palladium (0) catalyst (17.9 mg, 0.0158 mmol). The round-bottom flask containing the mixture was covered with aluminum foil and stirred for 1 h. TLC showed the completion of the reaction. The solvent was evaporated to dryness and the crude mixture subjected to flash column chromatography to give pure benzylic amine **10** (60 mg, 95% yield). ^{1}H NMR ($CDCl_3$, 400 MHz): 0.05 (s, 9H), 0.99 (t, J = 8.53 H_z, 2H), 3.40-3.48 (m, 4H), 3.57-3.66 (m, 2H), 3.82-3.84 (m, 2H), 4.17(t, J = 8.51H_z, 2H) 4.29(d, J = 5.52 H_z, 1H), 4.37-4.41(m, 1H), 5.0 (bs, 1H), 5.25(s, 2H0, 6.54-6.66 (m, 1H), 6.64 (dd, J = 2.0, 2.5H_z, 1H), 7.18 (d, J = 8.53 H_z, 1H); ^{13}C NMR ($CDCl_3$, 100 MHz): -1.0, 0.4, 18.1, 43.5, 56.6, 59.4, 63.7, 68.0, 71.9, 92.0, 94.0, 99.3, 109.6, 124.5, 125.2, 157.3, 159.3, 160.3; MS: (ES_+) m/z = 413 (M+1), 395 (M-NH_3) HPLC purity (>96%).

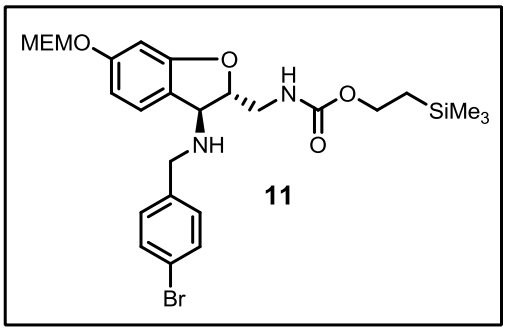

11

This compound is prepared following the similar procedure described for the compound **6** using the benzylic amine **10** (63 mg, 0.152 mmol), *p*-bromobenzaldehyde (31 mg, 0.168 mmol) and $NaCNBH_3$/AcOH/MeOH (15 mg, 0.228 mmol/12µL/120µL) in TMOF to afford compound **11** (79 mg, 90% yield). ^{1}H NMR ($CDCl_3$, 400 MHz): 0.05 (S, 9H), 1.00(t, J = 8.03 H_z) 3.25-3.32 (m, 1H), 3.40 (s, 3H), 3.53-3.59 (m, 3H), 3.82-3.85 (m, 4H), 4.15-4.20 (m, 3H), 4.63-4.66 (m, 1H), 4.97 (m, 1H), 5.25(s, 2H), 4.63-4.66 (m, 1H), 4.97 (m, 1H), 5.25 (s, 2H), 6.57 (d1 J = 2.0, 1H), 6.62 (dd, J = 2.0,

2.5, 1H), 7.19(d, *J* = 8.03, H_z, 1H), 7.25-7.28 (m, 2H), 7.45-7.48 (m, 2H); ^{13}C NMR (CDCl3, 100 MHz): -1.0, 0.4, 18.1, 44.4, 50.2, 59.4, 62.0, 63.7, 68.1, 71.9, 88.7, 94.0, 99.4, 109.5, 121.3, 126.0, 130.2, 131.9, 159.5, 160.6; MS: (ES_+) m/z = 581 (M+1), 583 (M+3) HPLC purity (>97%).

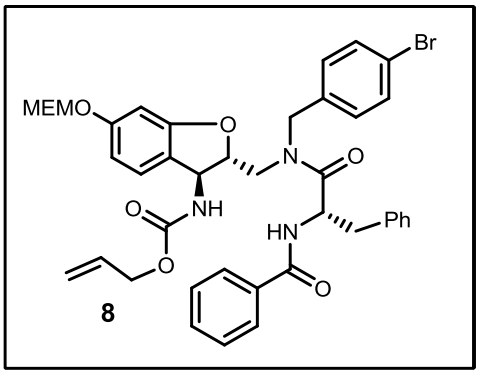

8

To a stirred solution of amine **6** (46 mg, 0.088 mmol) and amino acid **7** (28 mg, 0.106 mmol) in dry dichloromethane under organ atmosphere were added PyBrop (49 mg, 0.106 mmol) and DIPEA (31uL, 0.176 mmol) at room temperature. The reaction mixture was allowed to stir for overnight. After completion of the reaction as indicated by the TLC and LC-MS, organic layer evaporated and the crude mixture was dissolved in ethyl acetate (3x20 mL) and combined organic layers were concentrated and the crude mixture was purified by column chromatography using hexane and ethyl acetate (7:3) solvent system to give pure compound **8** (48 mg, 58% yield). ^1H NMR ($CDCl_3$, 400 MHz, 58 ^oC): 3.11-3.28 (m, 2H), 3.38-3.40 (m, 3H), 3.53-3.60 (m, 2H), 3.78-3.85 (m, 3H), 4.26-5.00 (m, 6H), 5.16-5.39 (m, 6H), 5.50 (bs, 1H), 5.83-6.00 (m, 1H), 6.49-6.76 (m, 3H), 6.83-7.00 (m, 2H), 7.11-7.28 (m, 4H), 7.35-7.54 (m, 6H), 7.71-7.82 (m, 2H); MS: (ES_+) m/z = 772 (M+1), 774 (M+3) HPLC purity (>95%).

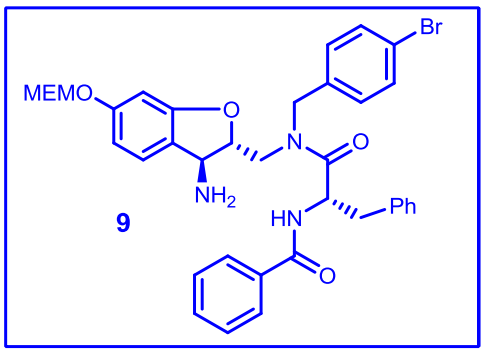

9

To a solution of **8** (48mg, 0.062 mmol) in dry CH_2Cl_2 (5 mL) under organ atmosphere at 0 °C, was added morpholine (10 µL, 0.124 mmol) and tetrakis(triphenylphosphine) palladium (0) catalyst (7 mg, 0.0062 mmol).

The round-bottom flask containing the mixture was covered with aluminum foil and stirred for 1 h. TLC showed the completion of the reaction. The reaction was quenched with saturated NH_4Cl solution and washed with water and brine. The organic layer was dried over anhy. $MgSO_4$, filtered, and concentrated under reduced pressure to give crude compound which upon flash column chromatography using ethyl acetate (100%) to afford amine **9** (40 mg, 95 % yield). ^{1}H NMR ($CDCl_3$, 400 MHz, 58 ^{o}C): 3.02-3.31 (m, 2H), 3.37 (m, 3H), 3.47-3.48 (m, 0.5H), 3.54-3.61 (m, 2.5H), 3.73-3.86 (m, 2.5H), 3.94-3.99 (m, 0.5H), 4.05-4.10 (m, 1H0, 4.14-4.24 (m, 1H), 4.36-4.49 (m, 1H), 4.51-4.63 (m, 1H), 4.70-4.81 (m, 0.5H), 5,02-5.06 (m, 0.5H), 5.19-5.31 (m, 2.5H), 5.36-5.59 (m, 1H), 6.49-6.55 (m, 1H), 6.61-6.65 (m, 1H), 6.79-7.02 (m, 3H), 7.09-7.16 (m, 2H), 7.20-7.34 (m, 3H), 7.39-7.54 (m, 5H), 7.73-7.80 (m, 2H); MS: (ES_+) m/z = 671 (M-NH_3+1), 673 (M-NH_3+3) HPLC purity (>97%).

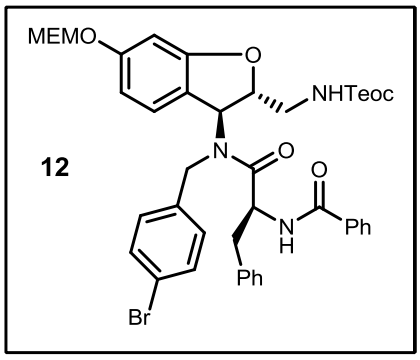

12

Compound **12** was prepared following the similar procedure described for the compound **8**, by using amine **11** (60 mg, 0.103 mmol), amino acid **7** (33 mg, 0.123 mmol), PyBrop (58 mg, 0.123 mmol) and DIPEA (36 L, 0.206 mmol) to afford the compound **12** (50 mg) 58 % yield. ^{1}H NMR (DMSO, 400 MHz, 120 ^{o}C): 0.01 (S, 9H), 0.89 (m, 2H), 3.05-3.17 (m, 2H), 3.22-3.34 (m, 5H), 3.48-3.50 (m, 2H), 3.71-3.74 (m, 2H), 4.02-4.06 (m, 2H), 4.20-4.36 (m, 3H), 4.52-4.65 (m, 2H), 5.16 (s, 2H), 5.72 (bs, 1H), 6.37-6.46 (m, 2H), 6.65-6.73 (bs, 1H), 6.89-7.00 (m, 3H), 7.17-7.35 (m, 6H), 7.41-7.53 (m, 4H), 7.78-7.85

(m, 2H), 8.48 (bs, 1H); MS: (ES+) m/z = 832 (M+1), 834 (M+3) HPLC purity (>97%).

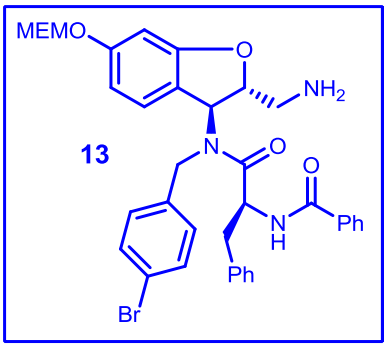

To a stirred solution of compound **12** (40 mg, 0.047 mmol) in dry THF under organ atmosphere was added TBAF (0.1 mL, 0.095 mmol) solution in THF at 0° C. The reaction mixture was allowed to warm to rt and stirred for overnight. After completion of the reaction as indicated by TLC and LC-MS, the solvent was evaporated under vacuum to give crude product which was subjected to flash chromatography using dichloromethane and methanol (9.8:0.2) solvent system on triethylamine neutralized silica gel to give pure amine **13** (30 mg, 93 % yield). ^{1}H NMR ($CDCl_3$, 400 MHz): 2.47-2.67 (m, 0.5 H), 2.83-3.03 (m, 1.5 H), 3.11-3.21 (m, 2H), 3.38-3.41 (m, 3H), 3.56-3.61 (m, 2H), 3.78-3.84 (m, 2H), 3.95-3.98 (m, 0.5), 4.14-4.27 (m, 2H), 4.36-4.47 (m, 0.5H), 5.19-5.28 (m, 2.5H), 5.69-5.83 (m, 1.5H), 6.46-6.54 (m, 2H), 6.69-7.02 (m, 4H), 7.14-7.16 (m, 1H), 7.25-7.35 (m, 4H), 7.45-7.57 (m, 4H), 7.77-7.81 (m, 2H); MS: (ES+) m/z = 688 (M+1), 690 (M+3) HPLC purity (>97%).

Experimental Section for the Synthesis of Small Molecule DAN004 (17)

Reductive amination of *tert*-butyl (3-aminopropyl)carbamate **14** with 4-bromobenzaldehyde gave rise to **15** the secondary amino functionality of which subsequently was coupled to *N*-benzoyl-*L*-phenylalanine yielding **16**. Final deprotection rendered **17** (DAN004**)** in good overall yield.

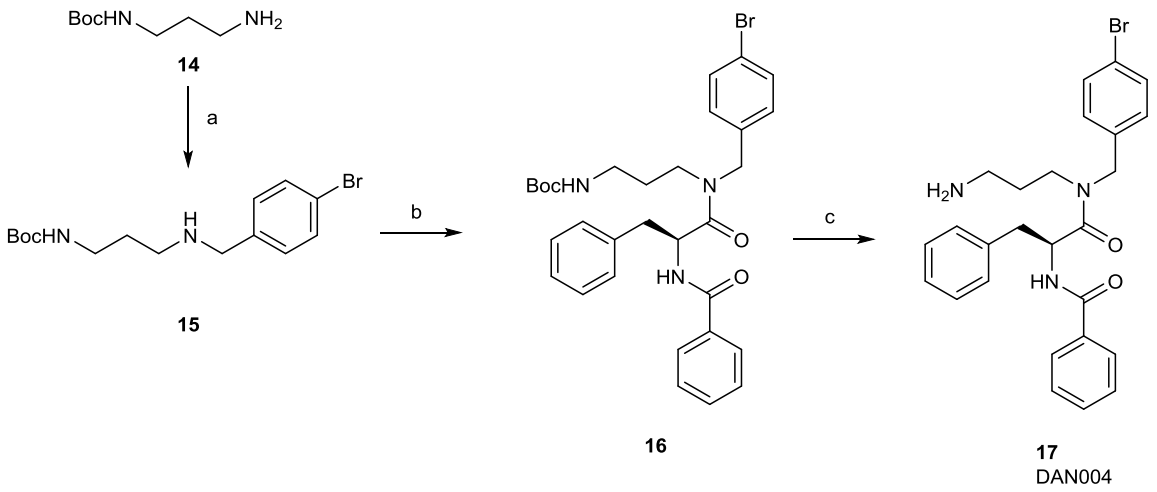

reagents and conditions: a) 4-bromobenzaldehyde, $NaBH_4$, MeOH, 0°C → RT, 16 h 77%; b) *N*-benzoyl-*L*-phenylalanine, HBTU, *N*-methylmorpholine, DMF, RT, 14h, 61%; c) TFA, DCM, RT, 72h, 92%.

General synthetic

Commercially available reagents and solvents were used without further purification, except for cyclohexane which was distilled prior to use. Thin layer chromatography (TLC) was performed on precoated TLC-plates (silica gel 60 F254, Merck). Flash column chromatography was performed on prepacked flash chromatography columns (PF 30-SIHPJP/ 12G) purchased from Interchim using a Büchi separation system.

Melting points were determined using the melting point meter MPM-H2 (Schorpp Gerätetechnik, Germany) and are uncorrected. 1H-NMR and 13C-NMR spectra were recorded either on a JEOL ECX-400 or a JEOL ECA-500 spectrometer. Chemical shifts (δ) are given in ppm with the residual solvent signal used as

reference [1H: DMSO-d_6 (30°C): quint, δ=2.49ppm; $CDCl_3$ (20°C): s, δ=7.26ppm; 13C: $DMSOd_6$ (30°C): quint, δ=39.50ppm, $CDCl_3$ (20°C): t, δ=77.16ppm. Coupling constants (J) are reported in hertz (Hz). Peak patterns are abbreviated as follows: s (singlet), d (doublet), dd (double doublet), dt (doublet of triplet), t (triplet), m (multiplet), sm (symmetric multiplet), br (broad), ps (pseudo). Mass spectra were either recorded on a triple quadrupole spectrometer type EP 10+ (MS Vision), a triple quadrupole spectrometer type Q-Trap 2000 (Applied Biosystems), or on a double-focusing sector field spectrometer type AutoSpec (Micromass). Elemental combustion analyses were performed on a vario MICRO cube (Elementar Analysensysteme GmbH, Hanau, Germany).

tert-butyl (3-((4-bromobenzyl)amino)propyl)carbamate **(15)**

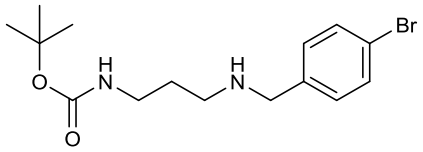

A solution of *tert*-butyl (3-aminopropyl)carbamate (**14**, 0.435 g, 2.50 mmol) and 4-bromobenzaldehyde (0.509 g, 2.75 mmol, 1.1 equiv.) in MeOH (10 mL) was stirred for 3h at RT under an argon atmosphere. The reaction mixture was subsequently cooled to 0 °C and sodium borohydride (0.378 g, 10.0 mmol, 4 equiv.) was added slowly, followed by further stirring of the mixture for additional 16h at RT. After concentrating in *vacuo*, the remaining residue was taken up in water (20 mL) and the mixture subsequently extracted with EtOAc (3 x 20 mL). The combined organic layers were extracted with aq. 0.5 M HCl (3 x 20 mL) and the separated aqueous layers combined and adjusted to pH 9-10 by addition of

an aq. NH_3 solution. After extraction with DCM (3 x 20 mL), the combined organic layers were washed with brine, dried over $MgSO_4$, filtered, and finally concentrated in *vacuo* to give crude **15** [0.659 g, 77%, 87% purity (qNMR)] which was used without further purification in the next step.

^{1}H-NMR (500MHz, DMSO-d_6): δ 1.36 (s, 9H), 1.51 (quint, ^3J = 6.9 Hz, 2H), 2.44 (t, ^3J = 6.7 Hz, 2H), 2.95 (dt, ^3J = 6.6 Hz, ^3J = 6.3 Hz, 2H), 3.29 (s, 1H), 3.62 (s, 2H), 6.74 (s, 1H), 7.26 (psd, ^3J + ^5J = 8.6 Hz, 2H), 7.47 (psd, ^3J + ^5J = 8.3 Hz, 2H). ^{13}C-NMR (125MHz, DMSO-d_6): δ 28.8, 30.3, 38.7, 46.7, 52.7, 77.9, 119.9, 130.6, 131.4, 141.1, 156.1. MS (ESI+) *m/z* (%): 342.15 (100) [^{79}Br, *M*+H]$^+$, 687.23 (80) [^{79}Br,^{81}Br, 2*M*+H]$^+$.HRMS (EI): calcd for $C_{15}H_{23}BrN_2O_2$ [^{79}Br, *M*+H]$^+$: 342.094289, found: 342.095397. HRMS-(EI): calcd for $C_{15}H_{23}BrN_2O_2$ [^{81}Br, *M*+H]$^+$: 344.092243, found: 344.093534.

(*S*)-*tert*-butyl (3-(2-benzamido-*N*-(4-bromobenzyl)-3-phenylpropanamido)propyl)-carbamate **(16)**

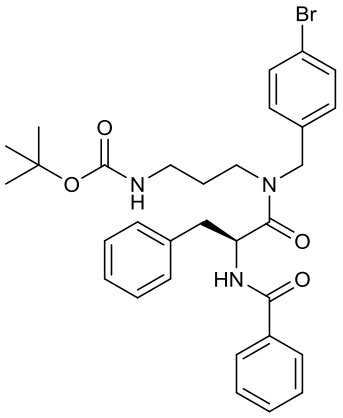

To a solution of *N*-benzoyl-*L*-phenylalanine (0.498 g, 1.85 mmol), HBTU (0.771 g, 2.04 mmol, 1.1 equiv.) and *N*-methylmorpholine (1.017 ml, 9.25 mmol, 5 equiv.)

in 8 ml DMF, **15** (0.699 g, 2.04 mmol, 1.1 equiv.) was added and the reaction mixture stirred at RT for 14h under an argon atmosphere. After addition of DCM (100 mL), the separated organic layer was exhaustively washed with an aqueous 5% LiOH solution (5 x 50 ml), dried over $MgSO_4$, filtered, and finally concentrated in *vacuo*. Flash chromatography (cyclohexanes/EtOAc, gradient from 0 → 5% over 15 min) of the remaining crude product gave rise to **16** as colorless solid (0.671 g, 61%).

Mp: 130-133°C. ^{1}H-NMR (500MHz, DMSO-d_6, mixture of rotamers): δ 1.35 (s, 9H), 1.53-1.71 (m, 2H), 2.81-2.96 (m, 2H), 2.98-3.11 (m, 2H), 3.15-3.27 (m, 1H), 4.40-4.73 (m, 2H), 4.97-5.12 (m, 1H), 6.67-6.82 (m, 1H), 7.09-7.31 (m, 6H), 7.32-7.54 (m, 6H), 7.76-7.85 (m, 2H), 8.79-8.82 (m, 1H). ^{13}C-NMR (100MHz, $CDCl_3$, mixture of rotamers): δ 27.5, 28.5, 28.7, 37.3, 37.8, 39.5, 39.9, 43.4, 44.5, 48.4, 50.3, 50.5, 51.2, 79.2, 79.4, 121.5, 121.8, 127.2, 128.5, 128.7, 128.75, 128.77, 129.6, 129.8, 131.8, 131.9, 132.1, 133.7, 133.8, 135.2, 135.8, 136.1, 136.3, 156.1, 156.3, 166.8, 167.0, 171.9, 172.5. MS (ESI+) *m/z* (%):594 (100) [^{79}Br, *M*+H]$^+$, 596 (100) [^{81}Br, *M*+H]$^+$. Anal. calcd for: $C_{31}H_{36}BrN_3O_4$: C, 62.63; H, 6.10; N, 7.07; found: C: 62.68; H, 6.20; N, 7.27.

(*S*)-*N*-(1-((3-aminopropyl)(4-bromobenzyl)amino)-1-oxo-3-phenylpropan-2-yl)-benzamide **(17)**

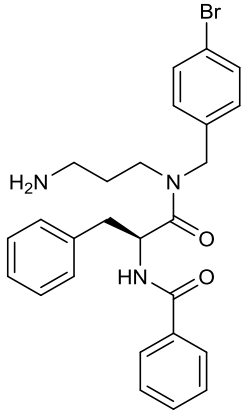

To a solution of **16** (0.719 g, 1.21 mmol) in DCM (6 mL), TFA (0.419 mL, 5.45 mmol, 4.5 equiv.) was added and the reaction mixture stirred at RT for 72h. The mixture was then quenched by addition of a sat. $NaHCO_3$ solution (10 mL) and the separated organic layer washed with brine, dried over $MgSO_4$, filtered, and concentrated in *vacuo*. Flash chromatography (DCM/MeOH gradient from 0 → 10% over 15 min) of the crude product yielded **17** as colorless, hygroscopic solid (0.550 g, 92%).

Mp: 46-50°C (hygroscopic). ^{1}H-NMR (500MHz, DMSO-d_6, mixture of rotamers): δ 1.70-1.83 (sm, 1.5H), 1.90-2.05 (sm, 0.5H), 2.70 (t, ^3J = 7.5 Hz, 1H), 2.78 (t, ^3J = 7.2 Hz, 1H), 2.96-3.04 (sm, 1H), 3.07-3.15 (m, 1H), 3.23-3.40 (m, 2H), 3.42-3.49 (sm, 1H), 4.40 (d, ^2J = 15.5 Hz, 0.5H), 4.60 (d, ^2J = 15.5 Hz, 0.5H), 4.61 (d, ^2J = 17.5 Hz, 0.5 H), 4.77 (d, ^2J = 17.2 Hz, 0.5H), 4.97 (dd, ^2J = 14.1 Hz, ^3J = 8.2 Hz, 0.5H), 5.12 (dd, ^2J = 14.9 Hz, ^3J = 8.0 Hz, 0.5H), 7.09-7.94 (m, 5H), 7.27 (pst, ^3J = 7.5 Hz, 1H), 7.37-7.55 (m, 6H), 7.78 (d, ^3J = 7.2 Hz, 1H), 7.81-7.92 (m, 3H), 8.86 (d, ^3J = 7.5 Hz, 1H). ^{13}C-NMR (125MHz, DMSO-d_6): δ 25.8, 27.1, 37.0, 37.2, 37.6, 37.7, 43.7, 45.0, 48.2, 50.2, 51.7, 52.1, 120.5, 120.9, 126.95, 127.02, 128.0, 128.1, 128.65, 128.68, 128.7, 128.8, 129.5, 129.8, 130.0, 130.1, 131.7, 1321.9, 132.0, 134.2, 134.3, 137.4, 137.8, 138.1, 138.3, 166.8, 167.0, 172.1, 127.6. MS (ESI) *m/z* (%): 494.10 (100) [^{79}Br, *M*+H]$^+$. HRMS (EI): calcd for $C_{26}H_{28}BrN_3O_2$ [^{79}Br, *M*+H]$^+$: 493.136489, found: 493.138102. HRMS (EI): calcd for $C_{26}H_{28}BrN_3O_2$: [^{81}Br, *M*+H]$^+$: 495.134442, found: 495.135035. Anal. calcd for: $C_{26}H_{28}BrN_3O_2$*2.5 H_2O: C, 57.89; H, 6.17; N, 7.79; found: C: 57.55; H, 5.66; N, 7.70.

CHAPTER III:

Small molecules reveal an alternative mechanism of Bax activation

Preface

The work presented here has been submitted to the *Biochemical Journal* (Submission # BJ2015/1347) as a research article.

Contribution of authors:

HB, BL and DWA designed the experiments, analyzed the data and wrote the paper. RA and DU assisted with the OICR766A analogs. DWA and BL directed the project, HB performed the experiments.

Research objective:

To identify and characterize small molecule activators of Bax

Research Highlights:

- Five structurally different compounds activate Bax by promoting the targeting to and oligomerization of Bax at the membranes.
- These compounds, but not recombinant activator BH3 proteins, induced the oligomerization of Bax in solution.
- Bax activated by the potent small molecule, OICR766A was poorly inhibited by Bcl-XL.
- OICR766A required cysteine at position 126 of Bax, a residue that is not critical for activation by BH3 activator proteins, for binding and activating Bax.

Small molecules reveal an alternative mechanism of Bax activation

Hetal Brahmbhatt[*,†], David Uehling[‡], Rima Al-awar[‡], Brian Leber[§], David Andrews[*,†,1]

[*] Department of Biochemistry and Biomedical Sciences, McMaster University, Hamilton, ON, Canada L8S 4L8
[†] Department of Biological Sciences, Sunnybrook Research Institute, University of Toronto, ON Canada M4N 3M5
[‡] Drug Discovery Program, Ontario Institute for Cancer Research, Toronto, ON, Canada M5G 0A3
[§] Department of Medicine, McMaster University, Hamilton, ON, Canada L8S 4L8

[1] To whom correspondence should be addressed (Email: david.andrews@sri.utoronto.ca)

Short title: Small molecule Bax activators

Abstract

The pro-apoptotic protein Bax commits a cell to death by permeabilizing the mitochondrial outer membrane. To obtain small molecule probes for elucidating the molecular mechanism(s) of Bax activation, we screened for compounds that induced Bax mediated liposome permeabilization. We identified five structurally different small molecules that promoted both Bax targeting to and oligomerization at membranes. All five compounds initiated Bax oligomerization in the absence of membranes by a mechanism unlike Bax activation by BH3 proteins. Some of the compounds induced Bax/Bak dependent apoptosis in cells. Activation of Bax by the most active compound was poorly inhibited by the anti-apoptotic protein, Bcl-XL, and requires a cysteine at position 126 of Bax, that is not required for

activation by BH3 proteins. Our results reveal a novel pathway for Bax activation independent of pro-apoptotic BH3 proteins that may have important implications for the regulation of Bax activity in cells.

Keywords: Bax activators, Apoptosis, Cysteine, Mechanism probes, Bax oligomerization, Membrane permeabilization

Summary Statement

We identified five structurally different compounds that trigger the pro-apoptotic protein Bax to permeabilize mitochondrial outer membranes leading to cellular demise. The molecular mechanisms by which these compounds and pro-apoptotic BH3 proteins trigger pore formation by Bax are different.

Introduction

Bcl-2 family proteins function as regulators and executors of apoptotic signals at the mitochondrial outer membrane (MOM) (Antonsson 2004). The fate of a cell is dictated by complex protein-protein and protein-membrane interactions of the pro- and anti-apoptotic Bcl-2 family members (Leber, Lin et al. 2007). For most cells, MOM permeabilization (MOMP) by the executor Bcl-2 family pro-apoptotic proteins Bax and Bak commits the cell to undergoing apoptosis. Since dysregulation of apoptosis is critical not only for tumor initiation, but also for tumor

maintenance and survival, small molecules that modulate Bax and Bak activity are of critical importance from a mechanistic and therapeutic point of view (Certo, Del Gaizo Moore et al. 2006; Hanahan and Weinberg 2011).

It is widely accepted that MOMP occurs when Bax and/or Bak undergo complex conformational changes including the exposure of a buried N-terminal region, insertion of parts of the protein into the bilayer, oligomerization, and the formation of a lethal pore (Hsu and Youle 1997; Annis, Soucie et al. 2005; Alsop, Fennell et al. 2015). However, there is a lack of consensus regarding the activation triggers of Bax and Bak in cells. According to some studies, Bax and Bak are inactive and activation is triggered by pro-apoptotic BH3 proteins such as cBid that target to the mitochondria, recruit and activate Bax and membrane bound Bak (Kuwana, Mackey et al. 2002; Lovell, Billen et al. 2008; Sarosiek, Chi et al. 2013). However results from other studies suggest that both Bax and Bak are constitutively active and held in check by the anti-apoptotic machinery. In this scenario MOMP occurs when BH3 proteins liberate activated Bax or Bak from the anti-apoptotic proteins (Chen, Willis et al. 2005; Willis, Chen et al. 2005). In these studies, it is unclear how Bax and Bak are activated since when purified both proteins are at best poorly active (Yethon, Epand et al. 2003; Leshchiner, Braun et al. 2013). Moreover, most Bax is found in the cytoplasm of asynchronously growing cells (Gilmore, Metcalfe et al. 2000).

Aside from BH3 proteins, additional reported triggers of Bax activation include: detergents, heat, alterations in pH and in cells, oxidative conditions, proteolytic cleavage and phosphorylation (Hsu and Youle 1997; Wood and Newcomb 2000; Cartron, Oliver et al. 2004; D'Alessio, De Nicola et al. 2005; Pagliari, Kuwana et al. 2005; Kim, Ryu et al. 2006; Nie, Tian et al. 2008). Furthermore three small molecules, BAM7, Compound 106 and SMBA1, have been reported to be activators of Bax (Gavathiotis, Reyna et al. 2012; Xin, Li et al. 2014; Zhao, Zhu et al. 2014). All three compounds were identified in virtual docking screens using Bax. Each of these docking studies was designed to identify molecules that can occupy specific sites on Bax. Compound 106 occupies the hydrophobic groove of Bax that binds BH3 proteins, SMBA1 docks in the small pocket around the S184 residue in the membrane binding domain of Bax and BAM7 selectively engages a site that binds a stapled Bim BH3 peptide. Virtual docking at previously identified BH3 peptide binding sites precludes identification of molecules that modulate Bax activity by binding to a different site and is unlikely to identify molecules that induce Bax activation by a mechanism different than that of the BH3 proteins.

To identify in an unbiased fashion small molecule probes that can be used to examine the molecular mechanism of Bax activation, we screened for compounds that trigger Bax mediated liposome permeabilization. We identified five structurally different small molecules that induce both the localization and

oligomerization of Bax at membranes. Unexpectedly all of these molecules activated Bax by a similar mechanism unlike that of Bax activation by BH3 proteins. Further analysis of the molecules in cells revealed as expected, that some of the compounds induced apoptosis in cells via a Bax/Bak dependent mechanism. Structure activity analysis of the most active of these compounds indicated that binding specificity rather than the physical-chemical properties of the molecule mediated Bax activation. Surprisingly, activation of Bax by the small molecule requires the cysteine residue at position 126 of Bax, a residue not required for BH3 protein mediated activation of Bax. This and other data strongly suggesting BH3 proteins and the small molecules activate Bax by different mechanisms provide insights into alternative mechanisms for regulating Bax activity in cells.

Results and Discussion

Five small molecules activate Bax in liposomes and enriched mitochondria

In order to identify probes of Bax activation, a screen was conducted for compounds that caused Bax mediated permeabilization of liposomes encapsulating a fluorophore (ANTS) and a quencher (DPX). Permeabilization of these liposomes results in an increase in fluorescence due to the increase in distance between the released dye and quencher (Yethon, Epand et al. 2003). As a positive control for membrane permeabilization, we used the known Bax

activator protein, cBid (Fig. S1A) (Lovell, Billen et al. 2008). To correct for intrinsic fluorescence of the compounds and to identify compounds that lyse liposomes directly, fluorescence intensity was also measured without adding Bax. Compounds with high background fluorescence, were re-assayed using liposomes encapsulating the fluorescent complex, terbium-dipicolinic acid (Tb/DPA) in a buffer containing EDTA. In this case, fluorescence is recorded at different wavelengths than for ANTS/DPX and liposome permeabilization causes a decrease in fluorescence because EDTA disrupts the Tb/DPA complex (Wilschut, Duzgunes et al. 1980).

After primary and secondary screening, five compounds met the criteria as bona fide hits including: OICR766A, phenylmercuric acid (PMA), ebselen, ZM39923 hydrochloride (referred to as ZM hereafter) and plumbagin. The relative potency of the compounds was established by re-assaying them at various concentrations. All five compounds permeabilized liposomes in a Bax and dose-dependent fashion (Fig 1A). In control experiments the highest dose of the compound alone had no effect on liposome integrity (Fig. S1A).

To further validate the compounds as Bax activators in biological membranes, we assayed their activity in mitochondria isolated from *bax-/- bak-/-* Baby Mouse Kidney (BMK) cells engineered to stably express Smac (1-56aa)-mCherry. This fusion protein includes residues 1-56 (the intermembrane mitochondrial targeting signal peptide) of Smac, an intermembrane space protein

released during apoptosis, fused to the fluorescence protein mCherry (Du, Fang et al. 2000). Bax activated by cBid leads to Smac-mCherry release that can be measured quantitatively using a fluorimeter (Fig. S1B). Consistent with the results using liposomes, the compounds triggered dose dependent Bax mediated permeabilization of mitochondria (Fig. 1B). Without Bax the compounds did not result in significant mitochondrial permeabilization at concentrations up to 10μM (Fig S1B). In both liposomes and mitochondria based assays, OICR766A had the greatest effect enhancing the pro-apoptotic activity of Bax with EC_{50}'s of ~ 0.1μM and ~0.9 μM, respectively (Table 1). Interestingly, the five molecules are structurally unrelated demonstrating that Bax can be activated by a variety of molecules (Fig 1C). That Bax responds to such diverse structures suggests that it may also respond to one of more chemical triggers that accumulate in cells in response to stress or intoxication.

Compounds induce oligomerization and membrane localization of Bax

To examine the molecular mechanism by which the small molecules induce Bax activation, compound induced oligomerization and membrane localization of Bax were measured biochemically. To determine if the compounds were inducing Bax to form oligomers, we performed cross-linking experiments using disuccinimidyl suberate (DSS) in reactions containing liposomes (Eskes, Desagher et al. 2000; Billen, Kokoski et al. 2008). As positive controls for Bax

oligomerization, we used cBid and Bim which have been shown to induce Bax oligomerization (Hsu and Youle 1997). As expected, the compounds induced the formation of higher order Bax complexes with OICR766A, and PMA having the most pronounced effects on Bax oligomerization (Fig. 1D, S1C).

Unlike pro-apoptotic BH3 proteins, in the absence of membranes both OICR766A and ebselen had pronounced effects on the formation of dimers and higher order Bax oligomers in solution (Fig. 1E, S1D). In control experiments no effects on Bax oligomerization were observed upon addition of cBid or Bim to Bax in solution (Fig. 1E), a result consistent with our previous observations that Bax inserts into membranes as monomers that then oligomerize (Lovell, Billen et al. 2008). Additionally, in solution Triton X-100 predominantly induced the formation of dimers with very little higher oligomers consistent with previous results showing that detergents such as Triton X-100 and octylmaltoside induce the formation of domain swapped Bax homodimers believed to be inactive (Hsu and Youle 1997; Hsu and Youle 1998; Czabotar, Westphal et al. 2013). Taken together, these data suggest that the molecular mechanism by which the compounds activate Bax differs significantly from that by cBid or Triton X-100.

Previously we have shown that in the presence of liposomes Bax undergoes a reversible conformational change that exposes a normally hidden epitope recognized by the monoclonal antibody 6A7 (Yethon, Epand et al. 2003). Exposure of this epitope strongly correlates with activation of the oligomerization

and pore forming activities of Bax. It was also possible to detect the formation of reversible Bax oligomers in the presence of liposomes (Billen, Kokoski et al. 2008). However, neither exposure of the 6A7 epitope nor the formation of these transient oligomers is sufficient to permeabilize membranes until an activator protein is introduced (Lovell, Billen et al. 2008). Therefore, although the compounds identified here induce changes to Bax in solution, it is possible that a substrate membrane is still required for Bax to undergo all the functional conformational changes associated with its activation to permeabilize membranes.

In unstressed cells Bax is typically a cytoplasmic or peripheral membrane protein that binds tightly to membranes only upon activation by a membrane bound BH3 protein (Shamas-Din, Bindner et al. 2013). To determine the effect of the compounds on Bax binding to membranes, Bax was incubated with the compounds in the presence of liposomes and then the reactions were passed over a size exclusion column to separate membrane bound Bax from unbound protein. Immunoblots of the fractions revealed that when incubated with the compounds or in control reactions with cBid most of the Bax elutes in the excluded fractions containing membranes (fraction 3-6) (Fig. S1E). The fraction of Bax that elutes in the bound fractions varies for each compound and correlates positively with membrane permeabilization (Fig. 1F). Taken together, these results indicate that the conformational changes that occur when the compounds

trigger Bax oligomerization in solution allow it to bind to membranes productively leading to membrane permeabilization.

Bax activation is not mediated by partitioning of the compounds into liposome membranes

Given that hydrophobic small molecules can partition into membranes, and that membranes trigger transient conformational changes in Bax, we sought to rule out the possibility that membrane permeabilization was due to the compound altering the physical properties of the membranes making them prone to spontaneous fusion such that the altered liposomes mediate Bax activation and oligomerization (Mondal Roy and Sarkar 2011). To test this hypothesis, we used a modified version of the dye release assay in which liposomes were first incubated with the compounds and then passed over a gel filtration column to separate the liposomes and any bound compound from unpartitioned compound. Thereafter, membrane permeabilization was compared for Bax and liposomes pre-incubated with the compounds to liposomes in which Bax and the compounds were added simultaneously as a control. Pre-incubation of the liposomes with the compounds did not result in Bax activation suggesting that that activation of Bax was unlikely due to an effect of the compounds on the liposome membranes (Fig. S1F).

OICR766A induces apoptosis in cells

To determine if the compounds induce Bax/Bak dependent apoptosis in cells, we examined their effects on wild type (Wt) and *bax-/- bak-/-* double knock out (DKO) BMK cells. Apoptotic cell death was monitored using triple staining with Annexin V, tetramethylrhodamine ethyl ester (TMRE) and DRAQ5 to measure externalization of phosphatidylserine (a hallmark of apoptosis), loss of mitochondrial membrane potential and nuclear/chromatin condensation, respectively. Among the five compounds tested, Annexin V staining indicated that OICR766A (Fig. 2A), PMA and plumbagin (Fig S2A) had the most pronounced effects on apoptosis of Wt compared to the DKO cells. Even though ebselen has been reported to kill leukemia cells, we found that it was not toxic to Wt or DKO BMK cells suggested that it may be either metabolized or pumped out of the cells (Brown, Burke et al. 2009). ZM killed both cell types with an EC_{50} of about 10 μM suggesting that in cells the drug has other more toxic activities than Bax activation, a result consistent with previous publications (Lai, Liu et al. 2008). Since OICR766A was the most effective Bax activator *in vitro* (Fig. 1), and had the largest differential kill between Wt and DKO cells (Fig. 2A) we analyzed the activity of this compound in more detail.

Annexin V staining revealed that 2.5-5μM OICR766A killed Wt but had limited activity in DKO cells. However, at 10 μM, it was equally toxic to both Wt and DKO cells suggesting significant off-target toxicity (Fig. 2A). These data were

further corroborated by reduced staining of the Wt cells with the membrane potential sensitive dye, TMRE, demonstrating a greater loss in membrane potential in Wt than in the DKO cells at similar doses (Fig. 2B). Interestingly, quantitative measurements of nuclear condensation indicated that OICR766A treatment decreased nuclear size of both Wt and DKO cells with only a marginally greater effect on the Wt cells between 2.5-5μM (Fig. 2C). Representative fluorescence images displaying staining with Annexin V, TMRE and DRAQ5 for cells treated with 2.5μM OICR766A are shown in Fig. 2D. At 2.5 μM OICR766A also killed DKO cells expressing exogenous human Bax (Fig. S2B). Consistent with the mechanism of cell death at lower concentrations being due to activation of Bax, almost 80% of cells stained with an antibody specific for the active form of Bax (6A7) after treatment with 2.5μM OICR766A (Fig. 2E).

Bax and Bak are functionally equivalent in many cell types therefore we tested cells expressing Bax or Bak for sensitivity to OICR766A (Wei, Zong et al. 2001; Degenhardt, Sundararajan et al. 2002). At 2.5μM the compound killed cells expressing either Bax or Bak (Fig. 2F). Off-target activity of the compound in cells could result in indirect activation of Bak, therefore, we measured direct activation of Bak by OICR766A *in vitro*. For these experiments mitochondria isolated from *bax-/-* BMK cells were incubated with increasing concentrations of OICR766A. Even at the maximum concentration assayed (40μM) there was no detectable release of the intermembrane space protein, cytochrome *c* (Fig. 2G). This

contrasts markedly with the effect of OICR766A on mitochondria with Bax and no Bak (Fig. 1B). Thus, these results suggest that in live cells OICR766A indirectly activated Bak to mediate apoptosis of *bax-/-* BMK cells. Consistent with this interpretation and the data in Fig. 2C, when the Wt and DKO cells were assayed for cell survival and regrowth post OICR766A treatment, no difference was observed in the survival response (Fig. S2C). Thus, Bax activation is only one mechanism by which OICR766A kills cells limiting the utility of the compound for cell based studies.

OICR766A activated Bax is poorly inhibited by Bcl-XL

To examine the molecular mechanism of Bax activation by OICR766A in more detail, we measured inhibition of compound activated Bax by the anti-apoptotic protein Bcl-XL. Bcl-XL functions as a dominant negative Bax to inhibit membrane permeabilization by binding to Bax directly and inhibiting its oligomerization (Mode 2). However, Bcl-XL also inhibits apoptosis by binding to the BH3 proteins thereby preventing activation of Bax (Mode 1) (Billen, Kokoski et al. 2008; Llambi, Moldoveanu et al. 2011). The two modes can be differentiated using cBid mt1, a mutant of Bid that activates Bax but does not bind to and therefore cannot be inhibited by Bcl-XL (Wang, Yin et al. 1996; Desagher, Osen-Sand et al. 1999; Billen, Kokoski et al. 2008). Therefore, we compared inhibition of Bax membrane permeabilizing activity by the anti-apoptotic protein,

Bcl-XL for Bax activated by OICR766A and cBid mt1. Preliminary experiments demonstrated that Bcl-XL inhibited liposome permeabilization by cBid mt1 and Bax much better than it inhibited OICR766A and Bax. Therefore Bcl-XL mediated inhibition of liposome permeabilization was compared for reaction conditions in which cBid mt1 and Bax permeabilized ~ 70% and OICR766A and Bax permeabilized ~40% of liposomes, respectively. As the concentration of Bcl-XL was increased cBid mt1/Bax mediated liposome permeabilization decreased from ~70% to ~10% at 160 nM Bcl-XL (Fig 3A, dotted line). In contrast, 300 nM Bcl-XL was required to decrease liposome permeabilization by OICR766A and Bax from roughly 40 to 18% (Fig. 3A, solid line). Thus, while OICR766A activated Bax mimics cBid mt1 activated Bax, given the difference in sensitivity to Bcl-XL and the data above suggesting the compound activates soluble Bax we speculated that the mechanism of Bax activation by OICR766A is different than activation by BH3 proteins.

OICR766A binds to Bax

To determine whether OICR766A binds directly to Bax and if so with what stoichiometry we monitored the binding thermodynamics by isothermal titration calorimetry (ITC). Titration of OICR766A into 20μM Bax yielded a dissociation constant (K_D) of 255nM ± 58nM and a compound:Bax stoichiometry of no more than 1:1 (Fig. 3B left panel). A structural analog of OICR766A, SRI-1, with similar

physical-chemical properties, failed to induce Bax mediated permeabilization in mitochondria (Fig. 3C,D). This compound also displayed no detectable binding to Bax in the ITC measurements (Fig. 3B right panel). In contrast four other analogues of OICR677A (SRI-2-SRI-5, Fig. 3D) all activated Bax to permeabilize mitochondria (Fig. 3C). These data demonstrate that OICR766A mediated Bax activation is induced by direct binding of OICR766A and that this interaction is structure specific.

Cysteine 126 of Bax is required for activation by OICR766A

Bax has two cysteines located at positions 62 and 126 (Suzuki, Youle et al. 2000). Conflicting reports exist on the role of the cysteines in Bax activation and oligomerization. It has been reported that for Bax activation in cells, cysteine 62 is required under oxidative conditions while cysteine 126 appears to be required for activation by DHHC protein acyltransferase family members or prostaglandins (Lalier, Cartron et al. 2011; Frohlich, Dejanovic et al. 2014). In contrast, the data presented in other studies suggest that in cells neither cysteine is required during Bax mediated cell death in response to etoposide or staurosporine (Dewson, Ma et al. 2012). Because all of these measurements were made in cells it is difficult to evaluate the relative importance of direct and indirect effects. To investigate the involvement of Bax cysteines for compound mediated Bax activation directly we used genetic elimination or chemical

modification of the cysteine residues with N-ethylmaleimide (NEM). Both treatments dramatically reduced activation of Bax by OICR766A but not by cBid (Fig. 4A) or Bim (Fig. S3A). To examine the individual cysteine residues, each was mutated to alanine. Bax C62A was activated while C126A Bax was almost completely resistant to chemical activation by OICR766A and the other two compounds that activated Bax at mitochondria, ZM and Ebselen (Fig. 4A and S3B). While it is possible that all three compounds react with C126, the differences in the structures of the compounds suggest that they are interacting with the C126 through distinct binding modes. Of note, covalent modification of C126 with other compounds (e.g. fluorophores (Lovell, Billen et al. 2008)) is not sufficient to activate Bax. These results suggest that C126 is most likely part of the compound binding site and modification or substitution alters the binding site sufficiently to prevent the compounds activating the protein.

To determine whether cysteine 126 is required for compound binding to Bax or for some other aspect of Bax activation (e.g. insertion into membranes) we measured OICR766A binding to the cysteine mutants using ITC. Consistent with C126 forming part of the compound binding site, a direct interaction between Bax and OICR766A was observed for Bax with a cysteine residue at this position (C62A) with a K_D of 266 ± 136nM but not for Bax C126A or for the double cysteine mutant (Fig 4B). Taken together these results indicate that cysteine 126 is required for OICR766A to bind to Bax. We could not address the cysteine

requirement for activation of Bax by OICR766A in cells due to off target effects. However, it is likely that the mechanism of Bax activation by the compound is similar in cells.

In summary, our data show that although cBid, Bim and OICR766A function to activate Bax, they differ in the mechanism by which this happens. Unlike cBid and Bim, OICR766A triggers oligomerization of Bax in the absence of membranes, is poorly inhibited by Bcl-XL and requires Bax cysteine 126. Thus multiple mechanisms exist for Bax activation and we speculate that the mechanism of Bax activation by small molecules allows Bax to respond to cellular signals, drug intoxication and/or metabolites independent of BH3 proteins. Our results may also explain why in some cells Bax and Bak appear to be constitutively activated without upregulation of BH3 proteins (Willis, Chen et al. 2005; Willis, Fletcher et al. 2007). In cells dual activation pathways may be particularly important for the integration of multiple stimuli. Insights gained into alternative mechanisms for targeting Bax using the small molecules here revealed a novel pathway for activation of Bax that is druggable and may prove to be an advantageous therapeutic target in some disease states including cancers where cells are dependent on sequestration of BH3 proteins (Mode 1) inhibition of apoptosis.

Materials and Methods

Materials

8-Aminonaphthalene-1,3,6-trisulfonic Acid, disodium salt (ANTS), p-Xylene-bis-pyridinium bromide (DPX), Dulbecco's Modified Eagle Medium (DMEM) and Fetal bovine serum (FBS) were obtained from Life Technologies. Terbium III chloride hexahydrate ($TBCl_3.6H_2O$) and pyridine-2,6-dicarboxylic acid (DPA) were obtained from Sigma. Lipids were obtained from Avanti Polar Lipids Inc. Disuccinimidyl suberate (DSS) and N-ethylmaleimide (NEM) were obtained from ThermoFisher. The Bax monoclonal antibodies, 6A7 and 2D2 were kind gifts from Richard Youle (Hsu and Youle 1997). The sheep polyclonal antibody against cytochrome c was purified in our laboratory (Billen, Kokoski et al. 2008). Immunoblotting of Bax and cytochrome c was conducted at a 1:5000 dilution. Immunofluorescence using 6A7 was performed at dilutions of 1:1000. All secondary antibodies were purchased from Jackson Immunoresearch laboratories. For immunoblotting, secondary antibodies conjugated to horseradish peroxidase were used at a 1:20,000 dilution. For immunofluorescence, secondary antibodies conjugated to FITC were used at a 1:1000 dilution. The plasmid encoding Annexin V was a generous gift from Seamus Martin. Alexa-488 was obtained from Life Technologies. DRAQ5 was obtained from Biostatus and used a final concentration of 5μM. Tetramethylrhodamine, ethyl ester (TMRE) was obtained from Life Technologies

and used at 10nM final concentration. Annexin V- conjugated to Alexa-488 was prepared in our laboratory and used as described previously (Logue, Elgendy et al. 2009). Baby mouse kidney (BMK) cells and their *bak-/-*, *bax-/-* and *bax-/- bak-/-* derivatives were generous gifts from Eileen White. All compounds except for OICR766A and its analogs were obtained from Sigma. OICR766A was obtained from Vitas M laboratory (cat # STL224013). Analogs of OICR766A, SRI-1 through 5 were obtained from Enamine (Cat # Z56176185, Z57301731, Z56976836, Z57301713, Z57301722).

Cell culture and transfection

BMK cells were cultured in DMEM, consisting of 10% FBS. BMK cells stably expressing Smac (1-56aa)-mCherry were generated as described previously (Shamas-Din, Satsoura et al. 2014). To generate BMK cells expressing human Bax, *bax-/- bak-/-* BMK cells were transfected with the mammalian expression vector (pvitro) expressing Wt human *bax*. Clones expressing Bax were maintained in 3µg/ml Blasticidin.

Protein Purification and labelling

Recombinant cBid, Bim, Bax and Bcl-XL were expressed and purified as described previously (Yethon, Epand et al. 2003; Billen, Kokoski et al. 2008; Lovell, Billen et al. 2008; Sarosiek, Chi et al. 2013). During the Bax and Bcl-XL

purification, the intein tag was cleaved by incubation of the chitin beads with 100mM β- mercaptoethanol for 48 hr at 4°C. Only batches of Bax with < 15% autoactivity in the liposome permeabilization assay were used. To modify cysteine residues, Bax was labelled with NEM by incubation with a 10 fold molar excess in buffer containing 10mM Hepes (pH 7.2), 200mM sodium chloride, 0.1mM EDTA and 10% Glycerol at room temperature for 2 hours. Excess NEM was removed by dialysis.

Liposome preparation

Mitochondria like liposomes with a lipid composition of 48% phosphatidylcholine, 28% phosphatidylethanolamine, 10% phosphatidylinositol, 10% dioleoyl phophatidylserine, and 4% tetraoleoyl cardiolipin were prepared as described previously in assay buffer containing 10mM Hepes (7.2), 200mM potassium chloride, 5mM magnesium chloride and 0.2mM EDTA (Yethon, Epand et al. 2003; Billen, Kokoski et al. 2008).

Liposome permeabilization assays

Liposomes encapsulating 12.5mM ANTS and 45mM DPX were prepared and assayed as described previously (Yethon, Epand et al. 2003; Billen, Kokoski et al. 2008). In this assay, background values (F_0) were obtained by measuring the fluorescence of liposomes in the presence of compounds at 1 min intervals for at

least 10 min at 37^0C (Ex: 355nm and Em: 520nm). Proteins (cBid and/or Bax) were added at t=0 and fluorescence was measured at 37^0C for 3 hours. F_{100} was obtained by adding Triton X-100 at a final concentration of 0.2% (w/v) and measuring fluorescence for 10 min at 37^0C. The % ANTS/ DPX release was calculated as $[(F- F_0 / F_{100} - F_{0)}]*100$. All reactions were carried out in the 96 half area non-binding plates (Corning # 3686). For the primary screen, compounds from the Canadian Compound Collection and the Ontario Institute for Cancer Research (OICR) diversity subset were screened at 10μM. Compounds with high background fluorescence were re-assayed with liposomes encapsulating Tb/DPA (0.8mM $TbCl_3$ and 2.4mM DPA) prepared in assay buffer without EDTA. The assay was conducted similar to the ANTS/ DPX assay described above except that the liposomes were assayed in assay buffer containing 5mM EDTA and F_{100} was obtained by permeabilizing the liposomes with 0.5% CHAPS (Ex: 276nm and Em: 545nm).

Mitochondria isolation and permeabilization assay

Heavy membranes containing mitochondria were isolated from baby mouse kidney (BMK) cells (Shamas-Din, Satsoura et al. 2014). Briefly, cells were harvested and washed twice in PBS. Cells were lysed by nitrogen cavitation at 150 psi for 10 min on ice in lysis buffer containing 250mM sucrose, 150mM potassium chloride, 20mM Hepes (7.2), 1mM EDTA supplemented with complete

protease inhibitor cocktail. To remove nuclei and cell debris, the lysate was centrifuged at 2000*g* for 4 min at 4°C. Mitochondria were then obtained by centrifugation of the supernatant at 13000*g* for 10 min at 4°C and washed once in lysis buffer. For Smac-mCherry release assays mitochondria and cytochrome c release assays, mitochondria were diluted to 0.2mg/ml and 1mg/ml protein concentration respectively. 50µl mitochondrial fractions were incubated with the indicated concentrations of compounds and protein at 37°C for 30 min. Another centrifugation step at 13000*g* for 10 min was performed post incubation. For Smac-mCherry release assays, fluorometric analysis was conducted on the supernatant (F_S) and pellet fractions (F_P) (Ex: 580nm and Em: 610nm). The % release of Smac-mCherry was calculated as (F_S/ F_S + F_P) *100. For cytochrome c release assays, supernatant and pellet fractions were analyzed by immunoblotting and densitometry analysis was carried out using Image J.

Membrane binding assay

Membrane binding assays were performed as described previously (Billen, Kokoski et al. 2008). Briefly, samples containing liposomes (300 µM lipids) were incubated with Bax and the compounds/cBid at 37 °C for 2 h. Membrane bound protein was separated from free protein by gel filtration chromatography on Sepharose CL-2B resin and fractions were analyzed using immunoblotting. Quantitative analysis of the fractions was performed using intensity

measurements in ImageJ. Membrane binding was measured by comparing the intensities of membrane bound proteins (Fraction 3-6) with the total protein in all the fractions.

Crosslinking

Crosslinking studies were carried out as described previously (Billen, Kokoski et al. 2008). Briefly, 100nM Bax and compounds at the indicated concentrations were incubated in the absence or presence of liposomes (300μM total lipids) for 2 hours at 37°C in a low protein binding plate (Corning 3686). Crosslinking was performed using DSS at a final concentration of 2mM for 30 min at room temperature. The reaction was subsequently quenched by the addition of Tris (pH 8) at a final concentration of 20mM. Bax oligomers were detected on immunoblots using the 2D2 antibody. Quantitative analysis of dimers and higher order Bax oligomers was performed using intensity measurements in Image J.

Liposome partitioning assay

Liposomes encapsulating ANTS/DPX or Tb/DPA were prepared as described above. To assess partitioning of the compounds into liposomes, liposomes were incubated with the compounds at 37 °C for 1 h. Membrane partitioned compounds were separated from free compound by passing the liposomes over

a Sepharose CL-2B gel filtration column. Bax was added to these liposomes and permeabilization was assayed as described above.

Isothermal Titration Calorimetry (ITC)

ITC runs were performed using the MicroCal ITC200 (Malvern Instruments). For sample preparation, Bax was dialyzed against 10mM Hepes (pH 7.2), 200mM sodium chloride and 0.1mM EDTA and diluted to a final concentration of 20μM. The compounds were diluted in Bax dialysis buffer and titrated from a 150μM solution. All experiments were performed at 25°C. Data analysis was performed using Origin software (MicroCal).

Live cell Imaging and Analysis

Cells were plated at a cell density of 2000 cells/ well in 384 well plates. 24 hours after plating, the cells were treated with the compounds at the indicated concentrations for 24 hours. 30min prior to imaging the cells were stained with DRAQ5, TMRE and Annexin-V-Alexa 488 in Annexin V binding buffer containing 10mM Hepes (7), 150mM sodium chloride, 5mM potassium chloride, 1mM magnesium chloride and 1.8mM calcium chloride (Logue, Elgendy et al. 2009). Image acquisition was performed using the Opera High Content Screening System (Perkin Elmer) with a 20x air objective. For every independent experiment, each treatment dose was conducted in a minimum of duplicate wells

and a minimum of 5 different fields of view (~50 cells /field) were acquired for each well. For each cell the nucleus and cytoplasm were identified using the DRAQ5 intensity as described previously (Shamas-Din, Bindner et al. 2013). Intensity features and morphology features were extracted using a custom Acapella high content imaging and analysis software (Perkin Elmer) script available for free download at www.andrewslab.ca. Thresholds were determined as the average intensity plus two standard deviations in the Annexin/TMRE channel in DMSO treated cells.

Immunofluorescence

BMK cells stably expressing human Wt Bax or empty vector were treated for 24 hours and at the end of the treatment, the cells were fixed and immunostained using the 6A7 primary monoclonal antibody and a secondary Donkey anti- mouse antibody conjugated to FITC. Cells were stained with DRAQ5 30 min prior to imaging. Image acquisition and analysis was performed as described above.

Cell survival and regrowth

BMK cells were treated with OICR766A for 24 hours as described above in 384 well plates. The compound was washed away post treatment and cells were left in regular media for 24 hours. Cells were trypsinized and re-plated in 96 well

plates and incubated in growth medium for 3 days. Surviving cells were stained with crystal violet and assessed by absorbance measurements at 600nm.

Acknowledgments and declaration of interest

We thank Dr. Eileen White for providing the BMK cells used in the study, Dr. Richard Youle for providing the 2D2 and 6A7 antibodies, Dr. Seamus Martin for providing the plasmid encoding Annexin-V and Jarkko Ylanko, Mina Falcone, Erin Wang and Annie Dahlgran for conducting the screen to identify Bax activators.

The authors declare no competing interests.

Funding

This work was supported by Canadian Institute of Health Research Grant [FRN 12517] to DWA and BL and Ontario Institute for Cancer Research/Terry Fox Research Institute Grant for Selective Therapies. Funding for the Ontario Institute for Cancer Research is provided by the Government of Ontario through the Ontario Ministry of Research and Innovation.

References

Alsop, A. E., S. C. Fennell, et al. (2015). "Dissociation of Bak alpha1 helix from the core and latch domains is required for apoptosis." Nat Commun **6**: 6841.

Annis, M. G., E. L. Soucie, et al. (2005). "Bax forms multispanning monomers that oligomerize to permeabilize membranes during apoptosis." EMBO J **24**(12): 2096-2103.

Antonsson, B. (2004). "Mitochondria and the Bcl-2 family proteins in apoptosis signaling pathways." Mol Cell Biochem **256-257**(1-2): 141-155.

Billen, L. P., C. L. Kokoski, et al. (2008). "Bcl-XL inhibits membrane permeabilization by competing with Bax." PLoS Biol **6**(6): e147.

Brown, R. D., G. A. Burke, et al. (2009). "Dependence of leukemic cell proliferation and survival on H2O2 and L-arginine." Free Radic Biol Med **46**(8): 1211-1220.

Cartron, P. F., L. Oliver, et al. (2004). "Impact of pH on Bax alpha conformation, oligomerisation and mitochondrial integration." FEBS Lett **578**(1-2): 41-46.

Certo, M., V. Del Gaizo Moore, et al. (2006). "Mitochondria primed by death signals determine cellular addiction to antiapoptotic BCL-2 family members." Cancer Cell **9**(5): 351-365.

Chen, L., S. N. Willis, et al. (2005). "Differential targeting of prosurvival Bcl-2 proteins by their BH3-only ligands allows complementary apoptotic function." Mol Cell **17**(3): 393-403.

Czabotar, P. E., D. Westphal, et al. (2013). "Bax crystal structures reveal how BH3 domains activate Bax and nucleate its oligomerization to induce apoptosis." Cell **152**(3): 519-531.

D'Alessio, M., M. De Nicola, et al. (2005). "Oxidative Bax dimerization promotes its translocation to mitochondria independently of apoptosis." FASEB J **19**(11): 1504-1506.

Degenhardt, K., R. Sundararajan, et al. (2002). "Bax and Bak independently promote cytochrome C release from mitochondria." J Biol Chem **277**(16): 14127-14134.

Desagher, S., A. Osen-Sand, et al. (1999). "Bid-induced conformational change of Bax is responsible for mitochondrial cytochrome c release during apoptosis." J Cell Biol **144**(5): 891-901.

Dewson, G., S. Ma, et al. (2012). "Bax dimerizes via a symmetric BH3:groove interface during apoptosis." Cell Death Differ **19**(4): 661-670.

Du, C., M. Fang, et al. (2000). "Smac, a mitochondrial protein that promotes cytochrome c-dependent caspase activation by eliminating IAP inhibition." Cell **102**: 33-42.

Eskes, R., S. Desagher, et al. (2000). "Bid induces the oligomerization and insertion of Bax into the outer mitochondrial membrane." Mol Cell Biol **20**(3): 929-935.

Frohlich, M., B. Dejanovic, et al. (2014). "S-palmitoylation represents a novel mechanism regulating the mitochondrial targeting of BAX and initiation of apoptosis." Cell Death Dis **5**: e1057.

Gavathiotis, E., D. E. Reyna, et al. (2012). "Direct and selective small-molecule activation of proapoptotic BAX." Nat Chem Biol **8**(7): 639-645.

Gilmore, A. P., A. D. Metcalfe, et al. (2000). "Integrin-mediated survival signals regulate the apoptotic function of Bax through its conformation and subcellular localization." J Cell Biol **149**(2): 431-446.

Hanahan, D. and R. A. Weinberg (2011). "Hallmarks of cancer: the next generation." Cell **144**(5): 646-674.

Hsu, Y. T. and R. J. Youle (1997). "Nonionic detergents induce dimerization among members of the Bcl-2 family." J Biol Chem **272**(21): 13829-13834.

Hsu, Y. T. and R. J. Youle (1998). "Bax in murine thymus is a soluble monomeric protein that displays differential detergent-induced conformations." J Biol Chem **273**(17): 10777-10783.

Kim, B. J., S. W. Ryu, et al. (2006). "JNK- and p38 kinase-mediated phosphorylation of Bax leads to its activation and mitochondrial

translocation and to apoptosis of human hepatoma HepG2 cells." J Biol Chem **281**(30): 21256-21265.

Kuwana, T., M. R. Mackey, et al. (2002). "Bid, Bax, and lipids cooperate to form supramolecular openings in the outer mitochondrial membrane." Cell **111**(3): 331-342.

Lai, T. S., Y. Liu, et al. (2008). "Identification of chemical inhibitors to human tissue transglutaminase by screening existing drug libraries." Chem Biol **15**(9): 969-978.

Lalier, L., P. F. Cartron, et al. (2011). "Prostaglandins antagonistically control Bax activation during apoptosis." Cell Death Differ **18**(3): 528-537.

Leber, B., J. Lin, et al. (2007). "Embedded together: the life and death consequences of interaction of the Bcl-2 family with membranes." Apoptosis **12**(5): 897-911.

Leshchiner, E. S., C. R. Braun, et al. (2013). "Direct activation of full-length proapoptotic BAK." Proc Natl Acad Sci U S A **110**(11): E986-995.

Llambi, F., T. Moldoveanu, et al. (2011). "A unified model of mammalian BCL-2 protein family interactions at the mitochondria." Mol Cell **44**(4): 517-531.

Logue, S. E., M. Elgendy, et al. (2009). "Expression, purification and use of recombinant annexin V for the detection of apoptotic cells." Nat Protoc **4**(9): 1383-1395.

Lovell, J. F., L. P. Billen, et al. (2008). "Membrane binding by tBid initiates an ordered series of events culminating in membrane permeabilization by Bax." Cell **135**(6): 1074-1084.

Mondal Roy, S. and M. Sarkar (2011). "Membrane fusion induced by small molecules and ions." J Lipids **2011**: 528784.

Nie, C., C. Tian, et al. (2008). "Cysteine 62 of Bax is critical for its conformational activation and its proapoptotic activity in response to H2O2-induced apoptosis." J Biol Chem **283**(22): 15359-15369.

Pagliari, L. J., T. Kuwana, et al. (2005). "The multidomain proapoptotic molecules Bax and Bak are directly activated by heat." Proc Natl Acad Sci U S A **102**(50): 17975-17980.

Sarosiek, K. A., X. Chi, et al. (2013). "BID preferentially activates BAK while BIM preferentially activates BAX, affecting chemotherapy response." Mol Cell **51**(6): 751-765.

Shamas-Din, A., S. Bindner, et al. (2013). "tBid undergoes multiple conformational changes at the membrane required for Bax activation." J Biol Chem.

Shamas-Din, A., D. Satsoura, et al. (2014). "Multiple partners can kiss-and-run: Bax transfers between multiple membranes and permeabilizes those primed by tBid." Cell Death Dis **5**: e1277.

Suzuki, M., R. J. Youle, et al. (2000). "Structure of Bax: coregulation of dimer formation and intracellular localization." Cell **103**(4): 645-654.

Wang, K., X. M. Yin, et al. (1996). "BID: a novel BH3 domain-only death agonist." Genes Dev **10**(22): 2859-2869.

Wei, M. C., W. X. Zong, et al. (2001). "Proapoptotic BAX and BAK: a requisite gateway to mitochondrial dysfunction and death." Science **292**(5517): 727-730.

Willis, S. N., L. Chen, et al. (2005). "Proapoptotic Bak is sequestered by Mcl-1 and Bcl-xL, but not Bcl-2, until displaced by BH3-only proteins." Genes Dev **19**(11): 1294-1305.

Willis, S. N., J. I. Fletcher, et al. (2007). "Apoptosis initiated when BH3 ligands engage multiple Bcl-2 homologs, not Bax or Bak." Science **315**(5813): 856-859.

Wilschut, J., N. Duzgunes, et al. (1980). "Studies on the mechanism of membrane fusion: kinetics of calcium ion induced fusion of phosphatidylserine vesicles followed by a new assay for mixing of aqueous vesicle contents." Biochemistry **19**(26): 6011-6021.

Wood, D. E. and E. W. Newcomb (2000). "Cleavage of Bax enhances its cell death function." Exp Cell Res **256**(2): 375-382.

Xin, M., R. Li, et al. (2014). "Small-molecule Bax agonists for cancer therapy." Nat Commun **5**: 4935.

Yethon, J. A., R. F. Epand, et al. (2003). "Interaction with a membrane surface triggers a reversible conformational change in Bax normally associated with induction of apoptosis." J Biol Chem **278**(49): 48935-48941.

Zhao, G., Y. Zhu, et al. (2014). "Activation of the proapoptotic Bcl-2 protein Bax by a small molecule induces tumor cell apoptosis." Mol Cell Biol **34**(7): 1198-1207.

Figures

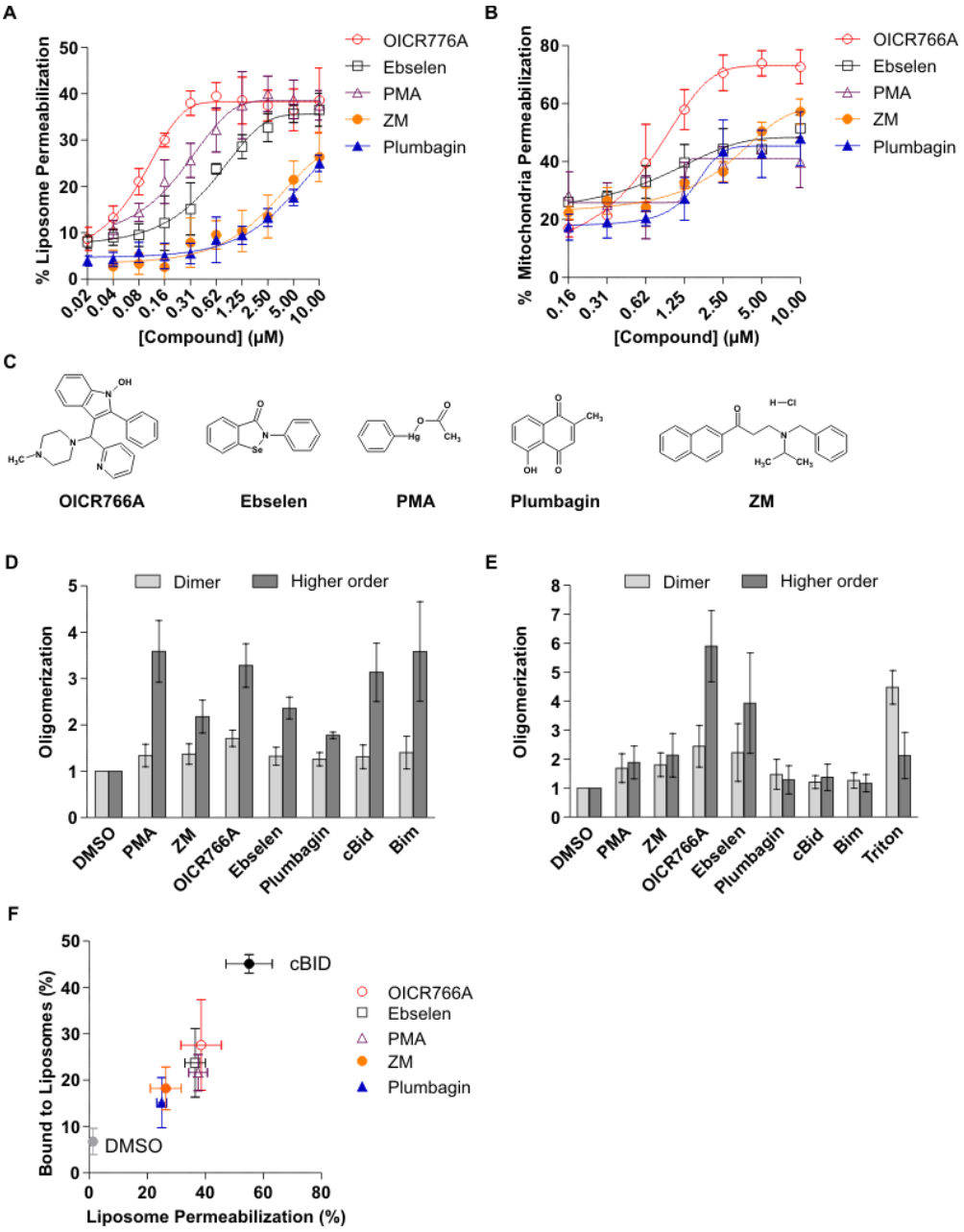

FIGURE 1: Structurally diverse compounds activate Bax.

A. Compounds Trigger Bax to Permeabilize Liposomes. Liposomes encapsulating ANTS and DPX were incubated with 100nM Bax and the indicated

concentrations of the compounds. Due to interfering fluorescence from the compound, ZM39923 was assayed using liposomes encapsulating Tb/DPA. Membrane permeabilization was assayed by measuring the increase in ANTS fluorescence or the decrease in Tb/DPA fluorescence. Results are compared to lysis with detergent (100%) and represented as mean ± std dev (n=3).

B. Compounds Trigger Bax to Permeabilize Mitochondria. Mitochondria from *bax-/- bak-/-* BMK cells containing Smac-mCherry were incubated with 20nM Bax and the indicated concentrations of the compounds. Permeabilization was assayed by pelleting the mitochondria and measuring the fluorescence of the supernatant and pellet fractions. The fraction of Smac-mCherry in the supernatant fraction was determined and results are represented as mean ± std dev (n=3).

C. **Structures of the five small molecule Bax activators.** PMA = Phenylmercuric acid; ZM= ZM39923 hydrochloride.

D. Compound induced Bax oligomerization in liposomes. 100nM Bax was incubated with 20nM cBid/Bim or 10μM of the indicated compounds in the presence of liposomes. Crosslinking was performed with DSS followed by immunoblotting (Fig. S1C). Band intensities of dimer ~42kDa and higher order oligomers (>42kDa) were quantified using Image J. Results are represented as the fold change in Bax intensity relative to the no compound (DMSO) lane ± std dev (n=3).

E. Compound induced Bax oligomerization in solution. Quantification of Bax oligomerization assessed by crosslinking in the absence of liposomes as described in D (Immunoblots: Fig. S1D). As a positive control, Bax was incubated with 1% Triton-X-100.

F. Compound induced Bax binding to liposomes correlates with permeabilization. 100nM Bax was incubated with 10μM of the compounds or 20nM cBid in the presence of liposomes. Membrane bound Bax was separated from soluble Bax using gel filtration chromatography and analyzed using immunoblotting. Results are represented as % membrane bound Bax vs % liposome permeabilization from Fig 1A (Error bars: std dev). Membrane binding was measured by comparing the intensities of membrane bound proteins (Fraction 3-6) with the total protein in all the fractions (Fig. S1E; n=3).

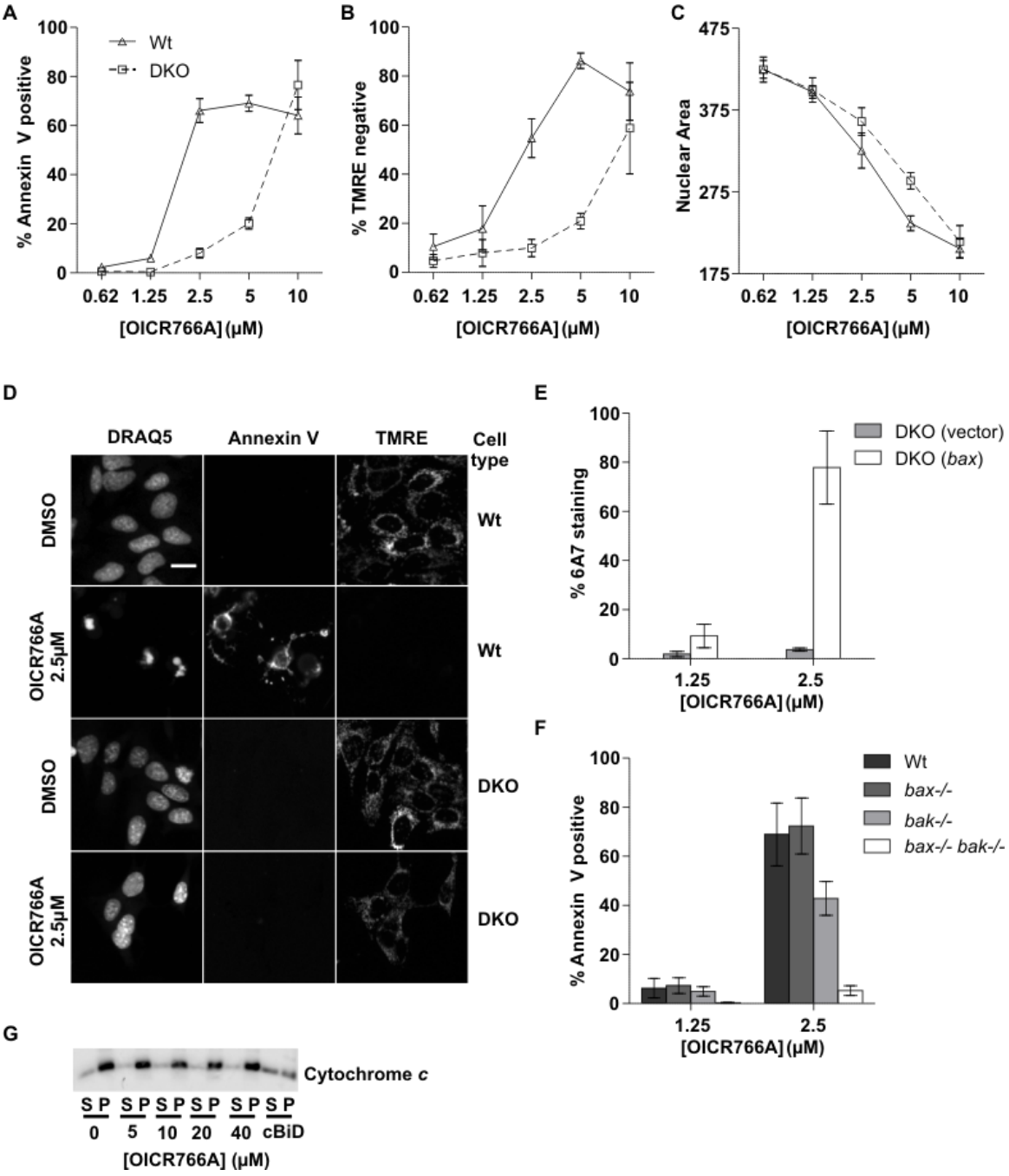

FIGURE 2: OICR766A induces cell death by a Bax/Bak dependent mechanism.

A-C. Cell death measured for Wt and *bax-/- bak-/-* (DKO) BMK cells treated with the indicated concentrations of OICR766A for 24 hours prior to imaging. Results are presented as percentage of cells scored as dead for duplicate wells from three independent experiments +/- SEM.

A. Externalization of phosphatidylserine. Cell death was assessed by Annexin V-Alexa 488 staining intensity above a calculated threshold.

B. Loss of mitochondrial transmembrane potential. Loss of mitochondrial transmembrane potential was assessed for the same cells from **A.** as decreased staining with TMRE below a calculated threshold.

C. Nuclear condensation. Nuclear area was measured for the same cells as **A**. by staining with DRAQ5.

D. Representative images of Wt and DKO BMK cells as indicated at the right, treated with DMSO or OICR766A as indicated to the left for 24 hours. Cells were stained with Annexin V (to detect externalized phosphatidylserine as indicative of loss of plasma membrane asymmetry), TMRE (mitochondrial membrane potential), and DRAQ5 (nuclear morphology) as indicated above the columns. The scale bar indicates 10 μm.

E. Bax activation. DKO BMK cells stably expressing human Wt *bax* or empty vector were treated for 24 hours with OICR766A as indicated. Immunofluorescence intensity above a threshold with an antibody (6A7) that binds an epitope exposed during activation of Bax was used to score cells as stained or unstained. Results are represented as the percentage increase in the number of cells with positive 6A7 staining relative to the DMSO control ± SEM of duplicate wells from n=3 independent experiments.

F. Externalization of phosphatidylserine. Wt, *bax-/-*, *bak-/-*, or *bax-/- bak-/-* BMK cells were treated at the indicated concentrations of OICR766A and analyzed as in A. (n=3)

G. Mitochondria Permeabilization. Mitochondria from *bax-/-* BMK cells were incubated with OICR766A at the indicated concentrations or 5nM cBid as a positive control and then the mitochondria were pelleted (P) by centrifugation. Permeabilization results in release of cytochrome *c* from the mitochondria into the supernatant (S). The blot is representative of 3 independent experiments.

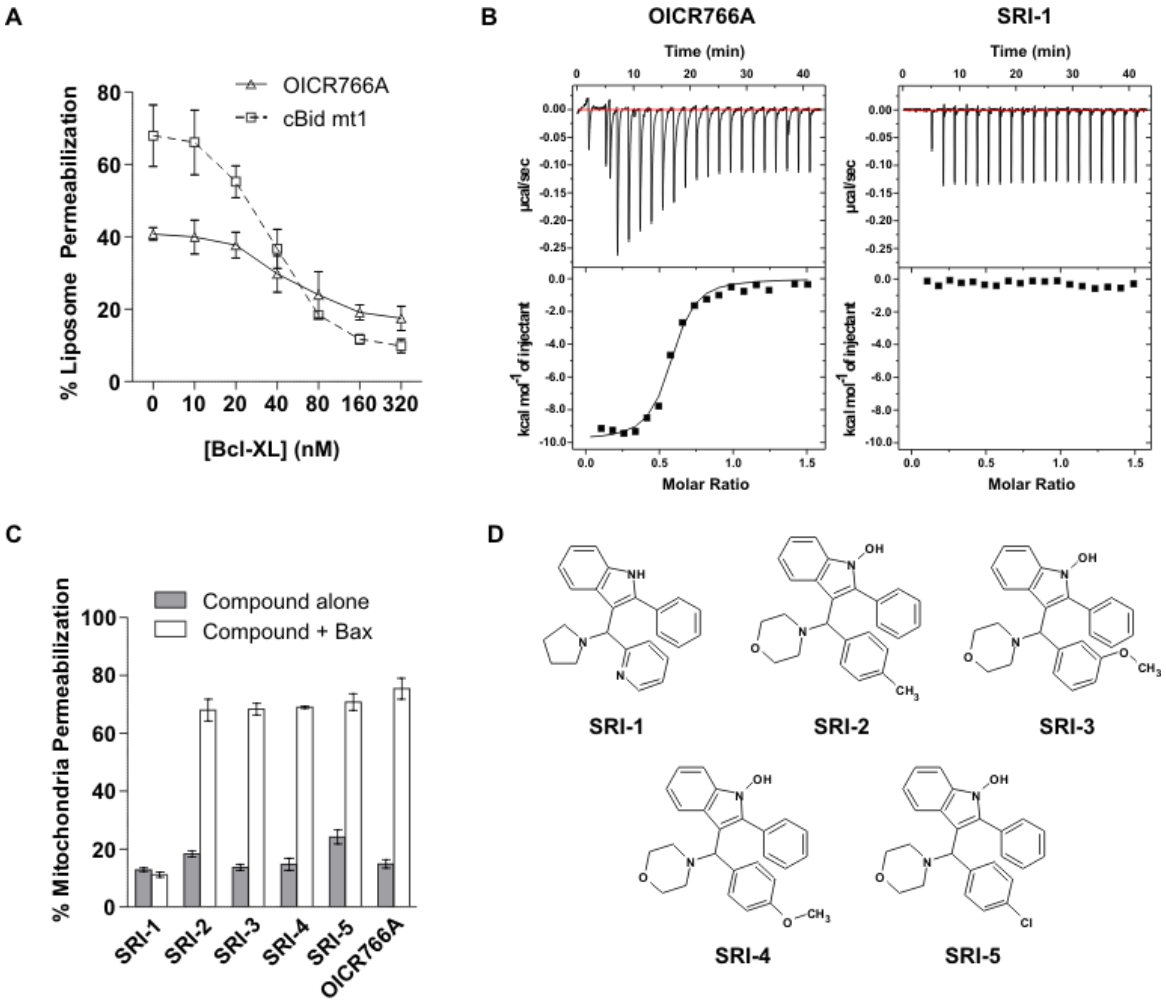

FIGURE 3: The molecular mechanisms of Bax activation by OICR766A and cBid are different.

A. Bcl-XL poorly inhibits OICR766A compared to cBid mt1 mediated activation of Bax. 100nM Bax and 1µM OICR766A or 20nM cBid mt1 were added to liposomes encapsulating ANTS/DPX and the indicated concentrations of Bcl-XL. Membrane permeabilization was assayed by the increase in fluorescence compared to liposome lysis with detergent (100%) as in Fig. 1A. (n=3)

B. OICR766A binds to Bax. Isothermal titration calorimetry analysis of 20µM Bax with successive additions of 2µl from a 150 µM stock of OICR766A (left panel) and SRI-1 (right panel). Raw injection heats are shown in the top panel

and corresponding isotherms fitted to a one site model in the bottom panel. Shown here is one representative titration of at three independent replicates.

C. Mitochondria Permeabilization. Mitochondria from *bax-/- bak-/-* BMK cells expressing smac-mCherry were incubated with 10 μM of the OICR766A analogs and 20nM Bax and assayed as described in Fig. 1B. (n=3)

D. Structures of OICR766A analogs tested in C. Names are indicated below the structures.

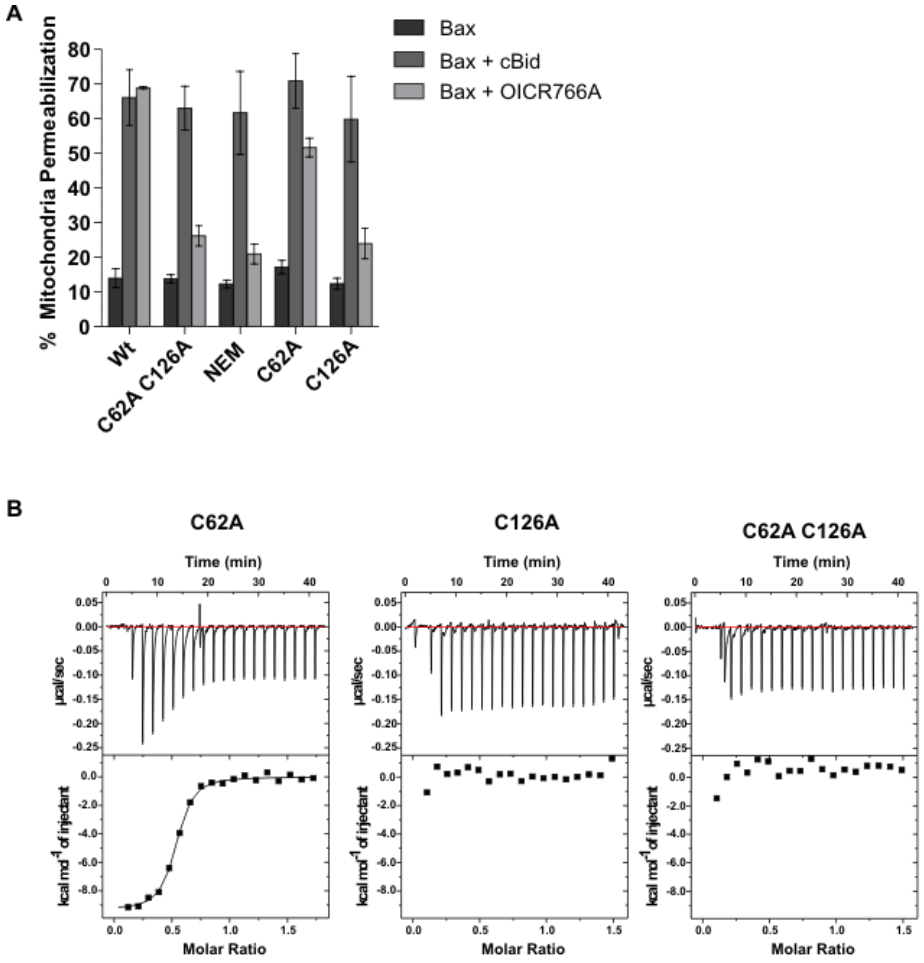

FIGURE 4: OICR766A mediated Bax activation requires cysteine 126.

A. Mitochondria Permeabilization. Mitochondria from *bax-/- bak-/-* BMK cells containing Smac-mCherry were assayed with 20nM Bax and 10µM OICR766A or 2nM cBid as a positive control and assayed as described in Fig. 1B. (n=3)

B. OICR766A-Bax binding. Isothermal titration calorimetry analysis of 20µM Bax mutants C62A, C126A, C62A C126A titrated with OICR766A as described in Fig. 3C.

Table

Table 1: Bax activation by compounds

Compound	EC_{50} in liposomes (μM)	EC_{50} in mitochondria (μM)
OICR766A	0.1	0.9
Ebselen	0.6	1.1
PMA	0.2	1.3
ZM	>3	3.5
Plumbagin	>3	1.5

Supplementary figures

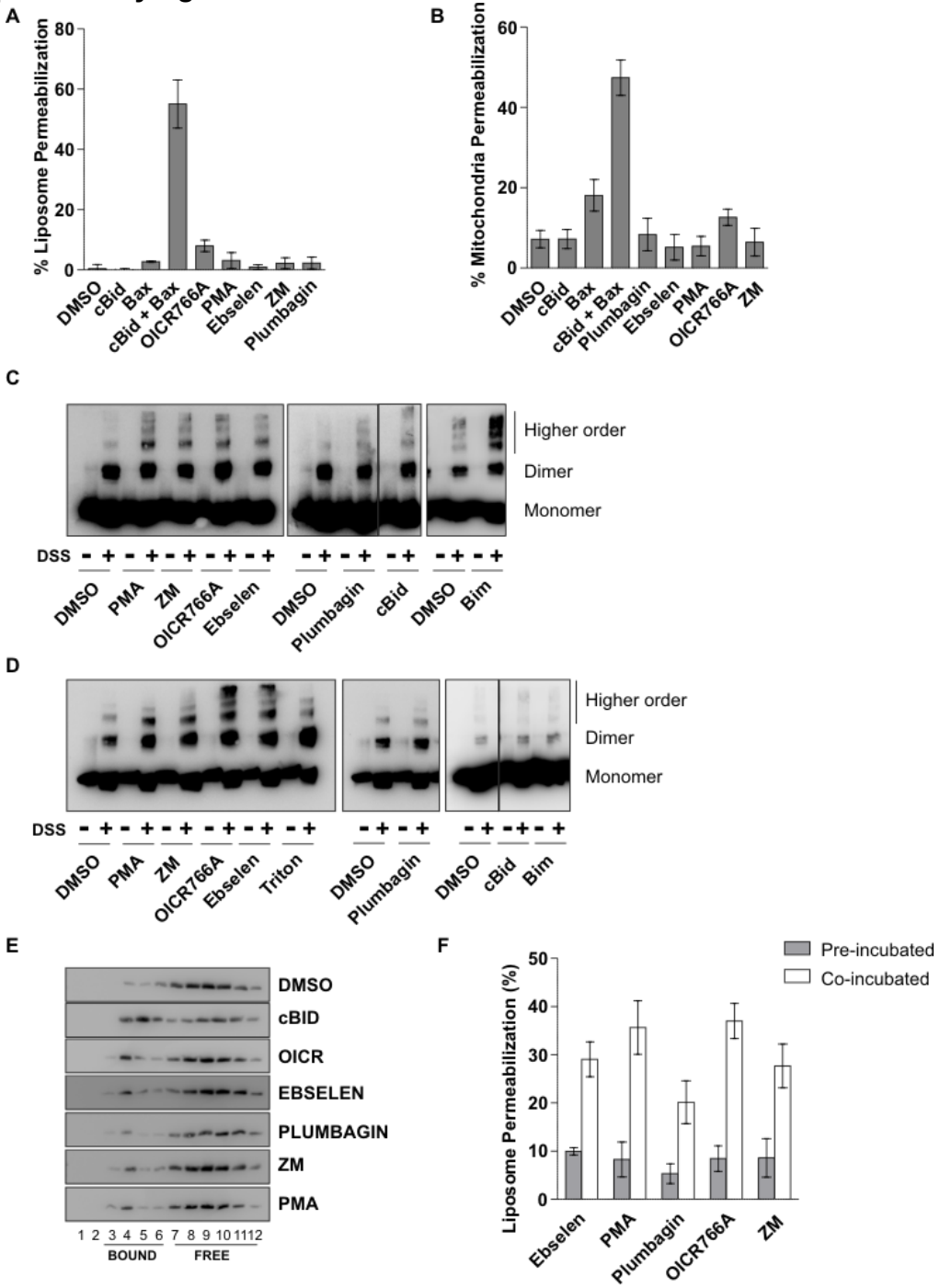

FIGURE S1: Compound mediated activation of Bax.

A. Liposome permeabilization. Liposomes encapsulating ANTS/DPX or Tb/DPA were incubated with 10μM of the compounds. As a positive control for liposome permeabilization, 20nM cBid was incubated with 100nM Bax. Liposome permeabilization was assayed as described in Fig. 1A.

B. Mitochondria Permeabilization. Mitochondria isolated from *bax-/- bak-/-* BMK cells expressing Smac-mCherry were incubated with 10 μM of each of the compounds. As a positive control, 2nM cBid was incubated with 20nM Bax. Membrane permeabilization was assayed as described in Fig. 1B.

C. Compound induced Bax oligomerization in liposomes. Representative immunoblots from Fig. 1D.

D. Compound induced Bax oligomerization in solution. Representative immunoblots from Fig. 1E.

E. Compound induced Bax binding to liposomes. Representative immunoblots from Fig. 1F.

F. Compounds do not activate Bax by partitioning into and altering liposome membrane properties. Liposomes containing ANTS and DPX or Tb and DPA were pre- incubated with the 10μM of the compounds and passed over the Sepharose CL-2B column followed by the addition of 100nM Bax (Pre-incubated). Controls contained liposomes passed over the CL-2B column and added to reactions containing both Bax and the indicated compounds (Co-incubated). Membrane permeabilization was assayed as described in Fig 1A. (mean +/- std dev, n=3).

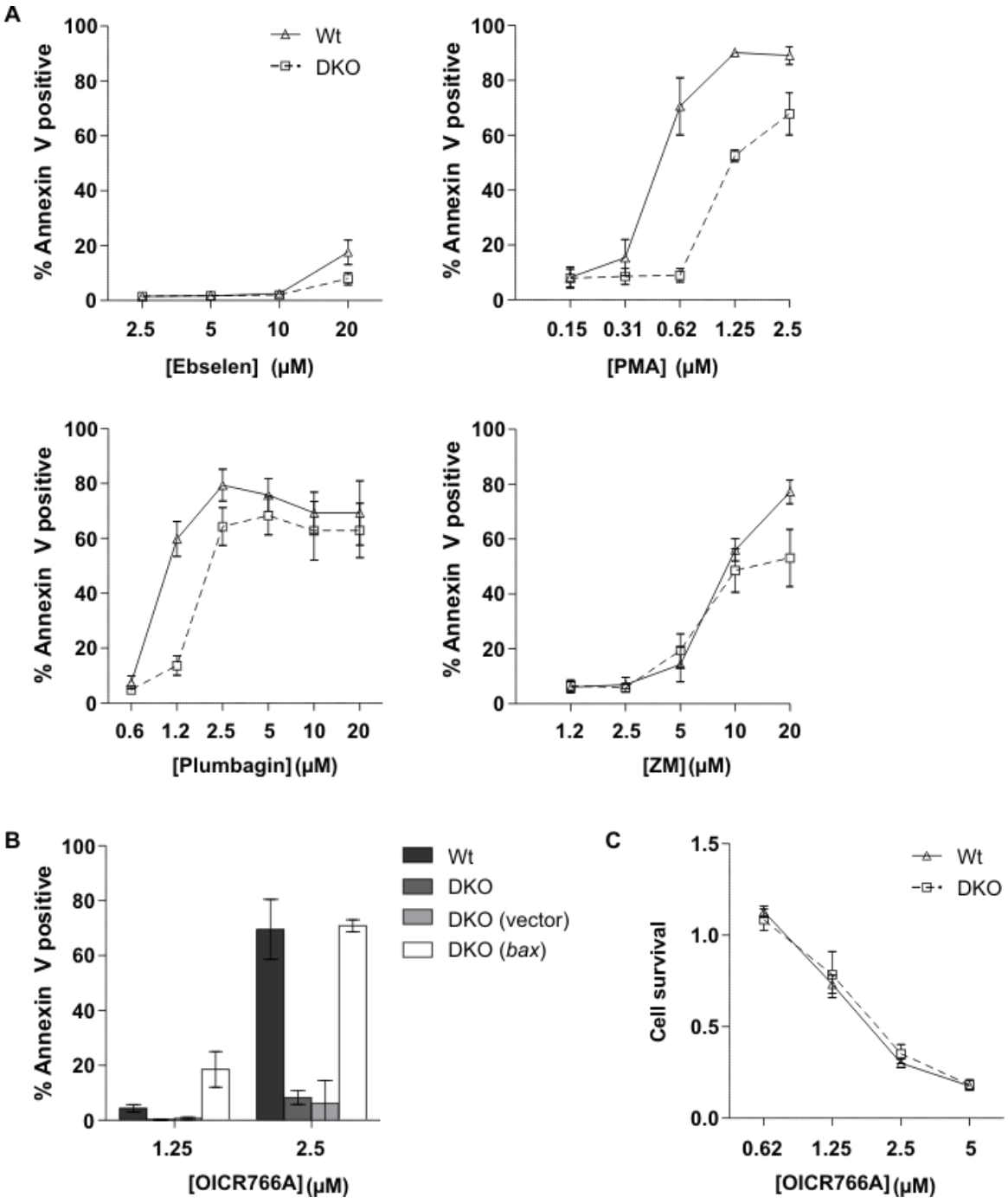

FIGURE S2. Bax dependent and independent cell death induced by compounds.

A. Externalization of phosphatidylserine. Wt and DKO BMK cells were treated with the compounds indicated below the graphs and assayed at the indicated concentrations for binding of Annexin V as in Fig. 2A.

B. Externalization of phosphatidylserine. Wt, DKO, and DKO BMK cells stably expressing the empty vector or exogenous Wt Bax were assayed at the indicated OICR766A concentrations as described in Fig. 2A.

C. Cell survival and regrowth. Wt and DKO BMK cells were treated with OICR766A at the indicated concentrations for 24hours and left in drug-free media for 24hours. Cells were replated and grown for 3 days. Cell survival was assessed by crystal violet staining. Each treatment point is normalized to the cell survival of DMSO control which is defined as 1 (mean ± SEM, n=3).

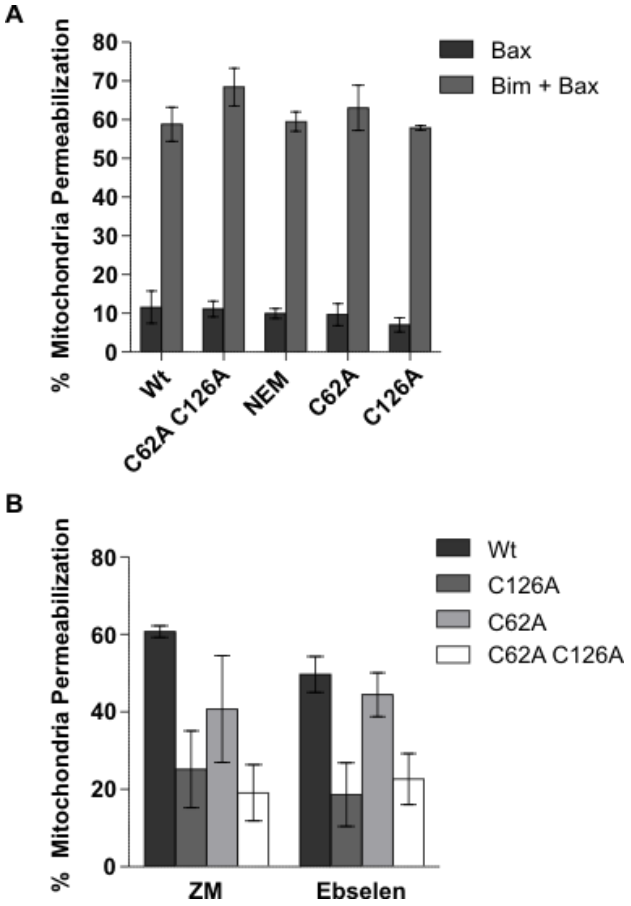

FIGURE S3: Cysteine residue requirements for Bax activation by compounds or Bim.

A. Activation of Bax by Bim does not require endogenous cysteines. Permeabilization assayed for mitochondria incubated with 20nM Bax and/or 2nM Bim as described in Fig. 4A. (n=3)

B. Cysteine 126 is required for activation of Bax by ZM and PMA. Permeabilization assayed for mitochondria incubated with 20nM Bax and 10μM of the indicated compounds as described in Fig. 4A. (n=3).

CHAPTER IV:

Enhancement of mitochondrial outer membrane permeabilization by the small molecule SRI-O13 as anti- cancer therapy

Preface

The work presented in this chapter has been prepared for submission as a research article and for submission as a patent application.

Contribution of authors:

BL, DWA and JY designed the screen and directed the project. DWA, DU and RA designed the SAR experiments. JS validated hits from the primary screen and conducted preliminary studies with SRI-O13 and its analogs. QL purified cBak. YS conducted all the experiments with the mice. The rest of the experiments described here were conducted by HB.

Research Objective

To identify small molecules that enable Bax to escape inhibition by Bcl-XL.

Research Highlights:

- The small molecule, SRI-O13 enabled Bax to escape inhibition by Bcl-XL in a dose dependent manner.
- Unlike ABT-737, SRI-O13 accelerated and enhanced Bax and Bak mediated membrane permeabilization.
- SRI-O13 displayed anti-tumor activity in mice.
- SRI-O13 synergized with various apoptosis inducers to potentiate cell death.

Enhancement of mitochondrial outer membrane permeabilization by the small molecule SRI-O13 as anti- cancer therapy

Hetal Brahmbhatt[1,3], Yuval Shaked[2], Jing Sang[3], David Uehling[4], Rima Al-awar[4], Qian Liu[3], Jing Yi[5], Brian Leber[6], David Andrews[1,3]

[1]Department of Biochemistry and Biomedical Sciences, McMaster University, Hamilton, ON.
[2]Department of Molecular Pharmacology, Rappaport Faculty of Medicine, Technion, Haifa.
[3]Department of Biological Sciences, Sunnybrook Research Institute, Toronto, ON.
[4]Drug Discovery Program, Ontario Institute for Cancer Research, Toronto, ON.
[5]Department of Biochemistry and Molecular Cell Biology, Institutes of Medical Sciences, Shanghai Jiao Tong University School of Medicine, Shanghai.
[6]Department of Medicine, McMaster University, Hamilton, ON.

Abstract

Overexpression of Bcl-2 family proteins mediates resistance to conventional and targeted anticancer agents by preventing apoptosis. Therefore, these proteins are attractive targets for therapeutic agents. Anti-apoptotic Bcl-2 proteins prevent MOMP by sequestering activator BH3 proteins and the pore forming proteins, Bax and Bak at the membrane. Most inhibitors of the anti-apoptotic proteins currently being developed disrupt the interactions between anti-apoptotic and BH3 proteins. Using high throughput screening we identified the small molecule SRI-O13 that enhances MOMP by a novel mechanism. *In vitro*, SRI-O13 functions by accelerating tBid or Bim mediated activation of Bax or Bak. As a single agent, SRI-O13 induced cell death of transplanted tumors in mice. As

expected, in cell lines SRI-O13 synergized with various apoptosis inducing agents. A secondary screen indicated that as a class, histone deacetylase (HDAC) inhibitors that are in clinical development strongly synergize with SRI-O13. Therefore by identifying the tool compound SRI-O13 we validated acceleration of Bax and Bak mediated MOMP as a novel druggable target for the enhancement of apoptosis that may have relevance for anti- cancer therapy.

Introduction

Resistance to conventional chemotherapy and targeted anti- cancer therapies remains a major clinical challenge. Most of these agents eliminate tumors by inducing apoptosis and consequently defects in apoptotic signaling contribute significantly to resistance (Kaufmann and Earnshaw 2000; Holohan, Van Schaeybroeck et al. 2013). A widely accepted model postulates that tumors are “addicted” to anti-apoptotic Bcl-2 family proteins which restrain the intrinsic apoptosis that would otherwise prevent tumor development (Deng, Carlson et al. 2007). Therefore there has been a strong rationale for therapeutically targeting these proteins to re-activate apoptosis to selectively kill cancer cells and for overcoming drug resistance.

The Bcl-2 family proteins play a pivotal role in regulating mitochondrial outer membrane permeabilization (MOMP), an event that commits a cell to death (Wang 2001; Leber, Lin et al. 2007). MOMP occurs when activator Bcl-2

homology 3 (BH3) proteins such as Bid or Bim sense apoptotic stimuli and induce the activation of the effector members, Bax and Bak, which oligomerize to permeabilize the mitochondrial outer membrane (MOM). After permeabilization, pro-apoptotic factors such as cytochrome c and Smac are released from the mitochondrial inter-membrane space which initiate a cascade of caspase activation culminating in cell death (Youle and Strasser 2008). Anti-apoptotic members such as Bcl-2, Bcl-XL, Mcl-1 inhibit this process by binding and inhibiting the activator and effector Bcl-2 family proteins at the MOM (Billen, Kokoski et al. 2008).

High expression levels of Bcl-2, Bcl-XL and Mcl-1 are present in various hematologic and solid tumors and contribute to both tumor development and resistance to diverse chemo- and radio- therapies (Minn, Rudin et al. 1995; Jameel, Rao et al. 2004; Deng, Carlson et al. 2007; Beroukhim, Mermel et al. 2010). Substantial progress has been made in identifying compounds targeting these anti-apoptotic members to restore apoptosis, and two compounds, ABT-199 and ABT-263 that mimic the binding of the BH3 protein Bad to anti-apoptotic proteins have been the most intensively investigated (Tse, Shoemaker et al. 2008; Souers, Leverson et al. 2013). To date most inhibitors have been identified in screens that use soluble fragments or recombinant proteins that lack the C-terminal binding domain as binding targets and therefore focus on disabling Mode 1 of inhibition whereby the BH3 proteins are sequestered by anti-apoptotic family

members (Petros, Olejniczak et al. 2004; Vogler 2014). Membrane binding causes conformational changes in all subclasses of the Bcl-2 family proteins, therefore, strategies that use soluble targets may not identify many potentially active agents and neglect other interactions that regulate MOMP (Annis, Soucie et al. 2005; Dlugosz, Billen et al. 2006; Billen, Kokoski et al. 2008; Billen, Shamas-Din et al. 2008; Lovell, Billen et al. 2008; Llambi, Moldoveanu et al. 2011; Shamas-Din, Bindner et al. 2013).

To address these issues we have developed a high-throughput *in vitro* liposome based assay to screen for compounds that enable Bax to escape inhibition by Bcl-XL. We report the identification of tool compound, SRI-O13, that potentiates Bax and Bak mediated apoptosis by accelerating their activation by BH3-proteins. SRI-O13 displays cytotoxic activity in xenotransplanted human cancer cells lines as a single agent. Furthermore by screening a library of anti-cancer compounds, we have identified HDAC inhibitors as potent synergizers of SRI-O13 across various cell types.

Results

SRI-O13 prevents inhibition of Bax by Bcl-XL enabling Bax mediated liposome permeabilization

To identify small molecules that enable Bax to escape inhibition by Bcl-XL on membranes, we used liposomes with a lipid composition mimicking the MOM

which encapsulated a fluorescent dye, 8-aminonaphthalene-1,3,6-trisulfonic acid (ANTS) and its collisional quencher, *p*-xylene-bis-pyridinium bromide (DPX). Membrane permeabilization mediated by cBid-activated Bax causes an increase in spatial separation with subsequent de-quenching of ANTS fluorescence (Yethon, Epand et al. 2003; Lovell, Billen et al. 2008). Drugs that compete with BH3 proteins for binding to Bcl-XL have already been identified and are in clinical trials. To bias our screen to selectively identify compounds that prevent or overcome inhibition of Bax but not cBid by Bcl-XL, a mutant of cBid (cBid-mt1) that does not bind to Bcl-XL but still activates Bax to permeabilize membranes was used (Wang, Yin et al. 1996). In this system Bcl-XL is recruited to the membrane; therefore compounds that enhance Bax activation or prevent the inhibition of Bax by Bcl-XL would lead to Bax mediated permeabilization (Fig. 1A). Consistent with previous findings Bcl-XL inhibits membrane permeabilization of Bax activated by cBid-mt1 in a dose dependent manner (Fig. S1A), and control reactions containing the proteins alone do not alter liposome integrity (Fig. S1B) (Billen, Kokoski et al. 2008).

To conduct the screen more than 20,000 structurally diverse compounds from the Ontario Institute for Cancer Research (OICR) library were incubated with Bcl-XL and cBid-mt1 in the presence of liposomes, followed by the addition of Bax. We identified and validated an active compound termed SRI-O13, with an IC_{50} of ~0.7 μM for overcoming the inhibition of Bax by Bcl-XL (Fig. 1B).

Importantly, it only increased the activity of Bax in the absence of cBid and Bcl-XL by ~20% at the highest concentration used in the screening assay, Fig. S2A). Furthermore SRI-O13 did not permeabilize liposomes directly (Fig. S1B).

SRI-O13 enhances Bax and Bak mediated membrane permeabilization by a novel mechanism

Based on the scheme of our screening system (Fig. 1A), the membrane permeabilization effect of SRI-O13 may be due to the compound 1) preventing Bcl-XL binding to and inhibiting Bax, or 2) dissociating of pre-existing Bcl-XL-Bax complexes. To discriminate between these two possibilities, liposome permeabilization was measured when SRI-O13 was added 1 hour after other components in the permeabilization assay, and compared with the results obtained with the screening conditions described earlier, where it was added to all the components before the addition of Bax. The delayed compound addition compromised the ability of SRI-O13 to enhance MOMP. By contrast the known Bcl-XL/ Bcl-2 inhibitor, ABT-737, was equally active regardless of the order of addition (Fig. 2A). The difference between ABT-737 and SRI-O13 was also evident when examining the kinetics of the assay in which the compounds were added prior to the addition of Bax. We observed that Bax mediated liposome permeabilization was not only much faster with SRI-O13 but importantly was also faster than the reaction containing cBid and Bax (Fig. 2B). Compound mediated

inhibition of Bcl-XL should theoretically yield liposome permeabilization kinetics comparable to or slower than that by cBid and Bax. Since we observed liposome permeabilization kinetics that were faster than that by cBid and Bax, we hypothesized that the mode of action of SRI-O13 was likely to be independent of Bcl-XL. Consistent with this hypothesis in the absence of Bcl-XL, although end-point liposome permeabilization was similar (Fig. S2A), SRI-O13 accelerated the rate of liposome permeabilization as measured by a decrease in the reaction half-time of liposome permeabilization whereas ABT-737 decreased the rate of liposome permeabilization (Fig. 2C, D). Taken together these results indicate a markedly distinct and novel mechanism of action for SRI-O13 compared to ABT-737.

To examine whether this enhancement of MOMP was unique to either cBid or Bax, we substituted cBid with the other well characterized activator BH3 protein, BimL, and Bax with calpain-proteolysed Bak (cBak) that is lacking the C-terminal membrane anchoring region, as it has been challenge to purify full length recombinant Bak (Moldoveanu, Liu et al. 2006; Liu and Gehring 2010; Sarosiek, Chi et al. 2013). Significantly, we noticed a similar acceleration and enhancement of Bax mediated liposome permeabilization by BimL (Fig. 2D, S2B) and cBak mediated liposome permeabilization triggered by activator BH3 proteins, BimL and cBid (Fig. S2C-D). Therefore, this suggested that either SRI-O13 mediated effects on the membrane to enhance pore forming activity by Bax and cBak or

that SRI-O13 mediated effects on one or multiple steps common to the activation of Bax and Bak by activator BH3 proteins.

To further examine the mechanism of action of SRI-O13, we assessed whether the enhancement of Bax activity triggered by the combination of SRI-O13 and cBid could be regulated by Bcl-XL. We observed that increasing the concentration of Bcl-XL resulted in a dose- dependent decrease in liposome permeabilization suggesting a direct inhibition of Bax by Bcl-XL (Fig. S2E). Additionally, we purchased a series of structurally similar compounds, and identified an analog 349A which does not accelerate liposome permeabilization (Fig. S2F). Therefore, our data indicate that that the activity of SRI-O13 is not dependent on chemical reactivity but rather structure specific and most likely not an indirect effect on membranes.

To extend these observations to the relevant physiologic target membrane for Bax/Bak pore formation, mitochondria were isolated from *Bax-/- Bak-/-* baby mouse kidney (BMK) cells that express the fluorescent fusion protein, Smac-mCherry. The latter is localized in the mitochondrial intermembrane space, and thus the release of Smac-mCherry serves as readout for MOMP. Consistent with the results observed in liposomes, SRI-O13 enhanced cBid/Bim-Bax (Fig. 2E-F) and cBid-cBak (Fig. S2G) mediated MOMP. Importantly, the addition of cBid, Bim, Bax, cBak or the highest dose of SRI-O13 as single agents did not compromise mitochondrial integrity (Fig. S2H).

SRI-O13 induces cell death of transplanted tumors in mice

Various cellular stress signals regulate the activity of BH3 proteins at the transcriptional and post- transcriptional levels (Kutuk and Letai 2008). Despite the various stresses, tumors have devised strategies to counter the pro-apoptotic stimulus to survive and proliferate (Brunelle and Letai 2009). To determine if SRI-O13 potentiated cell killing activity of tumors *in vivo* as a single agent¸ mice were implanted with human colon cancer cells (HCT116) and the effects of SRI-O13 on the size of the established tumors were measured after the maximum tolerated dose (MTD) was determined. Based on these results a dose of 25 mg/kg was used for these studies (Table S1). As shown in Fig. 3A, SRI-O13 treated mice had smaller tumor masses compared to the control group, with no significant changes in body weight during the treatment (Fig. 3B). To determine if the decreased tumor volume was due to delayed tumor growth and/or enhanced cell death, tumor sections were stained with terminal deoxynucleotidyl transferase dUTP nick end labeling (TUNEL) or Ki-67 to measure DNA fragmentation and cell proliferation, respectively (Fig. 3C left and middle panel). Corresponding cell nuclei were stained with 4',6-diamidino-2-phenylindole (DAPI). Cell death was also assessed by measuring the auto fluorescence of the tissue sections (Fig. 3C, right panel) (Shaked, Ciarrocchi et al. 2006). Our results indicated that both effects were present, as we measured an increase in DNA

fragmentation and cell death (Fig. 3D, left and right), as well as a decrease in cell proliferation (Fig. 3D, middle). This effect was not restricted to colon cancer as similar results were also noted in mice transplanted with murine (Fig. S3A-B) and human patient-derived breast cancer tumors (Fig. S3 C-D).

SRI-O13 synergizes with various inducers of apoptosis to potentiate cell death

Given that SRI-O13 exerts its effects by enhancing MOMP that has been initiated by activator BH3 proteins, we examined whether SRI-O13 will cooperate or synergize with other agents that activate BH3 proteins via diverse pathways. To ensure that we would detect enhancement of true apoptosis rather than non-specific toxicity we used wt BMK cells, with *Bax-/- Bak-/-* double knockout (DKO) cells as controls, where we anticipate no effect with the latter cell type. Cell death was assessed by triple staining with DRAQ5, Tetramethylrhodamine, ethyl ester (TMRE) and Annexin V to measure nuclei condensation, loss of membrane potential and exposure of phosphatidylserine, respectively. These three events are characteristic of cell death by apoptosis at different stages. Consistent with the effect we observed in the murine tumor transplants with monotherapy, SRI-O13 compromised the viability of wt (but not DKO) cells in a dose dependent fashion at 20 μM, as detected by an increase in Annexin-V staining and a decrease in membrane potential and in nuclear area (Fig. S4A).

To evaluate the ability of SRI-O13 to potentiate cell death, it was combined at a subtoxic dose of 10 μM with other drugs using a non- constant combination approach. Synergy was quantified by the Chou-Talalay method to determine a combination index (CI), where CI=1, <1 or >1 representing additive, synergistic or antagonistic effects respectively (Chou 2010). As shown in Fig. 4A and Supplementary Table 2, a combination of SRI-O13 with various doses of actinomycin D, staurosporine and cisplatin enhanced cell death of wt BMK as detected by an increase in Annexin V staining, and yielded CI values smaller than 1 for most drug combinations. Significantly the DKO cells were resistant to death at all drug combinations (Fig. 4A).

To identify additional clinically relevant agents that would synergize with SRI-O13, a combination screen was conducted on the wt BMK cells using a library of 160 compounds. The results displayed in Fig. 4B indicate the cell viability obtained after treatment with 1 μM of the compound alone compared to treatment in combination with 10 μM SRI-O13. Of the 160 compounds tested, 21 compounds displayed cell killing activity of >75% in the absence of SRI-O13. 17 of 139 compounds enhanced cell kill >25% in the presence of SRI-O13 and were classified as hits (Fig. 4B). Remarkably 6 of these 17 hits were histone deacetylase (HDAC) inhibitors (Fig. S4B). Interestingly, 5 of the 21 compounds which as single agents killed cells >75% were also HDAC inhibitors. The 11 HDAC inhibitors were re-assayed at various doses in combination with 10 μM

SRI-O13 in both wt and DKO BMK cells to confirm enhancement of apoptosis. From these 11, further synergy studies were conducted with four HDAC inhibitors: panobinostat, belinostat, pracinostat and vorinostat, as these compounds are already in clinical use or trials. Consistent with our observations in Fig. 4A, SRI-O13 potentiated HDAC inhibitor induced cell death of wt, but not DKO cells and exhibited synergy at most dose combinations (Fig. 4C, Supplementary Table 2). Since our results with the various HDAC inhibitors were similar, we focused further investigations using only one combination: the SRI-O13/panobinostat combination. To ensure that our observations were not cellular specific, we tested this combination on immortalized mouse embryonic fibroblasts (MEF). Consistent with the results in Fig. 4D, we observed a similar enhancement of cell death in wt MEF cells and the DKO cells were insensitive to this combination demonstrating that our observation were not cellular specific (Fig. S4C).

To investigate whether SRI-O13 enhances both Bax and Bak MOMP in cells similar to our observations with the liposome ANTS release assay, MEF DKO cells were transfected with expression vector for either human Bax or Bak and subjected to the combination treatment. Reconstitution of either Bax or Bak restored sensitivity to the combination (Fig. 5A).To determine if this combination was also effective in other types of tumor cells, we treated two different types of breast cancer tumors. Robust synergistic cell death was noted in murine EMT6

and human MDAM231 breast cancer cells (Fig. 5B, and Supplementary table 2). Taken together, our studies with SRI-O13 demonstrate that the acceleration of Bax and Bak is a druggable target that may have therapeutic potential as an anti-cancer strategy.

Discussion

Bax and Bak mediated MOMP is the point of no return for commitment to cell death in cancer cells. The anti-apoptotic Bcl-2 family proteins that prevent MOMP are often aberrantly expressed in tumors and therefore strategies to enhance “stalled” MOMP are highly desirable therapeutically (Ikegaki, Katsumata et al. 1994; Beroukhim, Mermel et al. 2010; Placzek, Wei et al. 2010). Although pharmacologic activation of Bax directly as anti-cancer avenue has been much less explored because of the presumed lack of selectivity for cancer cells, selective antagonism of the anti-apoptotic proteins to indirectly activate Bax and Bak has been investigated extensively (Vogler 2014; Liu, Ding et al. 2015). Here we report the discovery of the small molecule SRI-O13 that enhances MOMP via a mechanism distinct from previously identified anti-apoptotic protein inhibitors.

The small molecules discovered by AbbVie (ABT-737, 263 and 199) compete with the BH3 region of pro-apoptotic Bcl-2 proteins for binding the hydrophobic groove of anti-apoptotic proteins (Oltersdorf, Elmore et al. 2005; Tse, Shoemaker et al. 2008; Souers, Leverson et al. 2013). Our results

comparing the effects on liposome permeabilization when the order of addition of ABT-737 and SRI-O13 was altered suggest that ABT-737 potently prevented the formation of Bcl-XL-Bax complexes and dissociated pre-existing complexes, whereas SRI-O13 was only effective in the former. Furthermore in the absence of Bcl-XL, SRI-O13 accelerated the rate of Bax mediated MOMP whereas ABT-737 decreased the rate. Since Bax and Bcl-XL are structurally similar, we postulate that ABT-737 competed with cBid for the hydrophobic groove of Bax thereby delaying liposome permeabilization (Petros, Olejniczak et al. 2004). Alternatively, SRI-O13 accelerated and enhanced Bax mediated liposome permeabilization thereby enabling Bax to escape inhibition by Bcl-XL suggesting that the mechanism most likely does not involve competition for the hydrophobic groove of Bcl-XL.

We have previously shown that insertion of Bax into the membrane is the rate-limiting step during membrane permeabilization (Lovell, Billen et al. 2008). After interacting with BH3 activators, the alpha helix 9 of Bax is displaced from the hydrophobic pocket allowing Bax to insert into the membrane (Wolter, Hsu et al. 1997; Annis, Zamzami et al. 2001; Schinzel, Kaufmann et al. 2004). Although we see enhanced membrane permeabilization with SRI-O13, it is unlikely that this is mediated by dislodging of helix 9 since we see similar enhancement with cBak that is lacking this C- terminal membrane anchoring helix. Importantly since this enhancement was not specific to the activator or effector Bcl-2 proteins, we

speculate that SRI-O13 mediates its effects either by increasing the affinity of activator BH3 proteins for Bax or Bak by inducing a conformational change in the latter, or by altering these effector proteins such that they are more likely to adopt an oligomerization promoting conformation. A mechanistic dissection and assessment of potential binding sites on the proteins will be the subject of future investigations. In either case, SRI-O13 shifts the equilibria towards MOMP but only in circumstances where activator BH3 proteins and Bax/Bak are in close proximity as is the case in tumors where this activity is restrained by anti-apoptotic family members.

Consistent with the proposed mechanism of action, SRI-O13 displays anti-tumor activity as a single agent against HCT116 cells and breast cancer tumors by enhancing cell death. Tumors rapidly proliferate in a micro-environment lacking sufficient blood supply that results in hypoxia and decreased nutrient supplies which ultimately trigger acute stresses (Albini and Sporn 2007). Therefore, it is highly likely that these acute stresses trigger the activation of a pool of pro-apoptotic Bcl-2 family proteins to induce MOMP, whose effect can be amplified by SRI-O13.

Of all the inhibitors of the anti-apoptotic Bcl-2 family proteins, the drugs ABT-263 and ABT-199 as peptidomimetics of the BH3 sensitizer Bad are the furthest in clinical trials and have shown promising activities in small cell lung cancer and B lymphoid malignancies (Tse, Shoemaker et al. 2008; Rudin, Hann

et al. 2012; Souers, Leverson et al. 2013). ABT-263 was designed as a dual inhibitor of Bcl-2 and Bcl-XL but further clinical development was stopped after the appearance of dose-dependent on-target thrombocytopenia as a consequence of inhibiting Bcl-XL-Bim interactions (Roberts, Seymour et al. 2012). The newer agent ABT-199 was designed to avoid this problem by showing high specificity for Bcl-2 rather than Bcl-XL inhibition (Souers, Leverson et al. 2013; Vandenberg and Cory 2013). The more recently developed Bcl-XL inhibitor, A-1155463 is still associated with reversible thrombocytopenia (Tao, Hasvold et al. 2014). A challenge common to these inhibitors is the lack of inhibition of Mcl-1 which contributes to resistance to chemotherapies (Chen, Dai et al. 2007; Varin, Denoyelle et al. 2010; Bose and Grant 2013). Since SRI-O13 enhances and accelerates MOMP, it may therefore be useful in overcoming the challenges by faced by the current Bcl-2 inhibitors.

Emerging evidence demonstrates that combination treatment improves therapeutic potential and alleviates the side effects caused by higher doses of the component monotherapies (Kummar, Chen et al. 2010). Significantly SRI-O13 potentiates the cell death induced by multiple agents, and in our screen we have identified HDAC inhibitors as good candidates for combination treatment with SRI-O13. HDAC inhibitors are promising anti- cancer agents in a wide variety of solid and hematologic malignancies with positive results in clinical trials used either as monotherapy or in combination (Ververis, Hiong et al. 2013).

Therefore, our results suggest a potentially broad application for SRI-O13 as an important component of designing future anti- cancer therapies.

Materials and methods

Materials

8-Aminonaphthalene-1,3,6-Trisulfonic Acid, Disodium Salt (ANTS), p-Xylene-Bis-Pyridinium Bromide (DPX), Alexa-488, TMRE, Dulbecco's Modified Eagle Medium (DMEM), and MEM non- essential amino acids, and Fetal bovine serum (FBS) were obtained from Life Technologies. Lipids were obtained from Avanti Polar Lipids Inc. Blasticidin was obtained from BioShop. The plasmid encoding Annexin V was a kind gift from Seamus Martin. DRAQ5 was obtained from Biostatus. BMK cells were generous gifts from Eileen White. EMT6 and MDAMB231 were generous gifts from Dr. Kerbel. SRI-O13 and 370A were obtained from TCI chemicals, 364A was obtained from Sigma. 349A and 350A were provided by OICR. ABT-737 and ABT-199 were purchased from Selleck Chemicals. Cisplatin, actinomycin D and staurosporine were obtained from Sigma. The HDAC inhibitors were obtained from Adooq Bioscience.

Cell culture

BMK and MEF cells were cultured in DMEM supplemented with 10% FBS and 1X MEM non- essential amino acids. MEF clones stably expressing Bax or Bak were

maintained in 3 µg/ml Blasticidin. MDAMB231 and EMT6 cells were cultured in DMEM consisting of 10% FBS.

Protein purification

Recombinant murine cBid and human Bax and Bcl-XL were purified as described previously (Billen, Shamas-Din et al. 2008; Shamas-Din, Bindner et al. 2013). Murine BimL was purified as described previously (Sarosiek, Chi et al. 2013). Annexin V was purified and labelled with Alexa- 488 as described in (Logue, Elgendy et al. 2009). Calpain cleaved Bak lacking the C- terminus region was purified as described previously (Moldoveanu, Liu et al. 2006).

Liposome preparation and permeabilization assay

Mitochondria-like liposomes with a lipid composition of phosphatidylcholine, 48%; phosphatidylethanolamine, 28%; phosphatidylinositol, 10%; dioleoyl phosphatidylserine, 10%; and tetraoleoyl cardiolipin, 4% were prepared as described previously (Shamas-Din, Bindner et al. 2013). Membrane permeabilization assays with liposomes encapsulating ANTS and DPX were conducted as described previously with the exception that liposomes were incubated with all components (Bcl-XL, cBid-mt1 and compounds) and fluorescence was measured for 15-20 min at 37 ^{0}C to obtained background values. Bax was added at t=0 and fluorescence was measured at intervals of at

least 1 min for 3 hours at 37 ^{0}C (Billen, Kokoski et al. 2008). The screen was conducted using the Ontario Institute of Cancer Research (OICR) compound library. All compounds were screened at 10 μM. Unless indicated, we used 5 nM cBid or BimL, 100 nM Bax and 40 nM Bcl-XL. Reaction half times were obtained by fitting the time course liposome permeabilization data with a power law function in GraphPad prism.

Mitochondria Isolation and permeabilization assay

Mitochondria from BMK cells stably expressing Smac-mCherry in the intermembrane space were prepared and as described previously except mitochondria were incubated with various components for 30 min at 37 ^{0}C (Shamas-Din, Satsoura et al. 2014).

Live cell imaging and analysis

Cells were plated at a density of 1000 or 2000 cells/ well in 384 well plates for 48 and 24 hr time points respectively. After cells became adherent, they were treated with the compounds as indicated. Cells were stained with DRAQ (5 μM), TMRE (10 nM) and Annexin V- Alexa in cell culture media thirty minutes prior to imaging. Images were acquired using the Opera High Content Screen System using a 20X air objective. For each independent experiment, treatment was administered in duplicate wells and a minimum of 5 fields of view (~50 cells/ field)

per well were obtained. Feature extraction was conducted using a script written for Acapella (available from www.andrewslab.ca). Briefly, the nucleus and cytoplasmic regions were obtained using the DRAQ5 channel followed by extraction of intensity and morphology features. Intensity thresholds were determined using the mean value + 2 SD. Supervised classification for the screen was conducted using in-house classification software (MiClassify) in MATLAB as described previously (Collins, Ylanko et al. 2015). Briefly classifiers were trained using cell- level data from replicate wells of the positive and negative controls and the fraction of individual cells per well classified as either of the control groups was calculated.

Drug combinations and synergy quantification

For the synergy experiments, the drugs were combined at non-constant ratios and at least 3 pairs of drug combinations were examined for every experiment. Synergy was assessed using the Chou-Talalay method with the CompuSyn software (ComboSyn, Inc) (Chou and Talalay 1984; Chou 2010). For each combination experiment, the dose and the mean % cell death values (represented as fractional effect (Fa) over a range of 0.001 to 0.999) were entered into CompuSyn for each drug alone, and the combinations. The software was used to generate the dose- effect curves for the single and combination treatment and obtain combination index (CI) values at different Fa level.

Transplanted tumor studies

The use of animals and experimental protocols were approved by the Animal Care and Use Committee of Sunnybrook Research Institute. Human colon carcinoma cells (HCT116) were implanted subcutaneously into the flanks of 8-10 week old male SCID-YFP mice (grown in-house). The patient derived xenograft tumor HCI-002 line was provided by Dr. Alana Welm (Huntsman Cancer Institute, University of Utah) and was propagated in YFP-SCID mice by serial passages. Tumor tissue pieces 2-5 mm^3, were implanted in the mammary fat pads of new animals, as described previously (Paez-Ribes, Man et al. 2015). Tumor volume was measured regularly using Vernier calipers according to the formula $width^2 x$ length x 0.5. Tumors were removed at end point. For treatment purposes, O13 (25 mg/kg) or its appropriate vehicle (DMSO) were injected intraperitoneally. In order to evaluate toxicity, body weight was monitored regularly. For immunostaining, tumors were embedded in OCT (Sakura, Japan). Tumor OCT sections (5-8 μm thick) were fixed in cold acetone for 15 minutes. Subsequently, tumor sections were blocked with 10% horse serum for 20 minutes. To assess DNA fragmentation, fixed samples were stained using TUNEL (red) (in situ cell detection kit, Roche Diagnostic) as per the manufacturer's instructions. For the staining of proliferation, fixed samples were immunostained with Ki-67 (rabbit anti-Ki67, 1:150, Vector Laboratories VP-K451) followed by secondary Cy-3-

conjugated antibody (1:200, Jackson Immunoresearch Laboratories, PA, USA). DAPI was used to counterstain nuclei (Electron Microscopy Sciences, PA, USA). For assessment of tissue death, H&E staining was performed, and the tissue autofluorescence was detected in the fluorescein isothiocyanate (FITC) channel, as previously described (Shaked, Ciarrocchi et al. 2006). Images were acquired with a camera attached to an inverted microscope (Carl Zeiss Axioplan2 microscope with 10x objective with a Carl Zeiss AxioCam MRc camera).

References

Albini, A. and M. B. Sporn (2007). "The tumour microenvironment as a target for chemoprevention." Nat Rev Cancer **7**(2): 139-147.

Annis, M. G., E. L. Soucie, et al. (2005). "Bax forms multispanning monomers that oligomerize to permeabilize membranes during apoptosis." EMBO J **24**(12): 2096-2103.

Annis, M. G., N. Zamzami, et al. (2001). "Endoplasmic reticulum localized Bcl-2 prevents apoptosis when redistribution of cytochrome c is a late event." Oncogene **20**(16): 1939-1952.

Beroukhim, R., C. H. Mermel, et al. (2010). "The landscape of somatic copy-number alteration across human cancers." Nature **463**(7283): 899-905.

Billen, L. P., C. L. Kokoski, et al. (2008). "Bcl-XL inhibits membrane permeabilization by competing with Bax." PLoS Biol **6**(6): e147.

Billen, L. P., A. Shamas-Din, et al. (2008). "Bid: a Bax-like BH3 protein." Oncogene **27 Suppl 1**: S93-104.

Bose, P. and S. Grant (2013). "Mcl-1 as a Therapeutic Target in Acute Myelogenous Leukemia (AML)." Leuk Res Rep **2**(1): 12-14.

Brunelle, J. K. and A. Letai (2009). "Control of mitochondrial apoptosis by the Bcl-2 family." J Cell Sci **122**(Pt 4): 437-441.

Chen, S., Y. Dai, et al. (2007). "Mcl-1 down-regulation potentiates ABT-737 lethality by cooperatively inducing Bak activation and Bax translocation." Cancer Res **67**(2): 782-791.

Chou, T. C. (2010). "Drug combination studies and their synergy quantification using the Chou-Talalay method." Cancer Res **70**(2): 440-446.

Chou, T. C. and P. Talalay (1984). "Quantitative analysis of dose-effect relationships: the combined effects of multiple drugs or enzyme inhibitors." Adv Enzyme Regul **22**: 27-55.

Collins, T. J., J. Ylanko, et al. (2015). "A Versatile Cell Death Screening Assay Using Dye-Stained Cells and Multivariate Image Analysis." Assay Drug Dev Technol **13**(9): 547-557.

Deng, J., N. Carlson, et al. (2007). "BH3 profiling identifies three distinct classes of apoptotic blocks to predict response to ABT-737 and conventional chemotherapeutic agents." Cancer Cell **12**(2): 171-185.

Dlugosz, P. J., L. P. Billen, et al. (2006). "Bcl-2 changes conformation to inhibit Bax oligomerization." EMBO J **25**(11): 2287-2296.

Holohan, C., S. Van Schaeybroeck, et al. (2013). "Cancer drug resistance: an evolving paradigm." Nat Rev Cancer **13**(10): 714-726.

Ikegaki, N., M. Katsumata, et al. (1994). "Expression of bcl-2 in small cell lung carcinoma cells." Cancer Res **54**(1): 6-8.

Jameel, J. K., V. S. Rao, et al. (2004). "Radioresistance in carcinoma of the breast." Breast **13**(6): 452-460.

Kaufmann, S. H. and W. C. Earnshaw (2000). "Induction of apoptosis by cancer chemotherapy." Exp Cell Res **256**(1): 42-49.

Kummar, S., H. X. Chen, et al. (2010). "Utilizing targeted cancer therapeutic agents in combination: novel approaches and urgent requirements." Nat Rev Drug Discov **9**(11): 843-856.

Kutuk, O. and A. Letai (2008). "Regulation of Bcl-2 family proteins by posttranslational modifications." Curr Mol Med **8**(2): 102-118.

Leber, B., J. Lin, et al. (2007). "Embedded together: the life and death consequences of interaction of the Bcl-2 family with membranes." Apoptosis **12**(5): 897-911.

Liu, Q. and K. Gehring (2010). "Heterodimerization of BAK and MCL-1 activated by detergent micelles." J Biol Chem **285**(52): 41202-41210.

Liu, Z., Y. Ding, et al. (2015). "Direct Activation of Bax Protein for Cancer Therapy." Med Res Rev.

Llambi, F., T. Moldoveanu, et al. (2011). "A unified model of mammalian BCL-2 protein family interactions at the mitochondria." Mol Cell **44**(4): 517-531.

Logue, S. E., M. Elgendy, et al. (2009). "Expression, purification and use of recombinant annexin V for the detection of apoptotic cells." Nat Protoc **4**(9): 1383-1395.

Lovell, J. F., L. P. Billen, et al. (2008). "Membrane binding by tBid initiates an ordered series of events culminating in membrane permeabilization by Bax." Cell **135**(6): 1074-1084.

Minn, A. J., C. M. Rudin, et al. (1995). "Expression of bcl-xL can confer a multidrug resistance phenotype." Blood **86**(5): 1903-1910.

Moldoveanu, T., Q. Liu, et al. (2006). "The X-ray structure of a BAK homodimer reveals an inhibitory zinc binding site." Mol Cell **24**(5): 677-688.

Oltersdorf, T., S. W. Elmore, et al. (2005). "An inhibitor of Bcl-2 family proteins induces regression of solid tumours." Nature **435**(7042): 677-681.

Paez-Ribes, M., S. Man, et al. (2015). "Potential Pro-invasive or Metastatic Effects of Preclinical Antiangiogenic Therapy Are Prevented by Concurrent Chemotherapy." Clin Cancer Res.

Petros, A. M., E. T. Olejniczak, et al. (2004). "Structural biology of the Bcl-2 family of proteins." Biochim Biophys Acta **1644**(2-3): 83-94.

Placzek, W. J., J. Wei, et al. (2010). "A survey of the anti-apoptotic Bcl-2 subfamily expression in cancer types provides a platform to predict the efficacy of Bcl-2 antagonists in cancer therapy." Cell Death Dis **1**: e40.

Roberts, A. W., J. F. Seymour, et al. (2012). "Substantial susceptibility of chronic lymphocytic leukemia to BCL2 inhibition: results of a phase I study of navitoclax in patients with relapsed or refractory disease." J Clin Oncol **30**(5): 488-496.

Rudin, C. M., C. L. Hann, et al. (2012). "Phase II study of single-agent navitoclax (ABT-263) and biomarker correlates in patients with relapsed small cell lung cancer." Clin Cancer Res **18**(11): 3163-3169.

Sarosiek, K. A., X. Chi, et al. (2013). "BID preferentially activates BAK while BIM preferentially activates BAX, affecting chemotherapy response." Mol Cell **51**(6): 751-765.

Schinzel, A., T. Kaufmann, et al. (2004). "Conformational control of Bax localization and apoptotic activity by Pro168." J Cell Biol **164**(7): 1021-1032.

Shaked, Y., A. Ciarrocchi, et al. (2006). "Therapy-induced acute recruitment of circulating endothelial progenitor cells to tumors." Science **313**(5794): 1785-1787.

Shamas-Din, A., S. Bindner, et al. (2013). "tBid undergoes multiple conformational changes at the membrane required for Bax activation." J Biol Chem.

Shamas-Din, A., D. Satsoura, et al. (2014). "Multiple partners can kiss-and-run: Bax transfers between multiple membranes and permeabilizes those primed by tBid." Cell Death Dis **5**: e1277.

Souers, A. J., J. D. Leverson, et al. (2013). "ABT-199, a potent and selective BCL-2 inhibitor, achieves antitumor activity while sparing platelets." Nat Med **19**(2): 202-208.

Tao, Z. F., L. Hasvold, et al. (2014). "Discovery of a Potent and Selective BCL-XL Inhibitor with in Vivo Activity." ACS Med Chem Lett **5**(10): 1088-1093.

Tse, C., A. R. Shoemaker, et al. (2008). "ABT-263: a potent and orally bioavailable Bcl-2 family inhibitor." Cancer Res **68**(9): 3421-3428.

Tse, C., A. R. Shoemaker, et al. (2008). "ABT-263: A Potent and Orally Bioavailable Bcl-2 Family Inhibitor." Cancer Research **68**(9): 3421-3428.

Vandenberg, C. J. and S. Cory (2013). "ABT-199, a new Bcl-2-specific BH3 mimetic, has in vivo efficacy against aggressive Myc-driven mouse lymphomas without provoking thrombocytopenia." Blood **121**(12): 2285-2288.

Varin, E., C. Denoyelle, et al. (2010). "Downregulation of Bcl-xL and Mcl-1 is sufficient to induce cell death in mesothelioma cells highly refractory to conventional chemotherapy." Carcinogenesis **31**(6): 984-993.

Ververis, K., A. Hiong, et al. (2013). "Histone deacetylase inhibitors (HDACIs): multitargeted anticancer agents." Biologics **7**: 47-60.

Vogler, M. (2014). "Targeting BCL2-Proteins for the Treatment of Solid Tumours." Advances in Medicine **2014**: 14.

Wang, K., X. M. Yin, et al. (1996). "BID: a novel BH3 domain-only death agonist." Genes Dev **10**(22): 2859-2869.

Wang, X. (2001). "The expanding role of mitochondria in apoptosis." Genes Dev **15**(22): 2922-2933.

Wolter, K. G., Y. T. Hsu, et al. (1997). "Movement of Bax from the cytosol to mitochondria during apoptosis." J Cell Biol **139**(5): 1281-1292.

Yethon, J. A., R. F. Epand, et al. (2003). "Interaction with a membrane surface triggers a reversible conformational change in Bax normally associated with induction of apoptosis." J Biol Chem **278**(49): 48935-48941.

Youle, R. J. and A. Strasser (2008). "The BCL-2 protein family: opposing activities that mediate cell death." Nat Rev Mol Cell Biol **9**(1): 47-59.

Figures

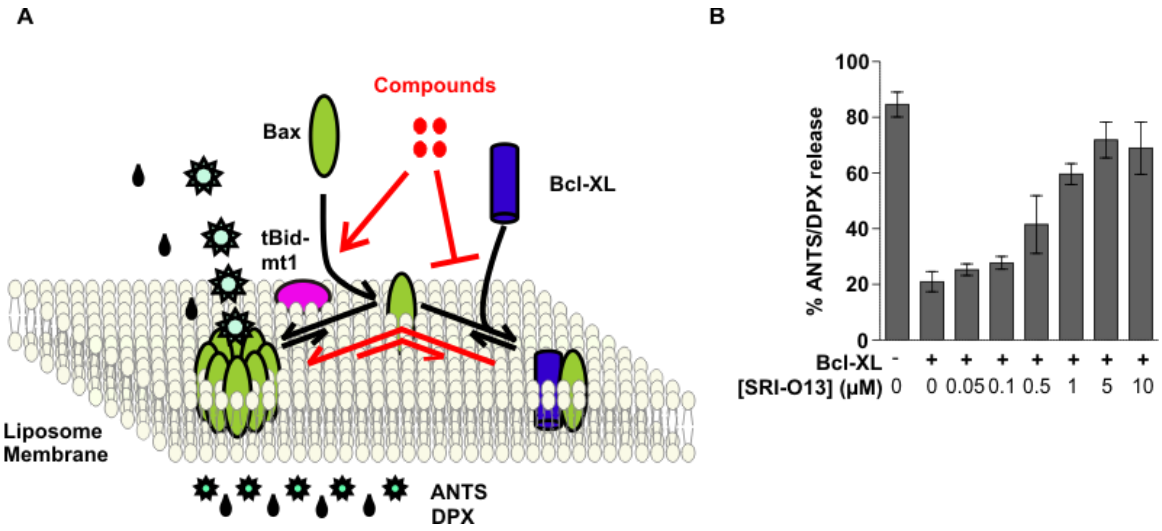

Figure 1: **SRI-O13 enables Bax to escape inhibition by Bcl-XL.**

A. Schematic of the liposome based screen to identify molecules that enable Bax to escape inhibition by Bcl-XL. Liposomes encapsulating the fluorophore, ANTS, and quencher, DPX, were incubated with cBid-mt1 (a mutant that binds Bax but not Bcl-XL), Bcl-XL, compounds, and Bax (added in that order). Bax translocates from the cytosol to the membrane after interacting with membrane bound tBid-mt1. Bcl-XL binds to activated Bax at the membrane and prevents further recruitment of Bax to the membrane thereby preventing Bax oligomerization. Compounds that directly activate Bax, prevent or overcome the inhibition of Bax by Bcl-XL will enable Bax to oligomerize and form pores at the liposome membrane resulting in de-quenching of ANTS fluorescence and an increase in the fluorescence signal.

B. Membrane permeabilization assayed after 3 hours for liposomes incubated Bcl-XL and SRI-O13 as indicated. All reactions have cBid and Bax. Data points: mean ± SD, n=3 independent experiments.

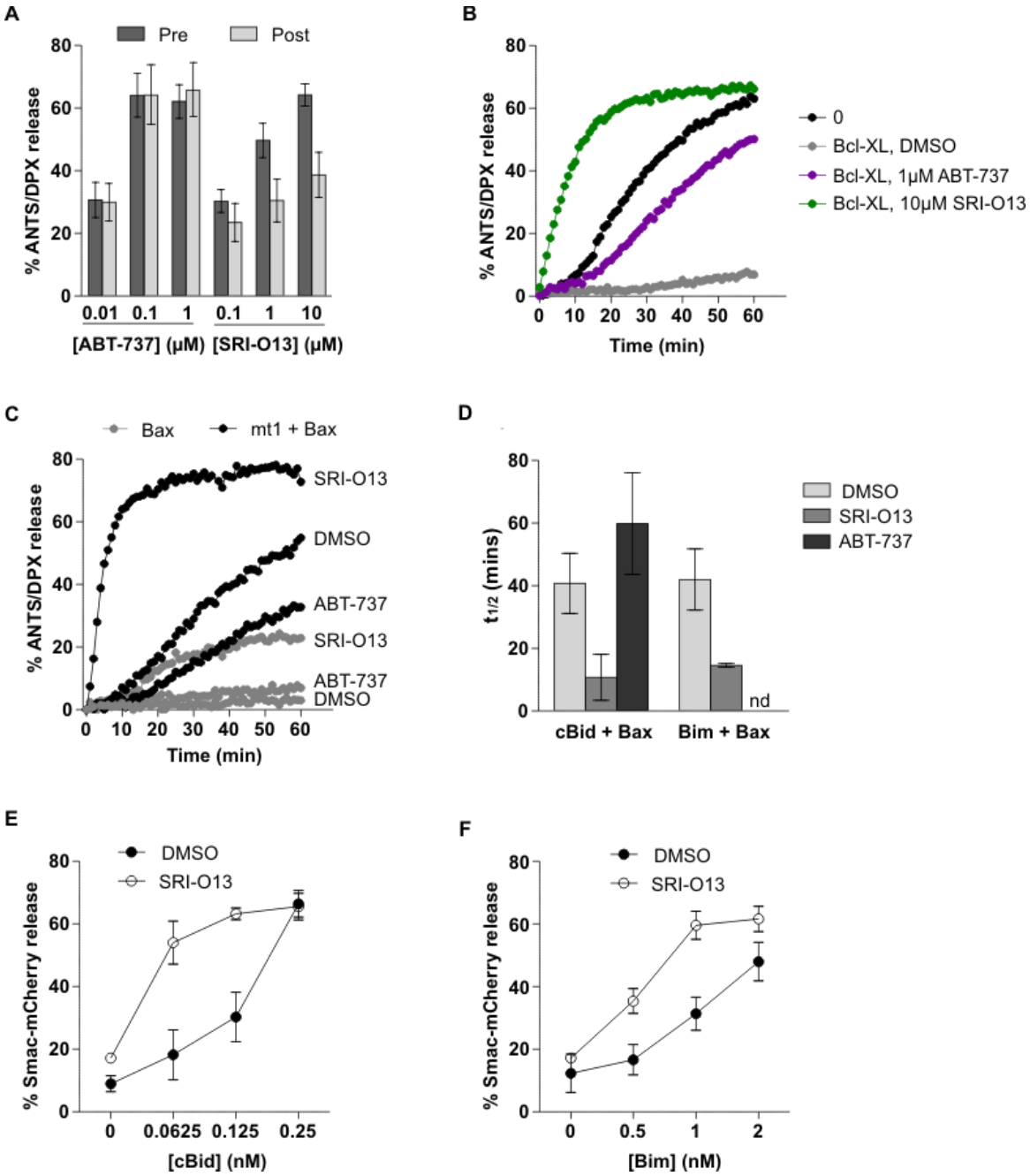

Figure 2: **SRI-O13 enhances Bax/cBak mediated membrane permeabilization.**

A. Liposome permeabilization measured after 3 hours when the indicated concentrations of ABT-737 or SRI-O13 were added to liposomes containing Bcl-XL and cBid-mt1 prior to the addition of Bax (Indicated as Pre) or 1 hour after the addition of Bax (Indicated as Post). Data points: mean ± SD, n=4.

B. Time courses of the permeabilization of liposomes for the first 60 min of the "Pre" reaction conditions from A. All reactions contain cBid-mt1 and Bax. One representative set of measurements from n=4 independent experiments is shown.

C. Time courses of the permeabilization of liposomes for the indicated reactions consisting 1 μM ABT-737 or 10 μM SRI-O13. One representative set of measurements from n=4 experiments is shown.

D. Time for 50% completion of liposome permeabilization for the indicated (Endpoint liposome permeabilization shown in Fig. S2A). Data points: Mean ± SD, n=3 independent experiments. nd= no data

E. Membrane permeabilization assayed for DKO BMK mitochondria incubated with 20 nM Bax and the indicated concentrations of cBid in the presence or absence of 10 μM SRI-O13. Mitochondria were pelleted after incubation and release of Smac-mCherry was detected by measuring the fluorescence in the supernatant and pellet fractions. Data points: mean ± SD, n=3.

F. Membrane permeabilization assayed as described in E. for reactions containing 5 nM BimL instead of cBid. Data points: mean ± SD, n=3.

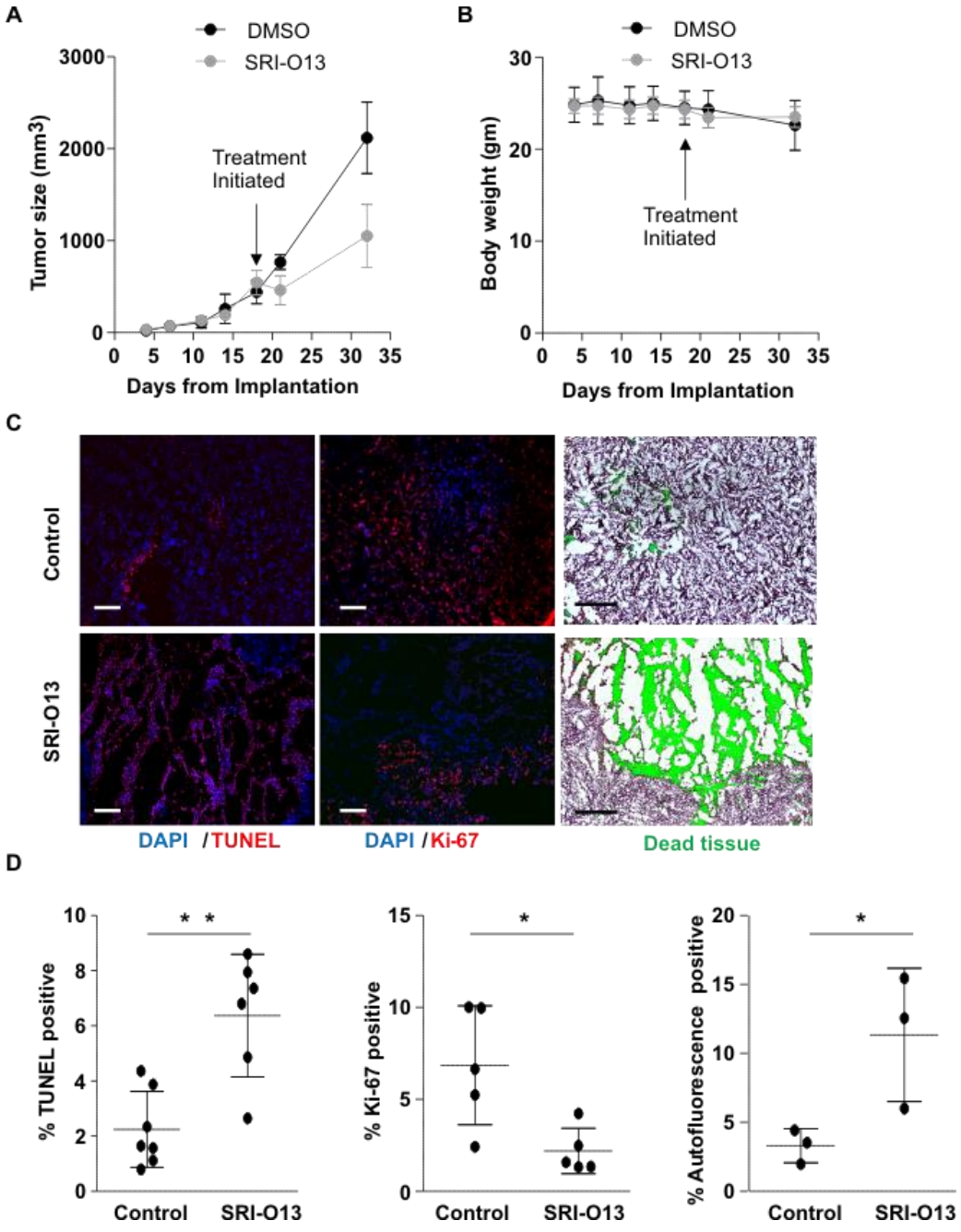

Figure 3: **SRI-O13 induces tumor cell death *in vivo.***

A. Tumor volume measurements of transplanted HCT116 tumors in male CB.17 SCID-YFP mice injected with 25 mg/kg SRI-O13 or DMSO at day 18 post implantation. Data points: Mean ± SD for 3 mice in each treatment group.

B. Body weight measurements of mice treated with SRI-O13 from A.

C. Representative images of tumor sections stained with DAPI, TUNEL (left), DAPI, Ki67 (middle) and H&E staining (right). Scale bar: 200 μm.

D. Quantification of tissue sections from C. Data points: mean ± SD; * indicates $p \leq 0.05$ and ** indicates $p \leq 0.01$ using students t- test.

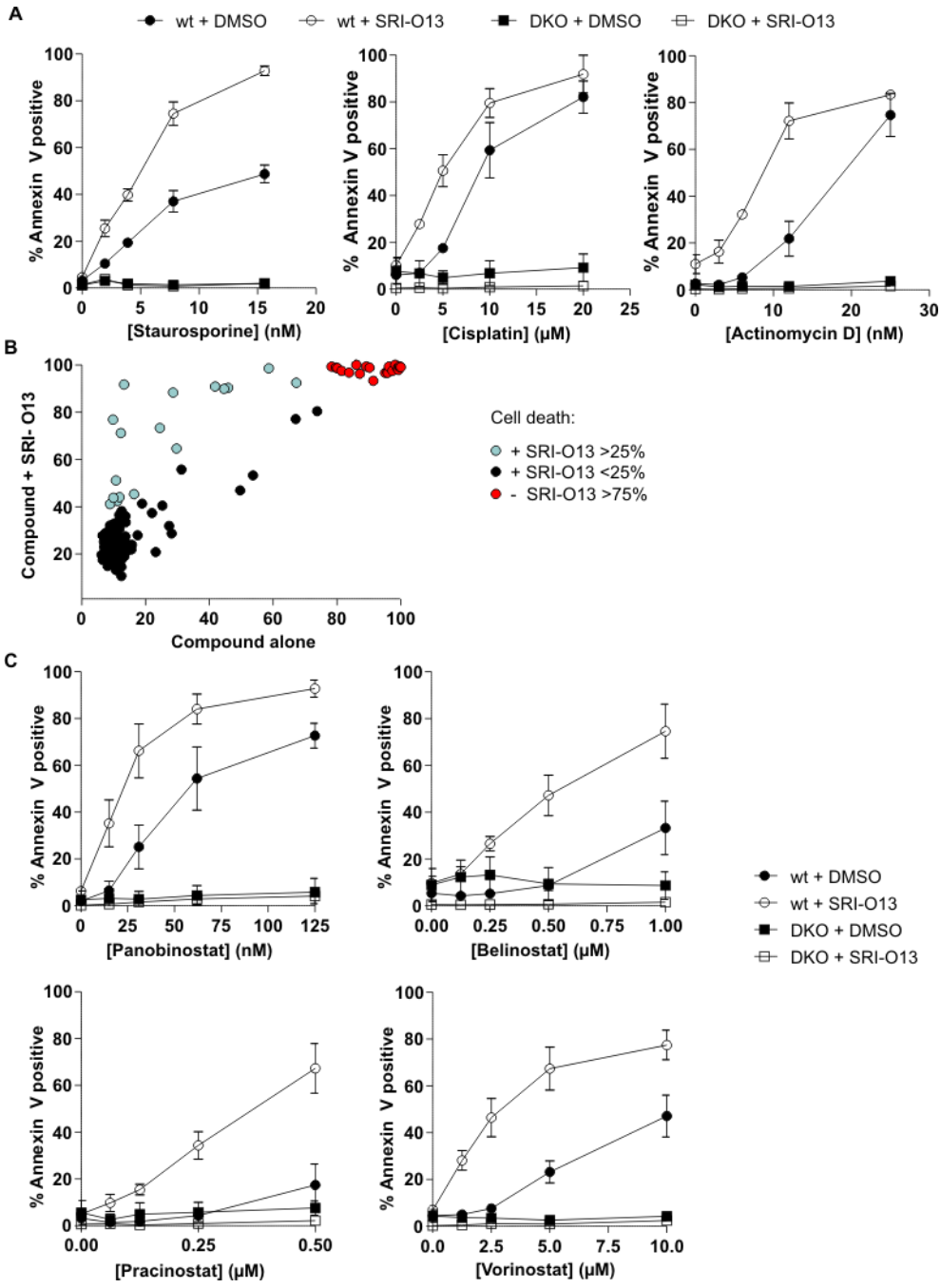

Figure 4: SRI-O13 synergizes with various apoptosis inducing agents.

A. Exposure of phophatidylserine detected by Annexin V staining in wt and DKO BMK cells treated with staurosporine, actinomycin D and cisplatin alone or in combination with 10 μM SRI-O13 for 24 hours. Data points: Mean ± SD, n=3 independent experiments.

B. wt BMK cells were treated with 1 μM of compound alone or in combination with 10 μM SRI-O13 for 24 hours. Cells were stained with DRAQ5, Annexin V and TMRE. Cell death was assessed by supervised classification using the DMSO treated cells as a negative control and cells treated with 10 μM SRI-O13 and 12 nM actinomycin D as a positive control. Cell killing activities of the compound alone and in combination with SRI-O13 are represented as the percentage of cells classified as the positive control.

C. Exposure of phophatidylserine detected by Annexin V staining in wt and DKO BMK cells treated with the indicated HDAC inhibitors alone or in combination with 10 μM SRI-O13 for 24 hours. Data points: Mean ± SD, n=3 independent experiments.

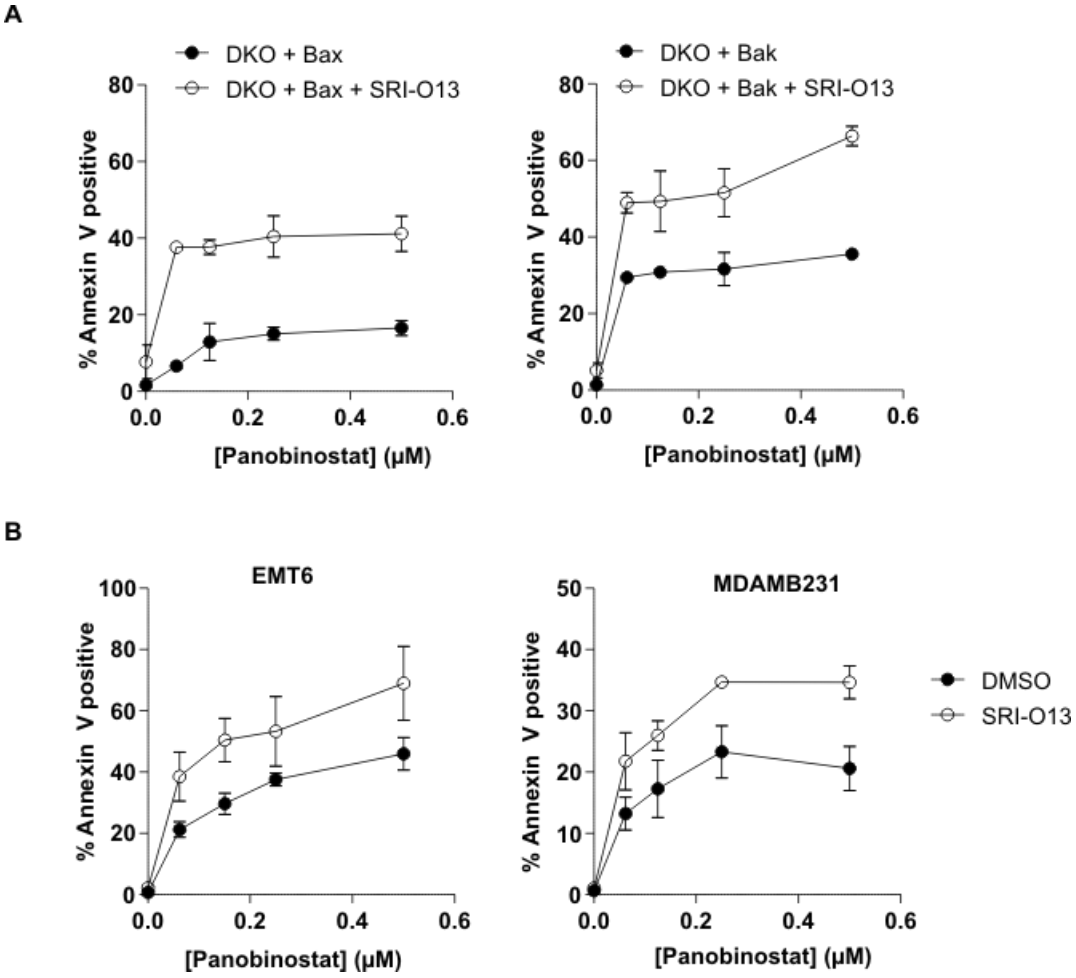

Figure 5: SRI-O13 synergizes with panobinostat to enhance Bax or Bak mediated MOMP in various cell lines.

A. Cell death assessed by Annexin V staining for DKO MEF cells reconstituted with human wt Bax (left) or Bak (right) treated with panobinostat alone or in combination with 10 μM SRI-O13 for 16 hrs. Data points: Mean ± SD, n=3 independent experiments.

B. Murine EMT6 and human MDAMB231 cells were treated with panobinostat alone or in combination with 20 μM SRI-O13 for 24 and 48 hrs. respectively. Cell death was assessed by staining using Annexin V. Data points: Mean ± SD, n=3 independent experiments.

Supplementary figures

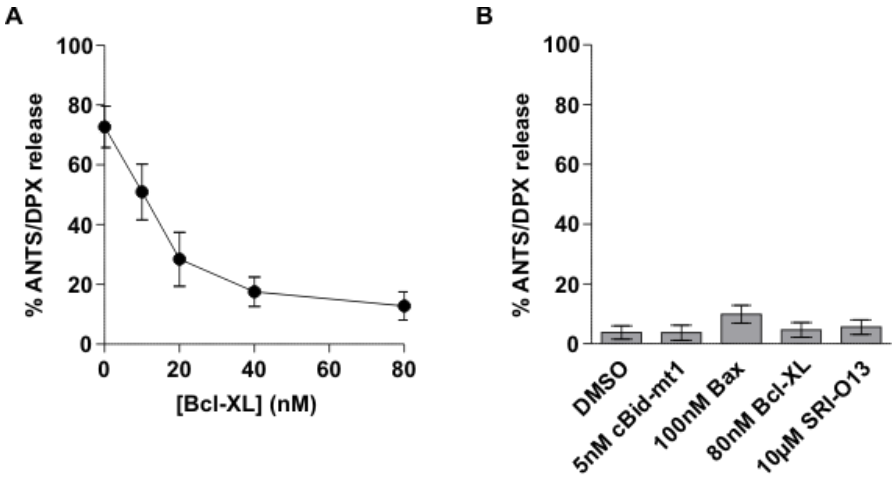

Figure S1: Bcl-XL inhibits cBid-Bax mediated liposome permeabilization.

A. Permeabilization assayed for liposomes incubated with cBid-mt1, Bax and the indicated concentrations of Bcl-XL after 3 hours. Data points: mean ± SD, n=3 independent experiments.

B. Liposome permeabilization measured for control reactions containing the indicated components. Data points: mean ± SD, n=3 independent experiments.

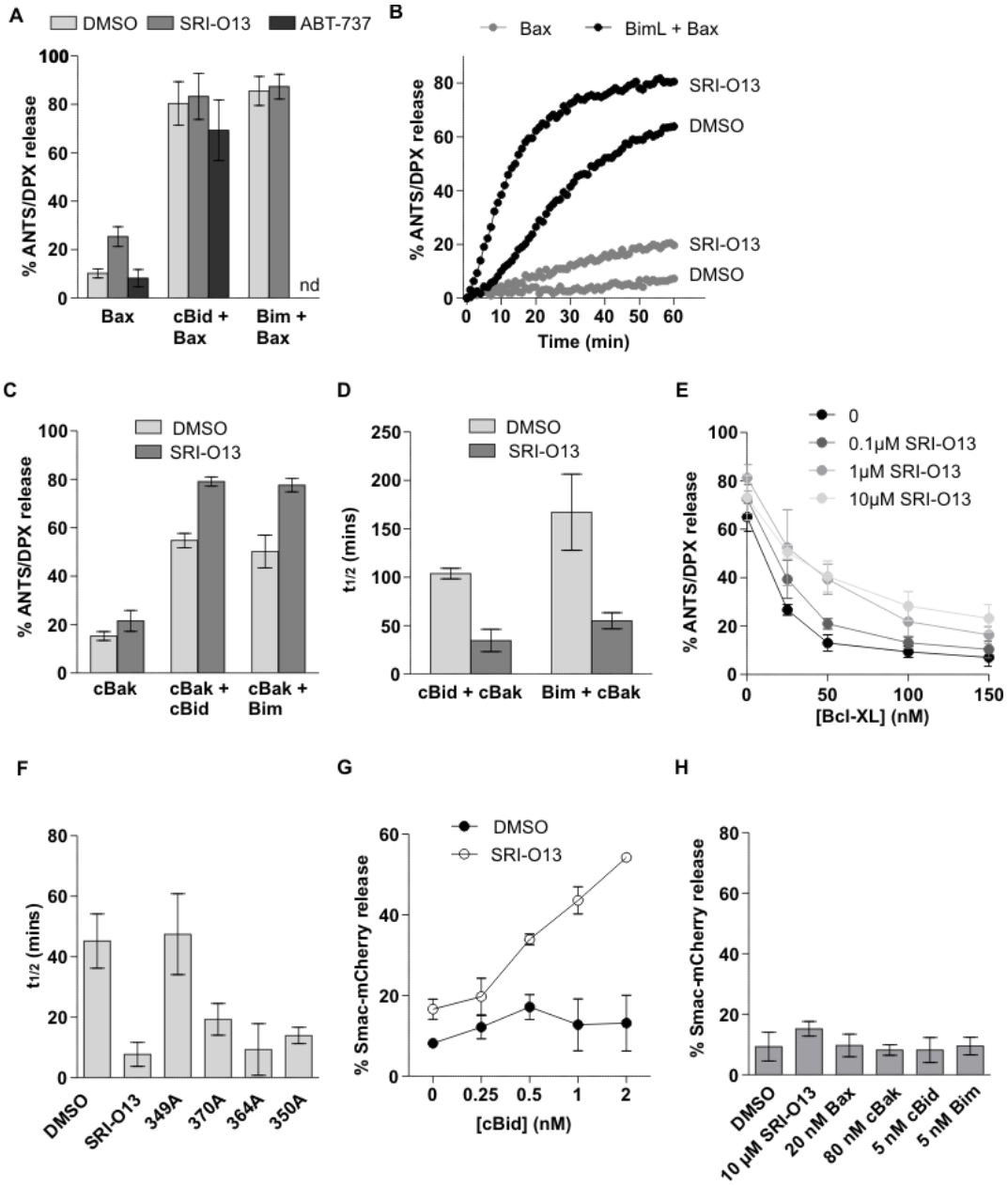

Figure S2: SRI-O13 enhances and accelerates Bax and cBak mediated membrane permeabilization.

A. Endpoint liposome permeabilization measured after 3 hours for the indicated reactions containing 10 μM SRI-O13 or 1 μM ABT-737. Data points: mean ± SD, n=3 independent experiments. nd=no data.

B. Time courses of liposome permeabilization measured during the first 60 min for the indicated reactions. SRI-O13 was used at 10 μM. Data points: mean ± SD, n=3 independent experiments.

C. Endpoint liposome permeabilization measured after 3 hours for indicated reactions containing 100 nM cBak or 100 nM cBak and 50 nM cBid/ BimL alone or combination with 10 μM SRI-O13. Data points: Mean ± SD, n=3 independent experiments.

D. Time for 50% completion of liposome permeabilization as described in D. Data points: Mean ± SD, n=3 independent experiments.

E. Permeabilization assayed for liposomes incubated with Bcl-XL and SRI-O13 as indicated. All reactions contain cBid-mt1 and Bax. Data points: Mean ± SD, n=3 independent experiments.

F. Time for 50% completion of liposome permeabilization for reactions containing cBid, Bax and 10 μM of the indicated analogs of SRI-O13. Data points: Mean ± SD, n=3 independent experiments.

G. Membrane permeabilization assayed as described in Fig. 2E for mitochondria incubated with 80 nM cBak and cBid and 10 μM SRI-O13 as indicated. Data points: Mean ± SD, n=3 independent experiments.

H. Mitochondrial permeabilization assayed as described in Fig. 2E for control reactions. Data points: Mean ± SD, n=3 independent experiments.

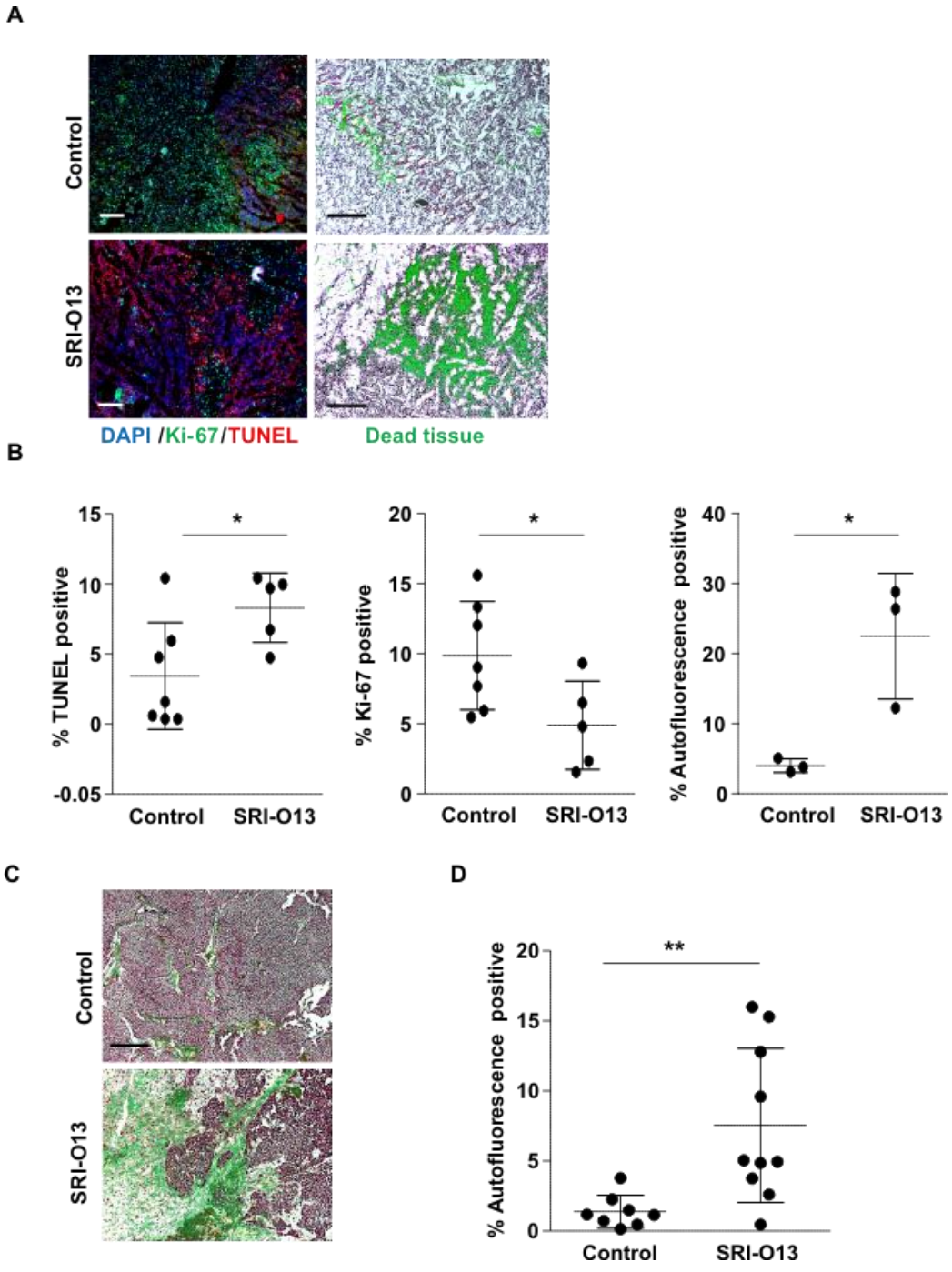

Figure S3: SRI-O13 induces cell death of transplanted tumors.

A. Representative tissue sections of transplanted murine EMT6 tumors treated with SRI-O13 and stained with DAPI, Tunel, Ki67 (left) or H&E stained (right).

B. Quantification of tissue sections from A. Data points: mean ± SD; * indicates $p \leq 0.05$ using student's test.

C. Representative H&E staining of transplanted patient derived xenografts treated with SRI-O13.
D. Quantification of tissue sections from C. ** indicates $p \leq 0.01$ using student's t-test.

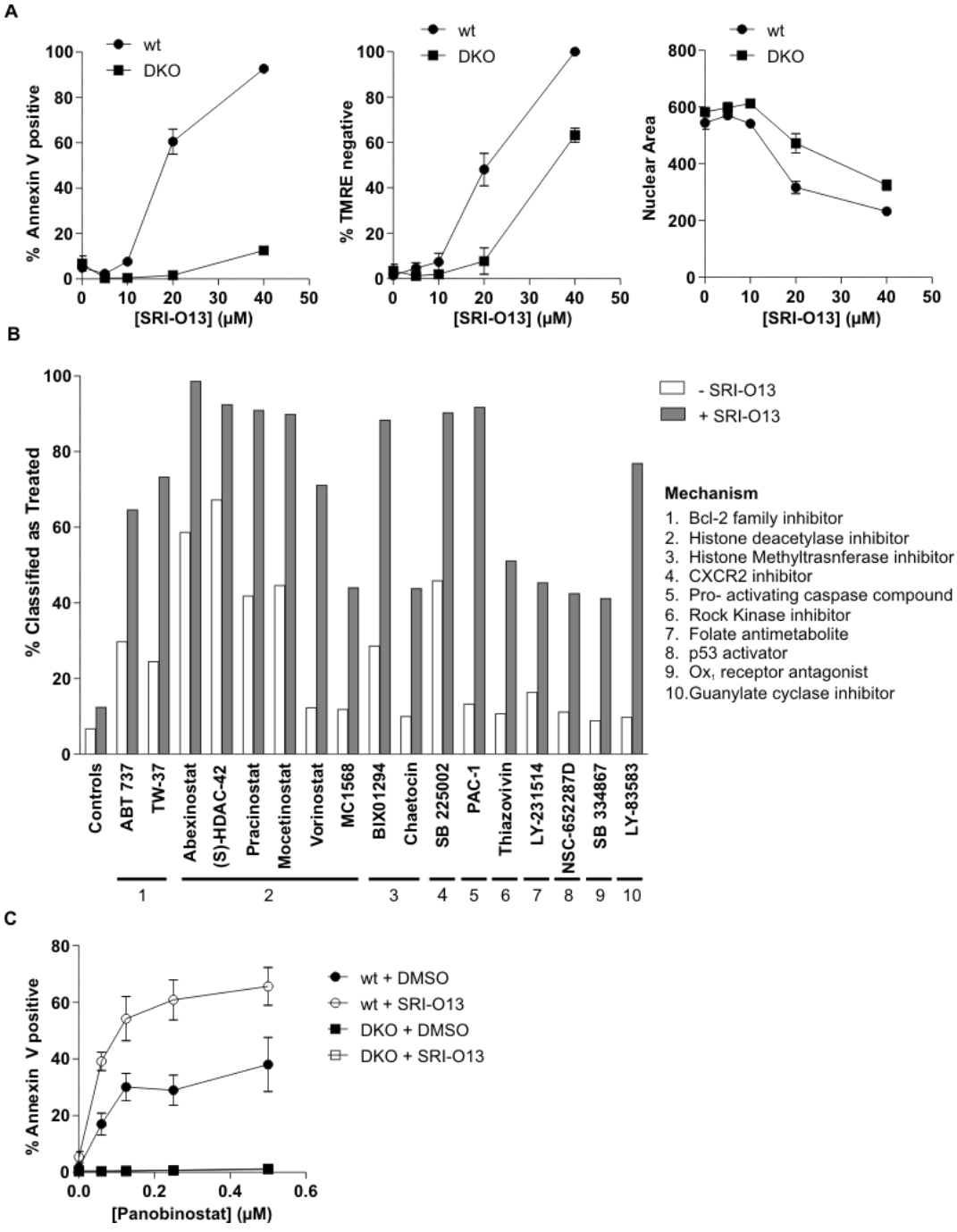

Figure S4: SRI-O13 synergizes with various compounds to enhance cell death.

A. Externalization of phophatidylserine as detected by Annexin V staining (left), loss of membrane potential as detected by TMRE staining (middle) and nuclear area as detected by DRAQ5 staining (right) for BMK cells treated with the indicated concentrations of SRI-O13 for 24 hours. Data points: Mean ± SD, n=3 independent experiments.

B. Cell death measurements for the top 17 hits obtained from the screen described in Fig. 4B categorized by their putative mechanism of action.

C. Externalization of phosphatidylserine as detected by Annexin V staining for wt and DKO MEF cells treated with panobinostat alone or in combination with 10 μM SRI-O13. Data points: Mean ± SD, n=3 independent experiments.

Supplementary tables

Table S1: Determining the maximum tolerated dose of SRI-O13 in mice

Dose	Comments on Mice
500 mg/kg	Mice died
100 mg/kg	Mice died
50 mg/kg	Mice were very sick but survived. Mice did not survive a second dose.
25 mg/kg	Mice survived and tolerated the toxicity. No second dose was assessed

Supplementary Table 2: Combination index measurements for assessment of synergy

Cell Line	Drug 1	Drug 2	[Drug 1]	[Drug2]	Mean combination Index	SD
wt BMK	SRI-O13	Actinomycin D	10μM	3nM	1.31	0.19
			10μM	6nM	1.15	0.03
			10μM	12nM	0.79	0.13
			10μM	25nM	0.81	0.38
wt BMK	SRI-O13	Cisplatin	10μM	2.5μM	1.15	0.05
			10μM	5μM	1.01	0.14
			10μM	10μM	0.78	0.14
			10μM	20μM	0.68	0.36
wt BMK	SRI-O13	Staurosporine	10μM	1.9nM	1.12	0.18
			10μM	3.9nM	0.99	0.08
			10μM	7.8nM	0.56	0.11
			10μM	15.6nM	0.33	0.06
wt BMK	SRI-O13	Panobinostat	10μM	15nM	0.99	0.18
			10μM	31nM	0.74	0.17
			10μM	62nM	0.66	0.14
			10μM	125nM	0.64	0.17
wt BMK	SRI-O13	Belinostat	10μM	0.125μM	1.15	1.15
			10μM	0.25μM	0.76	0.76
			10μM	0.5μM	0.56	0.56
			10μM	1μM	0.38	0.38
wt BMK	SRI-O13	Pracinostat	10μM	0.062μM	1.24	0.20
			10μM	0.125μM	1.05	0.08
			10μM	0.25μM	0.72	0.08
			10μM	0.5μM	0.44	0.08
wt BMK	SRI-O13	Vorinostat	10μM	1.25μM	0.90	0.21
			10μM	2.5μM	0.72	0.23
			10μM	5μM	0.54	0.23
			10μM	10μM	0.47	0.17
EMT6	SRI-O13	Panobinostat	20μM	0.062μM	0.52	0.16
			20μM	0.125μM	0.42	0.11
			20μM	0.25μM	0.63	0.32

			20µM	0.5µM	0.38	0.20
MDAMB231	SRI-O13	Panobinostat	20µM	0.062µM	0.52	0.16
			20µM	0.125µM	0.42	0.11
			20µM	0.25µM	0.63	0.32
			20µM	0.5µM	0.38	0.20

CHAPTER V:

Concluding remarks and future directions

Identifying small molecules targeting Bcl-2 family proteins

Low molecular weight compounds account for a wide variety of drugs including those in pre-clinical and clinical development (Imming, Sinning et al. 2006). Small molecules are attractive alternatives to peptides and proteins as they can be modified to be stable, resistant to proteolysis, selective, potent and orally available (Arkin and Wells 2004). Given the importance of Bcl-2 family proteins as critical players regulating and executing apoptosis, and that insufficient or excessive apoptosis is characteristic of many human diseases, extensive research has been conducted for over two decades to improve our understanding of apoptosis and identify novel strategies to exploit the activity of Bcl-2 family proteins (Hardwick and Soane 2013; Brahmbhatt, Oppermann et al. 2015).

To date, several small molecules targeting the Bcl-2 family proteins have been discovered and represent an important milestone in drug discovery and mechanistic research studies (Vogler 2014; Liu, Ding et al. 2015). For example, ABT-737, and various BH3 peptide mimetics have been incorporated in the BH3 profiling assay to dissect blocks in apoptosis in many cancers (Del Gaizo Moore, Schlis et al. 2008). BDA-366, has been used to show that targeting the BH4 domain of Bcl-2 is a potential alternative avenue for the treatment of lung cancer (Han, Park et al. 2015). Additionally, ABT-199 and ABT-263 have shown promising results in hematologic malignancies and have progressed the furthest

in clinical trials (Tse, Shoemaker et al. 2008; Souers, Leverson et al. 2013; Cang, Iragavarapu et al. 2015). Most recently, ABT-199 achieved orphan drug approval for the treatment of diffuse large B-cell lymphoma, an aggressive and most common form of non-Hodgkin lymphoma (Zelenetz 2015).

Despite this promising early success, the current small molecules target only a subset of the Bcl-2 family proteins representing an opportunity for the discovery of additional small molecules. This thesis was focused on the identification of small molecules that promote or inhibit Bax and Bak. We primarily focused on the evaluation of these compounds as important tools for mechanistic studies and as leads for potential therapeutics. Taken together, the findings presented in this thesis provide further mechanistic insights of the multiple steps leading to apoptosis, and highlight the potential of pharmacologically targeting multiple Bcl-2 family proteins.

Membranes in screening design for small molecules

Bcl-2 family proteins undergo multiple conformational changes upon interaction with membranes. The presence of the membrane as the locus of action of the Bcl-2 family proteins and its role as an active player governing subsequent binding interactions adds to the complexity of perturbing Bcl-2 family proteins (Leber, Lin et al. 2010). Previous strategies to identify small molecules to probe Bcl-2 family proteins have been influenced by challenges posed by

purifying membrane proteins and the lack of details of the dynamic conformations of these proteins in the membrane. As a result, the screens that have been conducted to date use the soluble forms of the proteins and lack membranes (Petros, Dinges et al. 2006; Gavathiotis, Reyna et al. 2012; Lessene, Czabotar et al. 2013). To target these proteins in ways mechanistically different than that obtained so far, we employed liposomes with a lipid composition mimicking the MOM and full length proteins in our primary screens. We used a functional assay to link modulation of the Bcl-2 family activity protein activity by small molecules with the important functional consequence of pore formation in this model membrane. Since the screening assays only measures the permeabilization of liposomes, we conducted additional confirmatory *in vitro* and *in vivo* studies to characterize and evaluate the hits as important tools for mechanistic dissection studies, and as a potential leads for therapeutic development.

Chapter II: Small molecule inhibitors of Bax and Bak

For most cells Bax and Bak mediated MOMP marks commitment to cell death and therefore understanding the mechanism by which this step occurs and inhibiting this step represents an attractive avenue for the treatment of diseases caused by excessive apoptosis (Leber, Lin et al. 2007). In this chapter, we reported the identification of MSN-50 and MSN-125 which inhibit Bax and Bak mediated MOMP. We used these compounds to examine the therapeutic benefit

of inhibiting apoptosis in cells and provide insights into the molecular mechanism of Bax and Bak oligomer formation.

Elucidating how Bax and Bak oligomerize has been the focus of several research groups. Although Bax and Bak undergo similar conformational changes upon activation, opposing models exist to describe the formation and propagation of the oligomers (Westphal, Kluck et al. 2014). According to the symmetric dimer mode, the exposed BH3 region of Bax/Bak engages in the canonical hydrophobic groove of a partnering Bax/Bak to form dimers and the transition of dimers to higher older oligomers occurs through interactions at two additional interfaces (Zhang, Subramaniam et al. 2015). By contrast, in the asymmetric model the exposed BH3 region of Bax/Bak engages an alternative “rear” pocket and oligomerization results from subsequential BH3 region-rear pocket interactions. Our study demonstrated that MSN-125, MSN-50 and DAN004 had a pronounced effect on the formation of larger Bax oligomers than dimers and that MSN-125 disrupted partial, and not all, interfaces of the Bax dimer. Therefore, MSN-125 served as an important tool to validate the formation of symmetric dimers as the first step in Bax oligomerization and subsequent pore formation. Importantly, our findings differ from reports suggesting that Bax monomers are the minimal functional units for pore formation; these differences may be attributed to the use of nanodiscs that restricted Bax to function as a monomer in the latter study (Xu, Zhai et al. 2013). Taken together, our studies with MSN-125 demonstrate that

Bax dimer interaction interfaces can be pharmacologically exploited. In line with this, since the compounds also inhibited Bak, it will be imperative to assess whether similar disulfide crosslinks of the Bak dimer are also disrupted. Since studies have supported the formation of symmetric dimers for Bak, we hypothesize that similar results will be observed (Westphal, Kluck et al. 2014).

A common conformational change that occurs in Bax and Bak after activation is the exposure of an N-terminal epitope which is assayed by the binding to epitope specific antibodies (Hsu and Youle 1997; Alsop, Fennell et al. 2015). Recent studies have reported that this region remains exposed in the Bak dimer (Alsop, Fennell et al. 2015). In our study, we observed that MSN-125 prevented the exposure of this N-terminal region of Bax in cells. Therefore, future studies can be used to determine if the Bax dimers have an exposed or buried N-terminal epitope in the presence of the compounds.

The observation that the compounds blocked Bax at the dimer stage after Bax activation has important implications in treatment regimens aimed to limit or prevent cell death after an apoptotic insult. Neuronal cell death or damage due to excitotoxicity has been observed in stroke, brain injury and various neurodegenerative conditions such as Huntington's and Alzheimer's diseases (Mergenthaler, Dirnagl et al. 2004; Dong, Wang et al. 2009). Commonly used neuroprotective agents comprise glutamate antagonists and antioxidants which function to reduce excitotoxicity and oxidative stress levels (Levi and Brimble

2004). In most neuroprotection studies assessing the therapeutic benefit of these agents, these agents are administered before the insult (Danton and Dietrich 2004). In our study, we see the protection of primary neuron cultures after glutamate exposure implying that MSN-125 has potential to be administered after the chemical insult that would otherwise kill the cell. Because of this property these compounds may be also be helpful in preventing apoptosis during reperfusion of ischemic tissues (Lopez-Neblina, Toledo et al. 2005). Additional studies can therefore be focused on altering the time-points of addition of MSN-125 after the apoptotic stimulus to determine the duration and magnitude of the apoptotic insult that can be tolerated. Additionally, to further validate this compound as a potential lead for future therapies, it will be exciting to extend these studies to model systems.

Although we saw promising results with MSN-50 and MSN-125, extensive optimization and further testing of these compounds will be required. Both MSN-50 and MSN-125 are poorly soluble in aqueous solutions, and the multi-step synthesis procedure of these compounds has proved to be challenging. By comparison, the synthesis of DAN004 is more feasible and this compound is much more soluble in aqueous solution. It is also more potent in inhibiting Bax and Bak in liposome and mitochondrial assays, but displays off- target effects in cells. Thus, future optimization studies should be focused on the development of

variants of DAN004 that inhibit Bax and Bak and also protect cells against apoptotic stimuli with limited to none off-target toxicities.

The poor solubility of MSN-125 and MSN-50 rendered protein-ligand binding studies difficult, and we were unable to detect direct binding to Bax with DAN004 using isothermal calorimetry. Since the mode of action of the compound is after activation of Bax at the membrane, the lack of the membranes and the absence of the active conformer of Bax in our isothermal calorimetry studies is one possible explanation for our negative results. Alternatively as an alternative approach we can use mutants of Bax that form dimers in solution (which are in different conformation than inactive Bax) for conducting future binding studies and elucidate the binding site.

Chapter III: Small molecule activators of Bax

Most chemotherapy agents induce intrinsic apoptosis leading to the indirect activation of Bax and Bak (Hannun 1997). Given the importance of Bax and Bak as the central players executing the commitment step during apoptosis, recent studies have focused on identifying small molecules activators of Bax and evaluate whether direct activation of Bax serves as an alternative avenue for cancer treatment. Interestingly the compounds identified so far activate Bax through different modes; BAM7 engages the rear pocket, SMBA1 engages the S184 binding pocket and Compound 106 engages the hydrophobic groove of Bax

(Gavathiotis, Reyna et al. 2012; Xin, Li et al. 2014; Zhao, Zhu et al. 2014). Although it has been postulated that activating Bax as an anti-cancer strategy may be too toxic to normal cells, other studies have suggested that cancers have an overwhelmed anti-apoptotic capacity and therefore may not be able to withstand activated Bax whereas normal cells have the anti-apoptotic reserve to counter activated Bax (Ryan, Brunelle et al. 2010). Consist with the latter hypothesis, BAM7, SMBA1 and Compound 106 have displayed anti-tumor activity in cell lines and transplanted tumors.

In this chapter, we report the discovery of additional small molecule activators of Bax. Due to the off- target activities of our most active compound OICR77A in cells, we could not use this compound to address whether there is any therapeutic benefit in pharmacologically targeting Bax for cancer therapies. However, we gained novel insights on the regulation of Bax activity using our compounds. We observed that the small molecules activated Bax by a mechanism different than Bax activation by pro-apoptotic BH3 proteins. Intriguingly, activation of Bax by OICR766A required a cysteine at position 126.

Bcl-2 family proteins are tightly regulated at the transcriptional, translational and post- translational level (Kutuk and Letai 2008). These multiple levels of regulation affect the expression and function of Bcl-2 family proteins to promote or prevent cell death in response to diverging stimuli (Kutuk and Letai 2008; Shamas-Din, Brahmbhatt et al. 2011). Therefore, we postulate that this

alternative mechanism exists for Bax to respond to certain stimuli that do not involve BH3 proteins (Hsu and Youle 1997; Cartron, Oliver et al. 2004; Pagliari, Kuwana et al. 2005; Lalier, Cartron et al. 2011; Frohlich, Dejanovic et al. 2014).

Although conflicting reports exist on the requirement of the two endogenous cysteines for the activation of Bax in cells; this may be attributed to differences in cellular context and the stimuli used (D'Alessio, De Nicola et al. 2005; Nie, Tian et al. 2008; Huang, Nie et al. 2009; Lalier, Cartron et al. 2011; Frohlich, Dejanovic et al. 2014). However, common to some of these studies is the importance of the cysteine residues for Bax activation under oxidative conditions (D'Alessio, De Nicola et al. 2005; Nie, Tian et al. 2008). Although most chemotherapy drugs induce intrinsic apoptosis initiating the activation of BH3 proteins to kill cells, these drugs have also been report to mediate oxidative stress in cells which activates Bax by an alternative mechanism (Deavall, Martin et al. 2012). Therefore, it is likely that multiple mechanisms exist in cells to amplify cell death stimuli in a cooperative and not competitive manner.

Although Bax and Bak are functionally similar and undergo similar conformational changes, they are different in localization in healthy cells and the number of BH3 protein binding sites (Wolter, Hsu et al. 1997; Zong, Li et al. 2003; Gavathiotis, Suzuki et al. 2008; Leshchiner, Braun et al. 2013). To date, no direct small molecule activators of Bak have been identified and this can be the subject of future investigations. Moreover, Bak has two endogenous cysteines

(Moldoveanu, Liu et al. 2006). Although neither cysteine is required for Bak mediated cell death in response to etoposide, a detailed assessment of the requirement of the cysteine residues in response to diverging stimuli has yet to be explored (Dewson, Ma et al. 2012; Iyer, Bell et al. 2015). Furthermore whether these cysteine residues are relevant druggable targets for activating Bak can be the subject of future studies.

An important observation in our study was that OICR766A activated Bax was poorly inhibited by Bcl-XL. Although further studies can be conducted to deduce this, our observations imply that this alternative mechanism may be particularly beneficial when other triggers of Bax activity are missing or their activity is inhibited. However, such an approach may be ineffective in cancers that are missing functional Bax/ Bak (Letai 2008).

Chapter IV: Small molecule enhancer of Bax and Bak

With emerging evidence indicating that cancers select for blocks in apoptosis that confer tumor survival and proliferation, strategies aimed to restore apoptosis are attractive for anti-cancer treatment (Deng, Carlson et al. 2007; Besbes, Mirshahi et al. 2015). In this chapter we reported the identification of SRI-O13 that accelerates and enhances apoptosis by a mechanism different from that by ABT-737. We used this compound as a tool to examine whether there is

any therapeutic benefit of enhancing Bax and Bak mediated MOMP as an anti-cancer strategy.

The rationale that small molecules which occupy the hydrophobic pocket of anti-apoptotic proteins will antagonize their activity and therefore “unleash” apoptosis has led the discovery of several small molecules over the past decade. Although the relatively large hydrophobic binding surfaces involved in the interactions between Bcl-2 family proteins have posed challenges and many of the small molecules discovered to date have been reported to have minimal on-target effects, ABT-263 and ABT-199 have mode promising progress (Petros, Olejniczak et al. 2004; Tse, Shoemaker et al. 2008; Vogler, Weber et al. 2009; Leber, Geng et al. 2010; Vogler, Hamali et al. 2011; Souers, Leverson et al. 2013). Although extensive research has been conducted to identify inhibitors of the anti-apoptotic proteins, pharmacologically manipulating Bax and Bak activity has been comparably less explored (Vogler 2014; Liu, Ding et al. 2015). Unlike the mode of action of the small molecules described above, SRI-O13 enhances and accelerates Bax and Bak mediated MOMP.

Functional interactions between the Bcl-2 family proteins are governed by a series of multiple reversible equilibria of protein- protein and protein- membrane interactions (Leber, Lin et al. 2010). In our *in vitro* studies, SRI-O13 enabled Bax to escape inhibition by Bcl-XL. SRI-O13 accelerates and enhances MOMP even in the absence of Bcl-XL and therefore we infer that it shifts the equilibria of Bax

activation to favour MOMP. Although a detailed assessment of the mode of action of SRI-O13 and potential binding sites have yet to be elucidated, we hypothesize that SRI-O13 may increase the affinity of the BH3 activator proteins for Bax/Bak, alter the conformation of Bax and Bak to an oligomer forming conformer, or stabilize the interaction interfaces of the Bax oligomers.

In our study SRI-O13 displayed anti-tumor activity in a mouse model system demonstrating the utility of this compound as a potential lead for pharmaceutical development. It is highly likely that the efficacy of this compound was reduced due to its poor solubility in aqueous solution, as compound aggregates were observed at sites of administration (data not shown). Thus, further studies can be focused on testing solvents that improve compound solubility without affecting compound action (Turner, Pekow et al. 2011). Alternatively it is important to conduct detailed SAR analysis studies on SRI-O13 to identify variants that have improved potency and reduced side effects in cells.

As an enhancer of MOMP, SRI-O13 synergized with various apoptosis inducing agents to potentiate cell death. By conducting a screen, we identified that SRI-O13 synergizes with HDAC inhibitors to promote cell death. In all these these studies the combinations were not toxic to cells lacking Bax and Bak. As a further measure of their effects it will be important to assess whether these cells have a delayed response after exposure to these combinations, and whether their replicative potential is prevented even if cell death is not complete.

In this study, we demonstrated that enhancing and accelerating Bax and Bak mediated MOMP can be triggered pharmacologically. Our results indicate that this pathway may be relevant for cancer therapies. Further testing of the combinatorial treatment of SRI-O13 with HDAC inhibitors in a broad range of cancers will be helpful in identifying the cancer types that can be targeted with this approach. Most importantly, whether this approach can circumvent resistance to conventional chemotherapies will be crucial to determine.

Targeting additional Bcl-2 family proteins

The major findings presented in this thesis so far have focused enhancing or inhibiting Bax and Bak mediated MOMP. Additional Bcl-2 family proteins such as the BH3 protein Bid are also potential drug targets. Bid is important as it plays a pivotal role in neuronal cell death by regulating MOM integrity and mitochondrial dynamics (Landshamer, Hoehn et al. 2008; Grohm, Plesnila et al. 2010; Tobaben, Grohm et al. 2011). This has driven the discovery of several small molecules targeting Bid for therapies against neurodegenerative diseases (Becattini, Sareth et al. 2004; Barho, Oppermann et al. 2014; Oppermann, Schrader et al. 2014). The Bid inhibitor BI-6C9 was the first published small molecule targeting Bid. It is proposed to inhibit Bid by occupying the deep hydrophobic crevice on the surface of the protein (Becattini, Sareth et al. 2004). Although BI-6C9 effectivity prevented cell death in cell culture models, it

displayed poor efficacy *in vivo* likely due to poor solubility in aqueous solutions. To overcome this, two follow up studies were conducted in which derivatives of BI-6C9 were synthesized (Barho, Oppermann et al. 2014; Oppermann, Schrader et al. 2014). From the latter studies, 15 compounds of interest were identified which protected immortalized neuronal HT22 cells against glutamate toxicity.

Bid is cleaved (termed cBid) by caspase 8 into two fragments, p7 and p15 (tBid), that are held together by non-covalent interactions and separate after tBid binds to membranes. Upon binding of tBid to the membrane, it undergoes conformational changes that are crucial for subsequent recruitment and oligomerization of Bax at the membrane (Shamas-Din, Bindner et al. 2013). To determine the mechanism of action of these compounds, we first examined their efficacy inhibiting tBid/cBid- Bax mediated liposome permeabilization. Two of these 15 molecules inhibited tBid/cBid – Bax mediated liposome permeabilization (Figure 1). Since these compounds inhibited both cBid and tBid, it suggests that inhibitory step was downstream of the separation of the two fragments. The remaining compounds either do not target Bid or target Bid upstream of the separation of the two fragments and this can be the subject of future studies.

In studies conducted to determine the step in permeabilization that was inhibited by the compounds, we observed that these two compounds disrupted the interaction between cBid and and Bax (Figure 2A) and decreased the insertion of Bax in the membrane (Figure 2B), two steps which can contribute to

reduced membrane permeabilization. Furthermore, when assessing the selectivity of the compounds for tBid, we observed that the compounds also inhibited Bim- Bax mediated liposome permeabilization in a dose dependent manner (Figure 3). It may be that the compounds inhibit steps commonly involved in the activation of Bax by either of the activator BH3 proteins or that the observed phenomena is due to partitioning of the compound in membranes altering physical properties such that pore formation is inhibited. These can be the subject of future investigations.

Similar to our observations with DAN004, we did not detect binding of these to compounds to full length Bid, cBid or tBid (data not shown), possibly due to the lack of membranes or other interaction partners in the ITC system. Taken together, our preliminary results indicate that these compounds may serve as important tools that can be used to dissect the steps involved in membrane permeabilization.

Summary

In this thesis, we reported the identification of various small molecules that modulate the activity of Bcl-2 family proteins. We used these compounds as tools to gain important insights into the regulation of Bax and Bak activity as well as examine the importance of targeting these proteins for diseases associated with insufficient or excessive apoptosis. Continued investigations of additional Bcl-2

family proteins that can be targeted and generating small molecules with favorable pharmaceutical properties will prove useful in the treatment of apoptosis- linked diseases.

References

Alsop, A. E., S. C. Fennell, et al. (2015). "Dissociation of Bak alpha1 helix from the core and latch domains is required for apoptosis." Nat Commun **6**: 6841.

Arkin, M. R. and J. A. Wells (2004). "Small-molecule inhibitors of protein-protein interactions: progressing towards the dream." Nat Rev Drug Discov **3**(4): 301-317.

Barho, M. T., S. Oppermann, et al. (2014). "N-acyl derivatives of 4-phenoxyaniline as neuroprotective agents." ChemMedChem **9**(10): 2260-2273.

Becattini, B., S. Sareth, et al. (2004). "Targeting apoptosis via chemical design: inhibition of bid-induced cell death by small organic molecules." Chem Biol **11**(8): 1107-1117.

Besbes, S., M. Mirshahi, et al. (2015). "New dimension in therapeutic targeting of BCL-2 family proteins." Oncotarget **6**(15): 12862-12871.

Brahmbhatt, H., S. Oppermann, et al. (2015). "Molecular Pathways: Leveraging the BCL-2 Interactome to Kill Cancer Cells-Mitochondrial Outer Membrane Permeabilization and Beyond." Clin Cancer Res **21**(12): 2671-2676.

Cang, S., C. Iragavarapu, et al. (2015). "ABT-199 (venetoclax) and BCL-2 inhibitors in clinical development." J Hematol Oncol **8**(1): 129.

Cartron, P. F., L. Oliver, et al. (2004). "Impact of pH on Bax alpha conformation, oligomerisation and mitochondrial integration." FEBS Lett **578**(1-2): 41-46.

D'Alessio, M., M. De Nicola, et al. (2005). "Oxidative Bax dimerization promotes its translocation to mitochondria independently of apoptosis." FASEB J **19**(11): 1504-1506.

Danton, G. H. and W. D. Dietrich (2004). "The search for neuroprotective strategies in stroke." AJNR Am J Neuroradiol **25**(2): 181-194.

Deavall, D. G., E. A. Martin, et al. (2012). "Drug-induced oxidative stress and toxicity." J Toxicol **2012**: 645460.

Del Gaizo Moore, V., K. D. Schlis, et al. (2008). "BCL-2 dependence and ABT-737 sensitivity in acute lymphoblastic leukemia." Blood **111**(4): 2300-2309.

Deng, J., N. Carlson, et al. (2007). "BH3 profiling identifies three distinct classes of apoptotic blocks to predict response to ABT-737 and conventional chemotherapeutic agents." Cancer Cell **12**(2): 171-185.

Dewson, G., S. Ma, et al. (2012). "Bax dimerizes via a symmetric BH3:groove interface during apoptosis." Cell Death Differ **19**(4): 661-670.

Dong, X. X., Y. Wang, et al. (2009). "Molecular mechanisms of excitotoxicity and their relevance to pathogenesis of neurodegenerative diseases." Acta Pharmacol Sin **30**(4): 379-387.

Frohlich, M., B. Dejanovic, et al. (2014). "S-palmitoylation represents a novel mechanism regulating the mitochondrial targeting of BAX and initiation of apoptosis." Cell Death Dis **5**: e1057.

Gavathiotis, E., D. E. Reyna, et al. (2012). "Direct and selective small-molecule activation of proapoptotic BAX." Nat Chem Biol **8**(7): 639-645.

Gavathiotis, E., M. Suzuki, et al. (2008). "BAX activation is initiated at a novel interaction site." Nature **455**(7216): 1076-1081.

Grohm, J., N. Plesnila, et al. (2010). "Bid mediates fission, membrane permeabilization and peri-nuclear accumulation of mitochondria as a prerequisite for oxidative neuronal cell death." Brain Behav Immun **24**(5): 831-838.

Han, B., D. Park, et al. (2015). "Small-Molecule Bcl2 BH4 Antagonist for Lung Cancer Therapy." Cancer Cell **27**(6): 852-863.

Hannun, Y. A. (1997). "Apoptosis and the dilemma of cancer chemotherapy." Blood **89**(6): 1845-1853.

Hardwick, J. M. and L. Soane (2013). "Multiple functions of BCL-2 family proteins." Cold Spring Harb Perspect Biol **5**(2).

Hsu, Y. T. and R. J. Youle (1997). "Nonionic detergents induce dimerization among members of the Bcl-2 family." J Biol Chem **272**(21): 13829-13834.

Huang, F., C. Nie, et al. (2009). "Selenite induces redox-dependent Bax activation and apoptosis in colorectal cancer cells." Free Radic Biol Med **46**(8): 1186-1196.

Imming, P., C. Sinning, et al. (2006). "Drugs, their targets and the nature and number of drug targets." Nat Rev Drug Discov **5**(10): 821-834.

Iyer, S., F. Bell, et al. (2015). "Bak apoptotic pores involve a flexible C-terminal region and juxtaposition of the C-terminal transmembrane domains." Cell Death Differ **22**(10): 1665-1675.

Kutuk, O. and A. Letai (2008). "Regulation of Bcl-2 family proteins by posttranslational modifications." Curr Mol Med **8**(2): 102-118.

Lalier, L., P. F. Cartron, et al. (2011). "Prostaglandins antagonistically control Bax activation during apoptosis." Cell Death Differ **18**(3): 528-537.

Landshamer, S., M. Hoehn, et al. (2008). "Bid-induced release of AIF from mitochondria causes immediate neuronal cell death." Cell Death Differ **15**(10): 1553-1563.

Leber, B., F. Geng, et al. (2010). "Drugs targeting Bcl-2 family members as an emerging strategy in cancer." Expert Rev Mol Med **12**: e28.

Leber, B., J. Lin, et al. (2007). "Embedded together: the life and death consequences of interaction of the Bcl-2 family with membranes." Apoptosis **12**(5): 897-911.

Leber, B., J. Lin, et al. (2010). "Still embedded together binding to membranes regulates Bcl-2 protein interactions." Oncogene **29**(38): 5221-5230.

Leshchiner, E. S., C. R. Braun, et al. (2013). "Direct activation of full-length proapoptotic BAK." Proc Natl Acad Sci U S A **110**(11): E986-995.

Lessene, G., P. E. Czabotar, et al. (2013). "Structure-guided design of a selective BCL-X(L) inhibitor." Nat Chem Biol **9**(6): 390-397.

Letai, A. G. (2008). "Diagnosing and exploiting cancer's addiction to blocks in apoptosis." Nat Rev Cancer **8**(2): 121-132.

Levi, M. S. and M. A. Brimble (2004). "A review of neuroprotective agents." Curr Med Chem **11**(18): 2383-2397.

Liu, Z., Y. Ding, et al. (2015). "Direct Activation of Bax Protein for Cancer Therapy." Med Res Rev.

Lopez-Neblina, F., A. H. Toledo, et al. (2005). "Molecular biology of apoptosis in ischemia and reperfusion." J Invest Surg **18**(6): 335-350.

Mergenthaler, P., U. Dirnagl, et al. (2004). "Pathophysiology of stroke: lessons from animal models." Metab Brain Dis **19**(3-4): 151-167.

Moldoveanu, T., Q. Liu, et al. (2006). "The X-ray structure of a BAK homodimer reveals an inhibitory zinc binding site." Mol Cell **24**(5): 677-688.

Nie, C., C. Tian, et al. (2008). "Cysteine 62 of Bax is critical for its conformational activation and its proapoptotic activity in response to H2O2-induced apoptosis." J Biol Chem **283**(22): 15359-15369.

Oppermann, S., F. C. Schrader, et al. (2014). "Novel N-phenyl-substituted thiazolidinediones protect neural cells against glutamate- and tBid-induced toxicity." J Pharmacol Exp Ther **350**(2): 273-289.

Pagliari, L. J., T. Kuwana, et al. (2005). "The multidomain proapoptotic molecules Bax and Bak are directly activated by heat." Proc Natl Acad Sci U S A **102**(50): 17975-17980.

Petros, A. M., J. Dinges, et al. (2006). "Discovery of a potent inhibitor of the antiapoptotic protein Bcl-xL from NMR and parallel synthesis." J Med Chem **49**(2): 656-663.

Petros, A. M., E. T. Olejniczak, et al. (2004). "Structural biology of the Bcl-2 family of proteins." Biochim Biophys Acta **1644**(2-3): 83-94.

Ryan, J. A., J. K. Brunelle, et al. (2010). "Heightened mitochondrial priming is the basis for apoptotic hypersensitivity of CD4+ CD8+ thymocytes." Proc Natl Acad Sci U S A **107**(29): 12895-12900.

Shamas-Din, A., S. Bindner, et al. (2013). "tBid undergoes multiple conformational changes at the membrane required for Bax activation." J Biol Chem.

Shamas-Din, A., H. Brahmbhatt, et al. (2011). "BH3-only proteins: Orchestrators of apoptosis." Biochim Biophys Acta **1813**(4): 508-520.

Souers, A. J., J. D. Leverson, et al. (2013). "ABT-199, a potent and selective BCL-2 inhibitor, achieves antitumor activity while sparing platelets." Nat Med **19**(2): 202-208.

Tobaben, S., J. Grohm, et al. (2011). "Bid-mediated mitochondrial damage is a key mechanism in glutamate-induced oxidative stress and AIF-dependent cell death in immortalized HT-22 hippocampal neurons." Cell Death Differ **18**(2): 282-292.

Tse, C., A. R. Shoemaker, et al. (2008). "ABT-263: A Potent and Orally Bioavailable Bcl-2 Family Inhibitor." Cancer Research **68**(9): 3421-3428.

Tse, C., A. R. Shoemaker, et al. (2008). "ABT-263: a potent and orally bioavailable Bcl-2 family inhibitor." Cancer Res **68**(9): 3421-3428.

Turner, P. V., C. Pekow, et al. (2011). "Administration of substances to laboratory animals: equipment considerations, vehicle selection, and solute preparation." J Am Assoc Lab Anim Sci **50**(5): 614-627.

Vogler, M. (2014). "Targeting BCL2-Proteins for the Treatment of Solid Tumours." Advances in Medicine **2014**: 14.

Vogler, M., H. A. Hamali, et al. (2011). "BCL2/BCL-X(L) inhibition induces apoptosis, disrupts cellular calcium homeostasis, and prevents platelet activation." Blood **117**(26): 7145-7154.

Vogler, M., K. Weber, et al. (2009). "Different forms of cell death induced by putative BCL2 inhibitors." Cell Death Differ **16**(7): 1030-1039.

Westphal, D., R. M. Kluck, et al. (2014). "Building blocks of the apoptotic pore: how Bax and Bak are activated and oligomerize during apoptosis." Cell Death Differ **21**(2): 196-205.

Wolter, K. G., Y. T. Hsu, et al. (1997). "Movement of Bax from the cytosol to mitochondria during apoptosis." J Cell Biol **139**(5): 1281-1292.

Xin, M., R. Li, et al. (2014). "Small-molecule Bax agonists for cancer therapy." Nat Commun **5**: 4935.

Xu, X. P., D. Zhai, et al. (2013). "Three-dimensional structure of Bax-mediated pores in membrane bilayers." Cell Death Dis **4**: e683.

Zelenetz, A. D. (2015). "Emerging treatment options for B-cell lymphomas." J Natl Compr Canc Netw **13**(5 Suppl): 666-669.

Zhang, Z., S. Subramaniam, et al. (2015). "BH3-in-groove dimerization initiates and helix 9 dimerization expands Bax pore assembly in membranes." EMBO J.

Zhao, G., Y. Zhu, et al. (2014). "Activation of the proapoptotic Bcl-2 protein Bax by a small molecule induces tumor cell apoptosis." Mol Cell Biol **34**(7): 1198-1207.

Zong, W. X., C. Li, et al. (2003). "Bax and Bak can localize to the endoplasmic reticulum to initiate apoptosis." J Cell Biol **162**(1): 59-69.

Figures

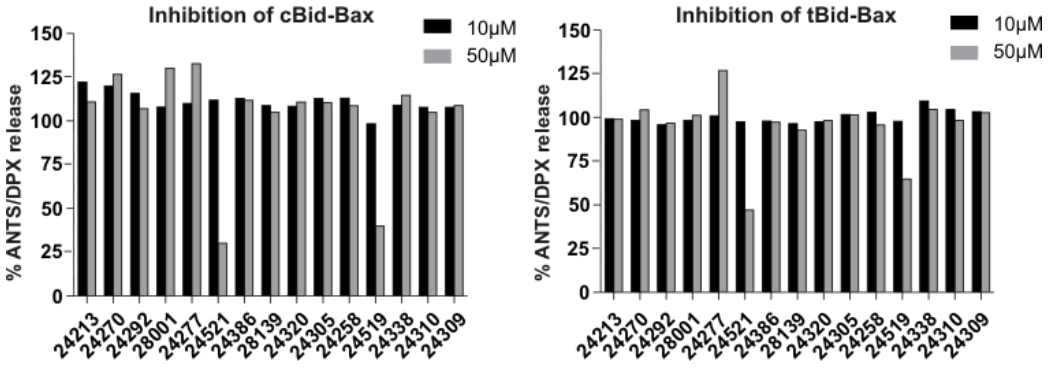

Figure 1: Two compounds inhibit tBid-Bax mediated liposome permeabilization.

Membrane permeabilization assayed for liposomes encapsulating ANTS/DPX incubated with 5nM cBid (Left) or 5nM tBid (Right), 100nM Bax and the indicated concentrations of the compounds. Permeabilization was assayed by measuring an increase in ANTS fluorescence. Results are represented as the % ANTS/DPX release and have been normalized to the no compound (DMSO) control.

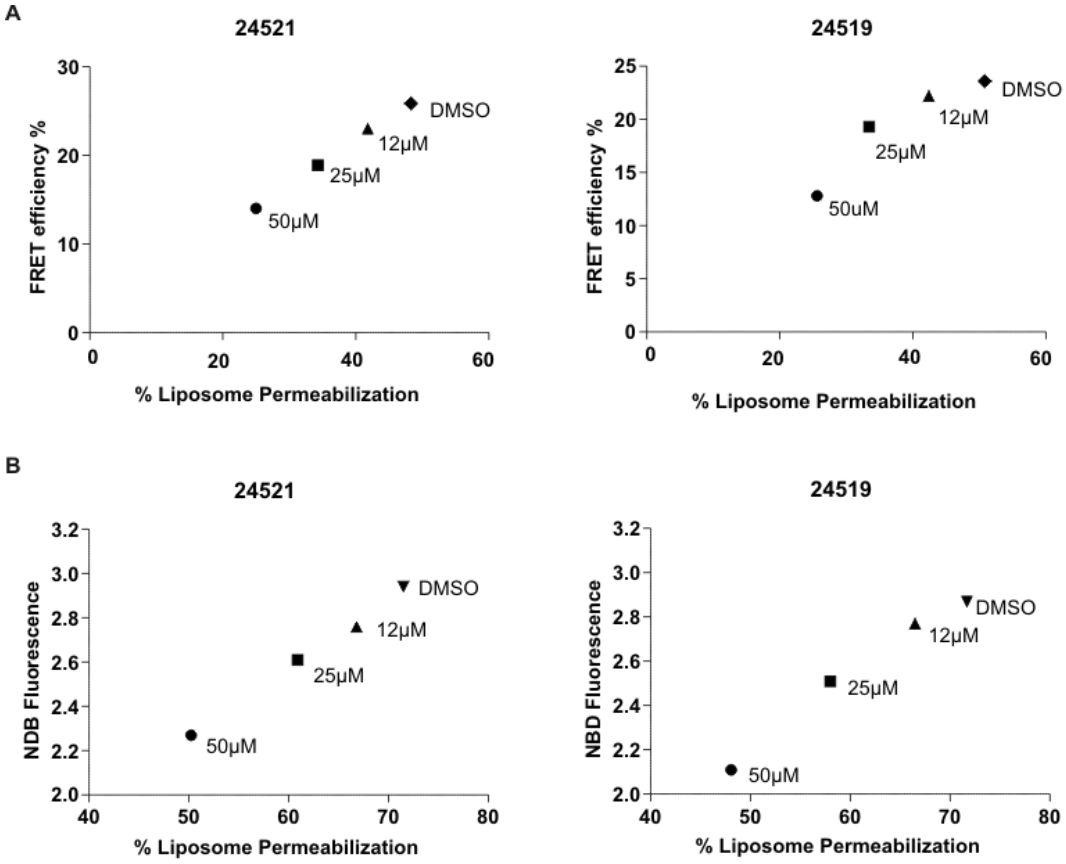

Figure 2: Compounds disrupt the interaction of Bax with cBid and reduce insertion of Bax in the membrane.

A. Compounds disrupt the interaction between cBid and Bax. Liposomes encapsulating Tb/DPA were incubated with 10nM 126C-Alexa 586 labelled cBid and 100nM 126C-Alexa 647 labelled Bax or unlabeled Bax and the compound at the indicated concentrations in the presence of liposomes. FRET was measured from reactions containing unlabeled Bax to obtained F_D or from reactions containing labelled Bax (F_{D+A}). FRET efficiency was calculated using the equation: 1- (F_{D+A} / F_D) * 100 at 3 hours. Liposome permeabilization was assayed by measuring the decrease in the fluorescence intensity of the Tb/DPA complex (n=1).

B. Compounds prevent the insertion of Bax in the membrane. Liposomes encapsulating Tb/DPA were incubated with 10nM cBid and 100nM 126C-NBD

labelled Bax. The fluorescence of NBD increases in a hydrophobic environment. After activation, Bax inserts into the liposomes and a corresponding increase in NBD fluorescence is measured. Results are represented as the fold increase in NBD fluorescence calculated as F/F_0 where F is the fluorescence at 3 hours and F_0 is the fluorescence at t=0. Liposome permeabilization is assayed as described in Fig. 2A (n=1).

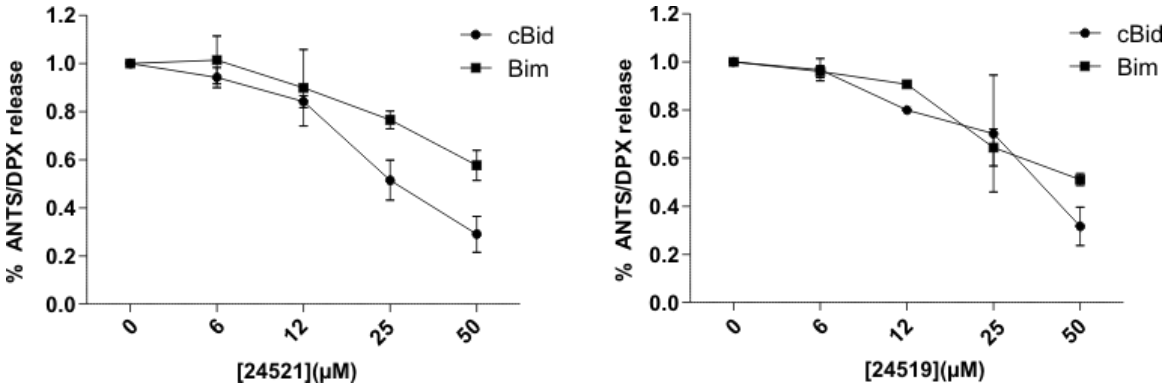

Figure 3: Compounds inhibit cBid/ Bim- Bax mediated liposome permeabilization.

Membrane permeabilization assayed for liposomes encapsulating ANTS/DPX incubated with 100nM Bax and 5nM cBid or 5nM Bim. Permeabilization assayed as described in Figure 1. Results have been normalized to the no compound (DMSO) control. Error bars: SD, n=3.